Master's thesis

2009 Christopher Sørum

Synthesis of New Tyrosine Kinase Inhibitors

NTNU
Norwegian University of
Science and Technology
Faculty of Natural Sciences
and Technology
Department of Chemistry

NTNU

Christopher Sørum

Synthesis of New Tyrosine Kinase Inhibitors

Master's Thesis for the Master of Technology/
Sivilingeniør Degree

Spring 2009

Supervisor: Associate Professor Bård Helge Hoff

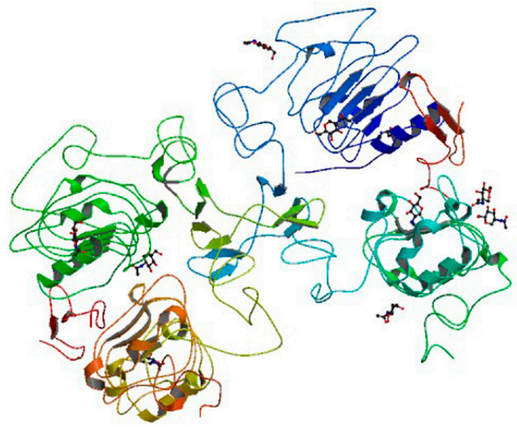

NTNU

The image on the front cover is a crystal structure of the complex human epidermal growth factor and extracellular domains.[1,2]

I hereby declare that this work is performed independently and in accordance with ”Reglement for sivilarkitekt- og sivilingeniøreksamen” at the Norwegian University of Science and Technology.

Christopher Sørum

Trondheim, 19th of June 2009

Acknowledgements

The work presented in this Master´s Thesis has been carried out at the Department of Chemistry at the Norwegian University of Science and Technology (NTNU) during the spring of 2009.

I would like to thank my supervisor, Associate Professor Bård Helge Hoff for his inspiration and valuble support during this work. His inputs and encouragement is most appreciated and has been of great importance to this thesis.

I want to thank the rest of the "Fluorine family" as well for all the fun we have had all year, and then especially PhD student Erik Fuglseth; even though Liverpool will never win the Barclays Premier League, you are a great organic chemist.

I want to thank engineer Roger Aarvik for providing all the chemicals to the right time, and everything else of a practical matter. Anders Brunsvik at Sintef is thanked for providing all of the MS spectra. A big thanks goes to Trygve Andreassen for helping me with the processing of the NMR spectra.

I would also like to thank my aunt and uncle, Dr. Anne Kari Nyhus and Dr. Steinar Hagen for useful feedback on this report.

For all the fun during these five years, I want to thank all of my friends. My family has been of tremendous support throughout these five years, which I am very grateful for. Finally, I want to thank my Benedicte for the patience and help in the course of this Master´s degree.

Christopher Sørum
Trondheim, June 2009

Abstract

The objective of this project was to synthesize new, novel low molecular compounds with tyrosine kinase inhibitory properties (Figure i). Some of these compounds (**1a** and **1e**) have already been reported to inhibit different kinases, and thus there was a great probability that the compounds set for synthesis also had these properties.

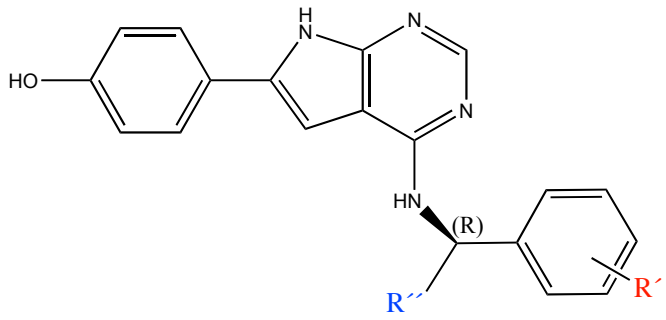

1a R´ = H, R´´ = CH_3
1b R´ = p-OH, R´´ = CH_3
1c R´ = o-F, R´´ = CH_3
1d R´ = m-F, R´´ = CH_3
1e R´ = p-F, R´´ = CH_3
1f R´ = o-F, R´´ = H
1g R´ = m-F, R´´ = H
1h R´ = p-F, R´´ = H

*Figure i: Existing (compounds **1a** and **1e**) and new potentially tyrosine kinase inhibitors.*

To assure that the eight compounds synthesized were the right molecules, NMR and MS were used in the characterization. Specific rotation was calculated, and the purity of the different compounds was determined by HPLC.

The second aim, given that the first goal was reached, was to have these compounds tested by *in vitro* enzymatic testing. Most of the compounds were synthesized successfully with a high degree of purity. A commercial enterprise was hired to perform the testing, and the results revealed that all of the compounds inhibited the tyrosine kinase EGFR (ErbB1) to a greater or lesser extent.

Table of Contents

List of Figures

Page

List of Schemes

List of Tables

Page

Symbols and Abbreviations

ATP	Adenosine Triphosphate
COSY	Correlation Spectroscopy (^{1}H,^{1}H)
DCM	Dichloromethane
DEPT	Distortionless Enhancement by Polarization Transfer
DEA	Diethylamine
DMF	Dimethylformamide
DMSO	Dimethylsulfoxide
EGFR	Epidermal Growth Factor Receptor
EI	Electron Ionization
ESI	Electron Spray Ionization
Eq.	Equivalent
h	Hour
HMBC	Heteronuclear Multiple Bond Correlation
HPLC	High Performance Liquid Chromatography
HRMS	High Resolution Mass Spectroscopy
HSQC	Heteronuclear Single Quantum Coherence
ICP-MS	Inductively Coupled Plasma Mass Spectrometry
J	Coupling Constant (Hz)
Mp	Melting Point
MS	Mass Spectroscopy
m/z	Mass per Charge
NMR	Nuclear Magnetic Resonance
ppm	Parts Per Million
Pr-i	Isopropyl-group
Pr-n	Propyl-group
PTK	Protein Tyrosine Kinase
r.t.	Room Temperature
rt.	Runtime
RPTK	Receptor Protein Tyrosine Kinase
RTK	Receptor Tyrosine Kinase
SAR	Structure-Activity Relationship
TEA	Triethylamine

TFA	Trifluoroacetic Acid
THF	Tetrahydrofuran
TK	Tyrosine Kinase
TLC	Thin Layer Chromatography
VEGF	Vascular Endothelial Growth Factor
Å	Ångström ($1*10^{-10}$ m)
α	Specific Rotation
δ	Chemical Shift
σ	Hammet constant

1. Introduction

The focus on low molecular compounds with tyrosine kinase inhibitory properties has increased tremendously during the last decade. Numerous patents containing both new, and existing molecules for use in new application area has been published continuously.[3-11] A breakthrough came in the late 1990s when the low molecular compounds Gefitinib (Iressa), Imatinib (Gleevec) and Erlotinib (Tarceva) (Figure 1.1) were found to have inhibitory activity against epidermal growth factor receptor (EGFR), a tyrosine kinase. The role of this receptor was first established during that time,[12] and was an important part of the research directed towards new anti-cancer agents.

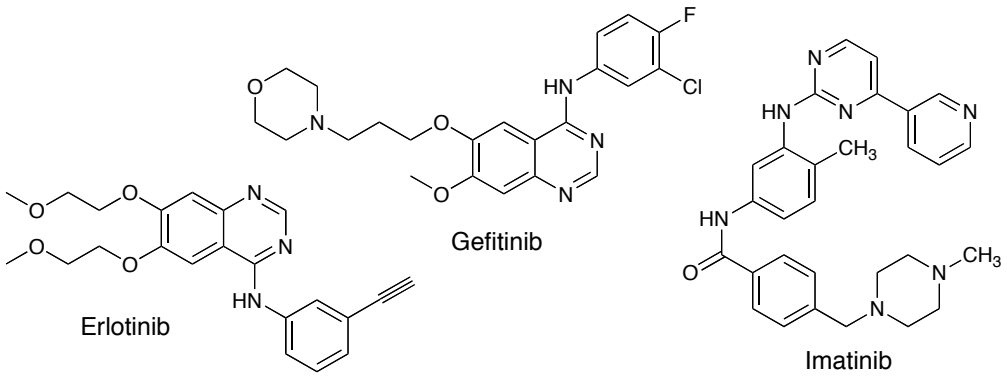

Figure 1.1: Tyrosine kinase inhibitors Erlotinib, Gefitinib and Imatinib.

The objective of this thesis is to synthesize both previously reported compounds, as well as novel molecules. The synthesis of compounds **2a**, **2b**, **2c**, **1a** (PKI 166) and **1e** (Figure 1.2 and 1.3) are earlier described in literature, while compounds **1a** and **1e** are also reported to have inhibitory activity towards tyrosine kinase.[5, 10, 13-15] Therefore, similar compounds will be set up for synthesis and biological testing. A convenient synthetic route is designed on the basis of previously reported work, and the biological testing should be performed if the syntheses and purification steps are shown to be successful. They will be tested for activity towards different receptor tyrosine kinases (RTKs).

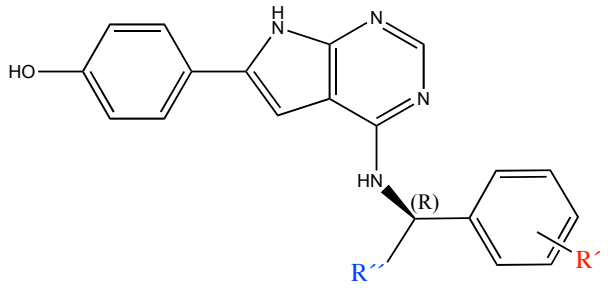

1a R´ = H, R´´ = CH_3
1b R´ = p-OH, R´´ = CH_3
1c R´ = o-F, R´´ = CH_3
1d R´ = m-F, R´´ = CH_3
1e R´ = p-F, R´´ = CH_3
1f R´ = o-F, R´´ = H
1g R´ = m-F, R´´ = H
1h R´ = p-F, R´´ = H

*Figure 1.2: End products in the synthetic route, compounds **1a-h**.*

The main products meant for testing, are compounds **1a-h** (Figure 1.2). However, some of the intermediates (**2a**, **2b**, **2e**) have also been reported to have good inhibitory activity towards tyrosine kinases. This means that one or more of these intermediates (Figure 1.3) may also be subjected to *in vitro* enzymatic testing.

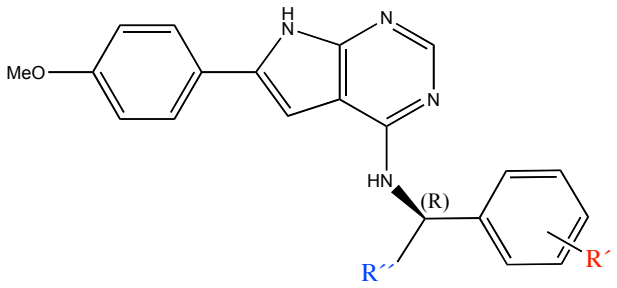

2a R´ = H, R´´ = CH_3
2b R´ = p-OMe, R´´ = CH_3
2c R´ = o-F, R´´ = CH_3
2d R´ = m-F, R´´ = CH_3
2e R´ = p-F, R´´ = CH_3
2f R´ = o-F, R´´ = H
2g R´ = m-F, R´´ = H
2h R´ = p-F, R´´ = H

*Figure 1.3: Compounds **2a-h** may also be biologically active.*

2. Theory

2.1 Fluorine in Medicinal Chemistry

A new era has arisen for the least natural abundant organohalogen. Widespread research is devoted towards the effects of fluorine, both in synthetic procedures and, more important, in drugs.[16, 17] Very few naturally occurring organic molecules contain any fluorine at all.[18] Chlorine is the preferred halogen from nature's side, and bacteria incorporate more often the chlorine atom than fluorine atom because it is more abundant in free ion form.[18] The industry also had a preference for the chlorine atom because of this, but in the latest years, this has changed. While fluorine was present in only 2% of pharmaceuticals in 1972, this has increased to 18% in 2006. In agrochemicals the number is even higher.[19] Fluorine is being included more frequently in pharmaceuticals than before, and several are on Forbes list of the top selling drugs worldwide in 2006,[20] e.g. Lipitor, a cholesterol lowering drug, and Seretide, an asthma drug (Figure 2.1). In addition, the known medicine Prozac is one of the most prescribed antidepressant in the world (Figure 2.1).

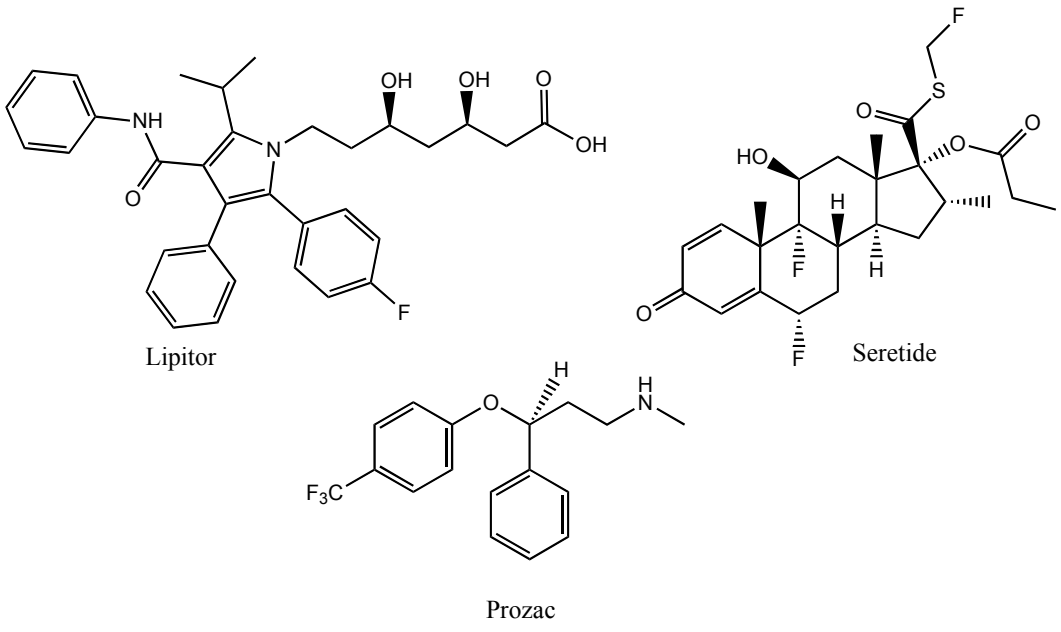

Figure 2.1: Different commercial drugs containing fluorine.

The influence of a fluorine atom in a molecule can be many, and the structure-activity relationship studies helps to predict the outcome in some cases.[19] But overall, the

pharmacokinetics is mostly a trial and error process until eventually the cryptic effects of fluorine are solved.

The fluorine atom is equivalent to hydrogen in size, which makes this a good replacement with regards to steric properties of the molecule. Fluorine is the smallest halogen with respect to the van der Waals radius, only a little bit larger than hydrogen (F 1.47 Å, Cl 1.75 Å, Br 1.85 Å, I 1.98 Å, H 1.20 Å).[21] This allows the structure to keep the molecular geometry and shape, in most cases without any disruption. However, when including a trifluoromethyl group, the steric change is estimated to correspond to the inclusion of an ethyl group, although the shape is significantly different. These steric variations make this element valuable when designing new drugs. The electron-withdrawing effects are quite strong, compare to other substituents. The Hammet constant (σ) that is used to predict the influence of a group on a neighboring site shows that fluorine has $\sigma_m = +0.34$, while the nitro group has $\sigma_m = +0.71$.[22] This means that a similar effect can be achived with regards to electron-withdrawing effects, by substituting a nitro group with a fluorine atom. The nitro group is much bigger in terms of the van der Waals radius, and influences sterically in a much stronger way than fluorine.[22] The highest known substituents with electron-withdrawing effect are highly fluorinated sulfimides (e.g. $SF(NSO_2CF_3)_2$, $\sigma_m = +1.78$).[23] The strong electron-withdrawing effect of fluorine is reflected in the electronegativity value (Pauling Scale 3.98),[24] and is the highest of the elements. This means that when fluorine is incorporated in the molecule, this affects the acidity or basicity of the nearby environment. It was found that fluorination in a series of 3-piperidinylindole decreased the basicity of the amine, which improved the bioavailability.[25]

Lipofilicity is also influenced by the incorporation of fluorine, both physiologically and on the molecular level. Better bioavailability (example above) and increased selectivity for target organs are two examples of the physiological advantageous fluorine brings. On the molecular level, electrostatic interactions with the target structure can be modulated, as well as inhibition of some metabolic pathways. This is especially important for the drugs designed to pass through the blood-brain barrier, for example anti-depressants.[23] Fluorination does not always lead to increased lipophilicity. In monofluorinated, or trifluorinated saturated alkyl groups, lipophilicity usually decreases due to strong electron-withdrawing effects of the

fluorine atom.[26] The electronegative fluorine can act as a hydrogen bond acceptor. This means that in molecules where a hydrogen and fluorine is spacially close, a hydrogen bridge will be able to stabilize the conformation intramolecularly (Figure 2.2).[23]

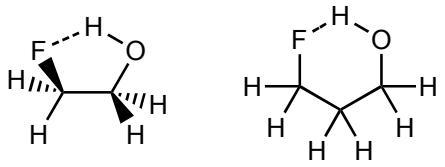

Figure 2.2: Conformational stabilization of gauche 2-fluoro-ethanol and 3-fluoropropanol by internal hydrogen bonding.

The stability of molecules is an important feature that has to be taken into consideration when developing drugs. After the drug has been administered, some of the active ingredients are lost by various detoxification mechanisms. This makes fluorine a valuable element in drug synthesis, since the size is approximately the same as hydrogen, but blocks e.g. the oxidation process mediated by cytochrome P450 enzymes. This means that the lipophilicity is not decreased due to oxidation, and the clearance is still the same.[27] This can be exemplified by the lead optimization of cholesterol inhibitor Ezetimib (Figure 2.3).

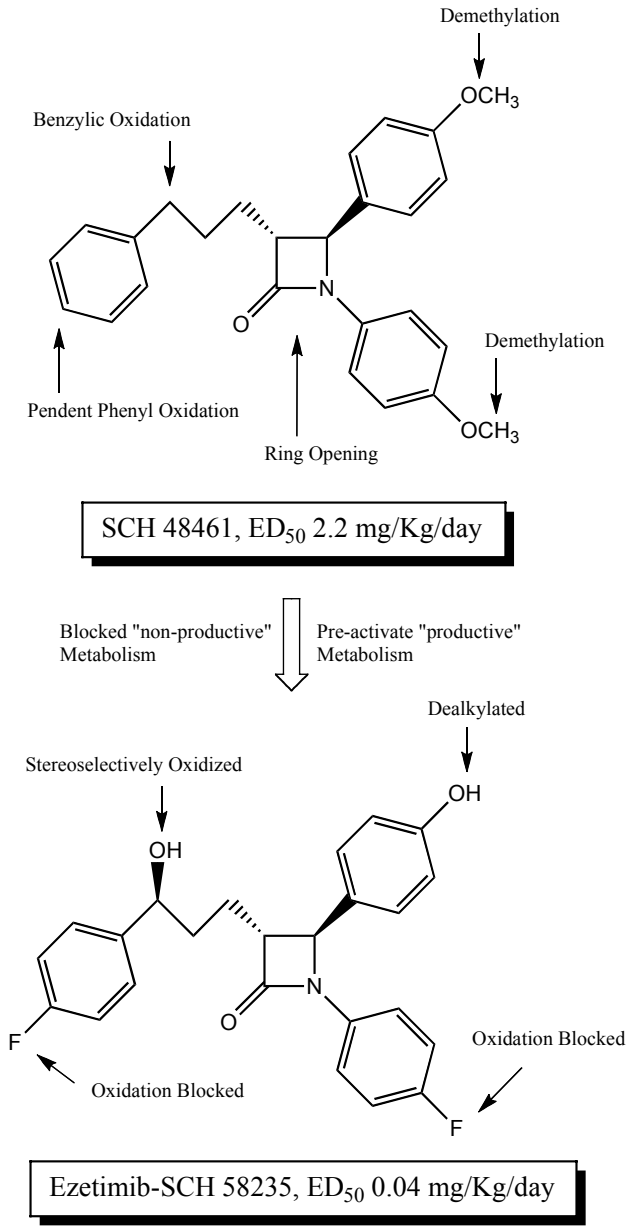

Figure 2.3: Lead optimization of Ezetimib[28]

The fluorine atom is often incorporated into a molecule to alter the rate of drug metabolism and thereby produce a drug with longer duration of action. Some drugs are found to be 400 times more potent because of structural modifications involving fluorine.[27] Another feature why fluorine substitution has become more important in drug design is that it can reduce the toxicity. This is achieved by blocking the formation of toxic and sometimes reactive metabolites, but this implies that fluorine is substituted on the appropriate site of the molecule.[29]

2.2 Tyrosine Kinase Signaling Pathway

Receptor tyrosine kinases trigger a chain of different signal transduction events inside the cell that eventually leads to cell growth, proliferation and differentiation. These processes are tightly controlled.[30] The EGFR is located extracellular and a ligand (e.g. EGF) binds to this receptor (Figure 2.4 a), the receptor is activated and a signal is sent to the intracellular tyrosine kinase domains. This further activates a set of signals, starting with the receptor aggregation, which leads to crossphosphorylation of a number of tyrosine amino acid residues (see Figure 2.4 b). Once the relay proteins are phosphorylated, in turn this initiates a cellular response.

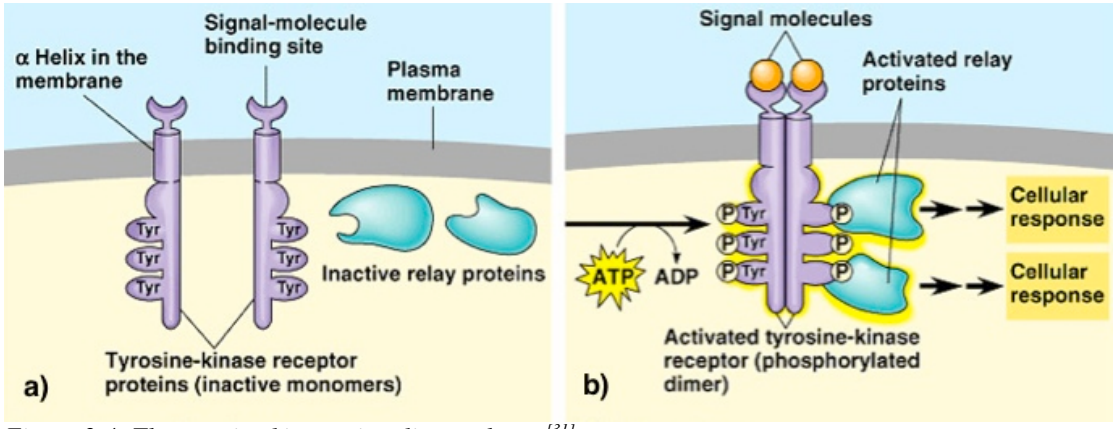

Figure 2.4: The tyrosine kinase signaling pathway.[31]
a) The inactive tyrosine-kinase receptor system, b) Activated system.

2.3 Tyrosine Kinases in Cancer

In the beginning of the 1990s various classes of compounds was reported as tyrosine kinase inhibitors.[32-34] Many of these compounds were potent, but lacked the selectivity. However, several examples of structurally different classes that were published afterwards proved to be more selective ATP-competitive tyrosine kinase inhibitors, e.g. phenylamino-compounds showed in Figure 2.5. Another class of low molecular compounds with the same selectivety is the class of pyrrolo-pyrimidines. These were identified in a random screening and optimized using a pharmacophore model of the adenosine triphosphate (ATP) binding site of the EGFR tyrosine kinase.[13, 35]

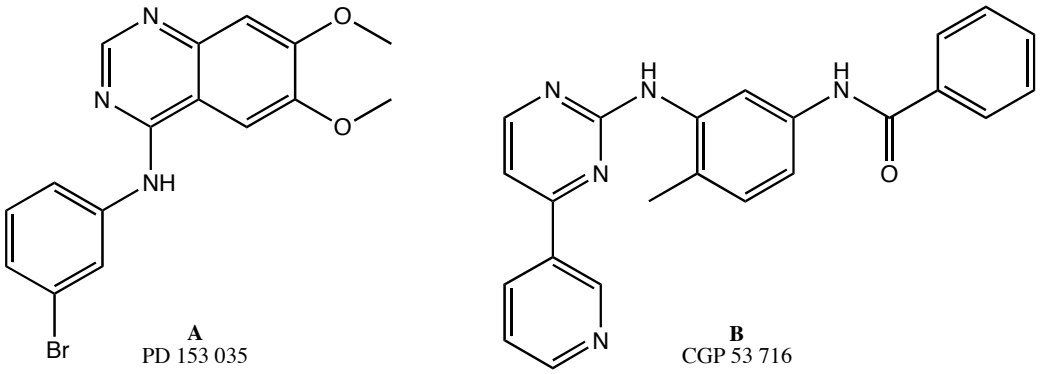

*Figure 2.5: **A** is an anilino-quinazoline while **B** is a phenylamino-pyrimidine, both are potent selective inhibitors of EGFR.*[35, 36]

Protein phosphorylation and dephosphorylation play a pivotal role in the mechanism for transmembrane and intracellular signaling.[37] Cell growth, differentiation, proliferation, cell cycle and survival are just some of the aspects that depend on these enzymes. Protein tyrosine kinases (PTKs) are a class of multiple enzymes that bind ATP and catalyze the transfer of γ-phosphate of ATP to hydroxyl groups of tyrosine residues on proteins. Activation occurs by phosphorylation, or in the case of receptor tyrosine kinases, activation by interaction of a protein with a receptor located within the extracellular domain of the kinase.[37] In the signal transduction machinery of healthy cells, the PTKs are central, and their deregulation plays an important role in many diseases, especially cancer. Activated RTKs are rapidly internalized in healthy cells. Because of this it is easy to control that their enzymatic activity is inhibited. In turn this ensures that signal cascades are only temporary and they can return to its

non-stimulated state in proper time. If not, it might happen that the kinases are locked in the activated form possibly caused by variable structural alterations, or deregulation of inhibitory signals and auto control mechanisms. Various diseases are proved to be due to active enzymes that lead to over-expression. Molecular characterizations of several human malignant tumors shows that many of the RPTKs have been mutated or over-expressed, e.g. EGF, ErB2, VEGF1, 2, 3.[38]

The ATP binding site has proven to be a highly selective target for several tyrosine kinase inhibitors active in the nanomolar range.[13] A number of inhibitors towards various tyrosine kinases are being described showing potent and selective *in vitro* activity.[13, 39] A known tyrosine kinase inhibitor, PKI166 (Figure 2.6) is one of many pyrrolo-pyrimidines that have been clinically evaluated. Although PKI166 is currently discontinued, there are many other tyrosine kinase inhibitors in different stages of clinical trial or already approved.[40-42]

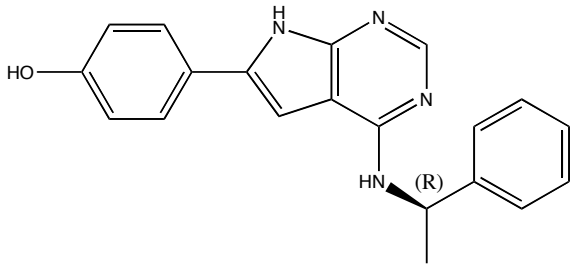

Figure 2.6: EGFR tyrosine kinase inhibitor PKI166.

The target of these novel molecules has been found due to greater understanding of the biological and molecular pathways. This has provided the knowledge on how to differentiate between malignant and normal cells, so that drugs can focus on the tumour cells, and leave the normal ones untouched. The abnormalities that characterize cancer cells have thus been a target for new drugs, and TK receptors represent one such target.[43] There are many RTPKs that cause cancer, but the most common seems to be the EGFR. The epidermal growth factor receptor (EGFR), also referred to as ErB1, is one receptor among many close related and was the first receptor in the ErbB family to be discovered and defined in 1984.[44] ErbB2 (HER2) was the second member to be discovered, then ErbB3 (HER3) and ErbB4 (HER4).[43] The different EGFRs can share ligands and form heterodimers, which initiates different signaling cascades.[39] Generally the ErbB receptors will comprise an extracellular domain, that may bind an ErbB ligand. Preferably the ErbB receptor is a

native sequence human ErbB receptor, but may also be an amino acid sequence variant thereof.[9] They are implicated in the development in numerous human tumors, e.g. breast, lung (the most frequent cause of cancer death),[45, 46] colorectal, ovarian and prostate. This is one of the main reasons the EGFR system was chosen as a new target for drug design.

There are numerous examples of tyrosine kinase inhibitors synthesized in the last two decades and many are still in clinical trial or already approved for the market. Several classes of compounds are found to have properties valuable in the search for potentially new anti-cancer drugs. Some examples are given in Figure 2.7.

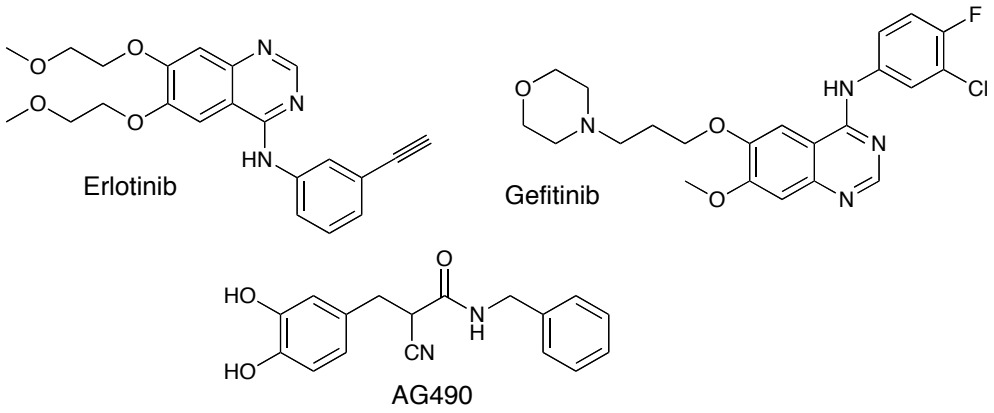

Figure 2.7: Tyrosine kinase inhibitors on the market or in clinical trials.

Erlotinib and Gefitinib are compounds that are on the market as anti-cancer drugs. Their mode of action is identical to the compounds shown in Figure 2.5. They target the EGFR tyrosine kinase to inhibit their ability to mutate or over-express further.[47] However, research and clinical evaluations are still underway to find new areas of use. AG490, shown in Figure 2.7 is also a potent inhibitor of tyrosine kinase, but in contrast to Erlotinib and Gefitinib, it inhibits JAK2, another class of PTK which is involved in development of leukemia when it is over-expressed.[48] This compound is still in clinical trial.[49]

2.4 Other Diseases

There has been work to find agents that treat microbial-induced diseases such as malaria and leishmania, as well as other diseases caused by parasitic protozoa, e.g. dyssenery and human African trypanosomiasis. Since there are no vaccines available and resistance towards existing drugs is emerging, the need of non-toxic, effective drugs are enormous.[50] Chemotherapy has been an important method in the treatment of individual patients and in vector-control measures to reduce the transmission of parasitic infections.[51] However, this method is not very effective in the long run, and does not kill nearly all of the parasitic infections known. This led to the need of more effective and selective agents, with less adverse effects. Drugs meant to inhibit tyrosine kinase in cancer were investigated if they also could be used in defeating protozoal diseases. The mode of action was early directed towards inhibiting tyrosine phosphorylation or dephosphorylation of proteins in trypanosomes.[52] Several of the already commercially available TK inhibitors Erlotinib, Gefitinib (Figure 2.7), Sunitinib and Axitinib (Figure 2.8) have been tested towards protozoans. The results provide evidence that these compounds not only possess inhibitory properties, but also kill the protozoans.[53]

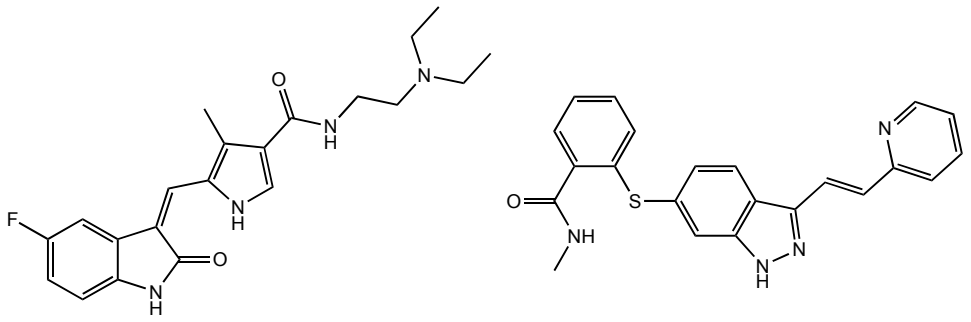

Figure 2.8: TK inhibitors used as antiprotozoal agents.

New research has found that other tyrosine kinases play a large role in the neurodegenerative disease leprosy (*Mycobacterium leprae*) as well. When the ErbB2 RTK signaling is activated without heterodimerization of ErbB2-ErbB3, this induces *Mycobacterium leprae* demyelination. PKI 166 has been found to inhibit this signaling, thus reducing the myelin damage.[54, 55]

3. Synthesis

3.1 Synthetic Route to Yield Compounds 1a-h

The synthetic route to give compounds **1a-1h** is showed in Scheme 3.1.[5, 10] The first step is an alcoholysis of ethyl cyanoacetate to yield ethyl 3-ethoxy-3-iminopropanoate hydrochloride. Second step includes the forming of the amidine hydrochloride salt using ammonium chloride.

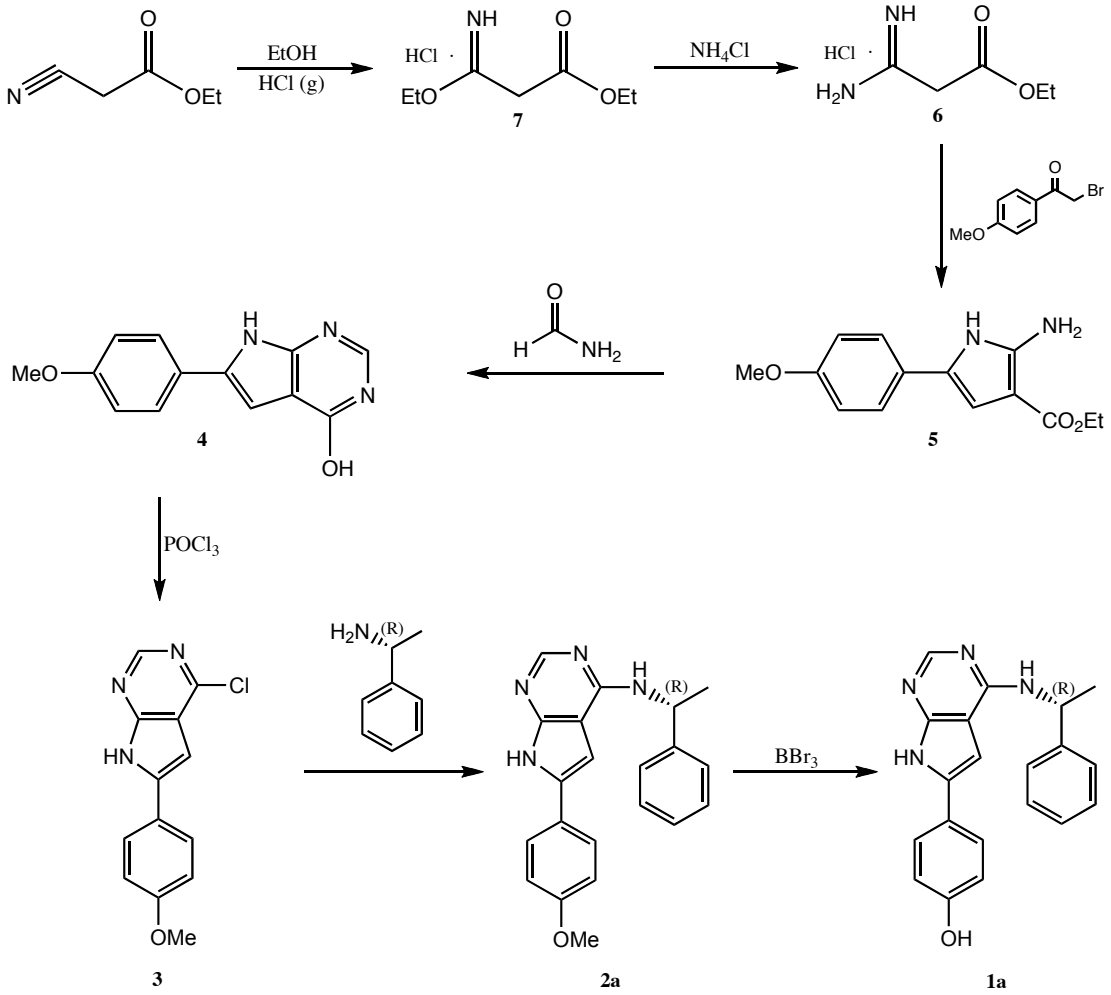

*Scheme 3.1: Synthetic route from ethyl cyanoacetate to (R)-4-(4-(1-phenylethylamino)-7H-pyrrolo[2,3-d]pyrimidin-6-yl)phenol (**1a**).*

Steps three and four are condensation and cyclization reactions, respectively.

Since the cyclization step was known to require harsh conditions (150°C, 19 h). The use of a microwave as a heating source was a practical solution (Scheme 3.2). Similar reactions were found in literature, and used as a starting point.[56, 57]

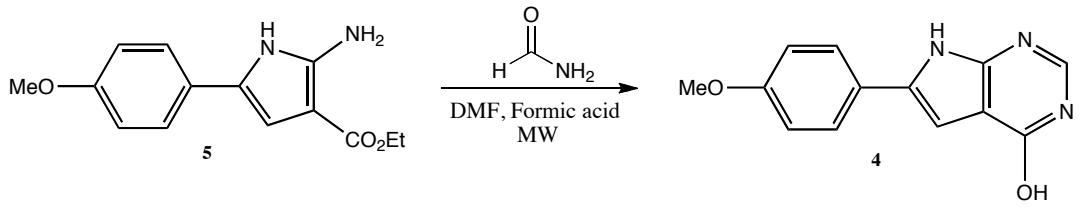

*Scheme 3.2: Microwave assisted cyclization reaction of compound **5** with formamide.*

The next step includes the chlorination of compound **3**, using phosphorus oxychloride.

In the second last step, a N-alkylation with purchased amines should be carried out. The literature suggests the use of three equivalents of amine per equivalent of 4-chloro-6-(4-methoxyphenyl)-7H-pyrrolo-[2,3-*d*]-pyrimidine (**3**).[5] Demethylation of compounds **2a-h** is accomplished with the use of boron tribromide and dichloromethane (DCM). This is a classical, well known method that is reported to give a decent yield in similar reactions.[58]

3.2 Mechanistic Reviews for Steps Five, Six and Seven

In the fifth step, chlorination with phosphorus oxychloride can take place in a number of different mechanisms, e.g. aromatic nucleophilic substitution. Another probable mechanism, which is described here (Scheme 3.3), involves a coordination of the hydroxyl group to the phosphorus molecule followed by an intramolecular exchange reaction.

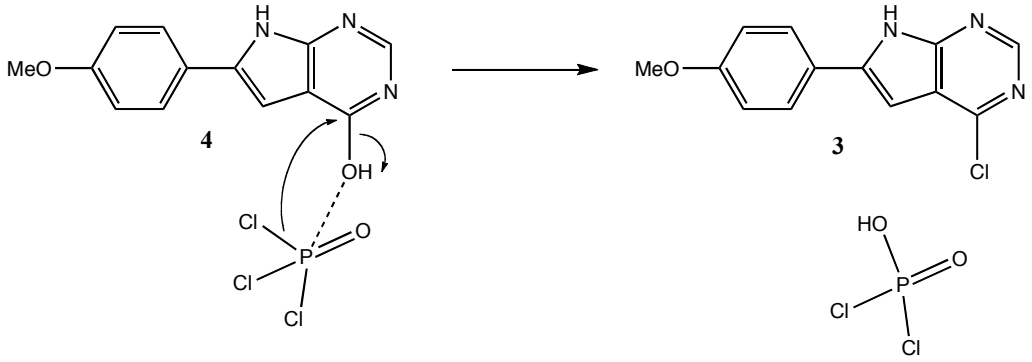

*Scheme 3.3: Mechanistic proposal for an intramolecular substitution of 4-hydroxy-6-(4-metoxyphenyl)-7H-pyrrolo-[2,3-d]-pyrimidine (**4**) with $POCl_3$.*

Step six in the synthesis includes an N-alkylation of the chloro-pyrrolo pyrimidine **3**. The mechanism proposed (Scheme 3.4) begins with the attack from the reacting amine onto the pyrimidine ring. The negative charge on the ring can be delocalized in the ring, stabilizing the intermediate. Chlorine as the leaving group is the final action that is taking place in this mechanism.

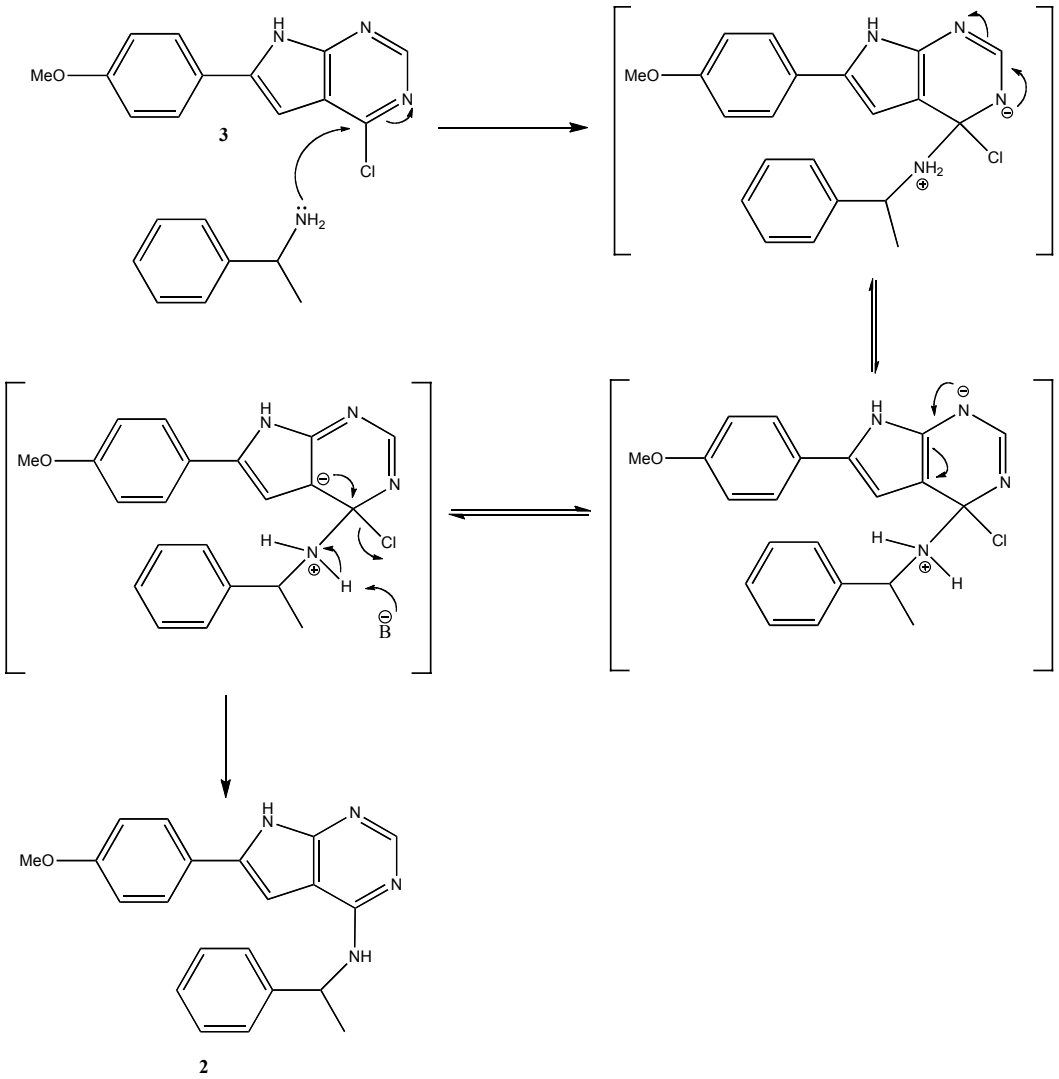

*Scheme 3.4: General mechanistic proposal yielding compounds **2a-h**.*

The ether cleavage is done under classical conditions (BBr_3/CH_2Cl_2), and one equivalent of boron tribromide can theoretically cleave three ether groups. However, an excess of BBr_3 is used to ensure full conversion in these reactions. The mechanism for the deprotection reaction is well established (Scheme 3.5).[59]

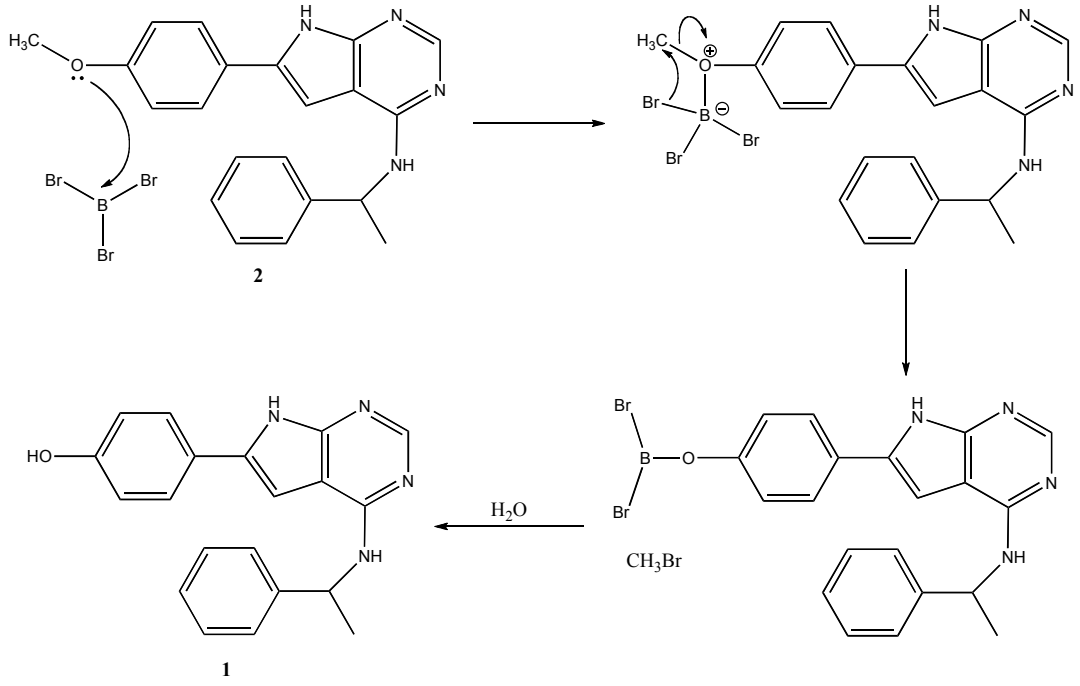

*Scheme 3.5: General mechanism for demethylation of compounds **2a-h**.*

3.3 Analogous Compounds and Reactions

The synthetic route described in Scheme 3.1 is the only route found in the literature to prepare these compounds. Focus on efficient, safe and ecologically friendly methods to synthesize 7*H*-pyrrolo[2,3-*d*]pyrimidine derivatives are growing, and are still an enormous challenge. Undesired intermediates that constitute an environmental hazard are to be avoided in these syntheses. A newly developed method focuses on this, and provide a more efficient way in the synthesis of 6-[4- (4-ethyl-piperazin-1-ylmethyl)-phenyl]-7H-pyrrolo[2,3-*d*]pyrimidin-4-yl]-((R)-1-phenyl-ethyl)- amine (Figure 3.1).[8] In the past syntheses of this compound it was produced a by-product that contained a benzyl-chloride moiety. This by-product constitutes a hazard in terms of safety and hygiene, and so, the development of a new synthesis that avoided the by-product was important.

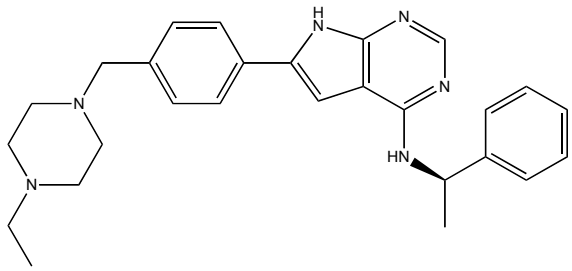

Figure 3.1: 6-[4- (4-ethyl-piperazin-1-ylmethyl)-phenyl]-7H-pyrrolo[2,3-d]pyrimidin-4-yl]-((R)-1-phenyl-ethyl)- amine.

Many more of 7*H*-pyrrolo[2,3-*d*]pyrimidine derivatives have been prepared and there are still more to come. Some examples are given in Figure 3.2.[7] Both *R* and *S* configuration has been found to have activity against tyrosine kinase, but molecules with *R* configuration seems generally to be the most potent.[13]

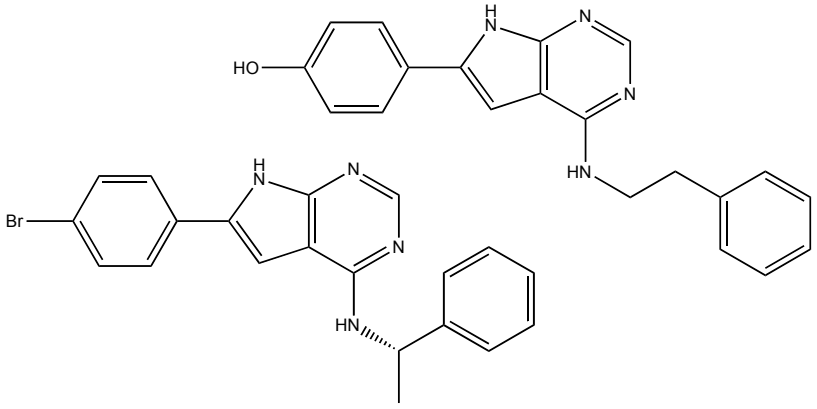

Figure 3.2: Potent inhibitors of tyrosine kinase EGFR.

Other halides have also been used in similar compounds with great success, both in preparing the compounds and regarding their activity.[13] Although the majority of the compounds found in literature have a phenyl ring substituted on each side of the 7*H*-pyrrolo[2,3-*d*]pyrimidine entity, there are examples of compounds with aliphatic chains on one or both sides of the pyrrolo-pyrimidine moiety (Figure 3.3).[7] These compounds are however, not synthesized with the intent to be used as inhibitor of cancer related kinases, but are reported to possess muscle relaxant, hypnotic and anticonvulsant activities,[60] or plant growth regulating properties.[61] As far as the literature reports, testing towards tyrosine kinases have never been performed. This could mean that there is a preference that at least one phenyl ring is substituted on one side of the entity. This is probably due to the ATP binding site, where the molecule possibly binds better to the site in case of the phenyl substituted compounds.

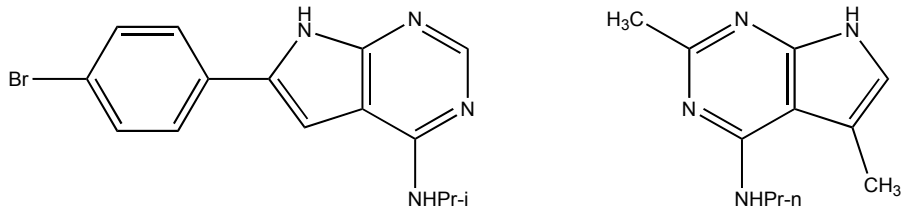

Figure 3.3: Examples of 7H-pyrrolo[2,3-d]pyrimidines substituted with aliphatic chains.

Besides pyrrolo-[2,3-*d*]pyrimidines, several furo-[2,3-*d*]pyrimidines have been synthesized (Scheme 3.6), and the condensation reaction was conducted in a different way than the pyrrolo-pyrimidines.[62] (Among others, THF was used instead of EtOH to avoid a retro-Claisen condensation.)

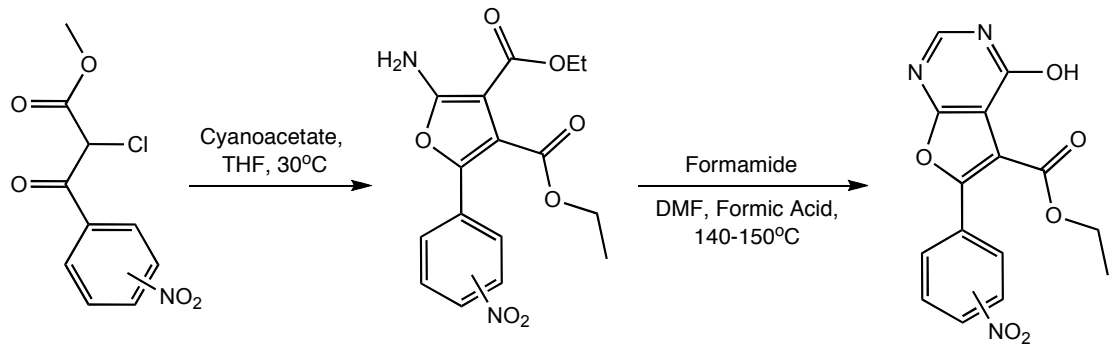

Scheme 3.6: Condensation reaction to yield a furo-[2,3-d]pyrimidine.

The cyclization reaction to yield the fused furo-pyrimidine was executed in the same manner as for the pyrrolo-pyrimidines. The further reaction was carried out with almost the same procedure as showed in Scheme 3.1. One difference however, was the saponification of the ester function before the resulting carboxylic acid was decarboxylated (Scheme 3.7).

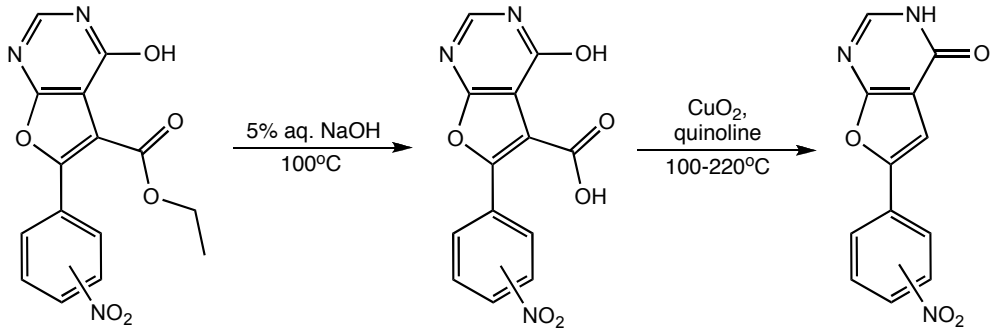

Scheme 3.7: Saponification and decarboxylation of the furo-[2,3-d]pyrimidine.

Testing of the inhibitory activity towards a number of tyrosine kinase showed that some of the furo-[2,3-*d*]pyrimidines was as active as PKI 166 (Figure 2.6).[62]

4. Results and Discussion

4.1 Scale-up of Previous Work

The synthetic steps from ethyl cyanoacetate to 4-Hydroxy-6-(4-metoxyphenyl)-7*H*-pyrrolo-[2,3-*d*]-pyrimidine (**4**) were done during the fall 2008 in the pre-project work (TKJ4520). The first four steps were conducted in a larger scale to ensure that the further synthetic steps could be carried out without any backtracking. The first two steps functioned reasonable well from the start, with regards to purity and yields. The yield was further increased in the scaled-up reactions (about 18 g of starting material was used in first step, and 28 g in the second step), and the purity remained high. The lowest yield was experienced for steps 3 and 4 (Scheme 4.1). Fortunately, when these reactions were scaled up, this resulted in an increase in yields (77% and 64%, respectively). Several grams of starting material were also used in steps 3 and 4 (13 g in each step). There were no changes in the procedure of step 3, the reaction time was still 1 h and the conversion of the bromo ketone was completed. Step 4 was performed in the same manner as before, but the large amount of starting material forced a prolonged reaction time (from 16 h to 19 h) to ensure full conversion. The larger scale made it easier to handle the product, and the small amount that was lost during multiple transfers, made less impact to the yield. NMR spectra obtained of compounds **4-7** are gathered in Appendices A.4-A.7.

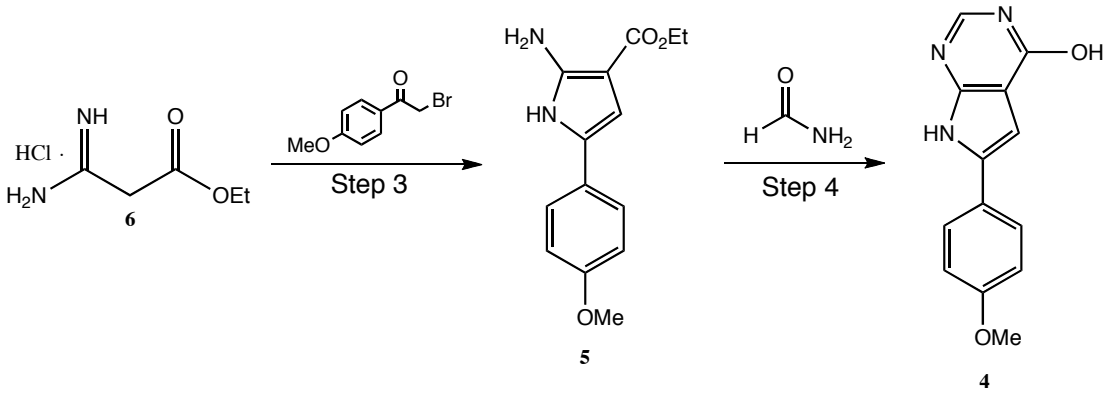

*Scheme 4.1: Steps 3 and 4 to yield 2-amino-3-carboxyethyl-5-(4-methoxyphenyl)-pyrrole (**5**) and 4-hydroxy-6-(4-metoxyphenyl)-7H-pyrrolo-[2,3-d]-pyrimidine (**4**).*

In an attempt to increase yield of 4-hydroxy-6-(4-metoxyphenyl)-7H-pyrrolo-[2,3-*d*]-pyrimidine (**4**), microwave heating was used (Scheme 4.2).

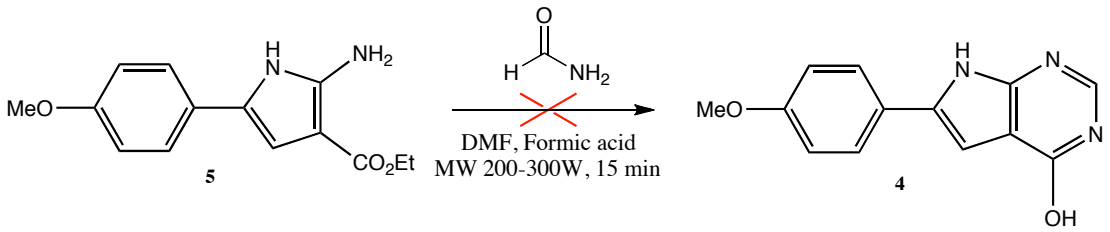

*Scheme 4.2: Microwave assisted cyclization reaction of compound **5** with formamide.*

Several attempts were made, with different settings, but the reaction mixture turned black every time. Analysis of the mixtures revealed that all of the starting material had decomposed, and nothing of the intended product was formed. This could mean that this reaction is not suited to be microwave heated, or that the reaction conditions were wrong, and has to be tested more extensively.

4.2 Synthesis of 4-chloro-6-(4-metoxyphenyl)-7H-pyrrolo-[2,3-*d*]-pyrimidine (3)

Compound **3** was made by dissolving 4-hydroxy-6-(4-metoxyphenyl)-7H-pyrrolo-[2,3-*d*]-pyrimidine (**4**) in phosphorus oxychloride (Scheme 4.3). The reaction was relatively fast, easy and without harsh conditions (90°C, 120 min.).

Scale-up to 13 g of compound **4** did not seem to affect the yield of the reaction in any way. The reaction was conducted several times, and all experiments resulted in good yields (96-98%).

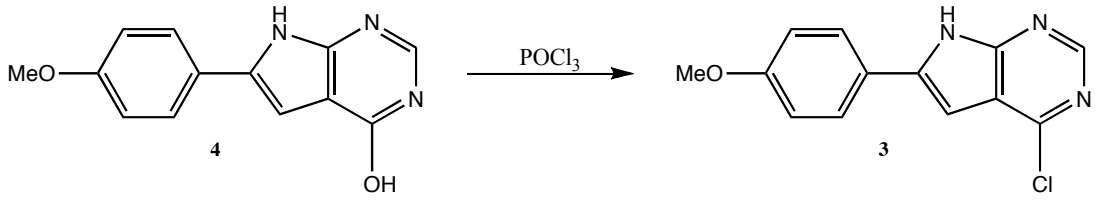

*Scheme 4.3: Nucleophilic aromatic substitution yielding 4-chloro-6-(4-methoxyphenyl)-7H-pyrrolo-[2,3-d]-pyrimidine (**3**).*

However, the large excess of phosphorus oxychloride required a large amount of ice in the quenching of the reaction mixture. In the following extraction, there had to be used large amounts of ethyl acetate, making this an environmentally unfriendly reaction because of all the waste. The amount of ice can probably be reduced to some extent, but the risk of the reaction mixture boils over (because of the exothermic reaction between water and the excess phosphorus oxychloride) increases, and product may be lost.

4.3 Synthesis of Compounds 2a-h

4.3.1 General features in the synthesis of compounds 2a-h

Compounds **2a-h** were synthesized using precursor **3** in reaction with purchased amines (Scheme 4.4). Because the prices of some of the amines were quite high, the amount of the reacting amine was kept low. This led to a prolonged reaction time for nearly all of the reactions. The different amines were either enantiomeric pure, or achiral so separation of enantiomers was not an issue. However, for some of the reactions, a by-product was formed. This mainly applied to the reactions with the achiral amines.

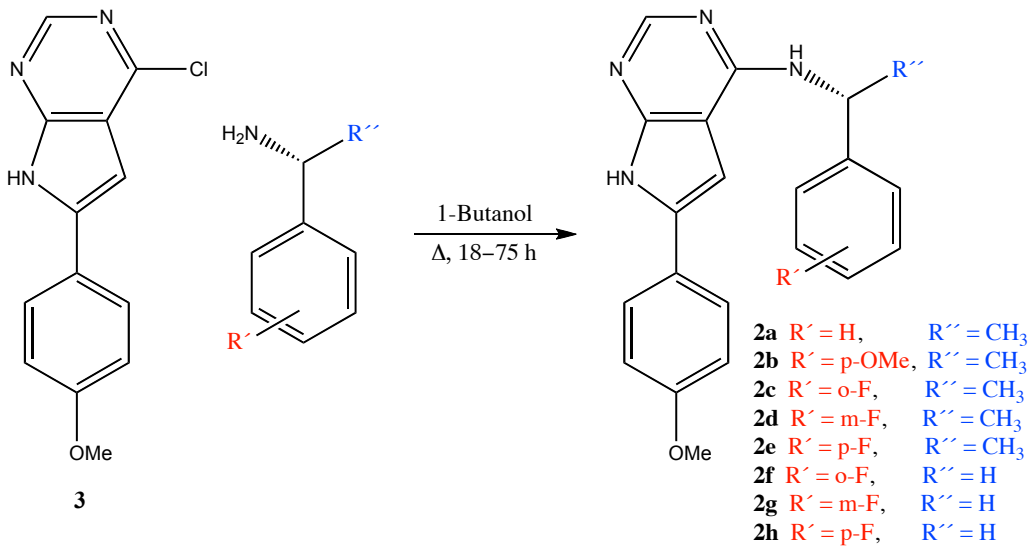

*Scheme 4.4: Reaction to yield compounds **2a-h**.*

To ensure a high conversion of 4-chloro-6-(4-methoxyphenyl)-7H-pyrrolo-[2,3-*d*]-pyrimidine (**3**) when only 2 equivalents of amine was used, the reaction was run up to 75 h. Triethylamine (TEA) was used in some reactions to deprotonate the amine; to ease the substitution. This has been reported in similar reactions, both in refluxing 1-butanol and under milder conditions.[63, 64] In the literature, the reaction times were 3-7 h, while for the reactions shown in Scheme 4.4, the reaction times were as long as 18-75 h.

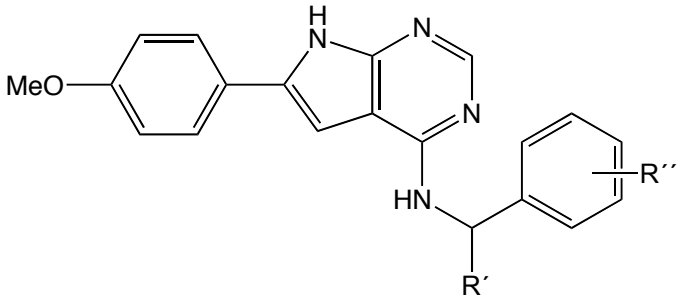

*Figure 4.1: The general structure of compounds **2a-h**.*

*Table 4.1: Yields of reactions to form compounds **2a-h** with, or without TEA. Inside the brackets are number of equivalents of the respective amine used totally in the reaction, and the reaction times. See Figure 4.1 for the general structure of compounds **2a-h***

Product:	R´	R´´	Isolated yield of reaction with TEA	Isolated yield of reaction without TEA
2a	H	CH_3	-	71% (3.8 Eq., 24 h)
2b	p-OMe	CH_3	57% (2 Eq., 44 h)	60% (3 Eq., 48 h), 63% (2 Eq., 75 h)
2c	o-F	CH_3	-	80% (2 Eq., 48 h)
2d	m-F	CH_3	-	60% (1.8 Eq., 51 h)
2e	p-F	CH_3	67% (2.5 Eq., 62 h)	65% (3.5 Eq., 24 h)
2f	o-F	H	74% (2 Eq., 28 h)	-
2g	m-F	H	76% (2 Eq., 18 h)	54% (2.4 Eq., 45 h)
2h	p-F	H	-	67% (2 Eq., 45 h), 70% (2.5 Eq., 28 h), 78% (2 Eq., 52 h)

Table 4.1 show that there are no overall trends either way. Too few experiments were carried out to determine the relationship between the use of TEA and the isolated yields. Some of the reactions (escpecially the one that yields compound **2g**) seemed to benefit from the use of TEA and the amount of amine was reduced, as well as the reaction times. Other reactions were conducted without the use of TEA and still gave high yields (compound **2c**), but the reaction time had to be prolonged. Theoretically, the extra steric hindrance of the chiral amines may cause deprotonation to be harder than for the achiral compounds. Another aspect is the donating effect of the methyl group that provides the chiral amines with more electrons. This makes them more

basic, and thus deprotonation may be more difficult. But, as stated above, these reactions have not been tested fully, which makes these only theories.

For all the products, the work-up was easy, and consisted only of a filtration with a following wash with diethyl ether. The achiral amines however, behaved differently from the chiral amines. After the filtration and rinsing, NMR revealed two different sets of signals in the spectra. Although nothing of the by-product was isolated, ^{1}H spectra of the crude material suggest that the by-product most likely was the hydrochloride salt of the amine substrate (Figure 4.1). The shift values in the ^{1}H spectrum corresponded well with literature.[65]

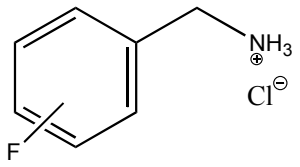

2f = o-F
2g = m-F
2h = p-F

*Figure 4.2: By-products in the amination reaction with achiral amines to yield **2f-h**.*

These by-products were separated from the product with an extraction, to leave the product pure.

4.4 Synthesis of Compounds 1a-h

4.4.1 General Features in the Synthesis of Compounds 1a-h

Compounds **2a-h** were demethylated using BBr_3 to yield **1a-h** (Scheme 4.5). The reactions were performed at r.t. under argon atmosphere, to ensure stable, dry conditions. Nitrogen was also used with good results. The boron tribromide was mixed with DCM and added to starting material **2** dissolved in DCM. The BBr_3 was added over a period of 1 h keeping the temperature at 0°C. The mixture was then heated to r.t., and was allowed to stir up to 24 h depending on the reaction. After the work-up the resulting oil was triturated with aceton (involved compounds **1a**, **1c-h**, while compound **1b** was recrystallized from diethyl ether). Because of the long reaction time, an attempt was made to use more boron tribromide in the reaction. However, the rate of reaction was not increased.

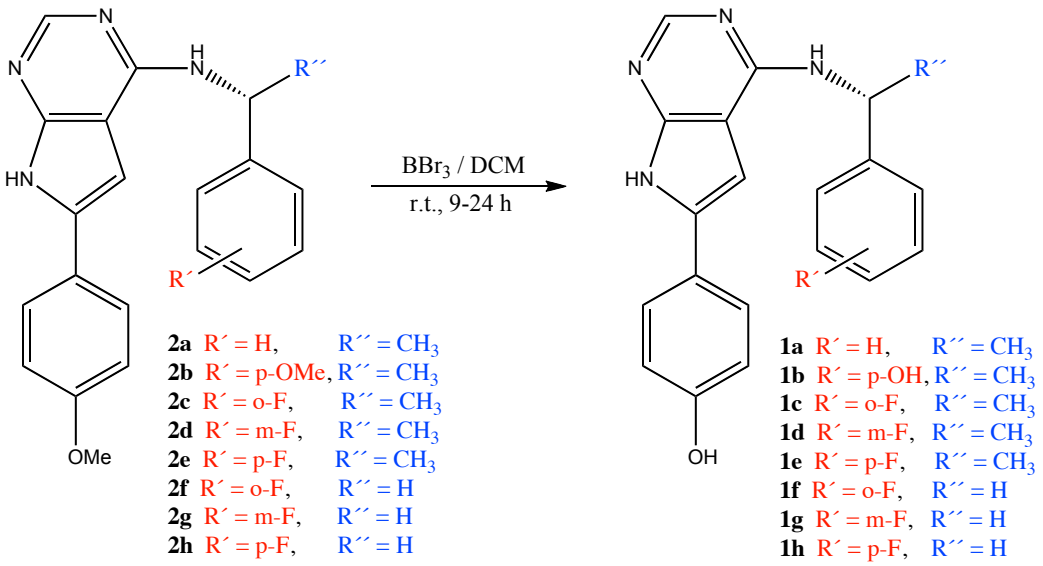

*Scheme 4.5: Deprotection reactions to yield **1a-h**.*

The reaction time exceeded the 5 h reported in the literature,[5] and varied from 9 h up to one day. This however, led to a better yield than reported.

Several of the deprotection reactions were conducted where little, or no product were formed. All of these reactions suffered from small quantities of the starting material (<50 mg). There was a tendency that when the amount of starting material was increased (~200 mg), the reaction went to completion, and the work-up yieled a pure compound.

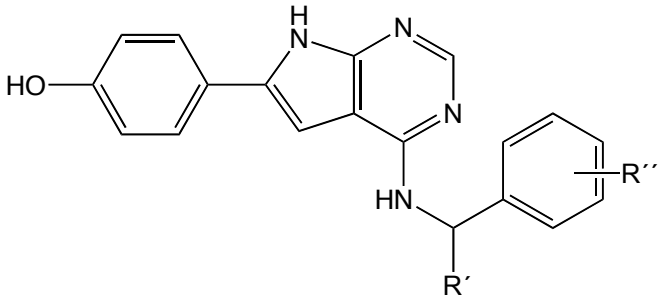

*Figure 4.3: The general structure of compounds **1a-h**.*

*Table 4.2: Yields of reactions to form compounds **1a-h**.*
*Reaction times are given in the brackets. Figure 4.3 shows the general structure of compounds **1a-h**.*

Product:	**R´**	**R´´**	**Isolated yields:**
1a	H	CH_3	68% (24 h)
1b	p-OMe	CH_3	8% (13 h)
1c	o-F	CH_3	48% (18 h)
1d	m-F	CH_3	71% (18 h)
1e	p-F	CH_3	54% (9 h)
1f	o-F	H	56% (24 h)
1g	m-F	H	33% (24 h)
1h	p-F	H	71% (12 h)

The yields of the demethylation reactions to give product **1a-h** are compiled in Table 4.2. There are large differences between the reactions, but the one that stands out, is the yield of product **1b**. The reaction was carried out in the same fashion as the others, but with a larger excess BBr_3 due to the extra site that needed to be demethylated. The work-up was also accomplished the same way, except for the trituration step. Instead, a recrystallization from diethyl ether was done to yield the colorless solid. The diethyl ether was analyzed to see if there was more product, but nothing else than impurities were found. Since this problem was discovered far out in the project, no further efforts towards this reaction were attempted.

An ICP MS analysis was carried out of the chiral para fluorine substituted amine (compound **1e**). This was done to ensure that the rinsing procedure, in all of the reactions, removed various elements (mostly Cl, Br and B). The analysis confirmed that the amount of B ($5*10^{-5}$ mg/g) and Cl ($3*10^{-3}$ mg/g) were very low, and are probably lower because only a fraction of the sample was dissolved (meaning that

while most of the elements present in the sample were dissolved, little of the actual compound was dissolved because of low solubility in water). Only a small amount of the product was used for this analysis (2.7 mg) and the amount of bromide was not detected due to the low quantity present in the sample.

The purity of these compounds was very important since they were intended for biological testing. Therefore, a HPLC method was developed. TEA was first used as a competing agent towards the solid phase in the column to help in the separation, since water alone led to tailing. This method gave two peaks in the chromatogram, and one of them was first thought to be an impurity. However, a recrystallization from ethanol did not remove this "impurity", and it was then thought that deprotonation of the phenol occurred during analysis. When TEA was replaced by trifluoroacetic acid (TFA), the second peak disappeared, which make the theory of deprotonation likely. The pKa of the phenol is probably around 10-11, and it is therefore possible for TEA (pKa 11) to deprotonate to some extent (Scheme 4.6), making this compound appear as a second peak in the chromatogram near the main peak.

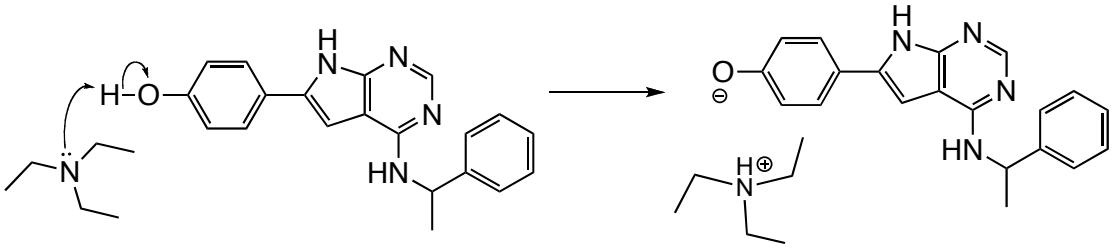

*Scheme 4.6: Reaction that was thought to happen for compounds **1a-h** in the HPLC column when TEA was used in the mobile phase.*

4.5 Structure elucidation of 4-Chloro-6-(4-metoxyphenyl)-7H-pyrrolo-[2,3-*d*]-pyrimidine (3)

Like the precursor **4**, the chemical shift values of both protons and carbons of compound **3** are changed due to change of electron distribution in the molecule. The chlorine atom is a more electronegative group than the hydroxyl group. This ultimately makes the shift values in the molecule to increase.

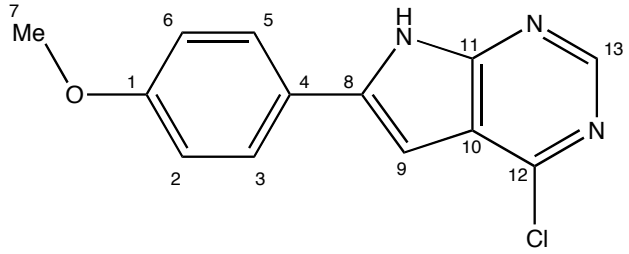

*Figure 4.4: 4-Chloro-6-(4-metoxyphenyl)-7H-pyrrolo-[2,3-d]-pyrimidine (**3**).*

^{1}H and ^{13}C NMR data (Table 4.3 and Table 4.4, respectively) from compound **3** (Figure 4.4) supports this theory (Appendix A.3). By comparing the different shift values of compound **3** and compound **4** (Experimental 8.5), one can see that every value has increased. MS was used to confirm the identity of the synthesized product (Appendix B.3)

*Table 4.3: ^{1}H NMR shifts, coupling constants and $^{1}H,^{1}H$ correlation for compound **3**.*

Position	^{1}H (ppm)	Multiplicity	J (Hz)	COSY (ppm)
2	7.06	d	8.8	7.95
3	7.95	d	8.8	7.06
5	7.95	d	8.8	7.06
6	7.06	d	8.8	7.95
7	3.82	s	-	-
9	6.96	d	2.1	12.90
13	8.55	s	-	-
NH	12.90	s	-	6.96

The signal of the single proton at C-9 in the ^{1}H spectrum is split into a doublet because of a weak coupling to the amine proton in the pyrrole ring. The size of the coupling constant (J=2.1 Hz) is within the expected value for this coupling.[66]

However, the signal of the amine proton in the pyrrole was not split into a doublet and therefore, a corresponding coupling constant was not identified.

*Table 4.4: Overview of ^{13}C-shifts, direct carbon-proton correlation (HSQC) and long-range carbon-proton correlation (HMBC) for compound **3**.*

Position	**^{13}C (ppm)**	**HSQC (ppm)**	**HMBC, couples to position:**
1	160.0	-	-
2	114.5	7.06	1, 4 and 6
3	127.5	7.95	1, 5 and 8
4	122.7		-
5	127.5	7.95	1, 3 and 8
6	114.5	7.06	1, 2 and 4
7	55.3	3.82	1
8	140.5	-	-
9	94.0	6.96	8, 10 and 11
10	118.0	-	-
11	153.0	-	-
12	149.2	-	-
13	150.0	8.55	11 and 12
NH	-	-	8, 9 and 10

The NMR data obtained corresponds well with the data reported by Cai *et al*.[5]

4.6 Characterization of Compounds 2a-h

4.6.1 General features of Compounds 2a-h

Specific rotation was calculated from the observed optical rotation, and every compound showed gave high values (the calculated values of each compound are found in the experimental part).

The ^{13}C shifts in positions 16-21 in the chiral, fluorine substituted compounds (**2c-e**), and positions 15-20 in the achiral compounds (**2f-h**), are doublets. This is due to coupling to fluorine. The large ^{1}J, ^{2}J, ^{3}J and even ^{4}J coupling constants seen in the different ^{13}C NMR spectra (Appendix A.2.3-A.2.8) are within the expected values for C-F couplings.[66] ^{19}F NMR experiment was run both proton- coupled and decoupled. Both are found in Appendixes A.2.3-A.2.8. The proton-coupled experiments uncover in five of the spectra, a higher order coupling pattern. In the proton-decoupled experiments, there are no fluorine impurities to be found in the spectra.

The MS that are recorded of the different compounds show clearly that the mass corresponds to the right compound in each case.

4.6.2 Structural Analysis of (*R*)-6-(4-methoxyphenyl)-*N*-(1-phenylethyl)-7*H*-pyrrolo[2,3-*d*]pyrimidin-4-amine (2a)

The shift values for the protons and carbons in the different positions of compound **2a** (Figure 4.5) are compiled in Table 4.5 and Table 4.6. To assign these shift values, 2D spectra of COSY, HSQC and HMBC were used together with the proton and carbon spectra (Appendix A.2.1). MS was also used to characterize the molecule (Appendix B.2.1).

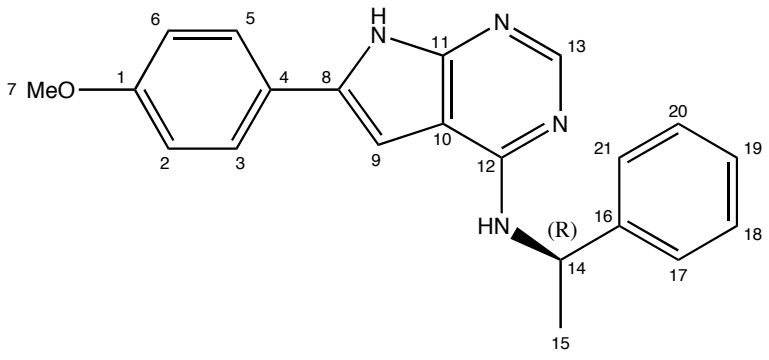

*Figure 4.5: (R)-6-(4-Methoxyphenyl)-N-(1-phenylethyl)-7H-pyrrolo[2,3-d]pyrimidin-4-amine (**2a**).*

*Table 4.5: ^{1}H NMR shifts, coupling constants and ^{1}H,^{1}H correlation for compound **2a**.*

Position	^{1}H (ppm)	Multiplicity	J (Hz)	COSY (ppm)
2	7.02	d	8.6	7.73
3	7.73	d	8.6	7.02
5	7.73	d	8.6	7.02
6	7.02	d	8.6	7.73
7	3.80	s	-	-
9	6.96	d	0.9	11.92
13	8.04	s	-	-
14	5.48-5.52	m	-	1.53, 7.73
15	1.53	d	7.0	5.48-5.52
17	7.42-7.44	m	-	7.30
18	7.30	t	7.6	7.18-7.21, 7.42-7.44
19	7.18-7.21	m	-	7.30
20	7.30	t	7.6	7.18-7.21, 7.42-7.44
21	7.42-7.44	m	-	7.30
Pyrrole-NH	11.92	s	-	6.96
NH	7.73	d	8.6	5.48-5.52

The chemical shift of the aromatic protons in positions 3 and 5 overlap the signal from the amine proton at 7.73 ppm. The signal of the single proton at C-9 in the ^{1}H spectrum is split into a doublet because of a weak coupling to the amine proton in the pyrrole ring. The size of the coupling constant (J=0.9 Hz) is within the expected value for this coupling.[66] However, the signal of the amine proton in the pyrrole was not split into a doublet and therefore, a corresponding coupling constant was not identified.

*Table 4.6: Overview of ^{13}C-shifts, direct carbon-proton correlation (HSQC) and long-range carbon-proton correlation (HMBC) for compound **2a**.*

Position	^{13}C (ppm)	HSQC (ppm)	HMBC, couples to position:
1	158.6	-	-
2	114.4	7.02	1, 4 and 6
3	125.9	7.73	1, 5 and 8
4	124.5	-	-
5	125.9	7.73	1, 3 and 8
6	114.4	7.02	1, 2 and 4
7	55.2	3.80	1

8	133.5	-	-
9	94.6	6.96	8, 10 and 11
10	103.9	-	-
11	151.4	-	-
12	154.8	-	-
13	151.3	8.04	11 and 12
14	50.0	5.48-5.52	15, 16, 17 and 21
15	22.9	1.53	14 and 16
16	145.6	-	-
17	126.0	7.42-7.44	14, 19 and 21
18	128.1	7.30	16 and 20
19	126.7	7.18-7.21	17 and 21
20	128.1	7.20	16 and 18
21	126.0	7.42-7.44	14, 17 and 19
Pyrrole-NH	-	-	8, 9 and 10
NH	-	-	12

4.6.3 Structural Analysis of (*R*)-6-(4-methoxyphenyl)-*N*-(1-(4-methoxyphenyl)ethyl)-7*H*-pyrrolo[2,3-*d*]pyrimidin-4-amine (2b)

The shift values for the protons and carbons in compound **2b** (Figure 4.6) are collected in Table 4.7 and Table 4.8. To assign these shift values, 2D spectra of COSY, HSQC and HMBC were used together with proton and carbon spectra (Appendix A.2.2). MS was used to determine the correct mass of the molecule as a part of the characterization (Appendix B.2.2).

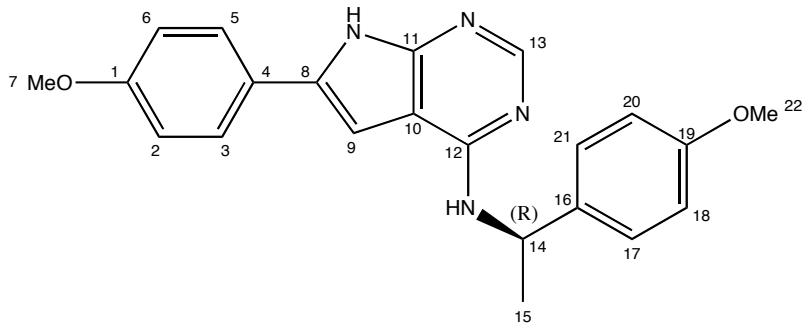

*Figure 4.6: (R)-6-(4-Methoxyphenyl)-N-(1-(4-methoxyphenyl)ethyl)-7H-pyrrolo[2,3-d]pyrimidin-4-amine (**2b**).*

*Table 4.7: ^{1}H NMR shifts, coupling constants and ^{1}H,^{1}H correlation for compound **2b**.*

Position	^{1}H (ppm)	Multiplicity	J (Hz)	COSY (ppm)
2	7.02	d	8.9	7.71
3	7.71	d	8.9	7.02
5	7.71	d	8.9	7.02
6	7.02	d	8.9	7.71
7	3.80	s	-	-
9	6.94	s	-	11.89
13	8.04	s	-	-
14	5.43-5.47	m	-	1.50, 7.64
15	1.50	d	7.0	5.43-5.47
17	7.34	d	8.7	6.86
18	6.86	d	8.8	7.34
20	6.86	d	8.8	7.34
21	7.34	d	8.7	6.86
22	3.71	s	-	-
Pyrrole-NH	11.89	s	-	6.94
NH	7.64	d	8.4	5.43-5.47

The two different methoxy groups were assigned with the aid of long-range correlation spectroscopy (HMBC) due to the similar shift values in proton and carbon spectra. The chiral carbon in position 14 was used as basis for this work since the surrounding carbons also are similar in shift values. The signal of the proton at 6.94 ppm is a singlet and is not fully understood since most of the other similar compounds report a doublet.

*Table 4.8: Overview of ^{13}C-shifts, direct carbon-proton correlation (HSQC) and long-range carbon-proton correlation (HMBC) for compound **2a**.*

Position	^{13}C (ppm)	HSQC (ppm)	HMBC, couples to position:
1	158.6	-	-
2	114.4	7.02	1, 4 and 6
3	125.9	7.71	1, 5 and 8
4	124.5	-	-
5	125.9	7.71	1, 3 and 8
6	114.4	7.02	1, 2 and 4
7	55.2	3.80	1
8	133.4	-	-

9	94.6	6.94	8, 10 and 11
10	103.9	-	-
11	151.3	-	-
12	154.8	-	-
13	151.3	8.04	11 and 12
14	48.0	5.43-5.47	15, 16, 17 and 21
15	22.9	1.50	15 and 16
16	137.5	-	-
17	127.2	7.34	14, 19 and 21
18	113.5	6.86	16, 19 and 20
19	157.9	-	-
20	113.5	6.86	16, 18 and 19
21	127.2	7.34	14, 17 and 19
22	55.0	3.71	19
Pyrrole-NH	-	-	8, 9 and 10
NH	-	-	12

As shown in Table 4.8, carbons in position 11 and 13 have the same shift value. HMBC show correlation between protons in position 9 and 13 to carbon in position 11, while in the HSQC, spectra shows that the proton in position 13 couples directly to the carbon in position 13.

The purity of this compound was determined using high performance liquid chromatography (HPLC, se Experimental 8.7.2 for conditions). Even with the simple work-up, the purity of the derivative **2b** was not compromised (>99%). This was the only compound of the protected molecules that were submitted to biologically testing, and therefore purity had to be determined.

4.6.4 Structural Analysis of (*R*)-*N*-(1-(2-fluorophenyl)ethyl)-6-(4-methoxyphenyl)-7*H*-pyrrolo[2,3-*d*]pyrimidin-4-amine (2c)

The ^{1}H-, ^{13}C and ^{19}F chemical shift values for compound **2c** (Figure 4.7) were interpreted from spectra given in Appendix A.2.3. The spectral data are summarized in Tables 4.9-4.11. To assign proton and carbon shift values, 2D spectra of COSY, HSQC and HMBC were used to aid the elucidation. MS was used to determine the correct mass of the molecule as a part of the characterization (Appendix B.2.3).

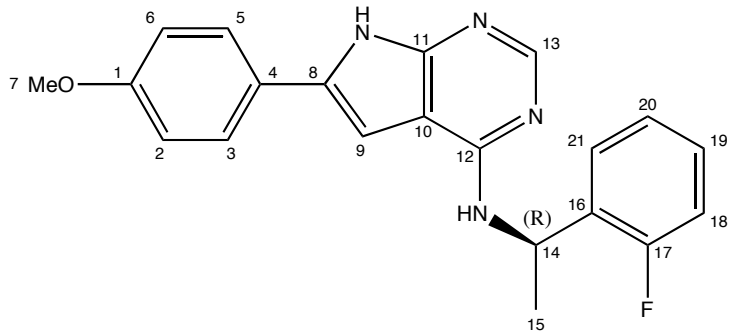

*Figure 4.7: (R)-N-(1-(2-Fluorophenyl)ethyl)-6-(4-methoxyphenyl)-7H-pyrrolo[2,3-d]pyrimidin-4-amine (**2c**).*

*Table 4.9: ^{1}H NMR shifts, coupling constants and ^{1}H,^{1}H correlation for compound **2c**.*

Position	^{1}H (ppm)	Multiplicity	J (Hz)	COSY (ppm)
2	7.03	d	8.8	7.73
3	7.73	d	8.8	7.03
5	7.73	d	8.8	7.03
6	7.03	d	8.8	7.73
7	3.80	s	-	-
9	6.98	d	1.4	11.94
13	8.03	s	-	-
14	5.67-5.74	m	-	1.53, 7.79
15	1.53	d	7.0	5.67-5.74
18	7.11-7.18	m	-	7.23-7.28
19	7.23-7.28	m	-	7.11-7.18
20	7.11-7.18	m	-	7.23-7.28, 7.45-7.49
21	7.45-7.49	m	-	7.11-7.18
Pyrrole-NH	11.94	s	-	6.98
NH	7.79	d	8.0	5.67-5.74

The proton in position 21 shows a splitting pattern in the ^{1}H spectrum that looks like a triplet of doublets. A proton that couples to two other magnetically equivalent protons and a third proton that is different normally causes this. It is therefore not obvious why these splittings are formed. However, an explanation could be that the proton in position 21 couple weakly to protons in positions 14 and 19, which act magnetically equivalent. Then, the strong coupling seen in COSY from proton in position 21 to the proton in position 20 is magnetically unequivalent to the protons in positions 14 and 19, splitting each of the peaks in the triplet. This is a higly unlikely scenario, but when the 2D COSY spectrum is amplified, a weak correlation between the proton in

position 21 and protons in positions 14 and 19 can be spotted. But, as the coupling constants measured in the triplet are larger than for doublet (meaning that coupling to the two equivalent protons, four bonds away, are larger than to the proton adjacent), makes this explanation unlikely.

The signal of the single proton at C-9 in the ^{1}H spectrum is split into a doublet because of a weak coupling to the amine proton in the pyrrole ring. The size of the coupling constant (J=1.4 Hz) is within the expected value for this coupling.[66] However, the signal of the amine proton in the pyrrole was not split into a doublet and therefore, a corresponding coupling constant was not identified.

*Table 4.10: Overview of ^{13}C-shifts, coupling constants for ^{13}C, direct carbon-proton correlation (HSQC) and long-range carbon-proton correlation (HMBC) for compound **2c**.*

Position	^{13}C (ppm)	Multiplicity (J, Hz)	HSQC (ppm)	HMBC, couples to position:
1	158.7	-	-	-
2	114.4	-	7.03	1, 4 and 6
3	125.9	-	7.73	1, 5 and 8
4	124.4	-	-	-
5	125.9	-	7.73	1, 3 and 8
6	114.4	-	7.03	1, 2 and 4
7	55.2	-	3.80	1
8	133.7	-	-	-
9	94.5	-	6.98	8, 10 and 11
10	104.0	-	-	-
11	151.4	-	-	-
12	154.5	-	-	-
13	151.3	-	8.03	11 and 12
14	43.2	-	5.67-5.74	15 and 16
15	21.9	-	1.53	14 and 16
16	132.5	d (14.1)	-	-
17	159.6	d (243.5)	-	-
18	115.1	d (22.1)	7.15-7.18	16 and 20
19	128.3	d (8.0)	7.23-7.28	17 and 21
20	124.3	d (3.0)	7.11-7.13	16 and 18
21	127.1	d (5.0)	7.45-7.49	17 and 19
Pyrrole-NH	-	-	-	8, 9 and 10
NH	-	-	-	12

*Table 4.11: ^{19}F NMR data and coupling constants for compound **2c**.*

Position	^{19}F (ppm)	Multiplicity
17	-119.2	s

The result from the ^{19}F NMR spectrum is a singlet, which is an unexpected outcome from this analysis. One would predict a multiplet, reflecting the surrounding protons.

4.6.5 Structural Analysis of (*R*)-*N*-(1-(3-fluorophenyl)ethyl)-6-(4-methoxyphenyl)-7*H*-pyrrolo[2,3-*d*]pyrimidin-4-amine (2d)

The information extracted from the spectra (Appendix A.2.4) was used to verify the structural identity of compound **2d** (Figure 4.8), and is given in Tables 4.12-4.14. An assignment of protons and carbons was aided by 2D spectra (COSY, HSQC and HMBC) together with proton and carbon spectra (Appendix A.2.4). MS was used to determine the correct mass of the molecule as a part of the characterization (Appendix B.2.4).

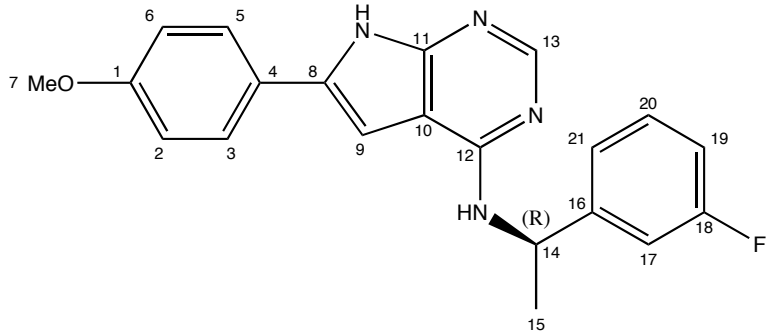

*Figure 4.8: (R)-N-(1-(3-Fluorophenyl)ethyl)-6-(4-methoxyphenyl)-7H-pyrrolo[2,3-d]pyrimidin-4-amine (**2d**).*

*Table 4.12: ^{1}H NMR shifts, coupling constants and $^{1}H,^{1}H$ correlation for compound **2d**.*

Position	^{1}H (ppm)	Multiplicity	J (Hz)	COSY (ppm)
2	7.02	d	8.8	7.73
3	7.73	d	8.8	7.02
5	7.73	d	8.8	7.02
6	7.02	d	8.8	7.73
7	3.80	s	-	-
9	6.94	d	1.8	11.94
13	8.04	s	-	-

14	5.45-5.53	m	-	1.53, 7.76
15	1.53	d	7.0	5.45-5.53
17	7.22-7.24	m	-	6.99-7.00
19	6.99-7.00	m	-	7.22-7.24, 7.32-7.37
20	7.32-7.37	m	-	6.99-7.00, 7.25-7.27
21	7.25-7.27	m	-	7.32-7.37
Pyrrole-NH	11.94	s	-	6.94
NH	7.76	d	8.2	5.45-5.53

The signal of the single proton at C-9 in the ^{1}H spectrum is split into a doublet because of a weak coupling to the amine proton in the pyrrole ring. The size of the coupling constant (J=1.8 Hz) is within the expected value for this coupling.[66] However, the signal of the amine proton in the pyrrole was not split into a doublet and therefore, a corresponding coupling constant was not identified.

*Table 4.13: Overview of ^{13}C-shifts, coupling constants for ^{13}C, direct carbon-proton correlation (HSQC) and long-range carbon-proton correlation (HMBC) for compound **2d**.*

Position	**^{13}C (ppm)**	**Multiplicity (J, Hz)**	**HSQC (ppm)**	**HMBC, couples to position:**
1	158.7	-	-	-
2	114.5	-	7.02	1, 4 and 6
3	126.0	-	7.73	1, 5 and 8
4	124.5	-	-	-
5	126.0	-	7.73	1, 3 and 8
6	114.5	-	7.02	1, 2 and 4
7	55.2	-	3.80	1
8	133.7	-	-	-
9	94.5	-	6.94	8, 10 and 11
10	103.9	-	-	-
11	151.4	-	-	-
12	154.7	-	-	-
13	151.3	-	8.04	11 and 12
14	48.4	-	5.45-5.53	15 and 16
15	22.8	-	1.53	14 and 16
16	148.9	d (28.2)	-	-
17	112.7	d (21.1)	7.22-7.24	21
18	162.3	d (242.4)	-	-
19	113.2	d (21.1)	6.99-7.00	21
20	130.1	d (9.1)	7.32-7.37	16 and 18

21	122.2	d (3.0)	7.25-7.27	17 and 19
Pyrrole-NH	-	-	-	8, 9 and 10
NH	-	-	-	12

*Table 4.14: ^{19}F NMR data and coupling constants for compound **2d**.*

Position	**^{19}F (ppm)**	**Multiplicity**
18	-113.0	m

The ^{19}F NMR proton coupled experiment was carried out to see if any coupling constants were found that corresponded to the coupling constants found in the ^{1}H spectrum. However, the coupling pattern turned out to be of higher order and therefore to difficult to elucidate. The ^{19}F NMR proton decoupled experiment was performed to find if there were any fluorine impurities in the sample since this is a very fluorine-sensitive detection method.

4.6.6 Structural Analysis of (*R*)-*N*-(1-(4-fluorophenyl)ethyl)-6-(4-methoxyphenyl)-7*H*-pyrrolo[2,3-*d*]pyrimidin-4-amine (2e)

The shift values for the ^{1}H-, ^{13}C- and the ^{19}F spectra for compound **2e** (Figure 4.9), are collected in Table 4.15, Table 4.16 and Table 4.17. 2D spectra of COSY, HSQC and HMBC were used together with proton and carbon spectra to assign these values (Appendix A.2.5). MS was also used to characterize the molecule (Appendix B.2.5).

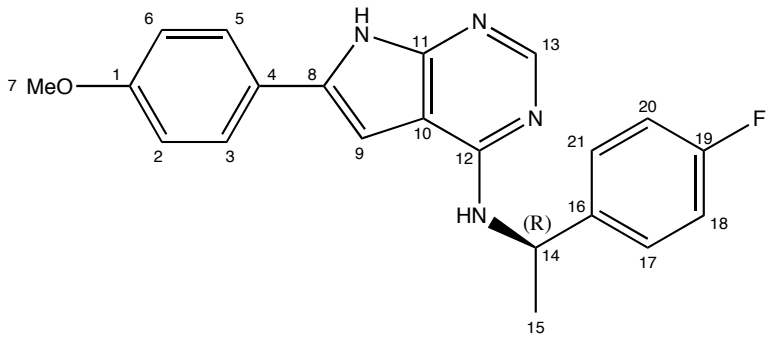

*Figure 4.9: (R)-N-(1-(4-Fluorophenyl)ethyl)-6-(4-methoxyphenyl)-7H-pyrrolo[2,3-d]pyrimidin-4-amine (**2e**)*

*Table 4.15: ^{1}H NMR shifts, coupling constants and ^{1}H,^{1}H correlation for compound **2e**.*

Position	^{1}H (ppm)	Multiplicity	J (Hz)	COSY (ppm)
2	7.02	d	8.6	7.72
3	7.72	d	8.6	7.02
5	7.72	d	8.6	7.02
6	7.02	d	8.6	7.72
7	3.80	s	-	-
9	6.94	s	-	11.93
13	8.04	s	-	-
14	5.47-5.50	m	-	1.52, 7.72
15	1.52	d	6.9	5.47-5.50
17	7.44-7.48	m	-	7.12
18	7.12	t	8.8	7.44-7.48
20	7.12	t	8.8	7.44-7.48
21	7.44-7.48	m	-	7.12
Pyrrole-NH	11.93	s	-	6.94
NH	7.72	d	-	5.47-5.50

The chemical shifts of the aromatic protons in positions 3 and 5 overlap the amine proton signal at 7.72 ppm. The triplet at 7.12 ppm is most likely a result of coupling between the neighboring protons and the fluorine atom. A difference in the ^{1}H spectrum, in comparison to compounds **2a-d**, was the shift value at 6.94 ppm that was a singlet and not the usual doublet due to coupling to the pyrrole amine.

*Table 4.16: Overview of ^{13}C-shifts, coupling constants for ^{13}C, direct carbon-proton correlation (HSQC) and long-range carbon-proton correlation (HMBC) for compound **2e**.*

Position	^{13}C (ppm)	Multiplicity (J, Hz)	HSQC (ppm)	HMBC, couples to position:
1	158.7	-	-	-
2	114.4	-	7.02	1, 4 and 6
3	125.9	-	7.72	1, 5 and 8
4	124.5	-	-	-
5	125.9	-	7.72	1, 3 and 8
6	114.4	-	7.02	1, 2 and 4
7	55.2	-	3.80	1
8	133.6	-	-	-
9	94.5	-	6.94	8, 10 and 11
10	103.9	-	-	-

11	151.4	-	-	-
12	154.7	-	-	-
13	151.3	-	8.04	11 and 12
14	48.1	-	5.47-5.50	15, 16, 17 and 21
15	22.9	-	1.52	14 and 16
16	141.8	d (3.0)	-	-
17	127.9	d (8.0)	7.44-7.48	14, 19 and 21
18	114.8	d (22.1)	7.12	16, 19 and 20
19	160.9	d (241.4)	-	-
20	114.8	d (22.1)	7.12	16, 18 and 19
21	127.9	d (8.0)	7.44-7.48	14, 17 and 19
Pyrrole-NH	-	-	-	8, 9 and 10
NH	-	-	-	12 and 14

*Table 4.17: ^{19}F NMR data and coupling constants for compound **2e**.*

Position	**^{19}F (ppm)**	**Multiplicity**
19	-116.2	m

The ^{19}F NMR proton coupled experiment was carried out to see if any coupling constants were found that corresponded to the coupling constants found in the ^{1}H spectrum. The coupling pattern turned out symmetrical, but the since the pattern was of higher order it was difficult to find a probable explanation. The ^{19}F NMR proton decoupled experiment was performed to find if there were any fluorine impurities in the sample since this is a very fluorine-sensitive detection method.

4.6.7 Structural Analysis of *N*-(2-fluorobenzyl)-6-(4-methoxyphenyl)-7*H*-pyrrolo[2,3-*d*]pyrimidin-4-amine (2f)

The chemical shift values for the protons, carbons and the fluorine for compound **2f** (Figure 4.10) are collected in Tables 4.18-4.20. To assign these shift values, 2D spectra of COSY, HSQC and HMBC were used in the process, with proton and carbon spectra (Appendix A.2.6). MS was used to determine the correct mass of the molecule as a part of the characterization (Appendix B.2.6).

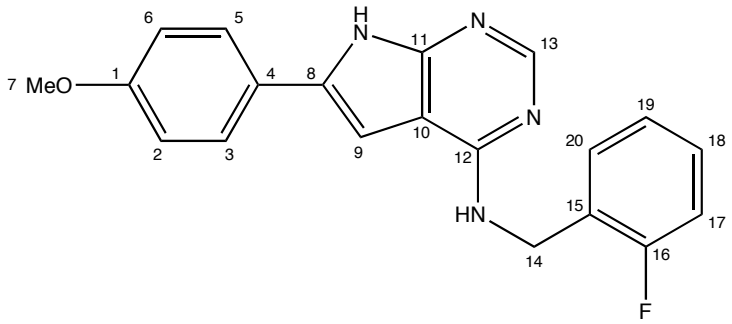

*Figure 4.10: N-(2-Fluorobenzyl)-6-(4-methoxyphenyl)-7H-pyrrolo[2,3-d]pyrimidin-4-amine (**2f**).*

*Table 4.18: ^{1}H NMR shifts, coupling constants and $^{1}H,^{1}H$ correlation for compound **2f**.*

Position	^{1}H (ppm)	Multiplicity	J (Hz)	COSY (ppm)
2	7.02	d	8.7	7.72
3	7.72	d	8.7	7.02
5	7.72	d	8.7	7.02
6	7.02	d	8.7	7.72
7	3.79	s	-	-
9	6.88	d	1.8	11.98
13	8.10	s	-	-
14	4.77	d	5.8	7.92
17	7.19-7.21	m	-	7.27-7.33
18	7.27-7.33	m	-	7.12-7.17, 7.19-7.21
19	7.12-7.17	m	-	7.27-7.33, 7.38-7.42
20	7.38-7.42	m	-	7.12-7.17
Pyrrole-NH	11.98	s	-	6.88
NH	7.92	t	5.8	4.77

The signal of the single proton at C-9 in the ^{1}H spectrum is split into a doublet because of a weak coupling to the amine proton in the pyrrole ring. The size of the coupling constant (J=1.8 Hz) is within the expected value for this coupling.[66] However, the signal of the amine proton in the pyrrole was not split into a doublet and therefore, a corresponding coupling constant was not identified.

*Table 4.19: Overview of ^{13}C-shifts, coupling constants for ^{13}C, direct carbon-proton correlation (HSQC) and long-range carbon-proton correlation (HMBC) for compound **2f**.*

Position	^{13}C (ppm)	Multiplicity (J, Hz)	HSQC (ppm)	HMBC, couples to position:
1	159.1	-	-	-
2	114.9	-	7.02	1, 4 and 6
3	126.4	-	7.72	1, 5 and 8
4	124.8	-	-	-
5	126.4	-	7.72	1, 3 and 8
6	114.9	-	7.02	1, 2 and 4
7	55.6	-	3.79	1
8	134.2	-	-	-
9	94.7	-	6.88	8, 10 and 11
10	104.4	-	-	-
11	151.8	-	-	-
12	155.8	-	-	-
13	151.8	-	8.10	11 and 12
14	37.4	-	4.77	12, 15 and 20
15	127.3	d (15.1)	-	-
16	160.6	d (244.5)	-	-
17	115.4	d (21.1)	7.19-7.21	19
18	129.1	d (8.0)	7.27-7.33	16 and 20
19	124.7	d (3.0)	7.12-7.17	15 and 17
20	129.8	d (5.0)	7.38-7.42	14, 16, and 18
Pyrrole-NH	-	-	-	8, 9 and 10
NH	-	-	-	12

The chemical shift of carbons in positions 11 and 13 overlap in the ^{13}C spectrum, and assignment were aided by HMBC and HSQC.

*Table 4.20: ^{19}F NMR data and coupling constants for compound **2f**.*

Position	^{19}F (ppm)	Multiplicity
16	-118.5	m

The ^{19}F NMR proton coupled experiment was carried out to see if any coupling constants were found that corresponded to the coupling constants found in the ^{1}H spectrum. However, the coupling pattern turned out to be of higher order and therefore to difficult to elucidate. The ^{19}F NMR proton decoupled experiment was

performed to find if there were any fluorine impurities in the sample since this is a very fluorine-sensitive detection method.

4.6.8 Structural Analysis of *N*-(3-fluorobenzyl)-6-(4-methoxyphenyl)-7*H*-pyrrolo[2,3-*d*]pyrimidin-4-amine (2g)

The ^{1}H-, ^{13}C- and ^{19}F shift values and coupling data extracted from spectra (Appendix A.2.7) for compound **2g** (Figure 4.11) are collected in Tables 4.21-4.23. Proton and carbon spectra, as well as 2D spectra of COSY, HSQC and HMBC were used in the assignment of the shift values. MS was used to determine the correct mass of the molecule as a part of the characterization (Appendix B.2.7).

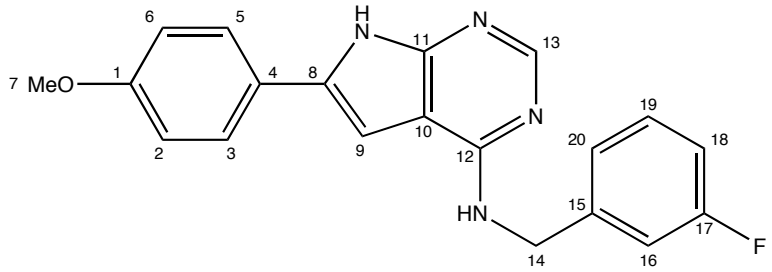

*Figure 4.11: N-(3-Fluorobenzyl)-6-(4-methoxyphenyl)-7H-pyrrolo[2,3-d]pyrimidin-4-amine (**2g**).*

*Table 4.21: ^{1}H NMR shifts, coupling constants and ^{1}H,^{1}H correlation for compound **2g**.*

Position	^{1}H (ppm)	Multiplicity	J (Hz)	COSY (ppm)
2	7.02	d	8.9	7.73
3	7.73	d	8.9	7.02
5	7.73	d	8.9	7.02
6	7.02	d	8.9	7.73
7	3.79	s	-	-
9	6.86	d	2.0	11.99
13	8.11	s	-	-
14	4.75	d	5.9	7.99
16	7.14-7.17	m	-	-
18	7.05-7.08	m	-	7.33-7.39
19	7.33-7.39	m	-	7.05-7.08, 7.19-7.21
20	7.19-7.21	m	-	7.33-7.39
Pyrrole-NH	11.99	s	-	6.86
NH	7.99	t	5.9	4.75

The signal of the single proton at C-9 in the ^{1}H spectrum is split into a doublet because of a weak coupling to the amine proton in the pyrrole ring. The size of the coupling constant (J=2.0 Hz) is within the expected value for this coupling.[66] However, the signal of the amine proton in the pyrrole was not split into a doublet and therefore, a corresponding coupling constant was not identified.

*Table 4.22: Overview of ^{13}C-shifts, coupling constants for ^{13}C, direct carbon-proton correlation (HSQC) and long-range carbon-proton correlation (HMBC) for compound **2g**.*

Position	^{13}C (ppm)	Multiplicity (J, Hz)	HSQC (ppm)	HMBC, couples to position:
1	158.7	-	-	-
2	114.4	-	7.02	1, 4 and 6
3	126.0	-	7.73	1, 5 and 8
4	124.4	-	-	-
5	126.0	-	7.73	1, 3 and 8
6	114.4	-	7.02	1, 2 and 4
7	55.2	-	3.79	1
8	133.8	-	-	-
9	94.2	-	6.86	8, 10 and 11
10	103.9	-	-	-
11	151.4	-	-	-
12	155.4	-	-	-
13	151.4	-	8.11	11 and 12
14	42.7	-	4.75	12, 15, 16 and 20
15	143.6	d (28.2)	-	-
16	113.7	d (21.1)	7.14-7.17	14, 17, 19 and 20
17	162.2	d (242.4)	-	-
18	113.3	d (21.1)	7.05-7.08	20
19	130.2	d (9.1)	7.33-7.39	15 and 17
20	123.1	d (3.0)	7.19-7.21	14, 16, and 18
Pyrrole-NH	-	-	-	8, 9 and 10
NH	-	-	-	12

Carbons in positions 11 and 13 overlap in the ^{13}C spectrum, but they were identified by HMBC and HSQC.

*Table 4.23: ^{19}F NMR data and coupling constants for compound **2g**.*

Position	^{19}F (ppm)	Multiplicity
17	-113.1	m

The ^{19}F NMR proton coupled experiment was carried out to see if any coupling constants were found that corresponded to the coupling constants found in the ^{1}H spectrum. However, the coupling pattern turned out to be of higher order and therefore to difficult to elucidate. The ^{19}F NMR proton decoupled experiment was performed to find if there were any fluorine impurities in the sample since this is a very fluorine-sensitive detection method.

4.6.9 Structural Analysis of *N*-(4-fluorobenzyl)-6-(4-methoxyphenyl)-7*H*-pyrrolo[2,3-*d*]pyrimidin-4-amine (2h)

The chemical shift values and coupling constants for the protons, carbons and the fluorine in the different positions of compound **2h** (Figure 4.12), are collected in Tables 4.24-4.26. To assign proton and carbon shift values, 2D spectra of COSY, HSQC and HMBC were used together with proton and carbon spectra (Appendix A.2.8). MS was also used to characterize the molecule (Appendix B.2.8).

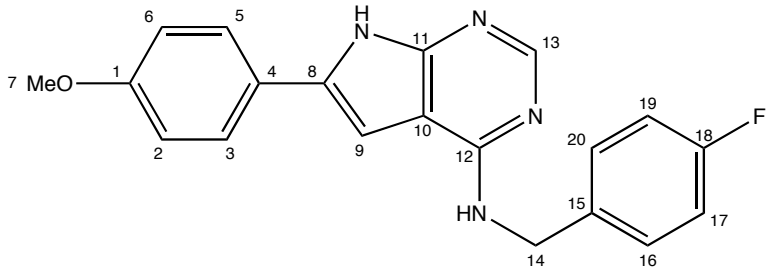

*Figure 4.12: N-(4-Fluorobenzyl)-6-(4-methoxyphenyl)-7H-pyrrolo[2,3-d]pyrimidin-4-amine (**2h**).*

*Table 4.24: ^{1}H NMR shifts, coupling constants and $^{1}H,^{1}H$ correlation for compound **2h**.*

Position	^{1}H (ppm)	Multiplicity	J (Hz)	COSY (ppm)
2	7.02	d	8.7	7.71
3	7.71	d	8.7	7.02
5	7.71	d	8.7	7.02
6	7.02	d	8.7	7.71
7	3.79	s	-	-
9	6.84	d	1.2	11.96
13	8.10	s	-	-
14	4.71	d	5.9	7.40, 7.95
16	7.40	dd	5.6, 8.5	4.71, 7.14

17	7.14	t	8.9	7.40
19	7.14	t	8.9	7.40
20	7.40	dd	5.6, 8.5	4.71, 7.14
Pyrrole-NH	11.96	s	-	6.84
NH	7.95	t	5.9	4.71

The signal of the single proton at C-9 in the ^{1}H spectrum is split into a doublet because of a weak coupling to the amine proton in the pyrrole ring. The size of the coupling constant (J=1.2 Hz) is within the expected value for this coupling.[66] However, the signal of the amine proton in the pyrrole was not split into a doublet and therefore, a corresponding coupling constant was not identified. The protons in positions 16 and 20 appear as a doublet of doublets in the ^{1}H spectrum. A coupling between protons in position 16 and 17, and between 19 and 20 would normally make only a doublet. A coupling from the fluorine to protons at C-16 and C-20 most likely causes this splitting.

*Table 4.25: Overview of ^{13}C-shifts, coupling constants for ^{13}C, direct carbon-proton correlation (HSQC) and long-range carbon-proton correlation (HMBC) for compound **2h**.*

Position	**^{13}C (ppm)**	**Multiplicity (J, Hz)**	**HSQC (ppm)**	**HMBC, couples to position:**
1	158.7	-	-	-
2	114.4	-	7.02	1, 4 and 6
3	126.0	-	7.71	1, 5 and 8
4	124.4	-	-	-
5	126.0	-	7.71	1, 3 and 8
6	114.4	-	7.02	1, 2 and 4
7	55.2	-	3.79	1
8	133.7	-	-	-
9	94.3	-	6.84	8, 10 and 11
10	103.9	-	-	-
11	151.3	-	-	-
12	155.4	-	-	-
13	151.4	-	8.10	11 and 12
14	42.5	-	4.71	12, 15, 16 and 20
15	136.5	d (3.0)	-	-
16	129.1	d (8.0)	7.40	14, 18 and 20
17	114.9	d (21.1)	7.14	15 and 18
18	161.1	d (241.4)	-	-

19	114.9	d (21.1)	7.14	15 and 18
20	129.1	d (8.0)	7.40	14, 16, and 18
Pyrrole-NH	-	-	-	8, 9 and 10
NH	-	-	-	-

*Table 4.26: ^{19}F NMR data and coupling constants for compound **2h**.*

Position	**^{19}F (ppm)**	**Multiplicity**
18	-115.9	m

The ^{19}F NMR proton coupled experiment was carried out to see if any coupling constants were found that corresponded to the coupling constants found in the ^{1}H spectrum. The coupling pattern turned out symmetrical, but the since the pattern was of higher order, a probable explanation was difficult to find. The ^{19}F NMR proton decoupled experiment was performed to find if there were any fluorine impurities in the sample since this is a very fluorine-sensitive detection method.

4.7 Characterization of Compounds 1a-h

4.7.1 General Features of Compounds 1a-h

Specific rotation was calculated from the observed optical rotation. Exceptional high rotation values were observed (although reduced in comparison to the protected compounds **2a-h**).

The NMR elucidation of these compounds showed that some of the carbons were suppressed in the ^{13}C spectra (Appendix A.1.1-A.1.8). This applies especially to carbons in positions 10 and 11. Reasons for this may be dynamic effects and/or the way these molecules orients themself. It was observed that some of the ^{13}C shift values for carbons in the pyrimidine ring were reduced significantly after the demethylation step. Table 4.27 shows a comparison of compound **2e** against compound **1e**. The structural moiety with assigned positions reffered to in Table 4.27 is shown in Figure 4.13.

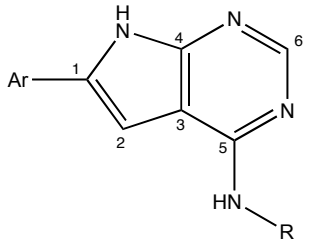

Figure 4.13: The structural moiety most influenced after the demethylation step as detected by ^{13}C NMR.

*Table 4.27: Comparison of some of the ^{13}C-shift values for carbons in the protected molecule **2e** and compound **1e**.*

Position	^{13}C (ppm) Compound 2e	^{13}C (ppm) Compound 1e
1	133.6	137.5
2	94.5	96.6
3	103.9	102.9
4	151.4	148.6
5	154.7	148.6
6	151.3	142.5

This may be due to a possible dimerization in solution, occuring more readily for the deprotected analogue because of hydrogen bonding (Figure 4.14).

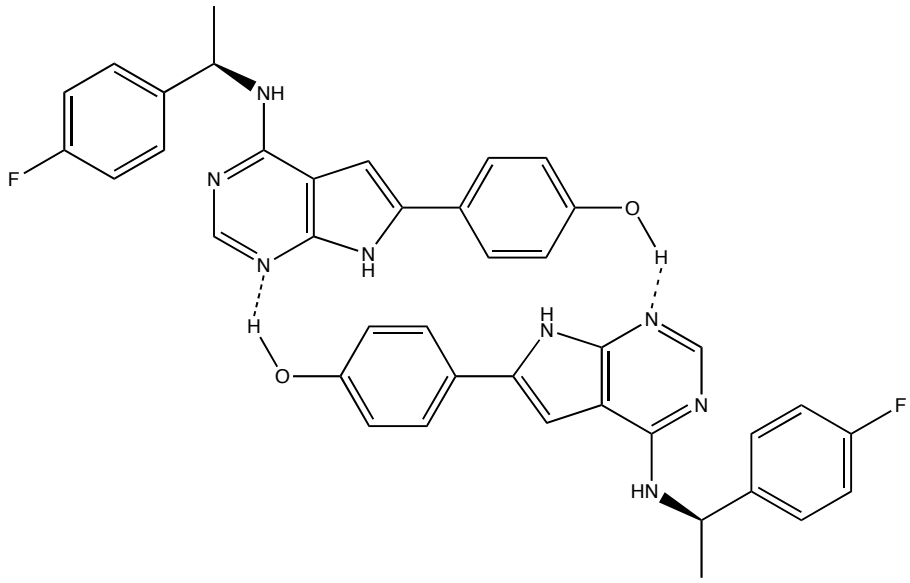

*Figure 4.14: A possible scenario after the demthylation step involving an intermolecular H-bonding of compound **1e**.*

If the proton in the hydroxyl group coordinate to the N1 in the pyrimidine ring, the electron density would be reduced and the nearby carbons would appear with reduced shift values (Figure 4.14). The carbon signal for position 4 would be less affected, because of the pyrrole amine. The ^{13}C shift values of positions 5 and 6 are the most altered carbon signals since they are close to both N1 and N2. Hydrogen bonding to N2 is not showed in this figure, but the shift values indicate that H-bonding may occur at this position instead, or in addition to the H-bonding at N1.

Attempts were made to overcome the dynamic effect in the molecule, by increasing the temperature and/or concentration of the sample while obtaining the ^{13}C spectra. Whereas this did not make the intensities of the peaks any higher in the ^{13}C spectrum, increasing the temperature or the concentration were apparent as the signals in ^{1}H spectrum broadened (Figure 4.15).

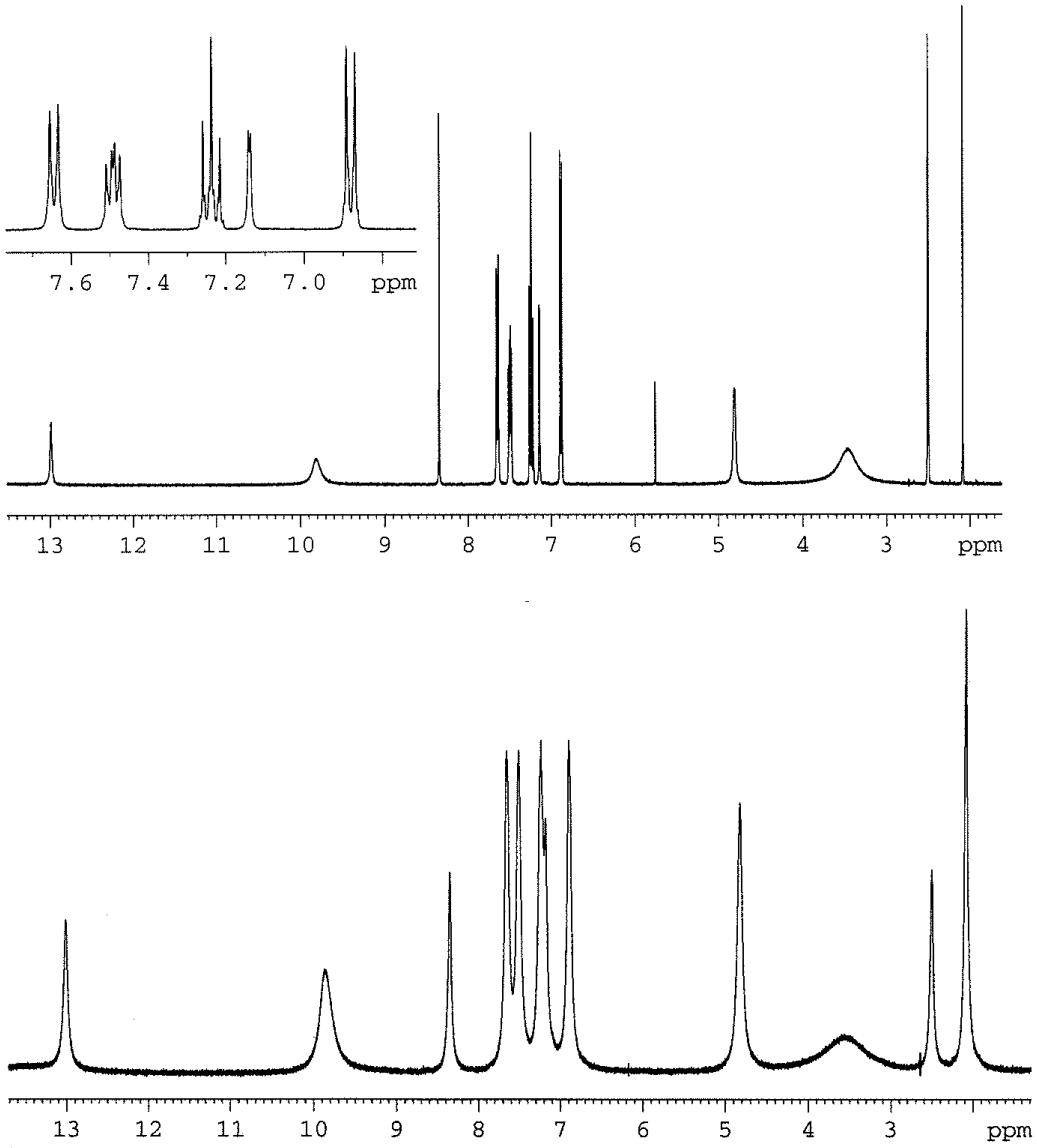

*Figure 4.15: ^{1}H spectrum of compound **1h** showing the dynamic effects present. The top spectrum is obtained at a low concentration (5 mg/mL), and the bottom spectrum is at an increased level of concentration (15 mg/mL).*

Using HMBC spectra, by increasing the line width in the different ^{13}C spectra, the peaks were revealed (although they were still small), and it was possible to obtain evidence that the missing carbons were present in the molecule. ^{19}F NMR yielded only singlets for compounds **1c-h**, which were unexpected seen that most of the analogous compounds **2a-h** yielded multiple peaks before the demethylation. Some kind of spacial arrangement of the molecule, where hydrogen bonding suppress the H-F coupling may be a plausible reason for this observation. There are reported in literature that intramolecularly bonding help stabilize the molecule,[23] but as seen in

Figure 4.16 at the top molecule, this conformation is somewhat strained. Instead, there may be intermolecular hydrogen bonding to fluorine that that causes this.

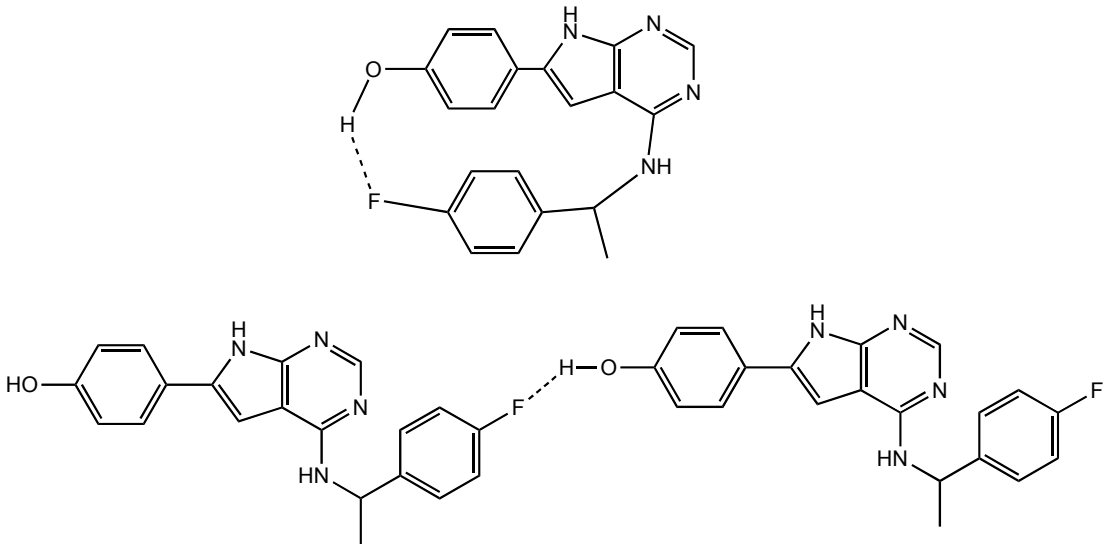

*Figure 4.16: Example of how hydrogen bonding to fluorine in compound **1e** may look like intramolecularly and intermolecularly.*

In the ^{1}H spectra of compounds **1a-h**, the signals of the single protons at C-8 are not split into a doublet, unlike most the corresponding protons in compounds **2a-h**. They are either singlets or overlapped by a multiplet. The reason for this is not found, but if the exchange rate of the amine proton is rapid, this leads to no splitting of the nearby protons.

The MS that are recorded of the different compounds show clearly that the mass corresponds to each compound and thus the right compound synthesized.

4.7.2 Structural Analysis of (*R*)-4-(4-(1-phenylethylamino)-7*H*-pyrrolo[2,3-*d*]pyrimidin-6-yl)phenol (1a)

Interpretation of NMR spectra obtained for compound **1a** (Figure 4.17) are collected in Table 4.28 and Table 4.29. To assign ^{1}H- and ^{13}C shift values, 2D spectra of COSY, HSQC and HMBC were used together with proton and carbon spectra (Appendix A.1.1). MS was also used to characterize the molecule (Appendix B.1.1).

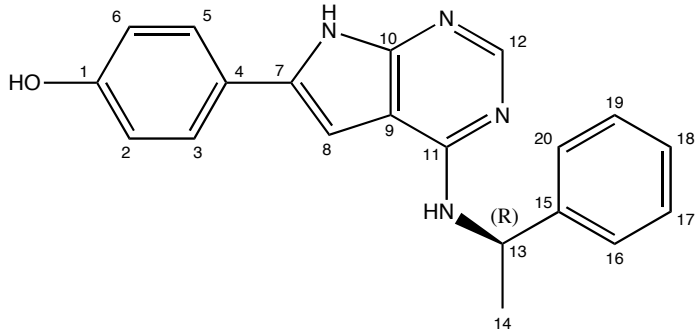

*Figure 4.17: (R)-4-(4-(1-Phenylethylamino)-7H-pyrrolo[2,3-d]pyrimidin-6-yl)phenol (**1a**).*

The purity of compound **1a** (>99%) was determined using HPLC.

*Table 4.28: ^{1}H NMR shifts, coupling constants and $^{1}H,^{1}H$ correlation for compound **1a**.*

Position	**^{1}H (ppm)**	**Multiplicity**	**J (Hz)**	**COSY (ppm)**
2	6.89	d	8.4	7.66
3	7.66	d	8.4	6.89
5	7.66	d	8.4	6.89
6	6.89	d	8.4	7.66
8	7.24	s	-	12.98
12	8.30	s	-	-
13	5.36-5.39	m	-	1.66, 9.55
14	1.66	d	6.5	5.38
16	7.48-7.50	m	-	7.39
17	7.39	t	7.5	7.29-7.32, 7.48-7.50
18	7.29-7.32	m	-	7.39
19	7.39	t	7.5	7.29-7.32, 7.48-7.50
20	7.48-7.50	m	-	7.39
OH	9.83	br	-	-
Pyrrole-NH	12.98	s	-	7.24
NH	9.55	br	-	5.38

*Table 4.29: Overview of ^{13}C-shifts, direct carbon-proton correlation (HSQC) and long-range carbon-proton correlation (HMBC) for compound **1a**.*

Position	^{13}C (ppm)	HSQC (ppm)	HMBC, couples to position:
1	158.0	-	-
2	116.0	6.89	1, 4 and 6
3	126.7	7.66	1, 5 and 7
4	121.2	-	-
5	126.7	7.66	1, 3 and 7
6	116.0	6.89	1, 2 and 4
7	137.6	-	-
8	96.6	7.24	7
9	102.9	-	-
10	148.8	-	-
11	148.8	-	-
12	142.3	8.30	10 and 11
13	50.9	5.38	-
14	22.3	1.66	13 and 15
15	141.9	-	-
16	126.1	7.48-7.50	13, 16 and 20
17	128.6	7.39	15 and 19
18	127.5	7.29-7.32	16 and 20
19	128.6	7.39	15 and 17
20	126.1	7.48-7.50	13, 16 and 18
OH	-	-	-
Pyrrole-NH	-	-	7 and 9
NH	-	-	-

The amine proton does not couple long range to any carbons, as observed with the protected analog **2a** (see Table 4.5).

4.7.3 Structural Analysis of (*R*)-4-(1-(6-(4-hydroxyphenyl)-7*H*-pyrrolo[2,3-*d*]pyrimidin-4-ylamino)ethyl)phenol (1b)

The structure elucidation of compound **1b** (Figure 4.18) is compiled in Table 4.30 and Table 4.31. To assign the proton and carbon shift values, 2D spectra of COSY, HSQC and HMBC were used together with the proton and carbon spectra (Appendix A.1.2).

MS was used to determine the correct mass of the molecule as a part of the characterization (Appendix B.1.2).

The NMR spectra of this compound seemed to be affected by the deprotection in an even stronger way than the rest of the compounds. Four carbons and the amine proton were not found in either of the spectra, and made the structure elucidation incompleted. Since this compound contains two phenolic units, hydrogen bonding and/or dynamic effects may have caused this.

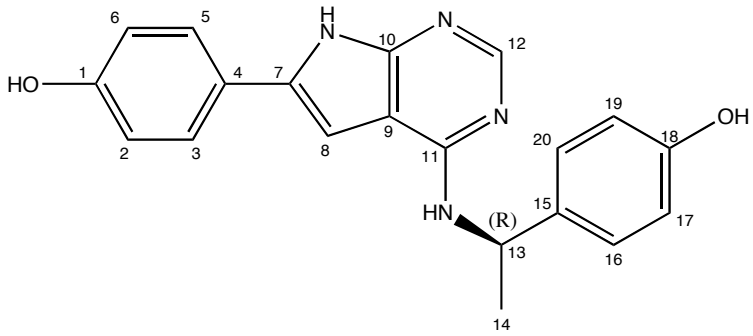

*Figure 4.18: (R)-4-(1-(6-(4-Hydroxyphenyl)-7H-pyrrolo[2,3-d]pyrimidin-4-ylamino)ethyl)phenol (**1b**).*

The purity of compound **1b** (83%) was determined using HPLC.

*Table 4.30: ^{1}H NMR shifts, coupling constants and $^{1}H,^{1}H$ correlation for compound **1b**.*

Position	^{1}H (ppm)	Multiplicity	J (Hz)	COSY (ppm)
2	6.86	d	8.7	7.62
3	7.62	d	8.7	6.86
5	7.62	d	8.7	6.86
6	6.86	d	8.7	7.62
8	7.07	s	-	12.45
12	8.18	s	-	-
13	5.30-5.34	m	-	1.55, 9.45
14	1.55	d	6.6	5.30-5.34
16	7.26	d	8.4	6.72
17	6.72	d	8.4	7.26
19	6.72	d	8.4	7.26
20	7.26	d	8.4	6.72
1-OH	9.76	s	-	-
18-OH	9.35	s	-	-
Pyrrole-NH	12.45	br	-	7.07
NH	-	-	-	-

The proton at 9.35 ppm was first thought to be the amine hydrogen, but since this proton couples to carbons 17 and 19 in the 2D HMBC spectrum, this is more likely to be the hydroxyl group in position 18. There was no other peak that could correspond to the amine hydrogen. It is a possibility that the amine proton is suppressed, if the rate of exchange is so slow that the peak becomes broad enough to disappear in the baseline.

*Table 4.31: Overview of ^{13}C-shifts, direct carbon-proton correlation (HSQC) and long-range carbon-proton correlation (HMBC) for compound **1b**.*

Position	**^{13}C (ppm)**	**HSQC (ppm)**	**HMBC, couples to position:**
1	157.8	-	-
2	115.8	6.86	1, 4 and 6
3	126.4	7.62	1, 5 and 7
4	121.8	-	-
5	126.4	7.62	1, 3 and 7
6	115.8	6.86	1, 2 and 4
7	136.2	-	-
8	95.1	7.07	-
9	-	-	-
10	-	-	-
11	-	-	-
12	-	8.18	-
13	48.9	5.30-5.34	14, 16 and 20
14	22.0	1.55	13 and 15
15	133.1	-	-
16	127.2	7.26	13, 18 and 20
17	115.1	6.72	15, 18 and 19
18	156.4	-	-
19	115.1	6.72	15, 17 and 18
20	127.2	7.26	13, 16 and 18
1-OH	-	-	2 and 6
18-OH	-	-	17 and 19
Pyrrole-NH	-	-	-
NH	-	-	-

None of the spectra showed signals from the carbons corresponding to 9, 10, 11 or 12. The ^{13}C spectrum shows only signals from positions 1, 2 and 6, 3 and 5, 13 (barely), 14, 16 and 20, 17 and 19, and 18. The rest was found using 2D spectra.

4.7.4 Structural Analysis of (*R*)-4-(4-(1-(2-fluorophenyl)ethylamino)-7*H*-pyrrolo[2,3-*d*]pyrimidin-6-yl)phenol (1c)

The chemical shift values and coupling constants for the protons, carbons and the fluorine for compound **1c** (Figure 4.19) were extracted from the NMR spectra (Appendix A.1.3). This is given in Tables 4.32-4.34. 2D spectra of COSY, HSQC and HMBC were used together with proton and carbon spectra to assign these values. MS was used to determine the correct mass of the molecule as a part of the characterization (Appendix B.1.3).

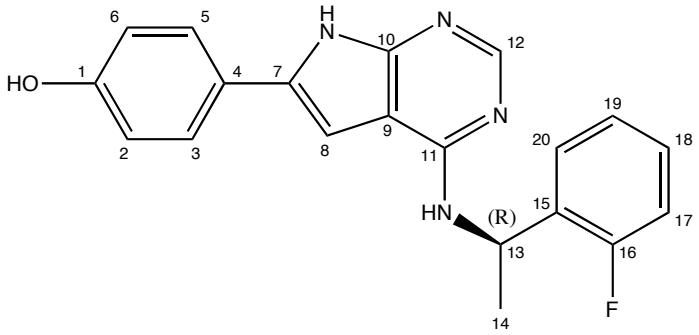

*Figure 4.19: (R)-4-(4-(1-(2-Fluorophenyl)ethylamino)-7H-pyrrolo[2,3-d]pyrimidin-6-yl)phenol (**1c**).*

The purity of compound **1c** (>99%) was determined using HPLC.

*Table 4.32: ^{1}H NMR shifts, coupling constants and $^{1}H,^{1}H$ correlation for compound **1c**.*

Position	^{1}H (ppm)	Multiplicity	J (Hz)	COSY (ppm)
2	6.88	d	8.7	7.64
3	7.64	d	8.7	6.88
5	7.64	d	8.7	6.88
6	6.88	d	8.7	7.64
8	7.26	s	-	12.98
12	8.31	s	-	-
13	5.55-5.58	m	-	-
14	1.65	d	6.7	5.55-5.58
17	7.19-7.24	m	-	7.48
18	7.48	t	7.4	7.19-7.24
19	7.19-7.24	m	-	7.48, 7.34-7.39
20	7.34-7.39	m	-	7.19-7.24
OH	9.83	br	-	-
Pyrrole-NH	12.98	s	-	7.26
NH	9.51	br	-	5.55-5.58

*Table 4.33: Overview of ^{13}C-shifts, coupling constants for ^{13}C, direct carbon-proton correlation (HSQC) and long-range carbon-proton correlation (HMBC) for compound **1c**.*

Position	^{13}C (ppm)	Multiplicity (J, Hz)	HSQC (ppm)	HMBC, couples to position:
1	158.0	-	-	-
2	116.0	-	6.88	1, 4 and 6
3	126.8	-	7.64	1, 5 and 7
4	121.2	-	-	-
5	126.8	-	7.64	1, 3 and 7
6	116.0	-	6.88	1, 2 and 4
7	137.6	-	-	-
8	96.5	-	7.26	-
9	103.0	-	-	-
10	147.5	-	-	-
11	149.2	-	-	-
12	142.7	-	8.31	10 and 11
13	45.8	-	5.55-5.58	-
14	20.8	-	1.65	13 and 15
15	128.8	d (13.1)	-	-
16	160.8	d (244.5)	-	-
17	115.7	d (21.1)	7.19-7.24	16 and 19
18	126.8	-	7.48	16 and 20
19	124.7	-	7.19-7.24	15, 16 and 17
20	129.7	d (8.0)	7.34-7.39	16 and 18
OH	-	-	-	-
Pyrrole-NH	-	-	-	-
NH	-	-	-	-

The carbons in position 15, 16, 17 and 20 appears as doublets, due to coupling to fluorine. The ^{1}J, ^{2}J and ^{3}J coupling constants seen in the ^{13}C NMR spectrum (Appendix A.1.3) are within the expected values for C-F couplings.[66] Signals from carbons in positions 3 and 5 overlap the signal for the carbon in position 18, which made it difficult to extract the coupling constant.

*Table 4.34: ^{19}F NMR data and coupling constants for compound **1c**.*

Position	^{19}F (ppm)	Multiplicity
16	-116.5	s

There was only a signal appearing as a singlet in the ^{19}F NMR proton-coupled experiment. The ^{19}F NMR proton decoupled experiment was performed to find if there were any fluorine impurities in the sample since this is a very fluorine-sensitive detection method.

4.7.5 Structural Analysis of (*R*)-4-(4-(1-(3-fluorophenyl)ethylamino)-7*H*-pyrrolo[2,3-*d*]pyrimidin-6-yl)phenol (1d)

The chemical shift values for the protons, carbons and the fluorine for compound **1c** (Figure 4.20), are gathered in Tables 4.35-4.37. The spectra are found in Appendix A.1.4. The assignment of protons and carbons were aided by 2D spectra (COSY, HSQC and HMBC) together with proton and carbon spectra. MS was used to determine the correct mass of the molecule as a part of the characterization (Appendix B.1.4).

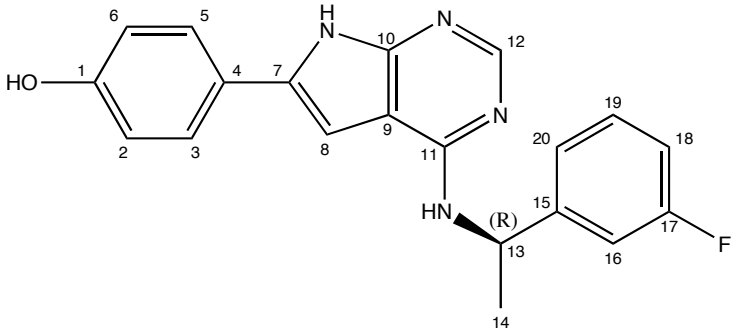

*Figure 4.20: (R)-4-(4-(1-(3-Fluorophenyl)ethylamino)-7H-pyrrolo[2,3-d]pyrimidin-6-yl)phenol (**1d**).*

The purity of compound **1d** (>99%) was determined using HPLC.

*Table 4.35: ^{1}H NMR shifts, coupling constants and $^{1}H,^{1}H$ correlation for compound **1d**.*

Position	^{1}H (ppm)	Multiplicity	J (Hz)	COSY (ppm)
2	6.89	d	8.7	7.66
3	7.66	d	8.7	6.89
5	7.66	d	8.7	6.89
6	6.89	d	8.7	7.66
8	7.23	s	-	12.95
12	8.29	s	-	-
13	5.43-5.46	m	-	1.65, 9.52
14	1.65	d	6.8	5.43-5.46

16	7.33-7.38	m	-	-
18	7.11-7.15	m	-	7.40-7.46
19	7.40-7.46	m	-	7.11-7.15, 7.33-7.38
20	7.33-7.38	m	-	7.40-7.46
OH	9.84	br	-	-
Pyrrole-NH	12.95	s	-	7.23
NH	9.52	br	-	5.43-5.46

Like in ^{1}H spectrum of compound **2c**, there is also for compound **1d** a splitting pattern appearing as a triplet of doublets. It is proton in position 18 that forms this pattern, and in this molecule that may be caused by coupling to the magnetically equivalent protons in positions 16 and 20. The splitting is thought to appear because of coupling to the proton in position 19. However, the size of the coupling constants makes this explanation unlikely.

*Table 4.36: Overview of ^{13}C-shifts, coupling constants for ^{13}C, direct carbon-proton correlation (HSQC) and long-range carbon-proton correlation (HMBC) for compound **1d**.*

Position	^{13}C (ppm)	Multiplicity (J, Hz)	HSQC (ppm)	HMBC, couples to position:
1	158.0	-	-	-
2	115.9	-	6.89	1, 4 and 6
3	126.7	-	7.66	1, 5 and 7
4	121.3	-	-	-
5	126.7	-	7.66	1, 3 and 7
6	115.9	-	6.89	1, 2 and 4
7	137.4	-	-	-
8	96.5	-	7.23	7
9	103.0	-	-	-
10	148.3	-	-	-
11	148.3	-	-	-
12	142.8	-	8.29	10 and 11
13	50.4	-	5.43-5.46	-
14	22.3	-	1.65	13 and 15
15	145.3	-	-	-
16	113.2	d (22.1)	7.33-7.38	18 and 20
17	162.2	d (244.5)	-	-
18	114.3	d (21.1)	7.11-7.15	20
19	130.6	d (8.0)	7.40-7.46	15 and 17
20	122.2	-	7.33-7.38	16 and 18

OH	-	-	-	-
Pyrrole-NH	-	-	-	9
NH	-	-	-	-

The carbons in position 16-19 appears as doublets, due to coupling to fluorine. The ^{1}J, ^{2}J and ^{3}J coupling constants seen in the ^{13}C NMR spectrum (Appendix A.1.4) are within the expected values for C-F couplings.[66]

*Table 4.37: ^{19}F NMR data and coupling constants for compound **1d**.*

Position	^{19}F (ppm)	Multiplicity
17	-112.2	s

There was only a signal appearing as a singlet in the ^{19}F NMR proton-coupled experiment. The ^{19}F NMR proton decoupled experiment was performed to find if there were any fluorine impurities in the sample since this is a very fluorine-sensitive detection method.

4.7.6 Structural Analysis of (*R*)-4-(4-(1-(4-fluorophenyl)ethylamino)-7*H*-pyrrolo[2,3-*d*]pyrimidin-6-yl)phenol (1e)

^{1}H-, ^{13}C- and the ^{19}F shift values and coupling data for compound **1e** (Figure 4.21) are collected in Table 4.38, Table 4.39 and Table 4.40. 2D spectra of COSY, HSQC and HMBC were used together with proton and carbon spectra to assign all positions (Appendix A.2.5). MS was used as well in the characterization of the molecule (Appendix B.2.5).

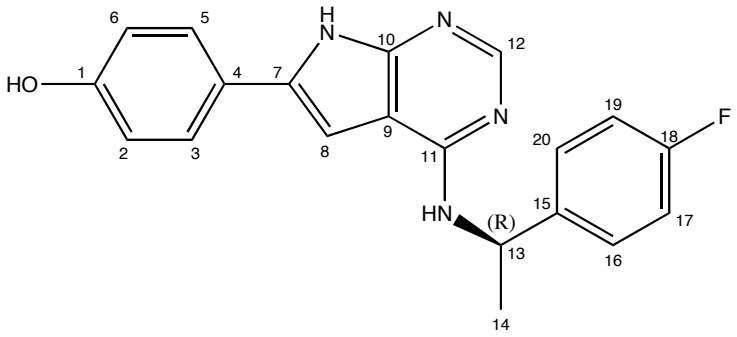

*Figure 4.21: (R)-4-(4-(1-(4-Fluorophenyl)ethylamino)-7H-pyrrolo[2,3-d]pyrimidin-6-yl)phenol (**1e**).*

The purity of compound **1e** (>99%) was determined using HPLC.

*Table 4.38: ^{1}H NMR shifts, coupling constants and ^{1}H,^{1}H correlation for compound **1e**.*

Position	^{1}H (ppm)	Multiplicity	J (Hz)	COSY (ppm)
2	6.89	d	8.7	7.65
3	7.65	d	8.7	6.89
5	7.65	d	8.7	6.89
6	6.89	d	8.7	7.65
8	7.20-7.25	m	-	12.97
12	8.31	s	-	
13	5.38-5.40	m	-	1.65, 9.51
14	1.65	d	6.7	5.38-5.40
16	7.52-7.56	m	-	7.20-7.25
17	7.20-7.25	m	-	7.52-7.56
19	7.20-7.25	m	-	7.52-7.56
20	7.52-7.56	m	-	7.20-7.25
OH	9.82	br	-	-
Pyrrole-NH	12.97	s	-	7.20-7.25
NH	9.51	br	-	5.39-5.40

The proton in position 13 appears as a broad singlet, but is regarded as a multiplet (see Appendix A.1.5). The aromatic protons in positions 17 and 19 overlap the signal from the amine proton in the multiplet reaching from 7.20-7.25 ppm.

*Table 4.39: Overview of ^{13}C-shifts, coupling constants for ^{13}C, direct carbon-proton correlation (HSQC) and long-range carbon-proton correlation (HMBC) for compound **1e**.*

Position	^{13}C (ppm)	Multiplicity (J, Hz)	HSQC (ppm)	HMBC, couples to position:
1	158.0	-	-	-
2	116.0	-	6.89	1, 4 and 6
3	126.7	-	7.65	1, 5 and 7
4	121.3	-	-	-
5	126.7	-	7.65	1, 3 and 7
6	116.0	-	6.89	1, 2 and 4
7	137.5	-	-	-
8	96.6	-	7.20-7.25	7
9	102.9	-	-	-
10	148.6	-	-	-
11	148.6	-	-	-

12	142.5	-	8.31	10 and 11
13	50.2	-	5.38-5.40	-
14	22.4	-	1.65	13 and 15
15	138.2	-	-	-
16	128.2	d (7.0)	7.52-7.56	18 and 20
17	115.4	d (22.1)	7.20-7.25	15, 18 and 19
18	161.5	d (243.4)	-	-
19	115.4	d (22.1)	7.20-7.25	15, 17 and 18
20	128.2	d (7.0)	7.52-7.56	16 and 18
OH	-	-	-	14, 17 and 19
Pyrrole-NH	-	-	-	8, 9 and 10
NH	-	-	-	12 and 14

The carbons in position 16-20 appears as doublets, due to coupling to fluorine. The ^{1}J, ^{2}J and ^{3}J coupling constants seen in the ^{13}C NMR spectrum (Appendix A.1.5) are within the expected values for C-F couplings.[66]

*Table 4.40: ^{19}F NMR data and coupling constants for compound **1e**.*

Position	^{19}F (ppm)	Multiplicity
18	-114.6	s

There was only a signal appearing as a singlet in the ^{19}F NMR proton-coupled experiment. The ^{19}F NMR proton decoupled experiment was performed to find if there were any fluorine impurities in the sample since this is a very fluorine-sensitive detection method.

4.7.7 Structural Analysis of 4-(4-(2-fluorobenzylamino)-7*H*-pyrrolo[2,3-*d*]pyrimidin-6-yl)phenol (1f)

The shift values and coupling constants for protons, carbons and the fluorine in compound **1f** (Figure 4.22) are collected in Tables 4.41-4.43. To assign the proton and carbon shift values, 2D spectra of COSY, HSQC and HMBC were used together with proton and carbon spectra (Appendix A.1.6). MS was used to determine the correct mass of the molecule as a part of the characterization (Appendix B.1.6).

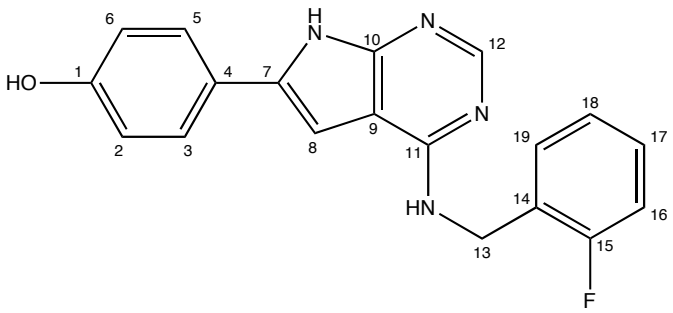

*Figure 4.22: 4-(4-(2-Fluorobenzylamino)-7H-pyrrolo[2,3-d]pyrimidin-6-yl)phenol (**1f**).*

The purity of compound **1f** (98%) was determined using HPLC.

*Table 4.41: ^{1}H NMR shifts, coupling constants and $^{1}H,^{1}H$ correlation for compound **1f**.*

Position	^{1}H (ppm)	Multiplicity	J (Hz)	COSY (ppm)
2	6.88	d	8.7	7.64
3	7.64	d	8.7	6.88
5	7.64	d	8.7	6.88
6	6.88	d	8.7	7.64
8	7.11	s	-	12.94
12	8.35	s	-	-
13	4.86	d	3.5	9.60
16	7.29-7.31	m	-	7.40-7.44
17	7.40-7.44	m	-	7.21-7.27, 7.29-7.31
18	7.21-7.27	m	-	7.40-7.44, 7.45-7.48
19	7.45-7.48	m	-	7.21-7.27
OH	9.82	br	-	-
Pyrrole-NH	12.94	br	-	7.11
NH	9.60	br	-	4.86

Unlike the pyrrolo-amine hydrogens in the other similar compounds, the pyrrolo-amine hydrogen in compound **1f** forms a broad singlet. There are no obvious reasons for this, but normally this is caused by an intermediate exchange rate. This would affect the proton signal at C-8 to appear as a singlet, since it would not be able to couple to the amine proton. This is confirmed in the ^{1}H spectrum, and the proton signal at C-8 appears in this case as a singlet. In contrast, it was observed that the corresponding proton in position 8, in compounds **2f-h**, appear as a doublet, and the pyrrole-amine hydrogens appear as sharp singlets (Tables 4.18, 4.21 and 4.24).

*Table 4.42: Overview of ^{13}C-shifts, coupling constants for ^{13}C, direct carbon-proton correlation (HSQC) and long-range carbon-proton correlation (HMBC) for compound **1f**.*

Position	^{13}C (ppm)	Multiplicity (J, Hz)	HSQC (ppm)	HMBC, couples to position:
1	158.0	-	-	-
2	116.0	-	6.88	1, 4 and 6
3	126.8	-	7.64	1, 5 and 7
4	121.2	-	-	-
5	126.8	-	7.64	1, 3 and 7
6	116.0	-	6.88	1, 2 and 4
7	137.6	-	-	-
8	96.3	-	7.11	7 and 9
9	103.0	-	-	-
10	147.4	-	-	-
11	149.8	-	-	-
12	142.4	-	8.35	10 and 11
13	39.5	-	4.86	14 and 19
14	123.5	d (13.1)	-	-
15	160.4	d (245.5)	-	-
16	115.5	d (21.1)	7.29-7.31	14 and 18
17	130.0	d (7.0)	7.40-7.44	15 and 19
18	124.7	-	7.21-7.27	14 and 16
19	129.6	-	7.45-7.48	15 and 17
OH	-	-	-	-
Pyrrole-NH	-	-	-	-
NH	-	-	-	-

The signal from carbon in position 13 is overlapped by DMSO-d_6, but was identified by HSQC. The carbons in position 14-17 appears as doublets, due to coupling to fluorine. The ^{1}J, ^{2}J and ^{3}J coupling constants seen in the ^{13}C NMR spectrum (Appendix A.1.6) are within the expected values for C-F couplings.[66]

*Table 4.43: ^{19}F NMR data and coupling constants for compound **1f**.*

Position	^{19}F (ppm)	Multiplicity
15	-117.1	s

There was only a signal appearing as a singlet in the ^{19}F NMR proton-coupled experiment. The ^{19}F NMR proton decoupled experiment was performed to find if

there were any fluorine impurities in the sample since this is a very fluorine-sensitive detection method.

4.7.8 Structural Analysis of 4-(4-(3-fluorobenzylamino)-7*H*-pyrrolo[2,3-*d*]pyrimidin-6-yl)phenol (1g)

The structural data for compound **1g** (Figure 4.23) is collected in Tables 4.44-4.46. To assign proton and carbon shift values, 2D spectra of COSY, HSQC and HMBC were used together with proton and carbon spectra (Appendix A.1.7). MS was used to determine the correct mass of the molecule as a part of the characterization (Appendix B.1.7).

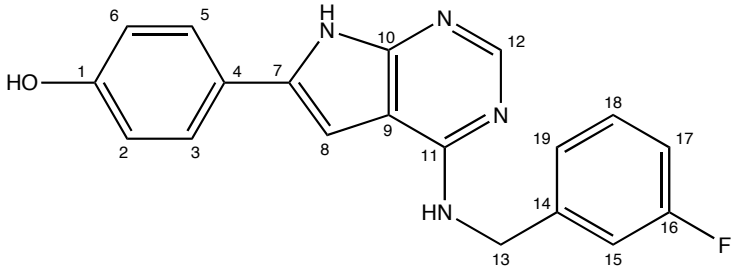

*Figure 4.23: 4-(4-(3-Fluorobenzylamino)-7H-pyrrolo[2,3-d]pyrimidin-6-yl)phenol (**1g**).*

The purity of compound **1g** (>99%) was determined using HPLC.

*Table 4.44: ^{1}H NMR shifts, coupling constants and $^{1}H,^{1}H$ correlation for compound **1g**.*

Position	^{1}H (ppm)	Multiplicity	J (Hz)	COSY (ppm)
2	6.87	d	8.7	7.64
3	7.64	d	8.7	6.87
5	7.64	d	8.7	6.87
6	6.87	d	8.7	7.64
8	7.04	s	-	12.73
12	8.29	s	-	-
13	4.82	d	4.9	9.31
15	7.25-7.27	m	-	-
17	7.12-7.17	m	-	7.40-7.46
18	7.40-7.46	m	-	7.12-7.17, 7.25-7.27
19	7.25-7.27	m	-	7.40-7.46
OH	9.78	s	-	-
Pyrrole-NH	12.73	br	-	7.04
NH	9.31	br	-	4.82

The pyrrolo-amine proton in this molecule (compound **1g**) forms a broad singlet similar to compound **1f**. The reason for this is not clear, but similar to compound **1f**, the amine proton is thought to be exchanged at an intermediate rate, and thus make a broad singlet.

*Table 4.45: Overview of ^{13}C-shifts, coupling constants for ^{13}C, direct carbon-proton correlation (HSQC) and long-range carbon-proton correlation (HMBC) for compound **1g**.*

Position	^{13}C (ppm)	Multiplicity (J, Hz)	HSQC (ppm)	HMBC, couples to position:
1	158.0	-	-	-
2	116.0	-	6.87	1, 4 and 6
3	126.8	-	7.64	1, 5 and 7
4	121.2	-	-	-
5	126.8	-	7.64	1, 3 and 7
6	116.0	-	6.87	1, 2 and 4
7	137.7	-	-	-
8	96.4	-	7.04	7, 9 and 10
9	103.0	-	-	-
10	147.4	-	-	-
11	149.6	-	-	-
12	142.2	-	8.29	10 and 11
13	44.3	-	4.82	14, 15 and 19
14	139.6	-	-	-
15	114.4	d (21.1)	7.25-7.27	13, 17 and 19
16	161.1	d (243.4)	-	-
17	114.5	d (21.1)	7.12-7.17	15, 16 and 19
18	130.7	d (8.0)	7.40-7.46	14 and 16
19	123.5	-	7.25-7.27	13, 15 and 17
OH	-	-	-	2 and 6
Pyrrole-NH	-	-	-	-
NH	-	-	-	-

The carbons in position 15-18 appears as doublets, due to coupling to fluorine. The ^{1}J, ^{2}J and ^{3}J coupling constants seen in the ^{13}C NMR spectrum (Appendix A.1.7) are within the expected values for C-F couplings.[66]

*Table 4.46: ^{19}F NMR data and coupling constants for compound **1g**.*

Position	^{19}F (ppm)	Multiplicity
16	-112.5	s

There was only a signal appearing as a singlet in the ^{19}F NMR proton-coupled experiment. The ^{19}F NMR proton decoupled experiment was performed to find if there were any fluorine impurities in the sample since this is a very fluorine-sensitive detection method.

4.7.9 Structural Analysis of 4-(4-(4-fluorobenzylamino)-7*H*-pyrrolo[2,3-*d*]pyrimidin-6-yl)phenol (1h)

The shift values and coupling data for the protons, carbons and the fluorine for compound **1h** (Figure 4.24), are collected in Tables 4.47-4.49. To assign the proton and carbon shift values, 2D spectra of COSY, HSQC and HMBC were used together with proton and carbon spectra (Appendix A.1.8). MS was also used to characterize the molecule (Appendix B.1.8).

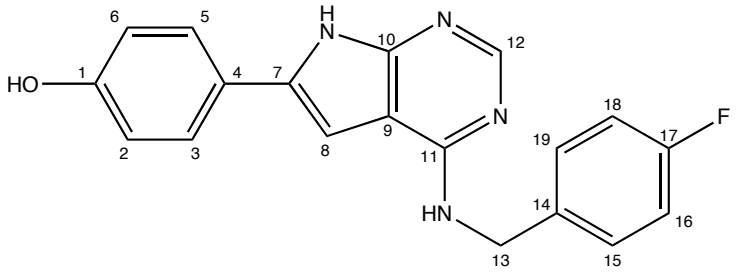

*Figure 4.24: 4-(4-(4-Fluorobenzylamino)-7H-pyrrolo[2,3-d]pyrimidin-6-yl)phenol (**1h**)*

The purity of compound **1h** (98%) was determined using HPLC.

*Table 4.47: ^{1}H NMR shifts, coupling constants and $^{1}H,^{1}H$ correlation for compound **1h**.*

Position	^{1}H (ppm)	Multiplicity	J (Hz)	COSY (ppm)
2	6.88	d	8.7	7.65
3	7.65	d	8.7	6.88
5	7.65	d	8.7	6.88
6	6.88	d	8.7	7.65

8	7.14	d	2.0	13.01
12	8.35	s	-	-
13	4.77	s	-	9.76
15	7.48-7.51	m	-	7.21-7.27
16	7.21-7.27	m	-	7.49
18	7.21-7.27	m	-	7.49
19	7.48.7.51	m	-	7.21-7.27
OH	9.81	br	-	-
Pyrrole-NH	13.01	s	-	7.14
NH	9.76	br	-	4.77

Signals from protons in positions 15 and 19 appear as a doublet of doublets in the ^{1}H spectrum like the similar methylated compound **2h**. A coupling between proton in positions 15 and 16, and between 18 and 19 would normally only make a doublet. The splitting of these peaks was most likely caused by a coupling to fluorine.

*Table 4.48: Overview of ^{13}C-shifts, coupling constants for ^{13}C, direct carbon-proton correlation (HSQC) and long-range carbon-proton correlation (HMBC) for compound **1h**.*

Position	**^{13}C (ppm)**	**Multiplicity (J, Hz)**	**HSQC (ppm)**	**HMBC, couples to position:**
1	158.0	-	-	-
2	116.0	-	6.88	1, 4 and 6
3	126.8	-	7.65	1, 5 and 7
4	121.2	-	-	-
5	126.8	-	7.65	1, 3 and 7
6	116.0	-	6.88	1, 2 and 4
7	137.6	-	-	-
8	96.5	-	7.14	7 and 10
9	102.8	-	-	-
10	147.5	-	-	-
11	149.4	-	-	-
12	142.1	-	8.35	10 and 11
13	44.2	-	4.77	14, 15 and 19
14	132.7	-	-	-
15	129.7	d (8.0)	7.49	13, 17 and 19
16	115.4	d (21.1)	7.21-7.27	14, 17 and 18
17	161.7	d (243.4)	-	-
18	115.4	d (21.1)	7.21-7.27	14, 16 and 17
19	129.7	d (8.0)	7.49	13, 15 and 17
OH	-	-	-	14, 16, and 18
Pyrrole-NH	-	-	-	8, 9 and 10
NH	-	-	-	-

The carbons in position 15-19 appears as doublets, due to coupling to fluorine. The ^{1}J, ^{2}J and ^{3}J coupling constants seen in the ^{13}C NMR spectrum (Appendix A.1.8) are within the expected values for C-F couplings.[66]

*Table 4.49: ^{19}F NMR data and coupling constants for compound **1h**.*

Position	^{19}F (ppm)	Multiplicity
17	-114.3	s

There was only a signal appearing as a singlet in the ^{19}F NMR proton-coupled experiment. The ^{19}F NMR proton decoupled experiment was performed to find if there were any fluorine impurities in the sample since this is a very fluorine-sensitive detection method.

5. Biological Testing

Compounds **1a**, **1c-1h** and **2b** were subjected to *in vitro* enzymatic testing. The testing was purchased from Life Technologies Corporation (former Invitrogen). All of the compounds were dissolved in DMSO (meets EP and USP testing specifications). The activity of the compounds was tested against one tyrosine kinase, EGFR (ErbB1). The ten points titration curves, representing the activities of these compounds in different concentrations are reported in Figure 5.1. The reported IC_{50} values are compiled in Table 5.1.

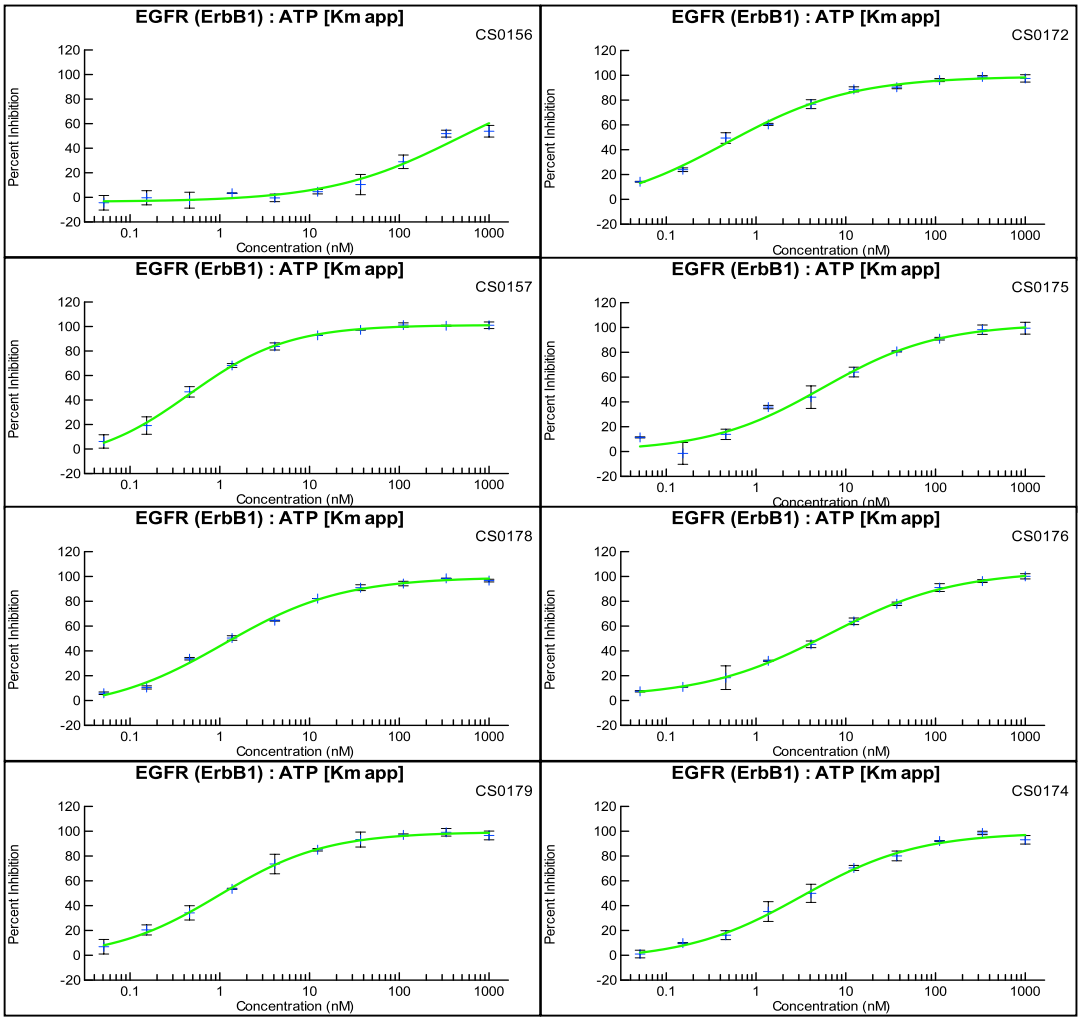

*Figure 5.1: Titration curves showing activities towards EGFR of compounds **2b**, **1a** and **1c-h** (Percent inhibition as a function of the logarithmic concentration in nM). The graph in top left corner is compound **2b**, and under it are compounds **1a**, **1c-d**. The graph in top right corner is compound **1e**, and under it are compounds **1f-h** (Each point is duplicated measurements).*

It is clear from these graphs, as well as the reported IC_{50} value, that compound **2b** has little activity compare to the other compounds. The highest activity measured in this test was for compounds **1a** (PKI 166) and **1e**. All of the demethylated chiral pyrrolo-pyrimidines had higher activity than the achiral ones.

Researchers has made a model of the ATP binding site of EGFR kinase and found how interactions may occur. Docking studies was made for PKI 166 and indicated what interactions that are essential for binding to the ATP binding site of the EGFR kinase.[13] Hydrogen-bonding involving the hydrogen donating phenolic unit, the pyrrole amine hydrogen and the other amine hydrogen were found to be of importance. Hydrogen accepting sites may be the nitrogen atoms in the pyrimidine ring.

*Table 5.1: IC_{50} values measured for compounds **2b**, **1a** and **1c-h**. The R^2 values indicate how well the IC_{50} values correlates with the corresponding graphs in Figure 5.1*

Compound	IC_{50} (nM)	R^2 Value	Kinase Type
2b	454	0.9614	EGFR (ErbB1)
1a	0.46	0.9988	EGFR (ErbB1)
1c	0.99	0.9987	EGFR (ErbB1)
1d	1.11	0.9958	EGFR (ErbB1)
1e	0.46	0.9945	EGFR (ErbB1)
1f	5.59	0.9838	EGFR (ErbB1)
1g	6.48	0.9995	EGFR (ErbB1)
1h	3.23	0.9956	EGFR (ErbB1)

Docking studies indicate that the phenyl ring of compound **1a** is placed in a hydrophobic pocket and interaction is induced between the phenyl ring and Cys 773 (see Figure 5.2). The selectivity PKI 166 shows towards EGFR is explained by this interaction with Cys 773.[13]

Compound **2b** does not contain any hydroxyl group, and the bonding interactions between the compound and binding site is hence reduced. Concerning the different activities of the chiral and achiral compounds, this may be explained by how the molecule fit in the binding site. The electron donating effect of the methyl group in the chiral compounds (**1a-1e**) increases the electron density of the amine function,

enabling the amine hydrogen to be a better H-bond acceptor towards the ATP site, than the amine in the achiral compounds (**1f-h**). Another trend in the test results, is that in the fluorine substituted compounds, the para substituted compounds are the most active derivative in each class (chiral and achiral). The least active compounds are the meta substituted. The effect of fluorine substitution on position 4 in the chiral molecules (compound **1a** and **1e**) has no effect on activity. This indicates that no steric or electronic effects influence this position.

Better lipophilicity for the chiral pyrrolo-pyrimidines because of the methyl group may explain the increased activity for compounds **1c-f** in comparison to the achiral derivatives **1f-h**. Steric, conformational or electronic interactions may also account for the difference in activity observed between the compounds.

The IC_{50} earlier reported for compound **1a** (1.7 nM) is a bit higher than the obtained value in this test (0.46 nM). This may be due to difference in testing methods and the values are not correlated with regard to this difference.

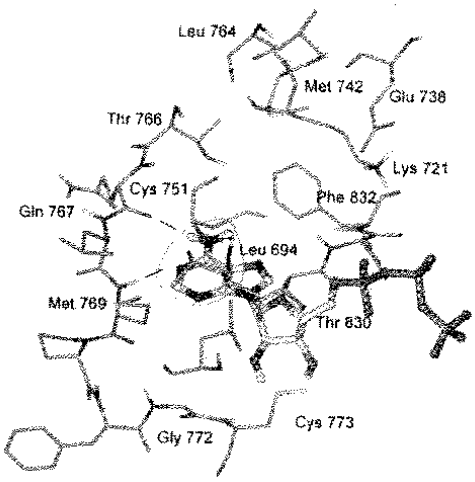

Figure 5.2: Model of the ATP binding site of the EGFR kinase.[13]

If these compounds were to be tested more extensively against a large number of kinases, the results between the different compounds, could give a different result. The binding sites of various kinases are quite different, and the interactions are varying amongst the separate receptors. The three dimensional structures of many TK receptors has not yet been determined, and there are mostly models used to calculate the interactions.

6. Conclusion

Eight compounds were synthesized pure in seven steps, and submitted for testing towards the TK EGFR. All of the compounds showed a high activity towards the kinase, and the chiral para-fluorine derivative **1e** together with the unsubstituted compound **1a,** gave the lowest IC_{50} values (0.46 nM for both compounds). The test results showed that the chiral demethylated compounds were most active, while the achiral were the least active. Compound **2b**, containing two methoxy groups gave the highest IC_{50} value.

Scale-up of the previous work (steps 1-4) was done in such a fashion that the overall yield increased from 23% to 46%. The larger scale made the crystallization easier and the compound lost in various transfers, made less impact.

Step five included chlorination with phosphorus oxychloride, and was carried out in a good yield (98%). In the sixth step, a N-alkylation was performed with yields varying from 54% to 80%. The reasons for the moderate yields in some of these reactions could be differences in electronic properties or steric hindrance, as well as various reaction conditions. The use of TEA to ease amination proved inconclusive, with yields varying from 62% to 79% at best. The demethylation step proved most difficult in this second part of the synthesis. Reactions turned out to require longer reaction time than earlier reported,[5] and more boron tribromide was added to reduce the reaction time. This proved invaluable, as there already were an excess of boron tribromide in the reaction mixture. The deprotection reaction of compound **2b** was less successful than for the rest of the compounds, and provided compound **1b** in only 8% yield. The yields of compounds **1a** and **1c-h** varied from 33-71%.

7. Further Work

The synthetic route towards compounds **1a-h** consists of seven steps with overall yields from 11% to 25%. This means that in some steps there are potential improvements. Some of these reactions have been performed in a small scale, which made the yield more dependent of a high accuracy in every operation. Especially in the reactions to give compounds **2a-h** and **1a-h**, the transfer of the solid from the filter to vial was difficult. Loss of only a small amount of compound makes a deep impact on the yield. This means that if these reactions were run in a larger scale, it could increase the yield substantially because of easier handling.

Reactions to form compounds **2a-h** provides decent yields with the reaction conditions described in this thesis. But these reactions can be carried out using a different approach; namely cross-coupling chemistry, which in similar reactions has been reported to give very good yields.[67, 68] In one of these reported reactions, Suzuki-Miyaura cross-coupling with arylchlorides was performed with good results.

The reaction time in the last step may be reduced if the reaction mixture is heated. In similar reactions where this has been performed, both the reaction time is significantly less, and the yield is good.[69] In addition, there are multiple methods to cleave methyl groups and they are all well examined, and may result in a better yield in this reaction.[58]

Docking studies with modeling of the ATP site could give clues on which interactions that are preferred, indicating what things that must be considerated when synthesizing new compounds. There are numerous possibilities to design new novel molecules that may have inhibitory properties, and only the creative mind can limit this. The pyrrolo-moiety can be replaced by either a furo- or thieno-ring, or another bi- or tri-heteroatom ring. The possibility to use a six-member ring with heteroatoms can also be a good alternative and has been investigated to some extent.[70] As for the substituents on the different rings, the options are endless. Some of these things will be investigated and tried out in the continuance of this project.

8. Experimental

8.1 General Experimental Procedures

8.1.1 Laboratory Techniques

Reactions were performed using dry glassware with rubber septa or condensers for refluxing conditions. Teflon-coated stir bars were used. Unless otherwise stated, the reactions were conducted under nitrogen atmosphere. To regulate reaction temperatures, oil baths were used for temperatures above r.t., while temperatures below r.t. were controlled using ice baths (0°C).

8.1.2 Separation Techniques

Thin layer chromatography (TLC) was used to monitor reaction progress (Silica gel on Al-sheets, 60, F_{254}, Merck and Alugram RP-18W/UV_{254}, 0.15 mm Silica gel C18, Macherey-Nagel). UV (254 nm) was used to visualize the spots. Flash chromatography was performed using Merck silica gel 230-400 mesh (particle size 0.040-0.063 mm). The eluent system is specified for the individual reactions.

HPLC (Agilent 1100-Series) with a G1379A degasser, G1311A Quatpump and an G1313A ALS autosampler and a UV-Bruker diode array detector (254 nm) was used to decide the purity of the end products. A Chirobiotic T2, 25cm x 4.6mm, 5µm column was used with a gradient eluent program specified for the individual reactions, flow rate 1.0 mL/min. Software used with the HPLC: Hystar 3.0 with Hystar Post Processing. Two different methods were used:

A) Linear gradient eluation, pump rt. 60 min., mobile phase start: (H_2O:TFA, 100:0.05):MeOH, 98:2, mobile phase after 45 min: (H_2O:TFA, 100:0.05):MeOH, 50:50.

B) Linear gradient eluation, pump rt. 70 min., mobile phase start: (H_2O:TFA, 100:0.05):MeOH, 98:2, mobile phase after 50 min: (H_2O:TFA, 100:0.05):MeOH, 50:50.

8.1.3 Spectroscopic Analysis

The mass spectroscopy spectra of compounds **6-4** were performed on a MAT 95XL instrument (TermoQuest Finnigan) using an electron ionization (EI) source. Spectra

of compounds **3**, **2a-h** and **1a-h** were recorded on an Agilent 6520 QTOF MS instrument equipped with a dual electrospray ion source.

Nuclear magnetic resonance spectroscopy (NMR) was recorded using a Bruker Avance DPX 300 and Bruker Avance DPX 400 spectrometer. The instruments were operating at 400 MHz for ^{1}H, 100 MHz for ^{13}C and 376 MHz for ^{19}F. The spectroscopic data were processed using Xwin-NMR (version 3.5). The different deuterated solvents are given for each individual compound. Chemical shifts are relative to TMS internal standard (0.00 ppm) or DMSO-d_6 (2.50) in ^{1}H-spectra.[71] In carbon spectra the shifts were calibrated with either chloroform (77.23 ppm) or DMSO (39.51 ppm).[71] For ^{19}F-NMR measurements, a QNP probe was used with hexafluorobenzene as an internal standard (-162.0 ppm)[72]. The peaks are abbreviated as follows: s, singlet; d (doublet), t (triplet), q (quartet), quintet, dd (doublet of doublets), td (triplet of doublets), br (broad singlet). The coupling constants (J) are reported in Hz.

8.1.4 Melting Point

The melting points were measured using Stuart Melting point apparatus SMP3 and are uncorrected.

8.1.5 Optical rotation

The optical rotation was found using a Perkin Elmer 243 B polarimeter with a Na source (D line, 589 nm). The different compounds were dissolved in DMSO and a 100 mm cell was used to measure the rotation.

8.2 Synthesis of Ethyl 3-ethoxy-3-propanoate hydrochloride (7)[73, 74]

Ethyl cyanoacetate (98+%, Aldrich) (18.16 g, 0.16 mole) was added to a solution of anhydrous ethanol (9.198 g, 0.200 mole) and diethyl ether saturated with HCl (70 mL). The solution was cooled in an ice-salt bath and stirred for 30 minutes. The mixture was allowed to stand in the refrigerator (5°C) over night. It was then filtered and washed with diethyl ether (30 mL) to give ethyl ethoxy-carbonyl acetimidate hydrochloride (**7**) as colorless crystals.

^{1}H NMR (400 MHz, $CDCl_3$, *Appendix A.7*), δ, ppm: 12.69 (s, 1H), 11.99 (s, 1H, NH). 4.72 (q, 2H, J=7.0), 4.23 (q, 2H, J=7.1), 3.88 (s, 2H), 1.50 (t, 3H, J=7.0), 1.29 (t, 3H, J=7.1)

^{13}C NMR (100 MHz, $CDCl_3$, *Appendix A.7*), δ, ppm: 172.1, 164.3, 71.7, 61.5, 39.1, 14.0, 13.5

Yield: 28.88 g, 0.15 mole, 94 %

8.3 Synthesis of Ethyl amidinoacetate hydrochloride (6)[74]

Ethyl 3-ethoxy-3-propanoate hydrochloride (**7**) (28.52 g, 0.15 mole) was added to a solution of K_2CO_3 (100 g) in water (150 mL) and was then extracted three times with diethyl ether (3x 150 mL). The combined organic layers were washed with brine (70 mL), dried over anhydrous Na_2SO_4, filtered and concentrated to give a colorless oil. Ammonium chloride (7.83 g, 0.15 mole) in anhydrous ethanol (20 mL) was added and the mixture refluxed for 6 h. The precipitate was filtered off and the filtrate was evaporated *in vacuo*. The residue was dried under reduced pressure over night to give the product **6** as colorless crystals.

Melting point: 105-107°C (Lit.[73] 104°C)

^{1}H NMR (400 MHz, DMSO-d_6, *Appendix A.6*), δ, ppm: 9.22 (s, 2H, NH_2), 8.95 (s, 2H, NH_2^+), 4.15 (q, 2H, J=7.1), 3.64 (s, 2H), 1.22 (t, 3H, J=7.1)

^{13}C NMR (100 MHz, DMSO-d_6, *Appendix A.6*), δ, ppm: 166.7, 164.2, 61.8, 38.0, 14.4

Yield: 22.99 g, 0.15 mole, >99 %

8.4 Synthesis of 2-Amino-3-carboxyethyl-5-(4-methoxyphenyl)-pyrrole (5)[15, 75]

Ethyl amidinoacetate hydrochloride (**6**) (13.78 g, 87 mmole) and abs. ethanol (60 mL) were added to a dry two-necked roundbottle, under Ar atmosphere, and maintained at 0°C. Sodium ethoxide (5.92 g, 87 mmole) was added and the mixture was allowed to stir for fifteen minutes before it was heated up to r.t.. 4-Methoxyphenacyl bromide (purum, ≥97%, Fluka) (10.78 g, 47 mmole) was then added and the temperature was increased to 50°C. After 1 h the solvent was evaporated at reduced pressure and the residue was extracted with water (30 mL) and ethyl acetate (70 mL). The organic layer was washed three times with water (3x 20 mL) and brine (30 mL). The combined water layers were washed two times with ethyl acetate (2x 50 mL) and all the organic fractions were collected, dried with anhydrous $MgSO_4$ and concentrated *in vacuo*. The crude material was purified by column chromatography by using n-hexane:ethyl acetate (4:6) as the eluent. The solvents were evaporated *in vacuo* and then triturated with diethyl ether (25 mL) and n-hexane (45 mL). This resulted in a beige solid that were filtered and washed with n-hexane (60 mL).

Melting point: 146-147°C (Lit.[15] 141-142°C)

TLC (DCM:MeOH, 9:1): $R_f = 0.54$

^{1}H NMR (400 MHz, DMSO-d_6, *Appendix A.5*),[5] δ, ppm: 10.63 (s, 1H, NH), 7.41 (d, $2H_{arom}$, J=8.9), 6.89 (d, $2H_{arom}$, J=8.9), 6.31 (d, 1H, J=2.9), 5.60 (s, 2H, NH_2), 4.13 (q, 2H, J=7.1), 3,74 (s, 3H), 1.24 (t, 3H, J=7.1)

^{13}C NMR (100 MHz, DMSO-d_6, *Appendix A.5*),[5] δ, ppm: 165.0, 157.1, 147.8, 125.2, 123.8 (2C), 123.3, 114.1 (2C), 101.8, 93.1, 58.0, 55.0, 14.7

Yield: 9.47 g, 36 mmole, 77%

8.5 Synthesis of 4-Hydroxy-6-(4-metoxyphenyl)-7*H*-pyrrolo-[2,3-*d*]-pyrimidine (4)[15]

To a solution of anhydrous DMF (40 mL) and formic acid (24 mL), 2-amino-3-carboxethyl-5-(4-methoxyphenyl)-pyrrole (**5**) (13.00 g, 50 mmole) and an excess formamide (76 mL, 1.5 mole) were added. The mixture was then heated to 150°C. After 19 h, isopropanol (20 mL) was added and the mixture was cooled down to 20°C. It was filtered, washed with isopropanol (30 mL), then three times with n-hexane (3x 10 mL) before it was dried under reduced pressure. The yield comprised a light beige solid.

Melting point: >300°C (Lit.[15] >300°C)

TLC (DCM:MeOH, 7:3): $R_f = 0.75$

^{1}H NMR (400 MHz, DMSO-d_6, *Appendix A.4*),[15] δ, ppm: 12.22 (s, br, 1H, NH), 11.81 (s, br, 1H, OH), 7.85 (s, 1H), 7.76 (d, $2H_{arom}$, J=9.0), 6.98 (d, $2H_{arom}$, J=9.0), 6.79 (s, 1H), 3.78 (s, 3H)

^{13}C NMR (100 MHz, DMSO-d_6, *Appendix A.4*),[15] δ, ppm: 159.1, 158.5, 149.5, 143.7, 133.7, 126.4 (2C), 124.6, 114.7 (2C), 109.5, 98.2, 55.6

Yield: 7.79 g, 32 mmole, 64%

8.6 Synthesis of 4-Chloro-6-(4-metoxyphenyl)-7*H*-pyrrolo-[2,3-*d*]-pyrimidine (3)[5]

To a dry roundbottle with 4-Hydroxy-6-(4-metoxyphenyl)-7*H*-pyrrolo-[2,3-*d*]-pyrimidine (**4**) (1.742 g, 7.22 mmole) was added phosphorus oxychloride (ReagentPlus®, 99%, Sigma Aldrich) (13.5 mL, 53.5 mmole) and heated to reflux for 2.5 h. The mixture was poured into a beaker filled with ice (200 mL) and 8M NaOH (75 mL) was used to adjust to pH 7. The residue was extracted with ethyl acetate (4x 400 mL) and the combined organic layers washed with brine (2x 200 mL), dried with $MgSO_4$ and concentrated *in vacuo* to afford the product as a yellow solid.

Melting point: 248-249°C (Lit.[15] 248-249°C)

TLC (DCM:MeOH, 85:15): $R_f = 0.80$

HRMS (ESI, *Appendix B.3*): m/z 260.0597 (calc. $C_{13}H_{10}ClN_3O$ 260.0591 M^+H)

^{1}H NMR (400 MHz, DMSO-d_6, *Appendix A.3*),[5] δ, ppm: 12.90 (s, 1H, NH), 8.55 (s, 1H), 7.95 (d, 2H$_{arom}$, J=8.8), 7.06 (d, 2H$_{arom}$, J=8.8), 6.96 (d, 1H, J=2.1), 3.82 (s, 3H)

^{13}C NMR (100 MHz, DMSO-d_6, *Appendix A.3*),[5] δ, ppm: 160.0, 153.0, 150.0, 149.2, 140.5, 127.5 (2C), 122.7, 118.0, 114.5 (2C), 94.0, 55.3

Yield: 1.834 g, 7.1 mmole, 98%

8.7 Synthesis of 2a-2h

8.7.1 Synthesis of 2a[5]

4-Chloro-6-(4-metoxyphenyl)-7*H*-pyrrolo-[2,3-*d*]-pyrimidine (**3**) (0.275 g, 1.1 mmole) was added to a dry roundbottle containing 1-butanol (3.5 mL). The (*R*)-(+)-α-methylbenzylamine (purity ≥99.0%, Fluka) (0.44 mL, 3.5 mmole) was added and the mixture was heated to 145°C for 24 h while stirring. 0.5 equivalent of the (*R*)-(+)-α-methylbenzylamine was then added and the mixture was cooled to 20°C. The light yellow precipitate was filtered off and washed with diethyl ether (25 mL).

TLC (EtOAc:EtOH, 96:4): $R_f = 0.29$

HRMS (ESI, *Appendix B.2.1*): m/z 345.1709 (calc. $C_{21}H_{20}N_4O$ 345.1715 M^+H)

^{1}H NMR (400 MHz, DMSO-d_6, *Appendix A.2.1*),[5] δ, ppm: 11.92 (s, 1H, NH), 8.04 (s, 1H), 7.73 (d, 3H, $2H_{arom}$ + NH, J=8.6), 7.43 (m, $2H_{arom}$), 7.30 (t, $2H_{arom}$, J=7.6), 7.19 (m, $1H_{arom}$), 7.02 (d, $2H_{arom}$, J=8.6), 6.96 (d, 1H, J=0.9), 5.48-5.52 (m, 1H), 3.80 (s, 3H)

^{13}C NMR (100 MHz, DMSO-d_6, *Appendix A.2.1*),[5] δ, ppm: 158.6, 154.8, 151.4, 151.3, 145.6, 133.5, 128.1 (2C), 126.7, 126.0 (2C), 125.9 (2C), 124.5, 114.4 (2C), 103.9, 94.6, 55.2, 50.0, 22.9

Specific Rotation: $[\alpha]_D^{25}$ = -353.3 ($c = 0.11$, DMSO)

Yield: 0.258 g, 0.75 mmole, 68%

8.7.2 Synthesis of 2b

4-Chloro-6-(4-metoxyphenyl)-7*H*-pyrrolo-[2,3-*d*]-pyrimidine (**3**) (0.238 g, 0.92 mmole) was added to a dry roundbottle containing 1-butanol (3.0 mL). The (*R*)-(+)-(4-methoxyphenyl)ethylamine (purity 99+%, ee 99+%, Alfa Aesar) (0.21 mL, 1.4 mmole) was added and the mixture was heated to 145°C for 28 h while stirring. 0.5 equivalent of the (*R*)-(+)-(4-methoxyphenyl)ethylamine was then added and stirred

for another 47 h before the mixture was cooled to 20°C. The colorless solid were filtered off and washed with diethyl ether (50 mL) and water (20 mL).

TLC (EtOAc:EtOH, 96:4): $R_f = 0.17$

Purity: >99% (determined by HPLC, Method A))

HRMS (ESI, *Appendix B.2.2*): m/z 375.1814 (calc. $C_{22}H_{22}N_4O_2$ 375.1821 M^+H)

^{1}H NMR (400 MHz, DMSO-d_6, *Appendix A.2.2*), δ, ppm: 11.89 (s, 1H, NH), 8.04 (s, 1H), 7.71 (d, $2H_{arom}$, J=8.9), 7.64 (d, 1H, NH, J=8.4), 7.34 (d, $2H_{arom}$, J=8.7), 7.02 (d, $2H_{arom}$, J=8.9), 6.94 (s, 1H), 6.86 (d, $2H_{arom}$, J=8.7), 5.43-5.47 (m, 1H), 3.80 (s, 3H), 3.71 (s, 3H), 1.50 (d, 3H, J=7.0)

^{13}C NMR (100 MHz, DMSO-d_6, *Appendix A.2.2*), δ, ppm: 158.6, 157.9, 154.8, 151.3 (2C), 137.5, 133.4, 127.2 (2C), 125.9 (2C), 124.5, 114.4 (2C), 113.5 (2C), 103.9, 94.6, 55.2, 55.0, 48.0, 22.9

Specific Rotation: $[\alpha]_D^{25}$ = -330.1 (c = 0.14, DMSO)

Yield: 0.215 g, 0.57 mmole, 62%

8.7.3 Synthesis of 2c

4-Chloro-6-(4-metoxyphenyl)-7*H*-pyrrolo-[2,3-*d*]-pyrimidine (**3**) (0.212 g, 0.82 mmole) was added to a dry roundbottle containing 1-butanol (3.0 mL). (R)-(+)-(2-Fluorophenyl)ethylamine (Apollo Scientific) (0.17 mL, 1.3 mmole) was added and heated to 145°C for 24 h while stirring under Ar atmosphere. 0.45 equivalent of the amine was then added and stirred for another 24 h at 145°C. The mixture was cooled to 20°C and the light yellow precipitate was filtered off and washed with diethyl ether (30 mL).

TLC (EtOAc:EtOH, 96:4): $R_f = 0.33$

HRMS (ESI, *Appendix B.2.3*): m/z 363.1615 (calc. $C_{21}H_{19}FN_4O$ 363.1621 M^+H)

^{1}H NMR (400 MHz, DMSO-d_6, *Appendix A.2.3*), δ, ppm: 11.94 (s, 1H, NH), 8.03 (s, 1H), 7.79 (d, 1H, NH, J=8.0), 7.73 (d, $2H_{arom}$, J=8.8), 7.45-7.49 (m, $1H_{arom}$), 7.23-7.28 (m, $1H_{arom}$), 7.11-7.18 (m, $2H_{arom}$), 7.03 (d, $2H_{arom}$, J=8.8), 6.98 (d, 1H, J=1.4), 5.67-5.74 (m, 1H), 3.80 (s, 3H), 1.53 (d, 3H, J=7.3)

^{13}C NMR (100 MHz, DMSO-d_6, *Appendix A.2.3*), δ, ppm: 159.6 (d, J=243.5), 158.7, 154.5, 151.4, 151.3, 133.7, 132.5 (d, J=14.1), 128.3 (d, J=8.0), 127.1 (d, J=5.0), 125.9 (2C), 124.4, 124.3 (d, J=3.0), 115.1 (d, J=22.1), 114.4 (2C), 104.0, 94.5, 55.2, 43.2, 21.9

^{19}F NMR (376 MHz, DMSO-d_6, C_6F_6 int. std., *Appendix A.2.3*), δ, ppm: -119.2 (s)

Specific Rotation: $[\alpha]_D^{25}$ = -375.9 (*c* = 0.13, DMSO)

Yield: 0.236 g, 0.65 mmole, 79%

8.7.4 Synthesis of 2d

4-Chloro-6-(4-metoxyphenyl)-7*H*-pyrrolo-[2,3-*d*]-pyrimidine (**3**) (0.229 g, 0.88 mmole) was added to a dry roundbottle containing 1-butanol (3.0 mL). The (*R*)-(+)-(3-fluorophenyl)ethylamine (Apollo Scientific) (0.18 mL, 1.3 mmole) was added and the mixture was heated to 145°C for 27 h while stirring under Ar atmosphere. 0.3 equivalent of the (*R*)-(+)-(3-fluorophenyl)ethylamine was then added and stirred for another 24 h. The mixture was cooled to 20°C and the light yellow precipitate was filtered off and washed with diethyl ether (30 mL).

TLC (EtOAc:EtOH, 96:4): R_f = 0.31

HRMS (ESI, *Appendix B.2.4*): m/z 363.1613 (calc. $C_{21}H_{19}FN_4O$ 363.1621 M^+H)

^{1}H NMR (400 MHz, DMSO-d_6, *Appendix A.2.4*), δ, ppm: 11.94 (s, 1H, NH), 8.04 (s, 1H), 7.76 (d, 1H, NH, J=8.2), 7.73 (d, $2H_{arom}$, J=8.8), 7.32-7.37 (m, $1H_{arom}$), 7.25-7.27 (m, $1H_{arom}$), 7.22-7.24 (m, $1H_{arom}$), 7.02 (d, $2H_{arom}$, J=8.8), 6.99-7.00 (m, $1H_{arom}$), 6.94 (d, 1H, J=1.8), 5.45-5.53 (m, 1H), 3.80 (s, 3H), 1.53 (d, 3H, J=7.0)

^{13}C NMR (100 MHz, DMSO-d_6, *Appendix A.2.4*), δ, ppm: 162.3 (d, J=242.4), 158.7, 154.7, 151.4, 151.3, 148.9 (d, J=28.2), 133.7, 130.1 (d, J=9.1), 126.0 (2C), 124.5, 122.2 (d, J=3.0), 114.5 (2C), 113.2 (d, J=21.1), 112.7 (d, J=21.1), 103.9, 94.5, 55.2, 48.4, 22.8

^{19}F NMR (376 MHz, DMSO-d_6, C_6F_6 int. std., *Appendix A.2.4*), δ, ppm: -113.0 (m)

Specific Rotation: $[\alpha]_D^{25}$ = -347.3 (*c* = 0.13, DMSO)

Yield: 0.236 g, 0.65 mmole, 79%

8.7.5 Synthesis of 2e[5]

4-Chloro-6-(4-metoxyphenyl)-7*H*-pyrrolo-[2,3-*d*]-pyrimidine (**3**) (0.142 g, 0.55 mmole) was added to a dry roundbottle containing 1-butanol (2.0 mL) and TEA (1.0 mL). The (*R*)-(+)-1-(4-fluorophenyl)ethylamine (purity 99%, ee 98%, Alfa Aesar) (0.15 mL, 1.11 mmole) was added and the mixture was heated to 140°C for 36 h while stirring. 0.5 equivalent of the (*R*)-(+)-1-(4-fluorophenyl)ethylamine was then added and stirred for an other 36 h before the mixture was cooled to 20°C. The light yellow precipitate was filtered off and washed with diethyl ether (15 mL).

TLC (EtOAc:EtOH, 92:8): R_f = 0.38

HRMS (ESI, *Appendix B.2.5*): m/z 363.1630 (calc. $C_{21}H_{19}FN_4O$ 363.1621 M^+H)

^{1}H NMR (400 MHz, DMSO-d_6, *Appendix A.2.5*),[5] δ, ppm: 11.93 (s, 1H, NH), 8.04 (s, 1H), 7.72 (d, 3H, $2H_{arom}$ + NH, J=8.6), 7.44-7.48 (m, $2H_{arom}$), 7.12 (t, $2H_{arom}$, J=8.8), 7.02 (d, $2H_{arom}$, J=8.6), 6.94 (s, 1H), 5.47-5.50 (m, 1H), 3.80 (s, 3H), 1.52 (d, 3H, J=6.9)

^{13}C NMR (100 MHz, DMSO-d_6, *Appendix A.2.5*),[5] δ, ppm: 160.9 (d, J=241.1), 158.7, 154.7, 151.4, 151.3, 141.8 (d, J=3.0), 133.6, 127.9 (d, 2C, J=8.0), 125.9 (2C), 124.5, 114.8 (d, 2C, J=22.1), 114.4 (2C), 103.9, 94.5, 55.2, 48.1, 22.9

^{19}F NMR (376 MHz, DMSO-d_6, C_6F_6 int. std., *Appendix A.2.5*), δ, ppm: -116.2 (m)

Specific Rotation: $[\alpha]_D^{25}$ = -315.9 (c = 0.16, DMSO)

Yield: 0.133 g, 0.37 mmole, 67%

8.7.6 Synthesis of 2f

4-Chloro-6-(4-metoxyphenyl)-7*H*-pyrrolo-[2,3-*d*]-pyrimidine (**3**) (0.186 g, 0.72 mmole) was added to a dry roundbottle containing 1-butanol (3.0 mL). TEA (1.5 mL) and 2-fluorobenzylamine (purity 97%, Alfa Aesar) (0.12 mL, 1.1 mmole) were added and the mixture was then heated to 135°C for 21 h while stirring under Ar atmosphere. 0.5 equivalent of the 2-fluorobenzylamine was added and stirred for another 7 h. The mixture was cooled to 20°C and the light yellow precipitate was filtered off and washed with diethyl ether (20 mL). The crude product was dissolved in a saturated potassium carbonate solution (40 mL) and extracted with ethyl acetate (3x 50 mL). It was washed with brine (30 mL), dried with $MgSO_4$ and concentrated on rotavapor to yield compound **2f** as a yellow solid.

TLC (EtOAc:EtOH, 96:4): R_f = 0.24

HRMS (ESI, *Appendix B.2.6*): m/z 349.1452 (calc. $C_{20}H_{17}FN_4O$ 349.1465 M^+H)

^{1}H NMR (400 MHz, DMSO-d_6, *Appendix A.2.6*), δ, ppm: 11.98 (s, 1H, NH), 8.10 (s, 1H), 7.92 (t, 1H, NH, J=5.8), 7.72 (d, 2H$_{arom}$, J=8.7), 7.38-7.42 (m, 1H$_{arom}$), 7.27-7.33 (m, 1H$_{arom}$), 7.19-7.21 (m, 1H$_{arom}$), 7.12-7.17 (m, 1H$_{arom}$), 7.02 (d, 2H$_{arom}$, J=8.7), 6.88 (d, 1H, J=1.8), 4.77 (d, 2H, J=5.8), 3.79 (s, 3H)

^{13}C NMR (100 MHz, DMSO-d_6, *Appendix A.2.6*), δ, ppm: 160.6 (d, J=244.5), 159.1, 155.8, 151.8 (2C), 134.2, 129.8 (d, J=5.0), 129.1 (d, J=8.0), 127.3 (d, J=15.1), 126.4 (2C), 124.8, 124.7 (d, J=3.0), 115.4 (d, J=21.1), 114.9 (2C), 104.4, 94.7, 55.6, 37.4

^{19}F NMR (376 MHz, DMSO-d_6, C_6F_6 int. std., *Appendix A.2.6*), δ, ppm: -118.5 (m)

Yield: 0.183 g, 0.53 mmole, 74%

8.7.7 Synthesis of 2g

4-Chloro-6-(4-metoxyphenyl)-7*H*-pyrrolo-[2,3-*d*]-pyrimidine (**3**) (0.097 g, 0.37 mmole) was added to a dry roundbottle containing 1-butanol (1.5 mL) and TEA (0.5 mL). The 3-fluorobenzylamine (purity 97%, Sigma Aldrich) (0.09 mL, 0.79 mmole) was added and the mixture was heated to 145°C for 18 h while stirring under Ar atmosphere. The mixture was cooled to 20°C and the light yellow precipitate was filtered off and washed with diethyl ether (15 mL). The crude product was dissolved in a saturated potassium carbonate solution (20 mL) and extracted with ethyl acetate (3x 25 mL). It was washed with brine (20 mL), dried with $MgSO_4$ and concentrated on rotavapor to yield compound **2g** as a yellow solid.

TLC (EtOAc:EtOH, 96:4): $R_f = 0.21$

HRMS (ESI, *Appendix B.2.7*): m/z 349.1455 (calc. $C_{20}H_{17}FN_4O$ 349.1465 M^+H)

^{1}H NMR (400 MHz, DMSO-d_6, *Appendix A.2.7*), δ, ppm: 11.99 (s, 1H, NH), 8.11 (s, 1H), 7.99 (t, 1H, NH, J=5.9), 7.73 (d, 2H_{arom}, J=8.9), 7.33-7.39 (m, 1H_{arom}), 7.19-7.21 (m, 1H_{arom}), 7.14-7.17 (m, 1H_{arom}), 7.05-7.08 (m, 1H_{arom}), 7.02 (d, 2H_{arom}, J=8.9), 6.86 (d, 1H, J=2.0), 4.75 (d, 2H, J=5.9), 3.79 (s, 3H)

^{13}C NMR (100 MHz, DMSO-d_6, *Appendix A.2.7*), δ, ppm: 162.2 (d, J=242.4), 158.7, 155.4, 151.4 (2C), 143.6 (d, J=28.2), 133.8, 130.2 (d, J=9.1), 126.0 (2C), 124.4, 123.1 (d, J=3.0), 114.4 (2C), 113.7 (d, J=21.1), 113.3 (d, J=21.1), 103.9, 94.2, 55.2, 42.7

^{19}F NMR (376 MHz, DMSO-d_6, C_6F_6 int. std., *Appendix A.2.3*), δ, ppm: -113.1 (m)

Yield: 0.098 g, 0.28 mmole, 76%

8.7.8 Synthesis of 2h

4-Chloro-6-(4-metoxyphenyl)-7*H*-pyrrolo-[2,3-*d*]-pyrimidine (**3**) (0.178 g, 0.69 mmole) was added to a dry roundbottle containing 1-butanol (3.0 mL). The 4-fluorobenzylamine (purity 97%, Sigma Aldrich) (0.12 mL, 1.0 mmole) was added and the mixture was heated to 145°C for 24 h while stirring. 0.5 equivalent of the 4-fluorobenzylamine was then added and stirred for another 28 h. The mixture was

cooled to 20°C and the light yellow precipitate was filtered off and washed with diethyl ether (30 mL). The crude product was dissolved in potassium carbonate (35 mL) and extracted with ethyl acetate (3x 40 mL). It was washed with brine (25 mL), dried with $MgSO_4$ and concentrated on *in vacuo* to yield compound **2h** as a yellow solid.

TLC (EtOAc:EtOH, 96:4): $R_f = 0.24$

HRMS (ESI, *Appendix B.2.8*): m/z 349.1460 (calc. $C_{20}H_{17}FN_4O$ 349.1465 M^+H)

^{1}H NMR (400 MHz, DMSO-d_6, *Appendix A.2.8*), δ, ppm: 11.96 (s, 1H, NH), 8.10 (s, 1H), 7.95 (t, 1H, NH, J=5.9), 7.71 (d, $2H_{arom}$, J=8.7), 7.40 (dd, $2H_{arom}$, J=5.6, 8.5), 7.14 (t, $2H_{arom}$, J=8.9), 7.02 (d, $2H_{arom}$, J=8.7), 6.84 (d, 1H, J=1.2), 4.71 (d, 2H, J=5.9), 3.79 (s, 3H)

^{13}C NMR (100 MHz, DMSO-d_6, *Appendix A.2.8*), δ, ppm: 161.1 (d, J=241.4), 158.7, 155.4, 151.4, 151.3, 136.5 (d, J=3.0), 133.7, 129.1 (d, 2C, J=8.0), 126.0 (2C), 124.4, 114.9 (d, 2C, J=21.1), 114.4 (2C), 103.9, 94.3, 55.2, 42.5

^{19}F NMR (376 MHz, DMSO-d_6, C_6F_6 int. std., *Appendix A.2.3*), δ, ppm: -115.9 (m)

Yield: 0.187 g, 0.54 mmole, 78%

8.8 Synthesis of 1a-1h

8.8.1 Synthesis of 1a[5]

(*R*)-6-(4-Methoxyphenyl)-*N*-(1-phenylethyl)-7*H*-pyrrolo[2,3-*d*]pyrimidin-4-amine (**2a**) (0.061 g, 0.18 mmole) was dissolved with DCM (2 mL) in a dry roundbottle under Ar atmosphere. BBr_3 (ReagentPlus®, 99.9%, Sigma Aldrich) (0.17 mL, 1.8 mmole) in DCM (1.5 mL) was added dropwise over 1 h at 0°C. The reaction mixture was heated to r.t., and stirred for 24 h under Ar atmosphere. Water (10 mL) was added, and the mixture was extracted with ethyl acetate (3x 25 mL). The combined organic layers were washed with brine (15 mL), dried over $MgSO_4$ and concentrated. The oil that appeared was triturated with acetone (0.5 mL) and the colorless solid were filtrated and washed with diethyl ether (10 mL).

TLC (Alugram RP-C18, Acetone:H_2O:DEA, 60:40:0.5): $R_f = 0.55$

Purity: >99% (determined by HPLC, method A))

HRMS (ESI, *Appendix B.1.1*): m/z 331.1555 (calc. $C_{20}H_{18}N_4O$ 331.1559 M^+H)

^{1}H NMR (400 MHz, DMSO-d_6, *Appendix A.1.1*), δ, ppm: 12.98 (s, 1H, NH), 9.83 (br, 1H, OH), 9.55 (br, 1H, NH), 8.30 (s, 1H), 7.66 (d, $2H_{arom}$, J=8.4), 7.48-7.50 (m, $2H_{arom}$), 7.39 (t, $2H_{arom}$, J=7.5), 7.29-7.32 (m, 1H), 7.24 (s, 1H), 6.89 (d, $2H_{arom}$, J=8.4), 5.36-5.39 (m, 1H), 1.66 (d, 3H, J=6.5)

^{13}C NMR (100 MHz, DMSO-d_6, *Appendix A.1.1*), δ, ppm: 158.0, 148.8 (2C), 142.3, 141.9, 137.6, 128.6 (2C), 127.5, 126.7 (2C), 126.1 (2C), 121.2, 116.0 (2C), 102.9, 96.6, 50.9, 22.3

Specific Rotation: $[\alpha]_D^{25}$ = -207.9 (c = 0.11, DMSO)

Yield: 0.258 g, 0.75 mmole, 68%

8.8.2 Synthesis of 1b

(*R*)-6-(4-Methoxyphenyl)-*N*-(1-(4-methoxyphenyl)ethyl)-7*H*-pyrrolo[2,3-*d*]pyrimidin-4-amine (**2b**) (0.228 g, 0.61 mmole) was dissolved with DCM (5 mL) in a dry roundbottle under Ar atmosphere. BBr_3 (ReagentPlus®, 99.9%, Sigma Aldrich) (0.89 mL, 9.2 mmole) in DCM (6 mL) was added dropwise over 1 h at 0°C. The reaction mixture was heated to r.t., and stirred for 13 h under Ar atmosphere. Water (30 mL) was added, and the mixture was extracted with ethyl acetate (3x 50 mL). The combined organic layers were washed with brine (30 mL), dried over $MgSO_4$ and concentrated under reduced pressure. The crude product was recrystallized from diethyl ether (2 mL), which resulted in a colorless solid.

TLC (Alugram RP-C18, H_2O:Acetone:DEA, 54:44:2): $R_f = 0.48$

Purity: 83% (determined by HPLC, Method B))

HRMS (ESI, *Appendix B.1.2*): m/z 347.1505 (calc. $C_{20}H_{18}N_4O_2$ 347.1508 M^+H)

^{1}H NMR (400 MHz, DMSO-d_6, *Appendix A.1.2*), δ, ppm: 12.45 (br, 1H, NH), 9.76 (s, 1H, OH), 9.35 (s, 1H, OH), 8.18 (s, 1H), 7.62 (d, $2H_{arom}$, J=8.7), 7.26 (d, $2H_{arom}$, J=8.4), 7.07 (s, 1H), 6.86 (d, $2H_{arom}$, J=8.7), 6.72 (d, $2H_{arom}$, J=8.4), 5.30-5.34 (m, 1H), 1.55 (d, 3H, J=6.6), (The amine proton was not found)

^{13}C NMR (100 MHz, DMSO-d_6, *Appendix A.1.2*), δ, ppm: 157.8, 156.4, 136.2, 133.1, 127.2 (2C), 126.4 (2C), 121.8, 115.8 (2C), 115.1 (2C), 95.1, 48.9, 22.0 (Four of the carbons in the molecule did not appear in the spectra)

Yield: 0.016 g, 0.05 mmole, 8%

8.8.3 Synthesis of 1c

(*R*)-*N*-(1-(2-Fluorophenyl)ethyl)-6-(4-methoxyphenyl)-7*H*-pyrrolo[2,3-*d*]pyrimidin-4-amine (**2c**) (0.218 g, 0.60 mmole) was dissolved with DCM (5 mL) in a dry roundbottle under Ar atmosphere. BBr_3 (ReagentPlus®, 99.9%, Sigma Aldrich) (0.58 mL, 6.0 mmole) in DCM (4 mL) was added dropwise over 1 h at 0°C. The reaction mixture was heated to r.t., and stirred for 18 h under Ar atmosphere. Water (20 mL)

was added, and the mixture was extracted with ethyl acetate (3x 50 mL). The combined organic layers were washed with brine (30 mL), dried over $MgSO_4$ and evaporated *in vacuo*. The oil that appeared was triturated with acetone (3 mL) and the colorless solid were filtrated and washed with diethyl ether (10 mL).

TLC (Alugram RP-C18, H_2O:Acetone:DEA, 54:44:2): $R_f = 0.34$

Purity: >99% (determined by HPLC, Method A))

HRMS (ESI, *Appendix B.1.3*): m/z 349.1465 (calc. $C_{20}H_{17}FN_4O$ 349.1465 M^+H)

^{1}H NMR (400 MHz, DMSO-d_6, *Appendix A.1.3*), δ, ppm: 12.98 (s, 1H, NH), 9.83 (br, 1H, OH), 9.51 (br, 1H, NH), 8.31 (s, 1H), 7.64 (d, $2H_{arom}$, J=8.7), 7.48 (t, $1H_{arom}$, J=7.4), 7.34-7.39 (m, $1H_{arom}$), 7.26 (s, 1H), 7.19-7.24 (m, $2H_{arom}$), 6.88 (d, $2H_{arom}$, J=8.7), 5.55-5.58 (m, 1H), 1.65 (d, 3H, J=6.7)

^{13}C NMR (100 MHz, DMSO-d_6, *Appendix A.1.3*), δ, ppm: 160.8 (d, J=244.5), 158.0, 149.2, 147.5, 142.7, 137.6, 129.7 (d, J=8.0), 128.8 (d, J=13.1), 126.8 (3C), 124.7, 121.2, 116.0 (2C), 115.7 (d, J=21.1), 103.0, 96.5, 45.8, 20.8

^{19}F NMR (376 MHz, DMSO-d_6, C_6F_6 int. std., *Appendix A.1.3*), δ, ppm: -116.5 (s)

Specific Rotation: $[\alpha]_D^{25}$ = -177.6 (c = 0.13, DMSO)

Yield: 0.101 g, 0.29 mmole, 48%

8.8.4 Synthesis of 1d

(*R*)-*N*-(1-(3-Fluorophenyl)ethyl)-6-(4-methoxyphenyl)-7*H*-pyrrolo[2,3-*d*]pyrimidin-4-amine (**2d**) (0.176 g, 0.49 mmole) was dissolved with DCM (4 mL) in a dry roundbottle under Ar atmosphere. BBr_3 (ReagentPlus®, 99.9%, Sigma Aldrich) (0.47 mL, 4.9 mmole) in DCM (3.5 mL) was added dropwise over 1 h at 0°C. The reaction mixture was heated to r.t., and stirred for 18 h under Ar atmosphere. Water (20 mL) was added, and the mixture was extracted with ethyl acetate (3x 50 mL). The combined organic layers were washed with brine (30 mL), dried over $MgSO_4$ and

concentrated *in vacuo*. The oil that appeared was triturated with acetone (2 mL) and the colorless solid were filtrated and washed with diethyl ether (10 mL).

TLC (Alugram RP-C18, H_2O:Acetone:DEA, 54:44:2): $R_f = 0.34$

Purity: >99% (determined by HPLC, Method A))

HRMS (ESI, *Appendix B.1.4*): m/z 349.1466 (calc. $C_{20}H_{17}FN_4O$ 349.1465 M^+H)

^{1}H NMR (400 MHz, DMSO-d_6, *Appendix A.1.4*), δ, ppm: 12.95 (s, 1H, NH), 9.84 (br, 1H, OH), 9.52 (br, 1H, NH), 8.29 (s, 1H), 7.66 (d, $2H_{arom}$, J=8.7), 7.40-7.46 (m, $1H_{arom}$), 7.33-7.38 (m, $2H_{arom}$), 7.23 (s, 1H), 7.11-7.15 (m, $1H_{arom}$), 6.89 (d, $2H_{arom}$, J=8.7), 5.43-5.46 (m, 1H), 1.65 (d, 3H, J=6.8)

^{13}C NMR (100 MHz, DMSO-d_6, *Appendix A.1.4*), δ, ppm: 162.2 (d, J=244.5), 158.0, 148.3 (2C), 145.3, 142.8, 137.4, 130.6 (d, J=8.0), 126.7 (2C), 122.2, 121.3, 115.9 (2C), 114.3 (d, J=21.1), 113.2 (d, J=22.1), 103.0, 96.5, 50.4, 22.3

^{19}F NMR (376 MHz, DMSO-d_6, C_6F_6 int. std., *Appendix A.1.4*), δ, ppm: -112.2 (s)

Specific Rotation: $[\alpha]_D^{25}$ = -195.2 (c = 0.13, DMSO)

Yield: 0.123 g, 0.35 mmole, 71%

8.8.5 Synthesis of 1e[5]

(*R*)-*N*-(1-(4-Fluorophenyl)ethyl)-6-(4-methoxyphenyl)-7*H*-pyrrolo[2,3-*d*]pyrimidin-4-amine (**2e**) (0.149 g, 0.41 mmole) was dissolved with DCM (4 mL) in a dry roundbottle under Ar atmosphere. BBr_3 (ReagentPlus®, 99.9%, Sigma Aldrich) (0.40 mL, 4.2 mmole) in DCM (4 mL) was added dropwise over 1 h at 0°C. The reaction mixture was heated to r.t., and stirred for 9 h under Ar atmosphere. Water (15 mL) was added, and the mixture was extracted with ethyl acetate (3x 40 mL). The combined organic layers were washed with brine (30 mL), dried over $MgSO_4$ and concentrated. The oil that appeared was triturated with acetone (2 mL) and the colorless solid were filtrated and washed with diethyl ether (10 mL).

TLC (Alugram RP-C18, Acetone:H_2O:DEA, 60:40:0.5): R_f = 0.54

Purity: >99% (determined by HPLC, Method A))

HRMS (ESI, *Appendix B.1.5*): m/z 349.1465 (calc. $C_{20}H_{17}FN_4O$ 349.1465 M^+H)

^{1}H NMR (400 MHz, DMSO-d_6, *Appendix A.1.5*), δ, ppm: 12.97 (s, 1H, NH), 9.82 (br, 1H, OH), 9.51 (br, 1H, NH), 8.31 (s, 1H), 7.65 (d, $2H_{arom}$, J=8.7), 7.52-7.56 (m, $2H_{arom}$), 7.20-7.25 (m, $2H_{arom}$+1H), 6.89 (d, $2H_{arom}$, J=8.7), 5.38-5.40 (m, 1H), 1.65 (d, 3H, J=6.7)

^{13}C NMR (100 MHz, DMSO-d_6, *Appendix A.1.5*), δ, ppm: 161.5 (d, J=243.4), 158.0, 148.6 (2C), 142.5, 138.2, 137.5, 128.2 (d, 2C, J=7.0), 126.7 (2C), 121.3, 116.0 (2C), 115.4 (d, 2C, J=22.1), 102.9, 96.6, 50.2, 22.4

^{19}F NMR (376 MHz, DMSO-d_6, C_6F_6 int. std., *Appendix A.1.5*), δ, ppm: -114.6 (s)

Specific Rotation: $[\alpha]_D^{25}$ = -142.2 (*c* = 0.12, DMSO)

Yield: 0.075 g, 0.22 mmole, 54%

8.8.6 Synthesis of 1f

N-(2-Fluorobenzyl)-6-(4-methoxyphenyl)-7*H*-pyrrolo[2,3-*d*]pyrimidin-4-amine (**2f**) (0.157 g, 0.45 mmole) was dissolved with DCM (3 mL) in a dry roundbottle under argon atmosphere. BBr_3 (ReagentPlus®, 99.9%, Sigma Aldrich) (0.44 mL, 4.6 mmole) in DCM (4 mL) was added dropwise over 1 h at 0°C. The reaction mixture was heated to r.t., and stirred for 24 h under Ar atmosphere. Water (15 mL) was added, and the mixture was extracted with ethyl acetate (3x 40 mL). The combined organic layers were washed with brine (20 mL), dried over $MgSO_4$ and evaporated *in vacuo*. The oil that appeared was triturated with acetone (2 mL) and the colorless solid were filtrated and washed with diethyl ether (10 mL).

TLC (Alugram RP-C18, Acetone:H_2O:DEA, 60:40:0.5): R_f = 0.41

Purity: 98% (determined by HPLC, Method A))

HRMS (ESI, *Appendix B.1.6*): m/z 335.1306 (calc. $C_{19}H_{16}FN_4O$ 335.1308 M^+H)

^1H NMR (400 MHz, DMSO-d_6, *Appendix A.1.6*), δ, ppm: 12.94 (br, 1H, NH), 9.82 (br, 1H, OH), 9.60 (br, 1H, NH), 8.35 (s, 1H), 7.64 (d, $2H_{arom}$, J=8.7), 7.45-7.48 (m, $1H_{arom}$), 7.40-7.44 (m, $1H_{arom}$), 7.29-7.31 (m, $1H_{arom}$), 7.21-7.27 (m, $1H_{arom}$), 7.11 (s, 1H), 6.88 (d, $2H_{arom}$, J=8.7), 4.86 (d, 2H, J=3.5)

^{13}C NMR (100 MHz, DMSO-d_6, *Appendix A.1.6*), δ, ppm: 160.4 (d, J=245.5), 158.0, 149.8, 147.4, 142.4, 137.6, 130.0 (d, J=7.0), 129.6, 126.8 (2C), 124.7, 123.5 (d, J=13.1), 121.2, 116.0 (2C), 115.5 (d, J=21.1), 103.0, 96.3, 39.5

^{19}F NMR (376 MHz, DMSO-d_6, C_6F_6 int. std., *Appendix A.1.6*), δ, ppm: -117.1 (s)

Yield: 0.083 g, 0.25 mmole, 56%

8.8.7 Synthesis of 1g

N-(3-Fluorobenzyl)-6-(4-methoxyphenyl)-7*H*-pyrrolo[2,3-*d*]pyrimidin-4-amine (**2g**) (0.139 g, 0.40 mmole) was dissolved with DCM (2.5 mL) in a dry roundbottle under Ar atmosphere. BBr_3 (ReagentPlus®, 99.9%, Sigma Aldrich) (0.39 mL, 4.0 mmole) in DCM (3 mL) was added dropwise over 1 h at 0°C. The roundbottle was heated to r.t., and it stirred for 24 h under Ar atmosphere. Water (15 mL) was added, and the mixture was extracted with ethyl acetate (3x 40 mL). The combined organic layers were washed with brine (20 mL), dried over $MgSO_4$ and evaporated *in vacuo*. The oil that appeared was triturated with acetone (2 mL) and the colorless solid were filtrated and washed with diethyl ether (10 mL).

TLC (Alugram RP-C18, Acetone:H_2O:DEA, 60:40:0.5): R_f = 0.40

Purity: >99% (determined by HPLC, Method A))

HRMS (ESI, *Appendix B.1.7*): m/z 335.1305 (calc. $C_{19}H_{16}FN_4O$ 335.1308 M^+H)

^1H NMR (400 MHz, DMSO-d_6, *Appendix A.1.7*), δ, ppm: 12.73 (br, 1H, NH), 9.78 (s, 1H, OH), 9.31 (br, 1H, NH), 8.29 (s, 1H), 7.64 (d, $2H_{arom}$, J=8.7), 7.40-7.46 (m,

$1H_{arom}$), 7.25-7.27 (m, $2H_{arom}$), 7.12-7.17 (m, $1H_{arom}$), 7.04 (s, 1H), 6.87 (d, $2H_{arom}$, J=8.7), 4.82 (d, 2H, J=4.9)

^{13}C NMR (100 MHz, DMSO-d_6, *Appendix A.1.7*), δ, ppm: 161.1 (d, J=243.4), 158.0, 149.6, 147.4, 142.2, 139.6, 137.7, 130.7 (d, J=8.0), 126.8 (2C), 123.5, 121.2, 116.0 (2C), 114.5 (d, J=21.1), 114.4 (d, J=21.1), 103.0, 96.4, 44.3

^{19}F NMR (376 MHz, DMSO-d_6, C_6F_6 int. std., *Appendix A.1.7*), δ, ppm: -112.5 (s)

Yield: 0.044 g, 0.13 mmole, 33%

8.8.8 Synthesis of 1h

N-(4-Fluorobenzyl)-6-(4-methoxyphenyl)-7*H*-pyrrolo[2,3-*d*]pyrimidin-4-amine (**2h**) (0.168 g, 0.48 mmole) was dissolved with DCM (4 mL) in a dry roundbottle under Ar atmosphere. BBr_3 (ReagentPlus®, 99.9%, Sigma Aldrich) (0.47 mL, 4.9 mmole) in DCM (3.5 mL) was added dropwise over 1 h at 0°C. The solution was heated to r.t., and stirred for 12 h under Ar atmosphere before water (15 mL) was added. Then it was extracted with ethyl acetate (3x 40 mL) and all the combined organic layers were collected. They were washed with brine (20 mL), dried over $MgSO_4$ and evaporated *in vacuo*. The oil that appeared was triturated with acetone (2 mL) and the colorless solid were filtrated and washed with diethyl ether (10 mL).
TLC (Alugram RP-C18, Acetone:H_2O:DEA, 60:40:0.5): R_f = 0.43

Purity: 98% (determined by HPLC, Method A))

HRMS (ESI, *Appendix B.1.8*): m/z 335.1303 (calc. $C_{19}H_{16}FN_4O$ 335.1308 M^+H)

^1H NMR (400 MHz, DMSO-d_6, *Appendix A.1.8*), δ, ppm: 13.01 (s, 1H, NH), 9.81 (br, 1H, OH), 9.76 (br, 1H, NH), 8.35 (s, 1H), 7.65 (d, $2H_{arom}$, J=8.7), 7.48-7.51 (m, $2H_{arom}$), 7.21-7.27 (m, $2H_{arom}$), 7.14 (d, 1H, J=2.0), 6.88 (d, $2H_{arom}$, J=8.7), 4.77 (s, 2H)

^{13}C NMR (100 MHz, DMSO-d_6, *Appendix A.1.8*), δ, ppm: 161.7 (d, J=243.4), 158.0, 149.4, 147.5, 142.1, 137.6, 132.7, 129.7 (d, 2C, J=8.0), 126.8 (2C), 121.2, 116.0 (2C), 115.4 (d, 2C, J=21.1), 102.8, 96.5, 44.2

^{19}F NMR (376 MHz, DMSO-d_6, C_6F_6 int. std., *Appendix A.2.3*), δ, ppm: -114.3 (s)

Yield: 0.114 g, 0.34 mmole, 71%

References

1. Ogiso, H., Ishitani, R., Nureki, O., Fukai, S., Yamanaka, M., Kim, J.-H., Saito, K., Sakamoto, A., Inoue, M., Shirouzu, M., and Yokoyama, S., *Cell*, 110, **2002,** 775-787

2. http://www.rcsb.org/pdb/explore/images.do?structureId=1IVO, Last Visited: **June 13th, 2009**

3. Bednarz, M.S., Kanamarlapudi, R.C., and Wu, W., US 20080097098A1 **2008**

4. Cai, X., WO 2008033747A9 **2008**

5. Cai, X., Qian, C., and Gould, S., WO 2008033745A2 **2008**

6. Christensen, J.G. and Zou, Y., WO 2007066187A2 **2007**

7. Grotzfeld, R.M., Patel, H.K., Mehta, S.A., Milanov, Z.V., Lai, A.G., and Lockhart, D.J., US 2005153989A1 **2005**

8. Portmann, R. and Scherrer, W., WO 2007017468A2 **2007**

9. Tharaux, P.L., WO 2008053270A2 **2008**

10. Traxler, P., Bold, G., Brill, W.K.-D., and Frei, J., WO 9702266A1 **1997**

11. Traxler, P., Bold, G., Brill, W.K.-D., and Frei, J., WO 9702266A1 **1997**

12. Baselga, J., *J. Clin. Oncol.*, 19, **2001,** 41-44

13. Caravatti, G., Bruggen, J., Buchdunger, E., Cozens, R., Furet, P., Lydon, N., O'Reilly, T., and Traxler, P., *ACS Symp. Ser.*, 796, **2001,** 231-244

14. Traxler, P. and Furet, P., *Pharmacol. Ther.*, 82, **1999,** 195-206

15. Traxler, P., Furet, P., and Brill, W., EP 682027A1 **1995**

16. Hagmann, W.K., *J. Med. Chem.*, 51, **2008,** 4359-4369

17. Muller, K., Faeh, C., and Diederich, F., *Science*, 317, **2007,** 1881-1886

18. Swinson, J., *PharmaChem*, 4, **2005,** 26-30

19. Isanbor, C. and O'Hagan, D., *J. Fluorine Chem.*, 127, **2006,** 303-319

20. http://www.forbes.com/, Last Visited: **June 10th, 2009**

21. Bondi, A., *J. Phys. Chem.* , 68, **1964,** 441-451

22. Carey, F.A. and Sundberg, R.J., *Advanced Organic Chemistry, Part A: Structure and Mechanisms*, Fifth ed., Springer, **2007**

23. Kirsch, P., *Modern Fluoroorganic Chemistry*, First ed., Wiley-VCH, **2004**

24. Aylward, G. and Findlay, T., *Si Chemical Data*, Fifth ed., John Wiley & Sons, **2002**

25. Rowley, M., Hallett, D.J., Goodacre, S., Moyes, C., Crawforth, J., Sparey, T.J., Patel, S., Marwood, R., Patel, S., Thomas, S., Hitzel, L., O'Connor, D., Szeto, N., Castro, J.L., Hutson, P.H., and MacLeod, A.M., *J. Med. Chem.*, 44, **2001,** 1603-1614

26. Smart, B.E., *J. Fluorine Chem.*, 109, **2001,** 3-11

27. Purser, S., Moore, P.R., Swallow, S., and Gouverneur, V., *Chem. Soc. Rev.*, 37, **2008,** 320-330

28. Rosenblum, S.B., Huynh, T., Afonso, A., Davis, H.R., Yumibe, N., Clader, J.W., and Burnett, D.A., *J. Med. Chem.*, 41, **1998,** 973-980

29. Park, B.K., Kitteringham, N.R., and O'Neill, P.M., *Annu. Rev. Pharmacol. Toxicol.*, 41, **2001,** 443-470

30. Becker, W.M., Kleinsmith, L.J., and Hardin, J., *The World of the Cell*, Sixth ed., Pearson Education Inc., **2006**

31. http://www.uic.edu/classes/bios/bios100/mike/spring2003/lect07.htm, Last Visited: **28. November 2008**

32. Fry, D.W., *Expert Opin. Invest. Drugs*, 3, **1994,** 577-595

33. Levitzki, A. and Gazit, A., *Science*, 267, **1995,** 1782-1788

34. Spada, A.P. and Myers, M.R., *Expert Opin. Ther. Pat.*, 5, **1995,** 805-817

35. Traxler, P.M., Furet, P., Mett, H., Buchdunger, E., Meyer, T., and Lydon, N., *J. Med. Chem.*, 39, **1996,** 2285-2292

36. Traxler, P.M., *Expert Opin. Ther. Pat.*, 7, **1997,** 571-588

37. Manley, P.W., Cowan-Jacob, S.W., Buchdunger, E., Fabbro, D., Fendrich, G., Furet, P., Meyer, T., and Zimmermann, J., *Eur. J. Cancer Prev.*, 38, **2002,** S19-S27

38. Grosios, K. and Traxler, P., *Drugs Fut.*, 28, **2003,** 679-697

39. Fabbro, D., Ruetz, S., Buchdunger, E., Cowan-Jacob, S.W., Fendrich, G., Liebetanz, J., Mestan, J.r., O'Reilly, T., Traxler, P., Chaudhuri, B., Fretz, H., Zimmermann, J.r., Meyer, T., Caravatti, G., Furet, P., and Manley, P.W., *Pharmacol. Ther.*, 93, **2002,** 79-98

40. Gangjee, A., Namjoshi, O.A., Yu, J., Ihnat, M.A., Thorpe, J.E., and Warnke, L.A., *Bioorg. Med. Chem.*, 16, **2008,** 5514-5528

41. Personal Communication, Prous Science Integrity, **2008**

42. Rucci, N., Susa, M., and Teti, A., *Anti-Cancer Agents Med. Chem.*, 8, **2008,** 342-349

43. Hamid, O., *J. Am. Pharm. Assoc.*, 44, **2004,** 52-58

44. Ullrich, A., Coussens, L., Hayflick, J.S., Dull, T.J., Gray, A., Tam, A.W., Lee, J., Yarden, Y., Libermann, T.A., Schlessinger, J., Downward, J., Mayes, E.L.V., Whittle, N., Waterfield, M.D., and Seeburg, P.H., *Nature*, 309, **1984,** 418-425

45. Hirsch, F.R., Herbst, R.S., Olsen, C., Chansky, K., Crowley, J., Kelly, K., Franklin, W.A., Bunn, P.A., Jr., Varella-Garcia, M., and Gandara, D.R., *J. Clin. Oncol.*, 26, **2008,** 3351-3357

46. http://www.who.int/mediacentre/factsheets/fs297/en/index.html, Last Visited: **November 19th, 2008**

47. Johnston, J.B., Navaratnam, S., Pitz, M.W., Maniate, J.M., Wiechec, E., Baust, H., Gingerich, J., Skliris, G.P., Murphy, L.C., and Los, M., *Curr. Med. Chem.*, 13, **2006,** 3483-3492

48. Miyamoto, N., Sugita, K., Goi, K., Inukai, T., Iijima, K., Tezuka, T., Kojika, S., Nakamura, M., Kagami, K., and Nakazawa, S., *Leukemia*, 15, **2001,** 1758-1768

49. http://clinicaltrials.gov/, Last Visited: **24. November 2008**

50. Murray, H.W., Pepin, J., Nutman, T.B., Hoffman, S.L., and Mahmoud, A.A.F., *BMJ*, 320, **2000,** 490-494

51. Liu, L.X. and Weller, P.F., *N. Engl. J. Med.*, 334, **1996,** 1178-1184

52. Parsons, M., Ledbetter, J., and Schieven, G.L., EP 507256A2 **1992**

53. Mensa-Wilmot, K., WO 2008066755A2 **2008**

54. Franklin, R.J.M. and Zhao, C., *Nat. Med.*, 12, **2006,** 889-890

55. Tapinos, N., Ohnishi, M., and Rambukkana, A., *Nat. Med.*, 12, **2006,** 961-966

56. Goswami, S. and Adak, A.K., *Tetrahedron Lett.*, 43, **2002,** 8371-8373

57. Larhed, M. and Olofsson, K., *Microwave Methods in Organic Synthesis*, First ed., Springer, **2006**

58. Wuts, P.G.M. and Greene, T.W., *Greene's Protective Groups in Organic Synthesis*, Fourth ed., Wiley, **2006**

59. Benton, F.L. and Dillon, T.E., *J. Am. Chem. Soc.*, 64, **1942,** 1128-1129

60. Joergensen, A., Girgis, N.S., and Pedersen, E.B., *Liebigs Ann. Chem.*, 1985, **1985,** 142-148

61. Iwamura, H., Masuda, N., Koshimizu, K., and Matsubara, S., *Phytochemistry*, 18, **1979,** 217-222

62. Martin-Kohler, A., Widmer, J., Bold, G., Meyer, T., Sèquin, U., and Traxler, P., *Helv. Chim. Acta*, 87, **2004,** 956-975

63. Dolezal, K., Popa, I., Krystof, V., SpÌchal, L.s., FojtÌkov·, M., Holub, J., Lenobel, R., Schm¸lling, T., and Strnad, M., *Bioorg. Med. Chem.*, 14, **2006,** 875-884

64. Fujii, T., Ohba, M., Kawamura, H., Nakashio, Y., Honda, K., and Matsubara, S., *Chem. Pharm. Bull.*, 42, **1994,** 1045-1049

65. Pal, B., Jaisankar, P., and Giri, V.S., *Synth. Commun.* , 34, **2004,** 1317 - 1323

66. Silverstein, R.M., Webster, F.X., and Kiemle, D.J., *Spectrometric Identification of Organic Compounds*, Seventh ed., John Wiley & Sons, Inc., **2005**

67. Dai, Q., Gao, W., Liu, D., Kapes, L.M., and Zhang, X., *J. Org. Chem.*, 71, **2006,** 3928-3934

68. Therkelsen, F.D., Rottlander, M., Thorup, N., and Pedersen, E.B., *Org. Lett.*, 6, **2004,** 1991-1994

69. Keil, S., Glien, M., Schaefer, H.-L., Wendler, W., Bernardelli, P., Terrier, C., and Ronan, B., WO 2006029699A1 **2006**

70. Traxler, P., Green, J., Mett, H., Sequin, U., and Furet, P., *J. Med. Chem.*, 42, **1999,** 1018-1026

71. http://www.isotope.com/cil/products/images/nmrchart.pdf, Last Visited: **14. November 2008**

72. Vargov, A., Hrncarikov·, K., VÈgh, D., Lukes, V., Fedorko, P., and Rapta, P., *Electrochim. Acta*, 52, **2007,** 7885-7894

73. Collins, D.J., *J. Chem. Soc.*, **1963,** 1337-1339

74. Kobayashi, T., Inoue, T., Nishino, S., Fujihara, Y., Oizumi, K., and Kimura, T., *Chem. Pharm. Bull.*, 43, **1995,** 797-817

75. Toja*, E., Depaoli, A., Tuan, G., and Kettenring, J., *Synthesis*, **1987,** 272-274

Appendices

Page

Appendix A – NMR Spectra

A.1 – NMR Spectra of Compounds 1a-h

A.1.1 – NMR spectra of Compound 1a

^{1}H – Spectrum of Compound 1a

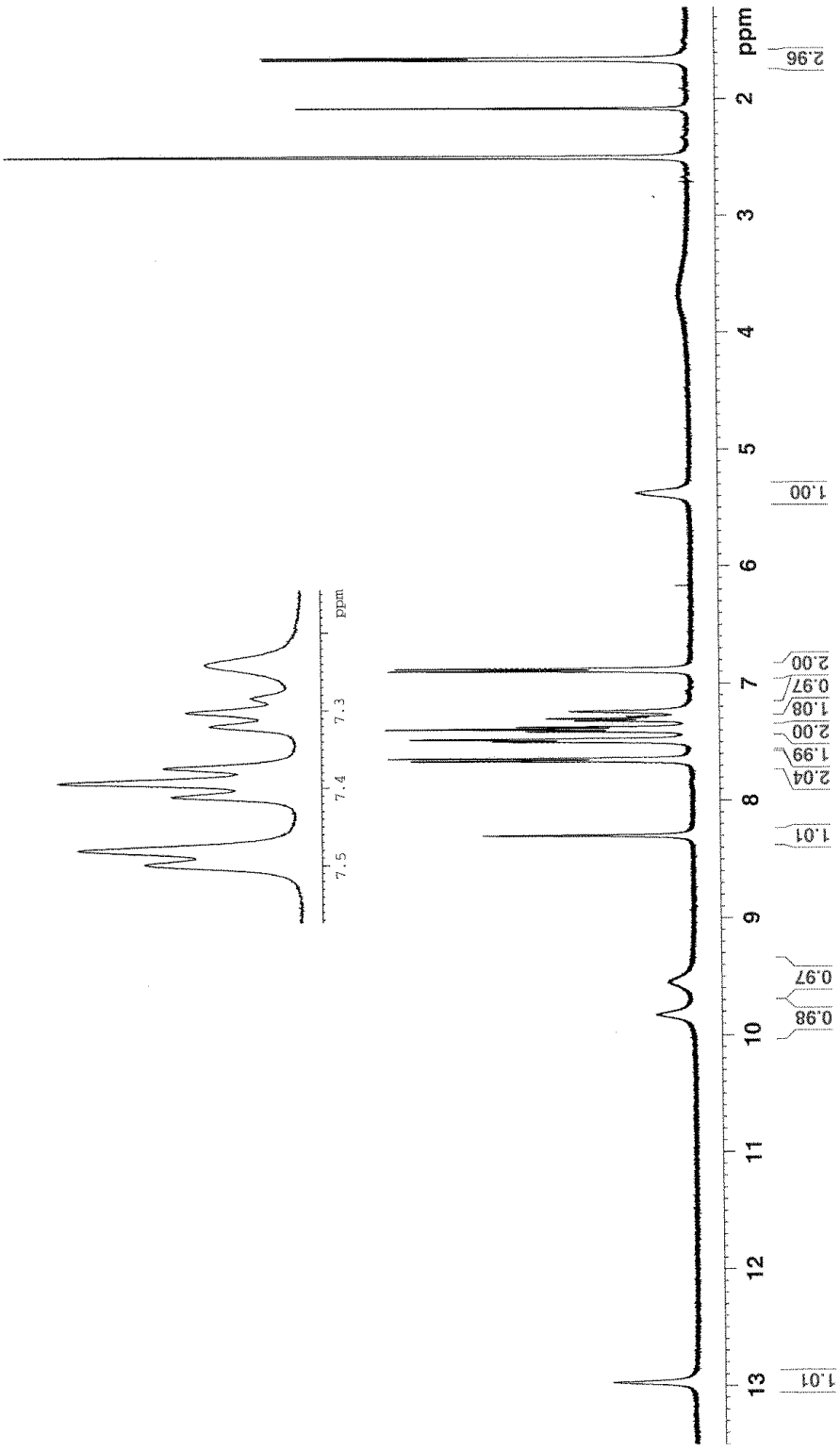

Residual peaks of DMSO, aceton and H_2O are found at 2.50 ppm, 2.09 ppm and 3.33 ppm, respectively.

^{13}C – Spectrum of Compound 1a

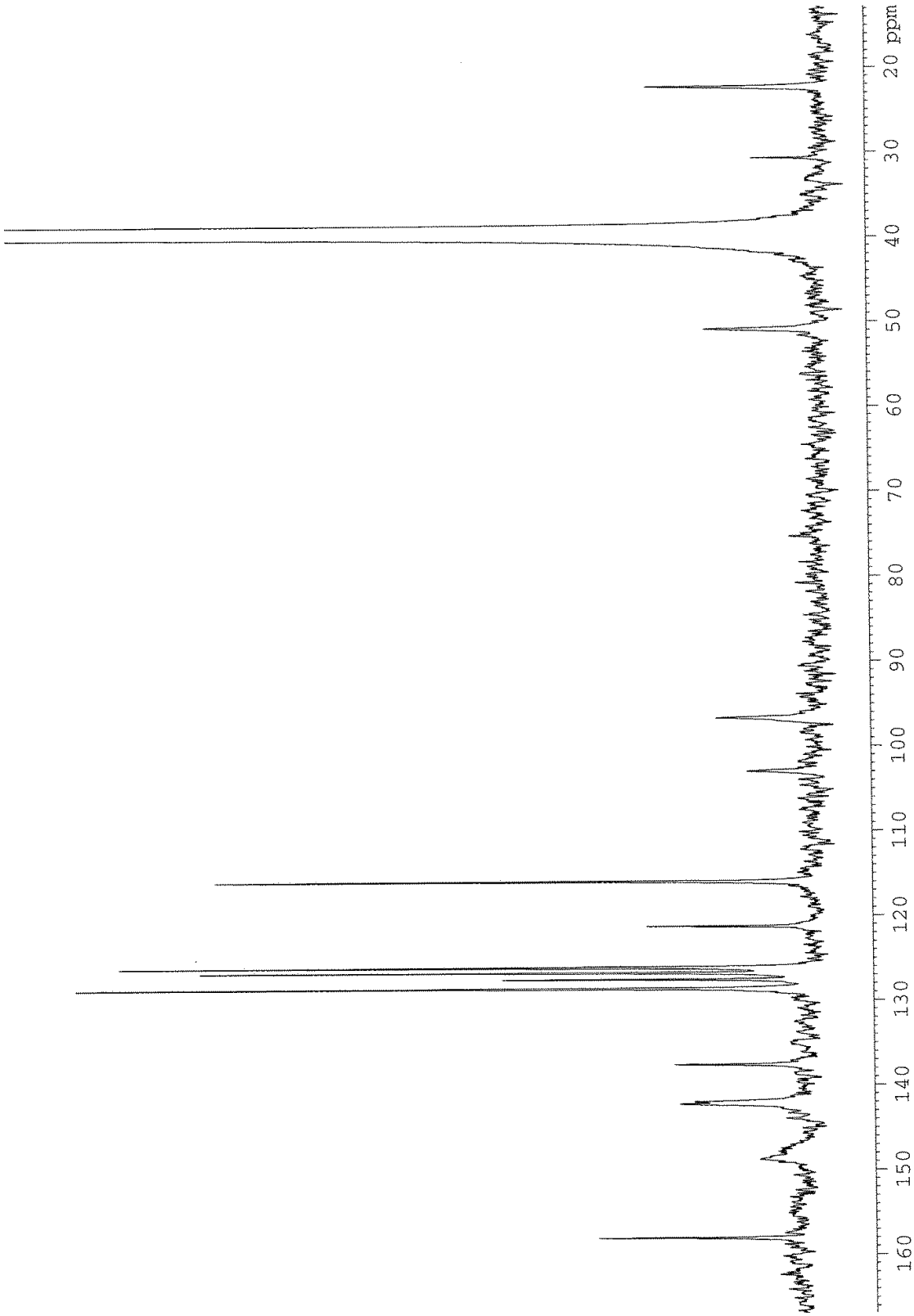

Residual peak of DMSO and acetone is found at 39.51 ppm and 30.56 ppm, respectively.

COSY, 2D Spectrum of Compound 1a

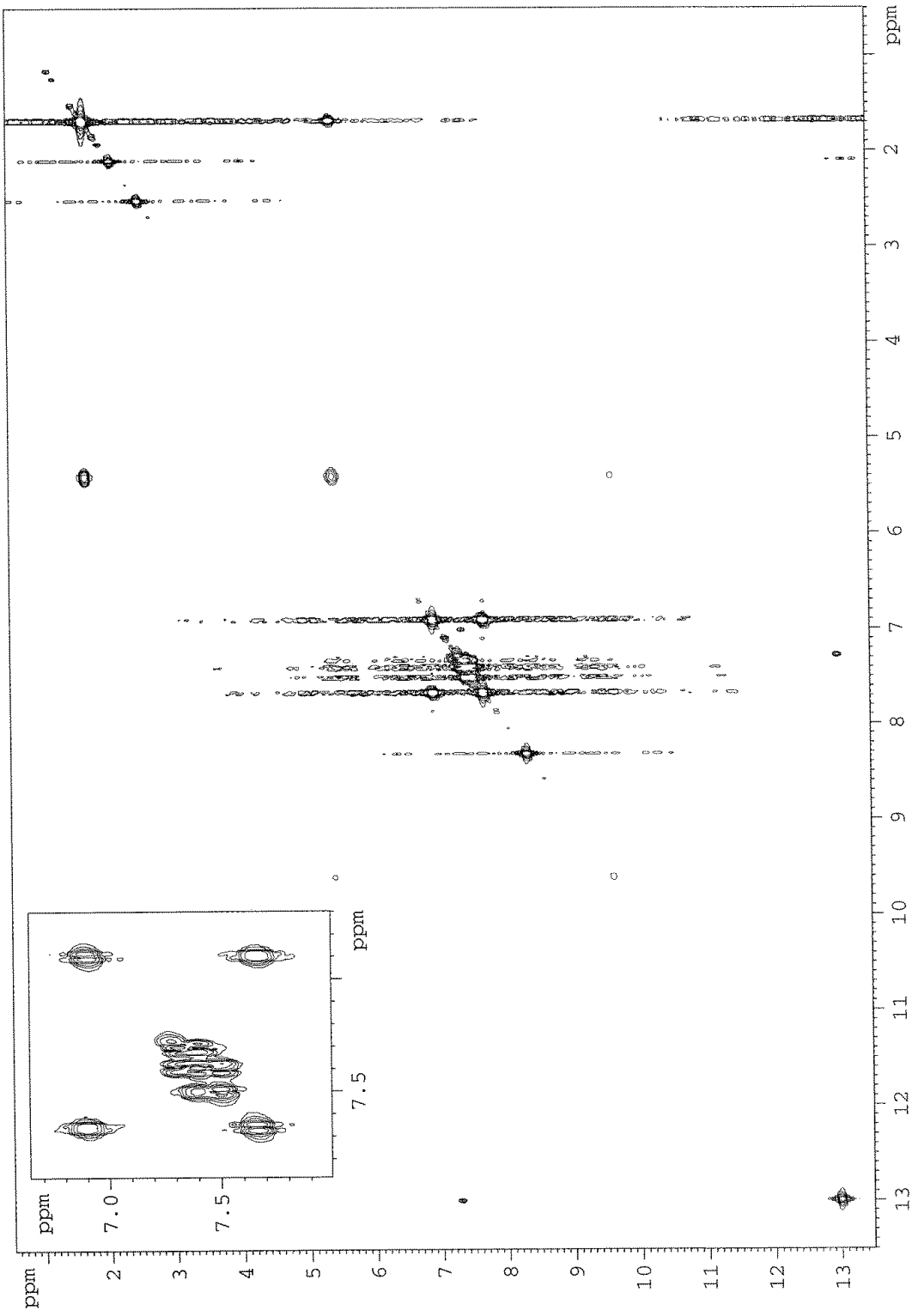

HSQC, 2D Spectrum of Compound 1a

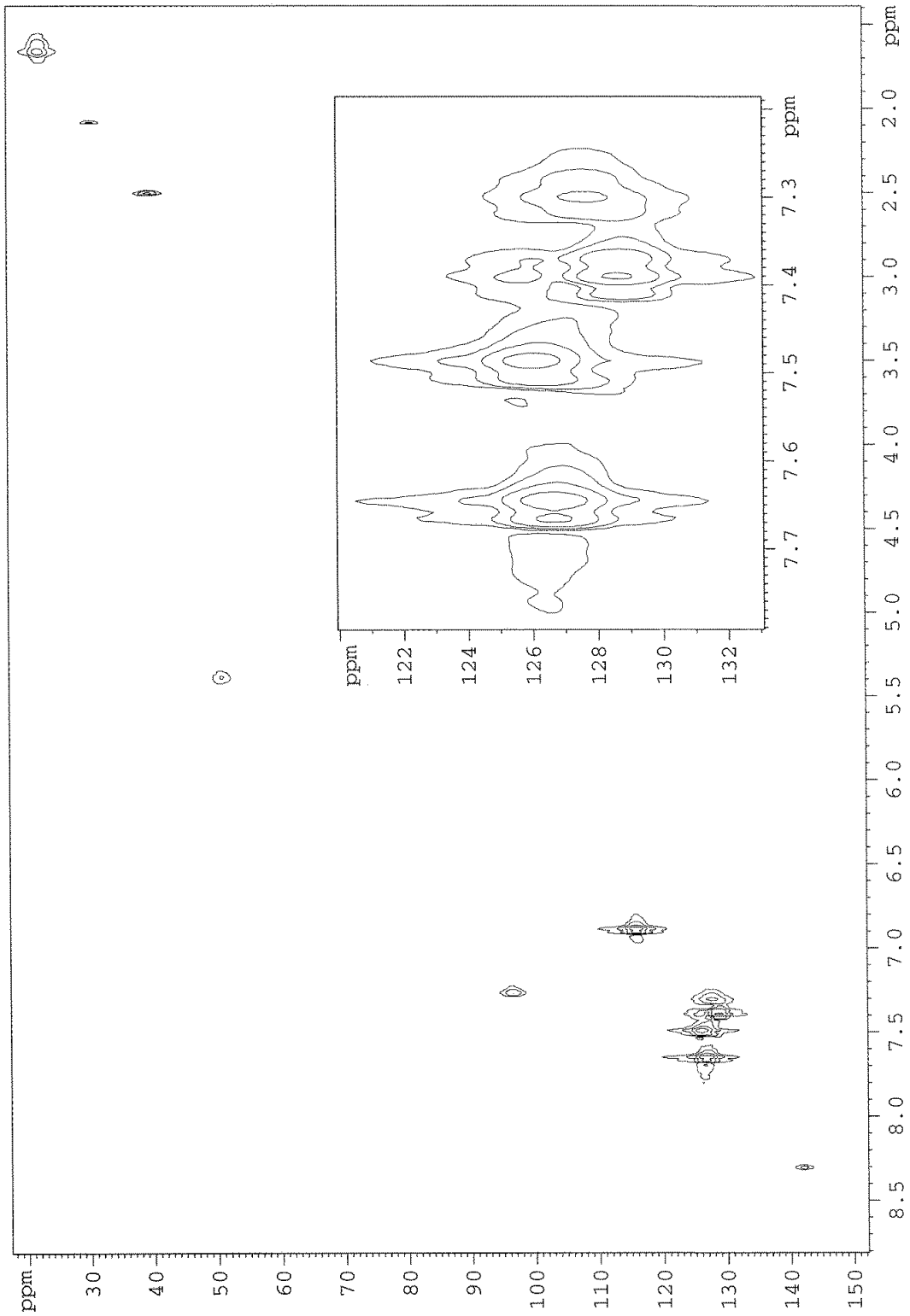

HMBC, 2D Spectrum of Compound 1a

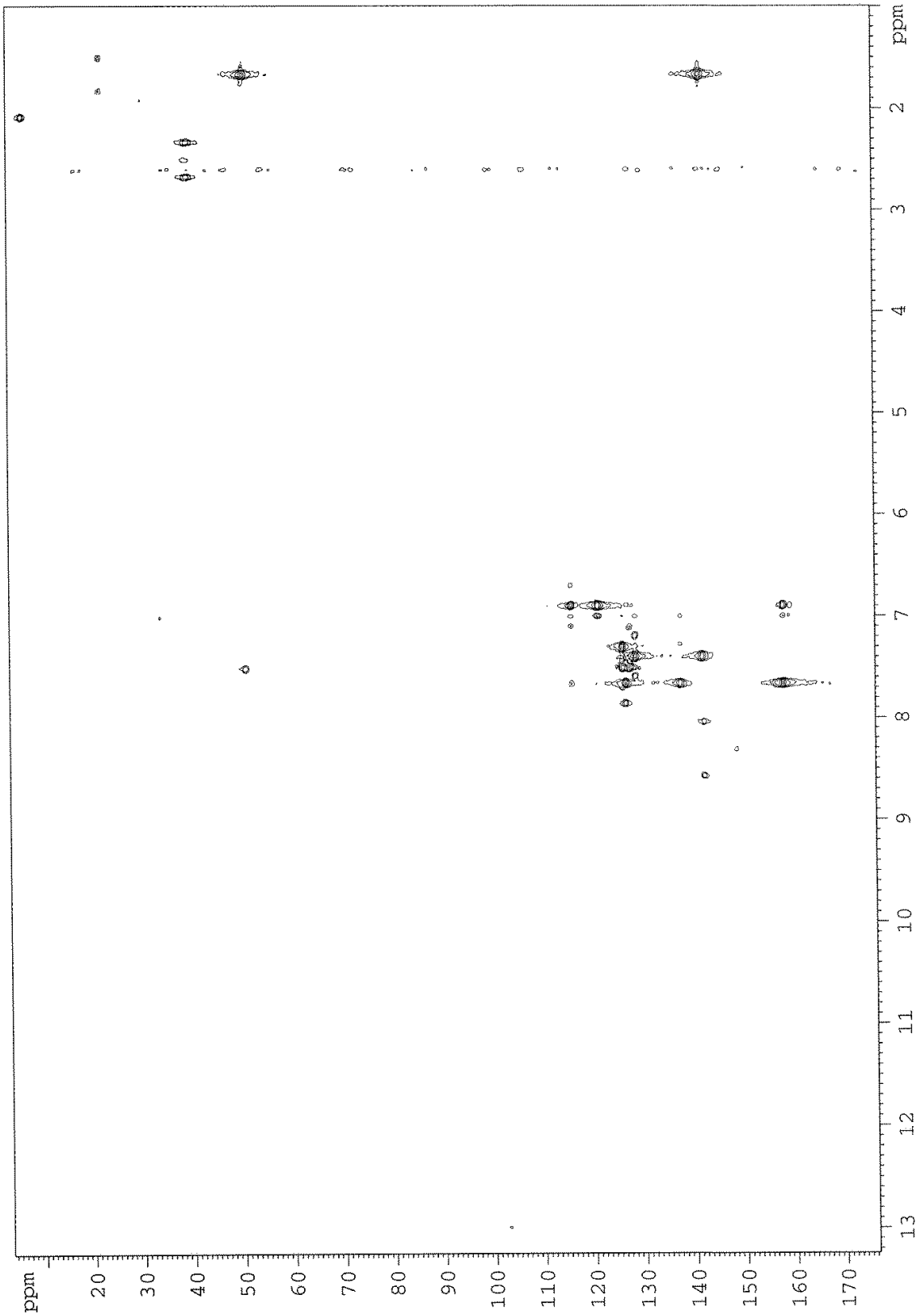

A.1.2 – NMR spectra of Compound 1b

^{1}H – Spectrum of Compound 1b

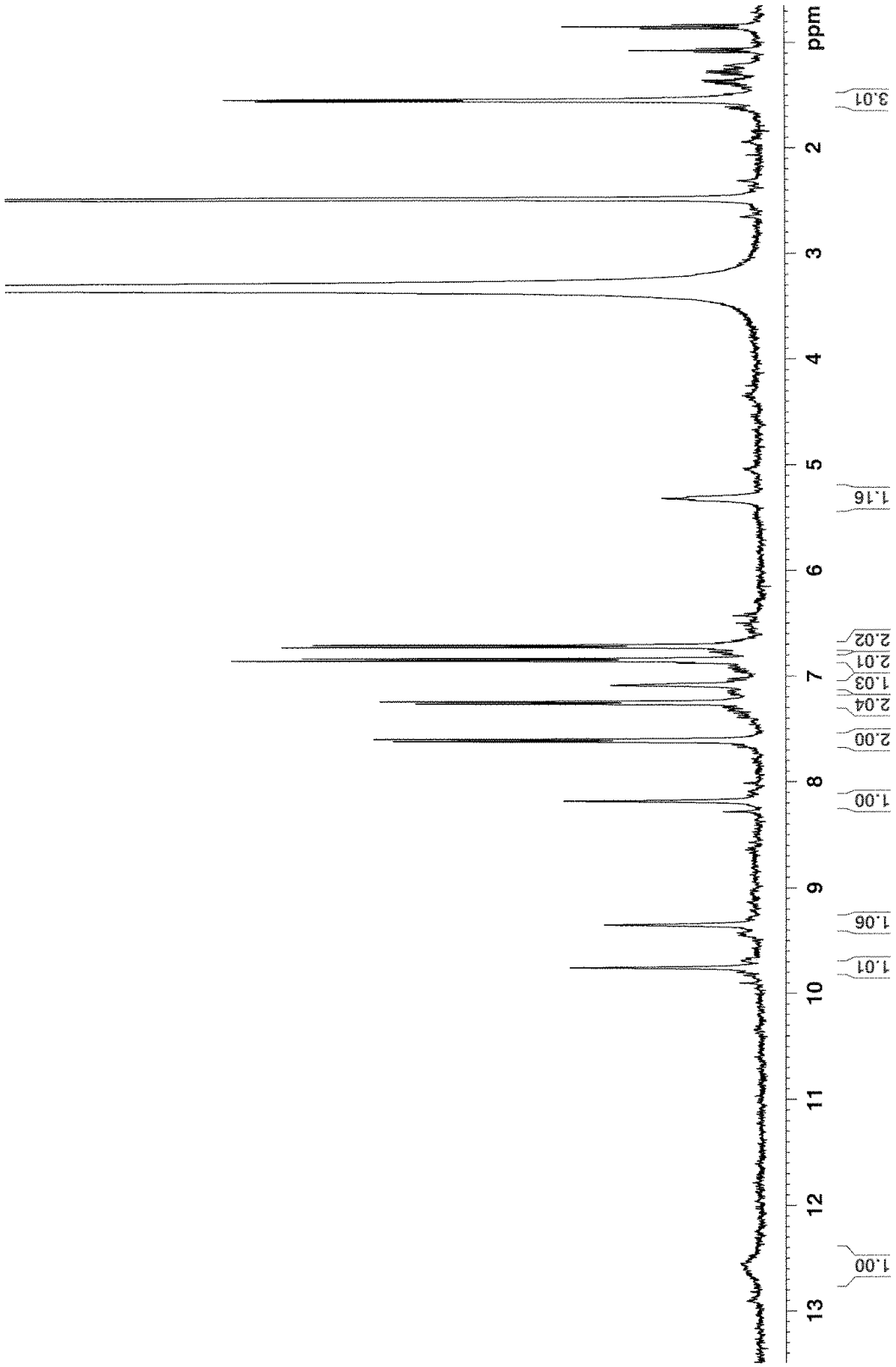

Residual peaks of: DMSO (2.50 ppm), n-pentane (0.86 and 1.27 ppm), diethyl ether (1.09 ppm) and H_2O (3.33 ppm).

^{13}C – Spectrum of Compound 1b

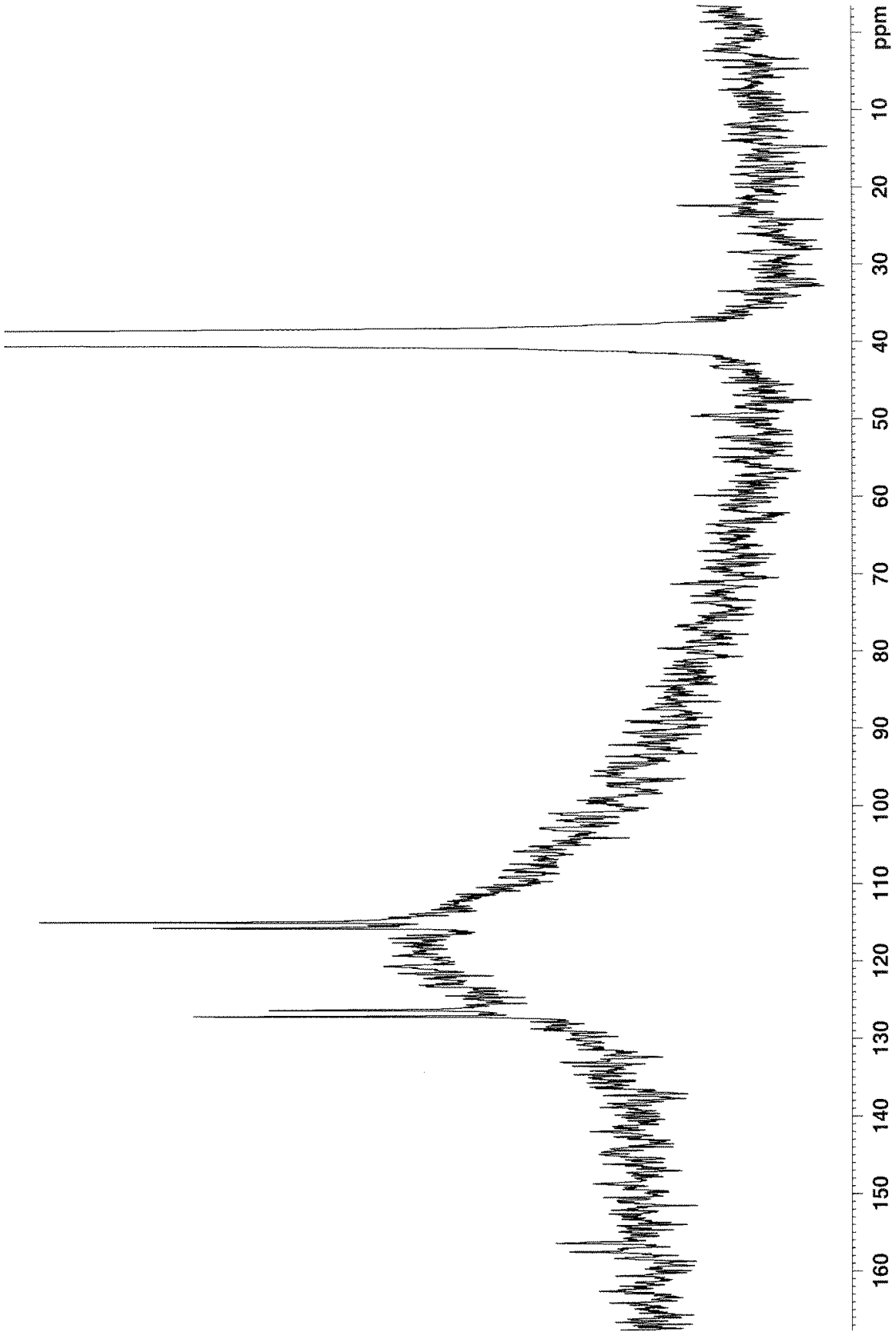

Residual peak of DMSO is found at 39.51 ppm.

COSY, 2D Spectrum of Compound 1b

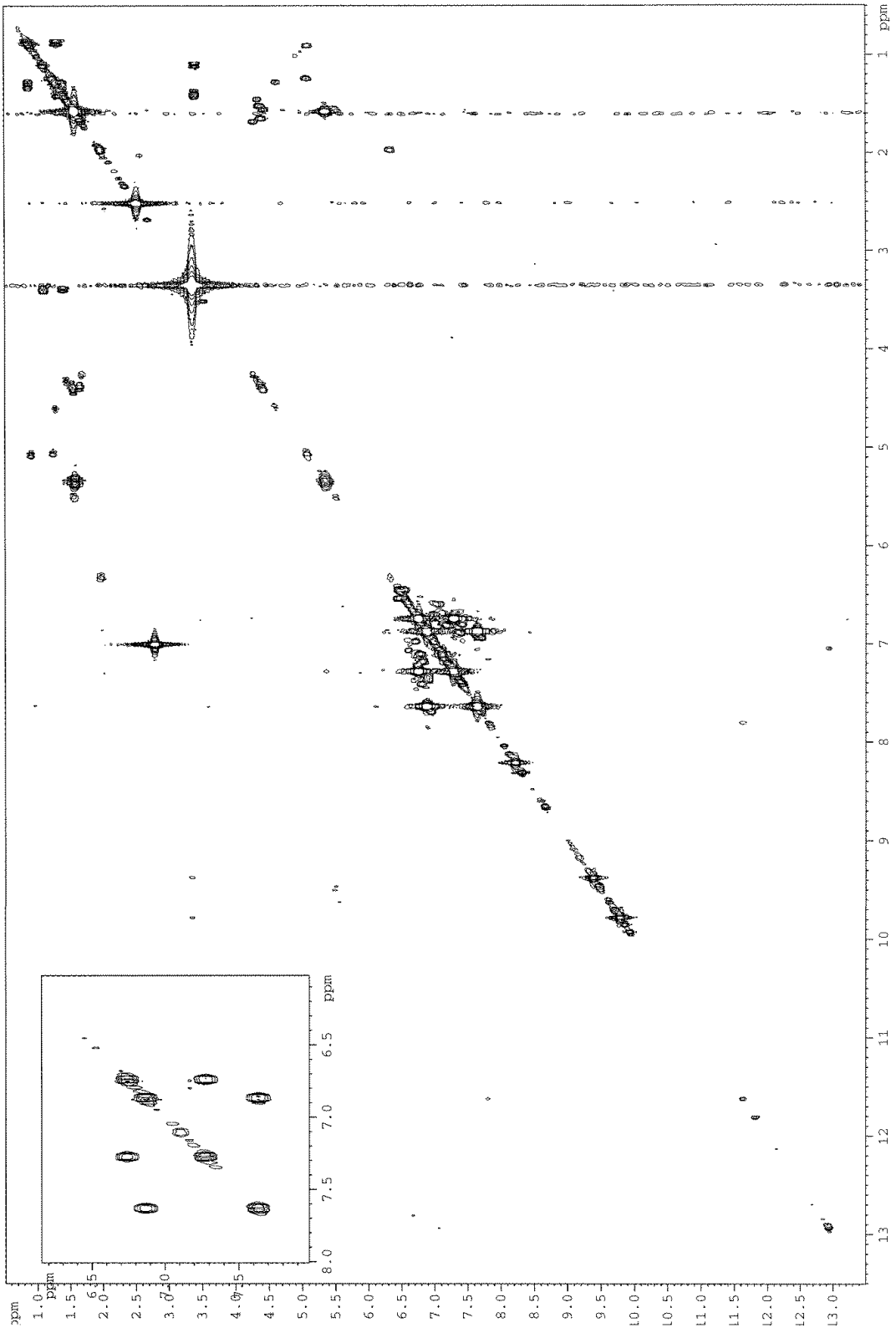

HSQC, 2D Spectrum of Compound 1b

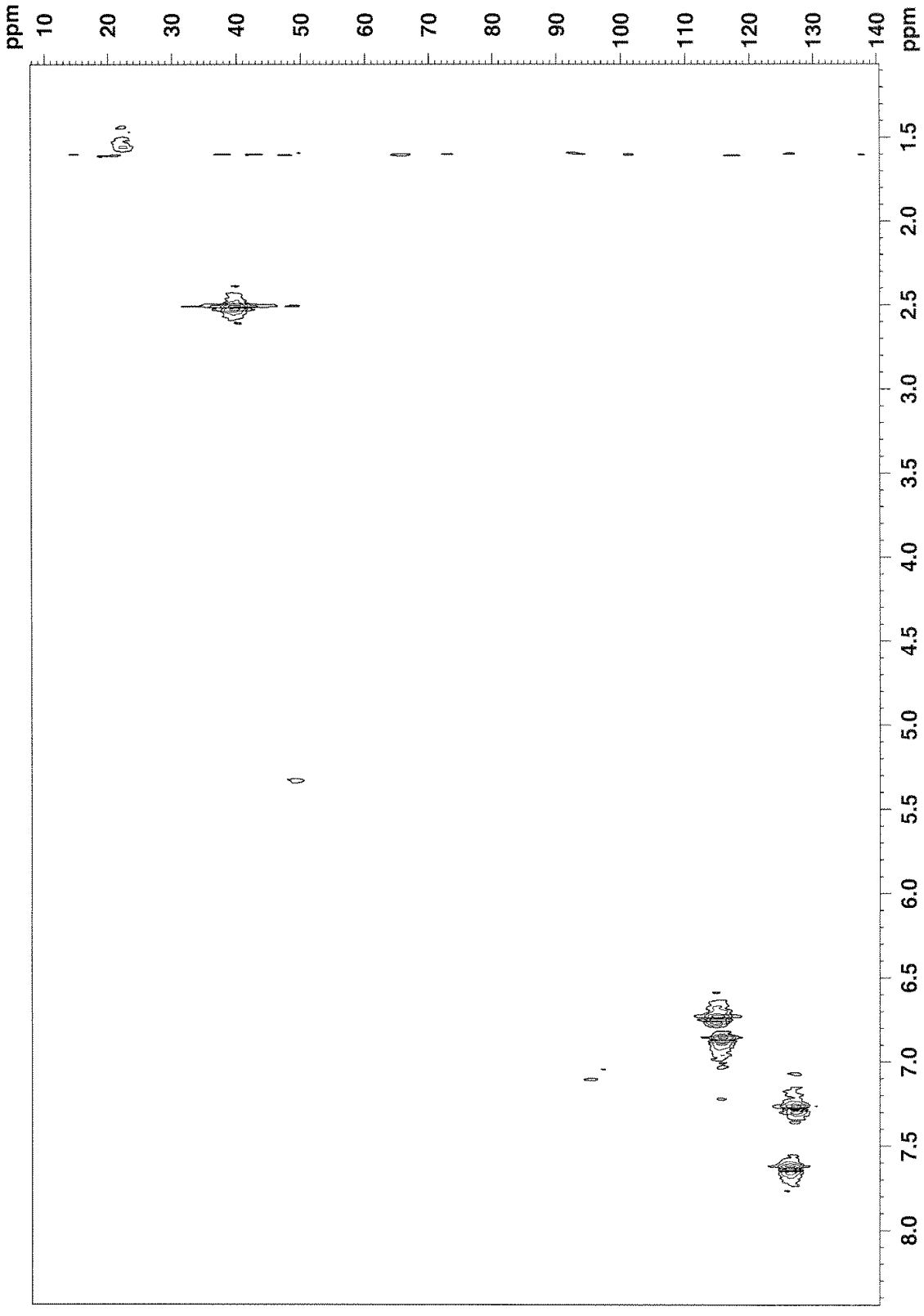

HMBC, 2D Spectrum of Compound 1b

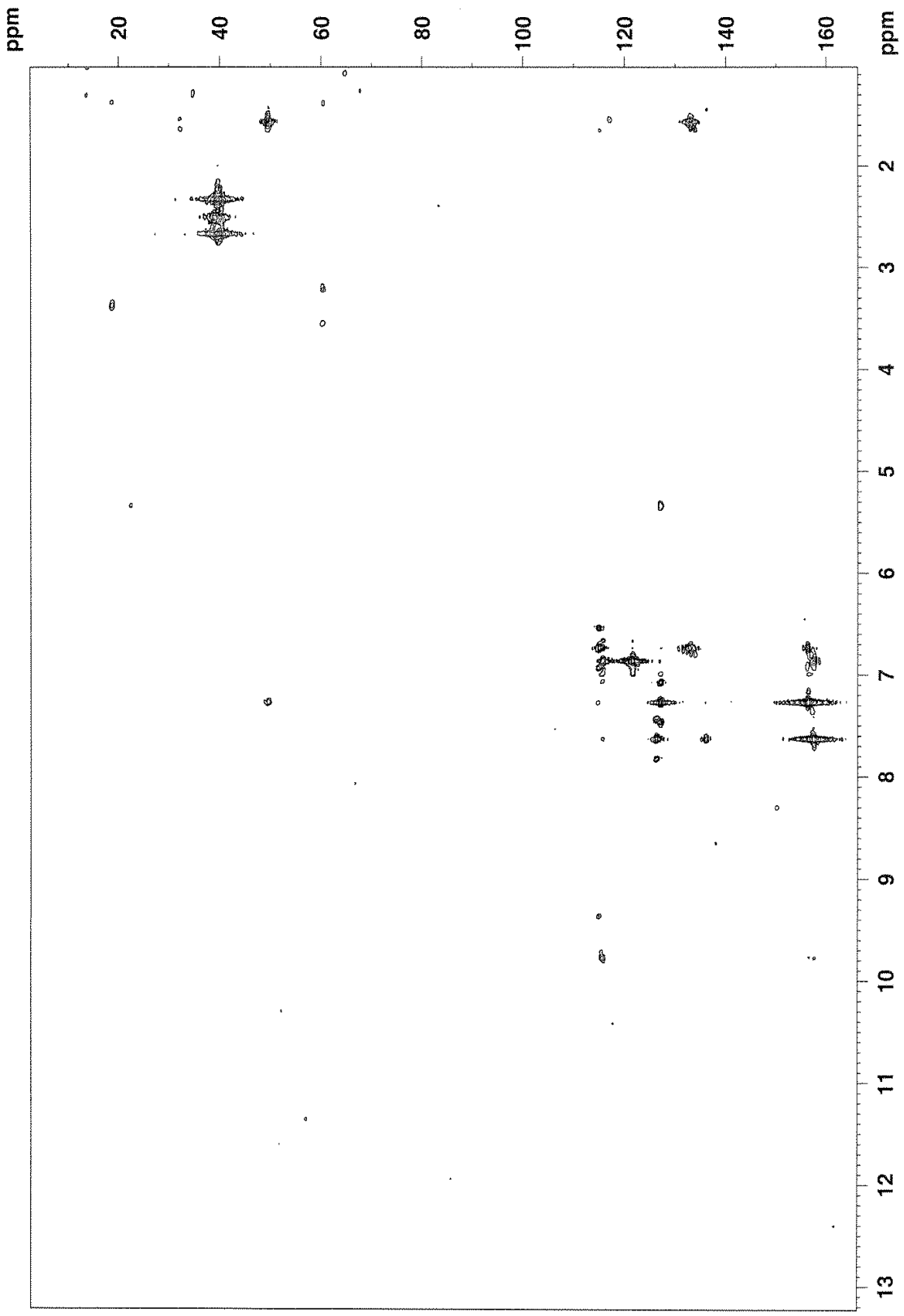

A.1.3 – NMR spectra of Compound 1c

^{1}H – Spectrum of Compound 1c

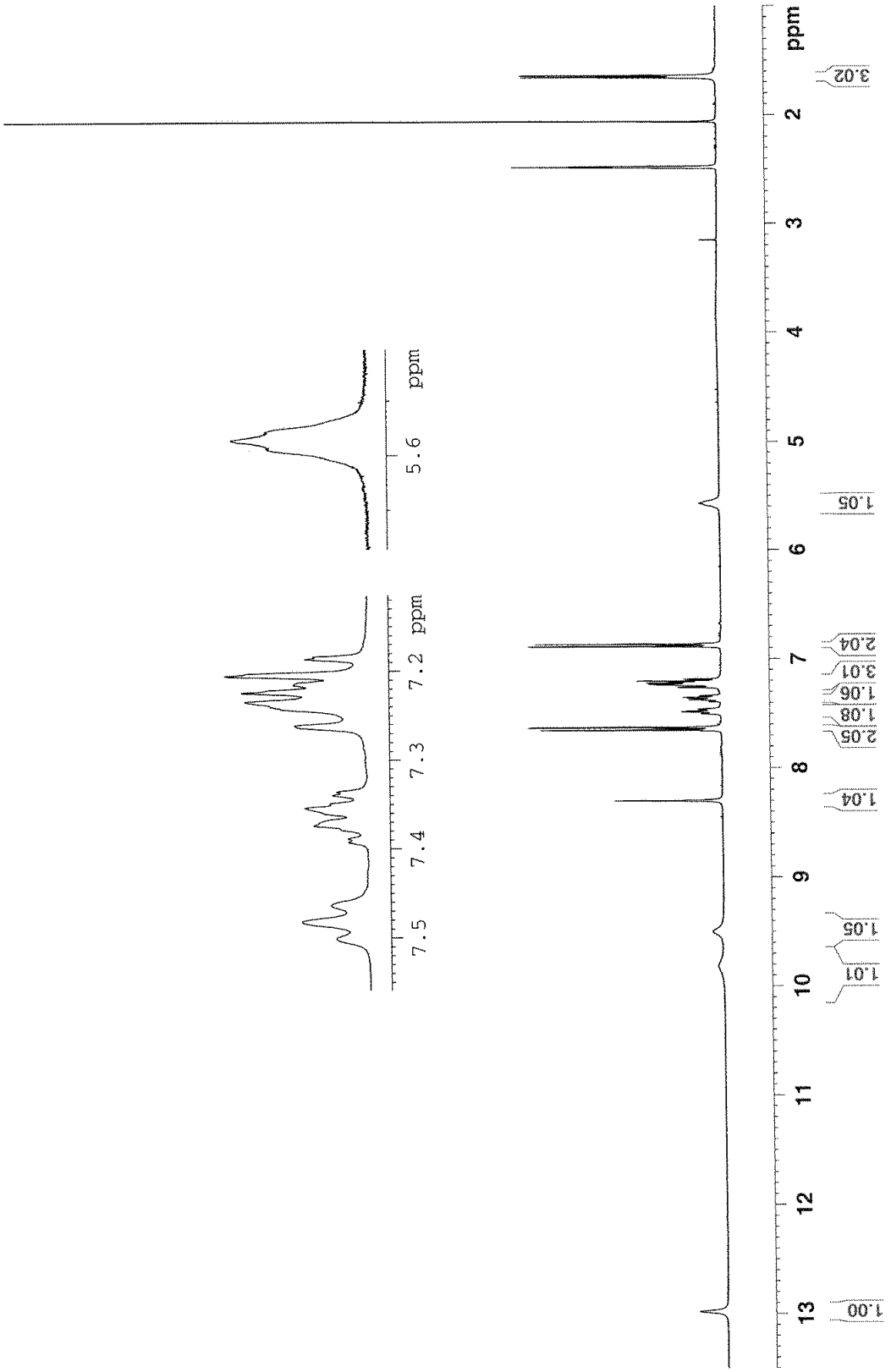

Residual peaks of DMSO, aceton and H_2O are found at 2.50 ppm, 2.09 ppm and 3.33 ppm, respectively.

^{13}C – Spectrum of Compound 1c

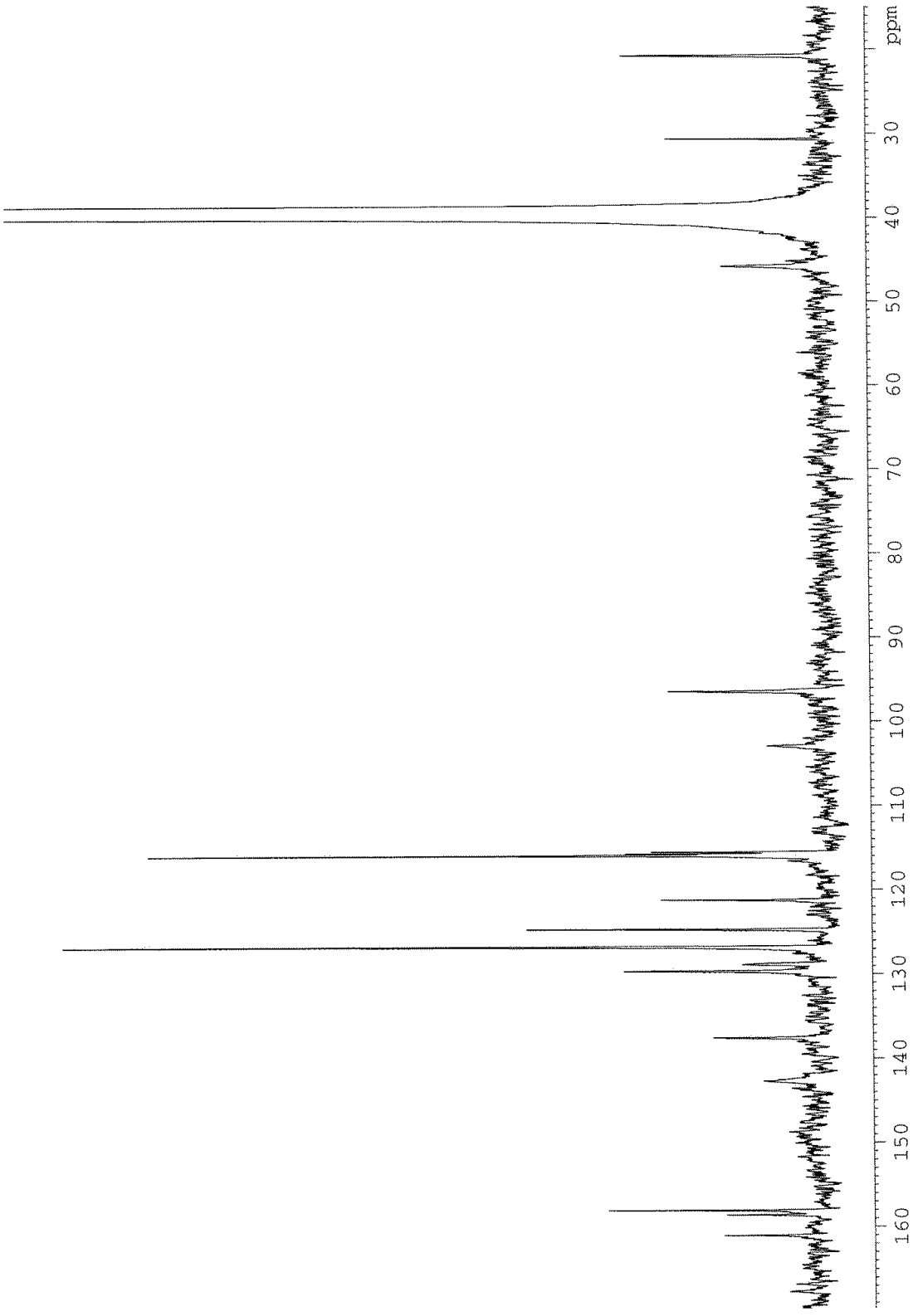

Residual peak of DMSO and acetone is found at 39.51 ppm and 30.56, respectively.

COSY, 2D Spectrum of Compound 1c

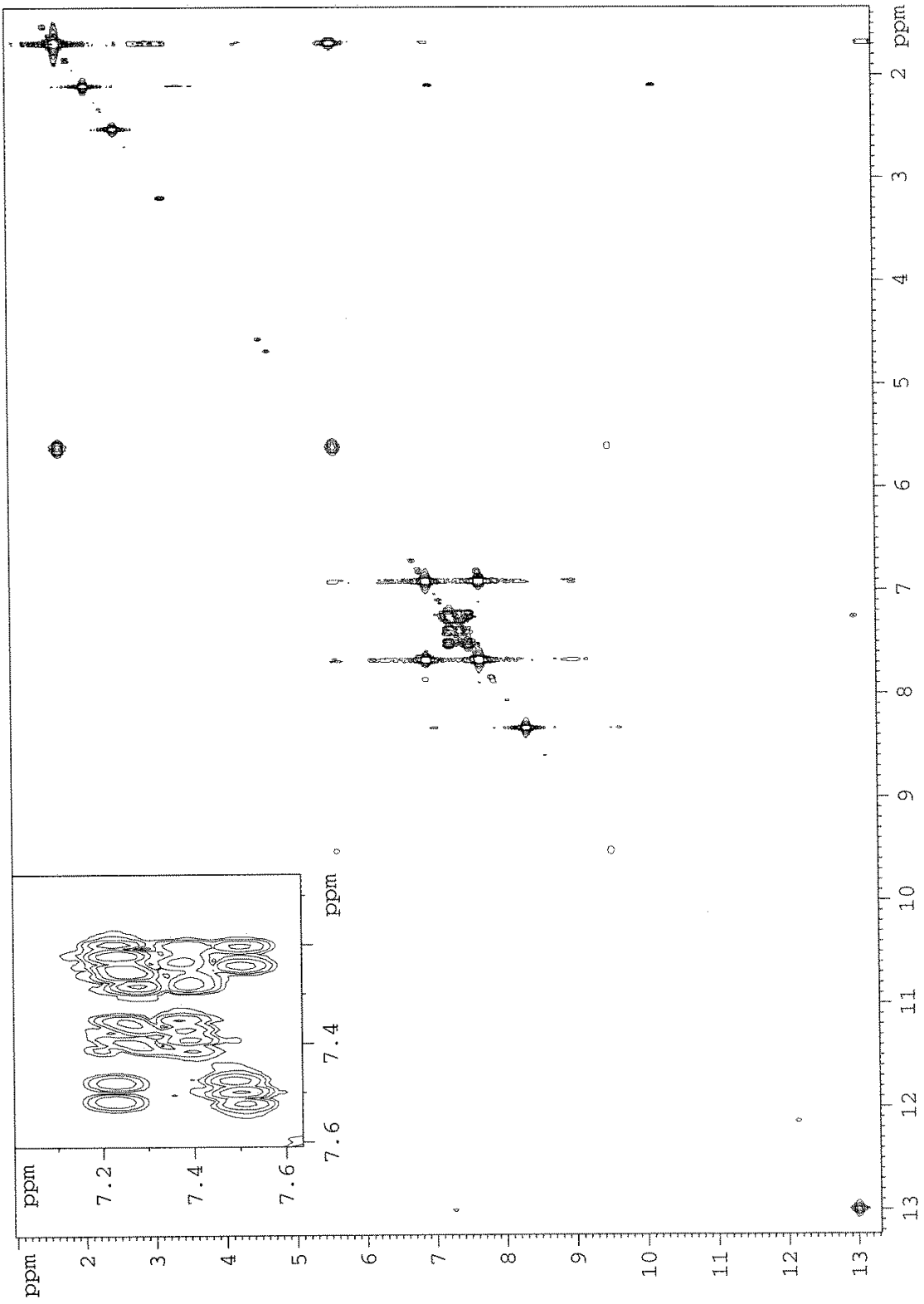

HSQC, 2D Spectrum of Compound 1c

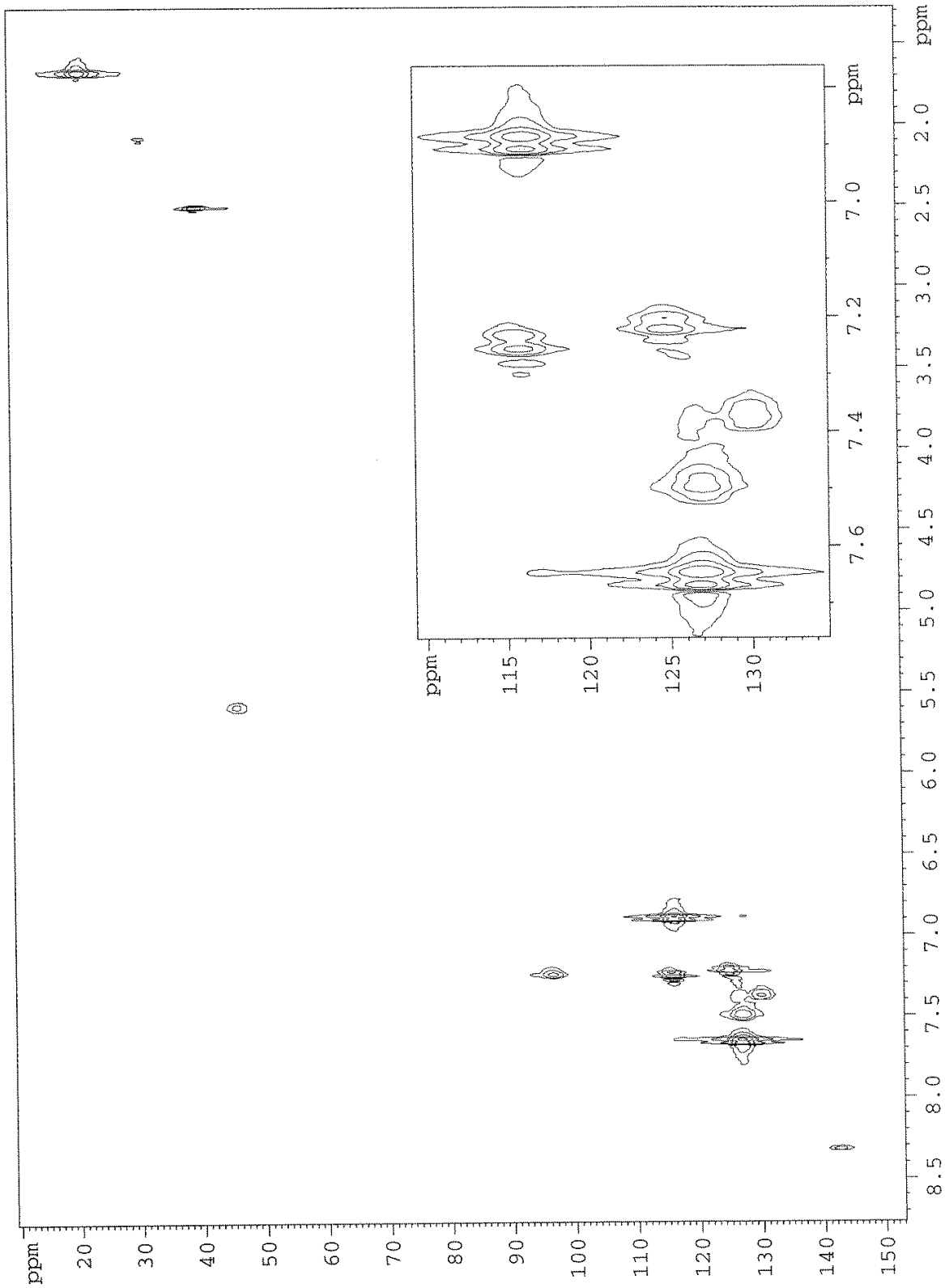

HMBC, 2D Spectrum of Compound 1c

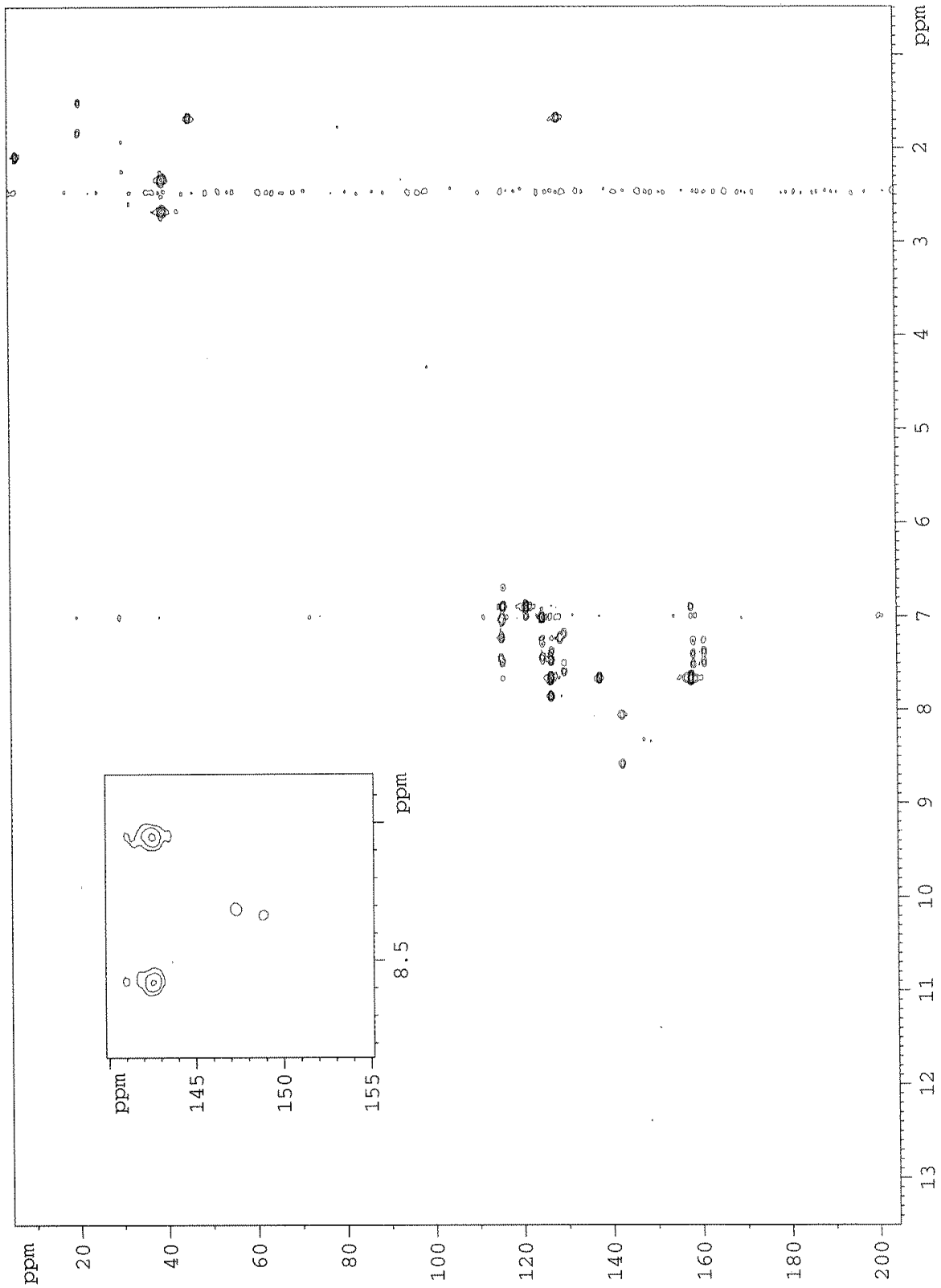

^{19}F – Spectrum of Compound 1c

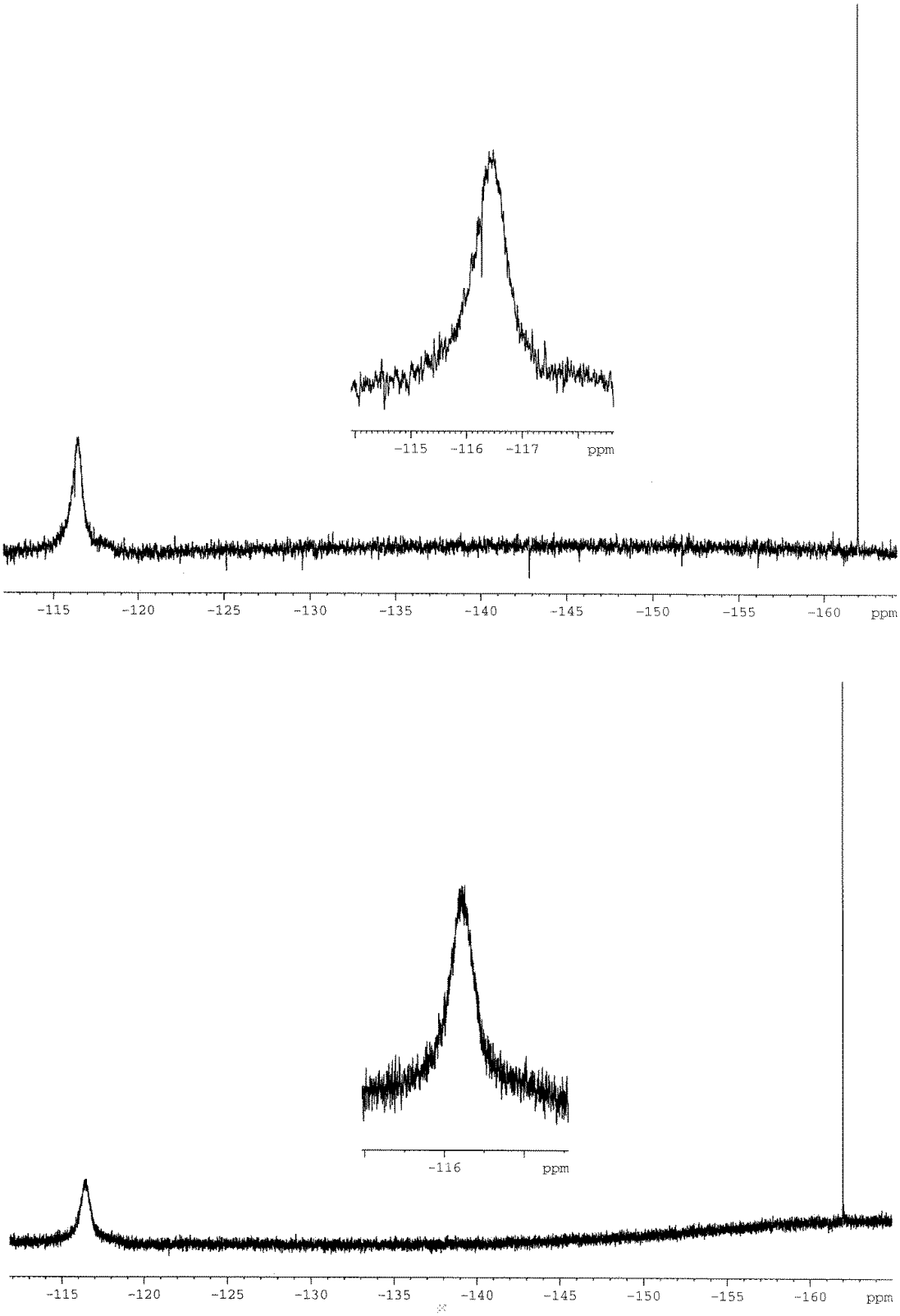

Residual peak of hexafluorobenzene is found at -162.0 ppm. Proton decoupled ^{19}F-NMR experiment is found in the top spectrum, while proton coupled ^{19}F-NMR experiment is found in the bottom spectrum.

A.1.4 – NMR spectra of Compound 1d

^{1}H – Spectrum of Compound 1d

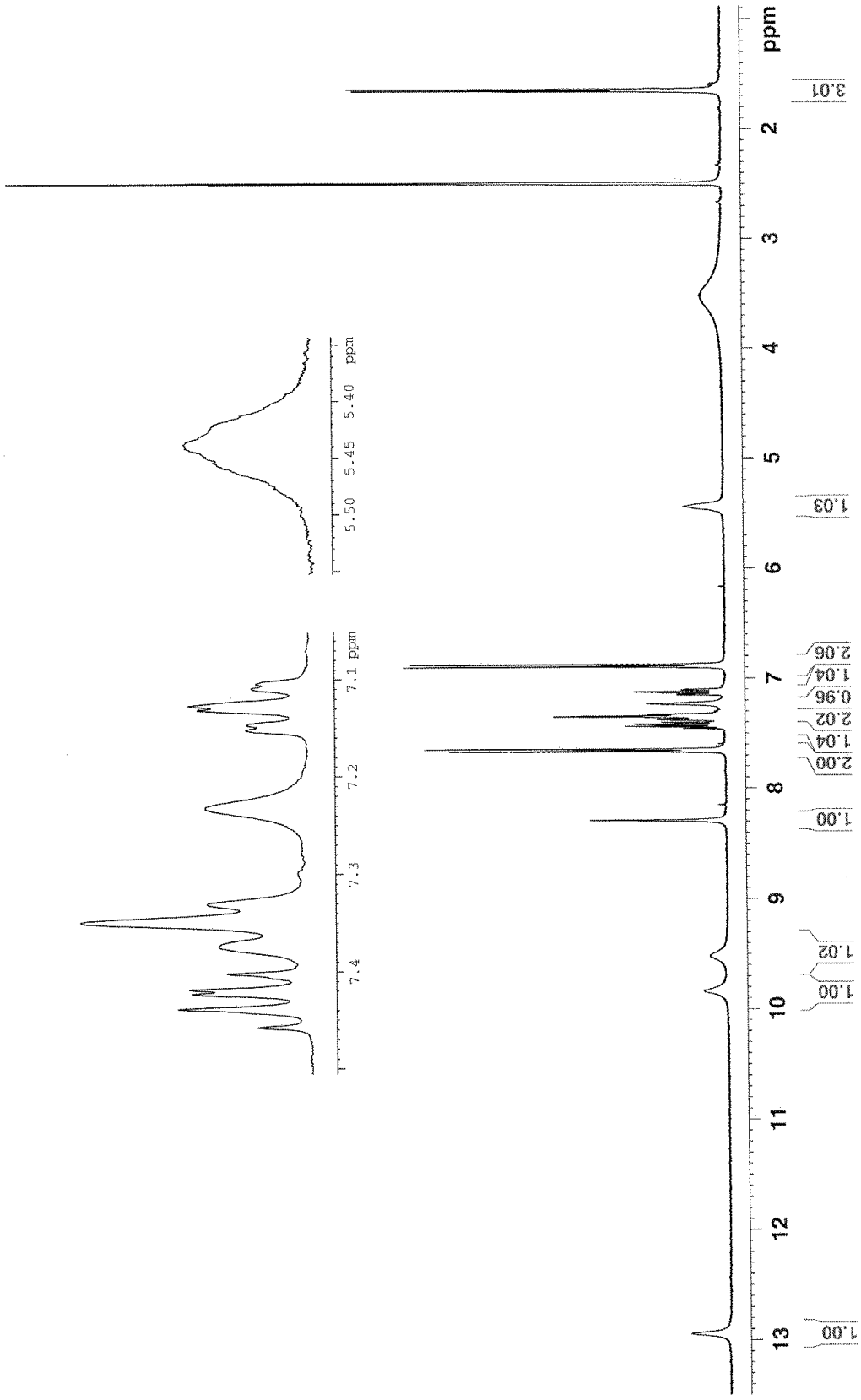

Residual peaks of DMSO and H_2O are found at 2.50 ppm and 3.33 ppm, respectively.

^{13}C – Spectrum of Compound 1d

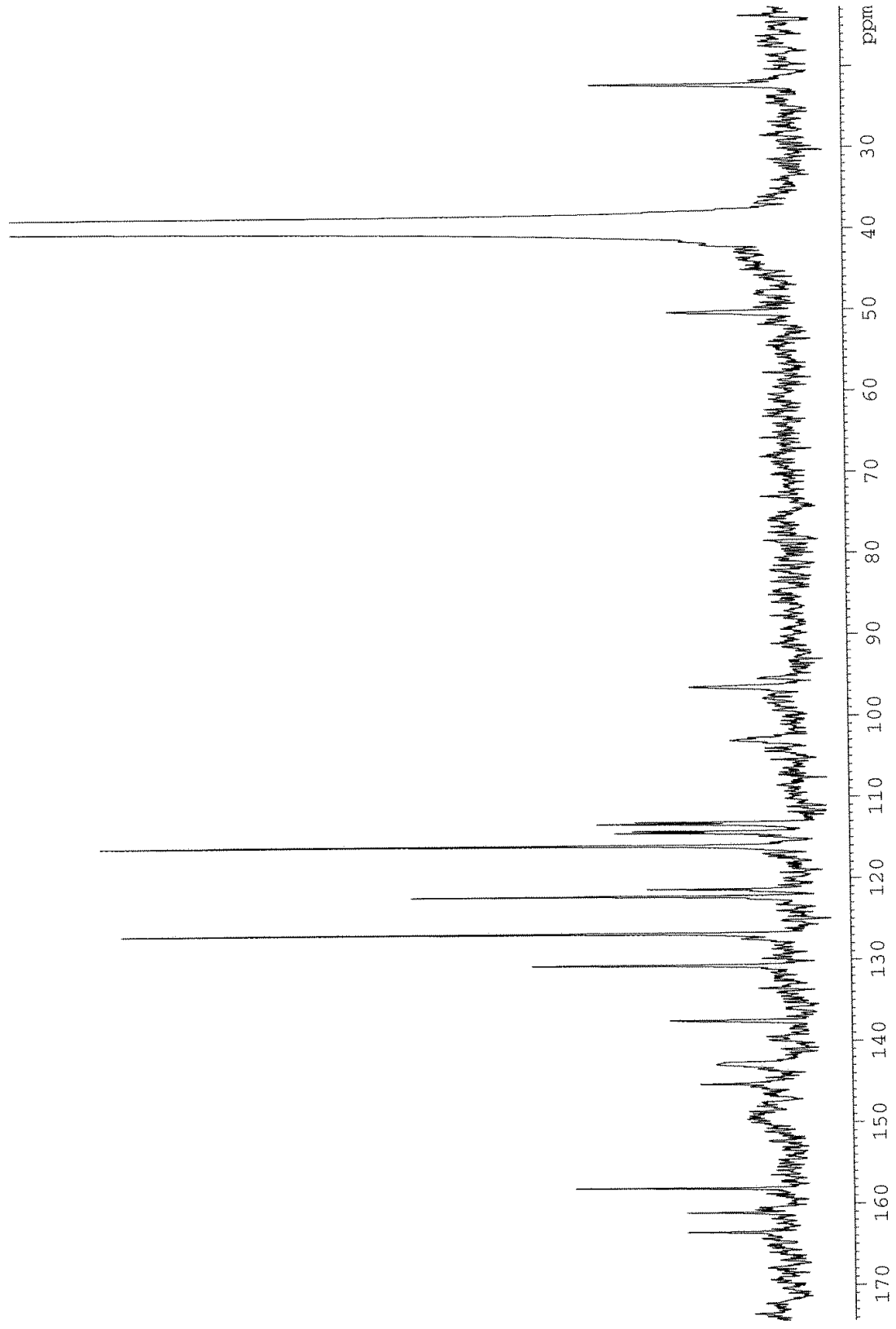

Residual peak of DMSO is found at 39.51 ppm.

COSY, 2D Spectrum of Compound 1d

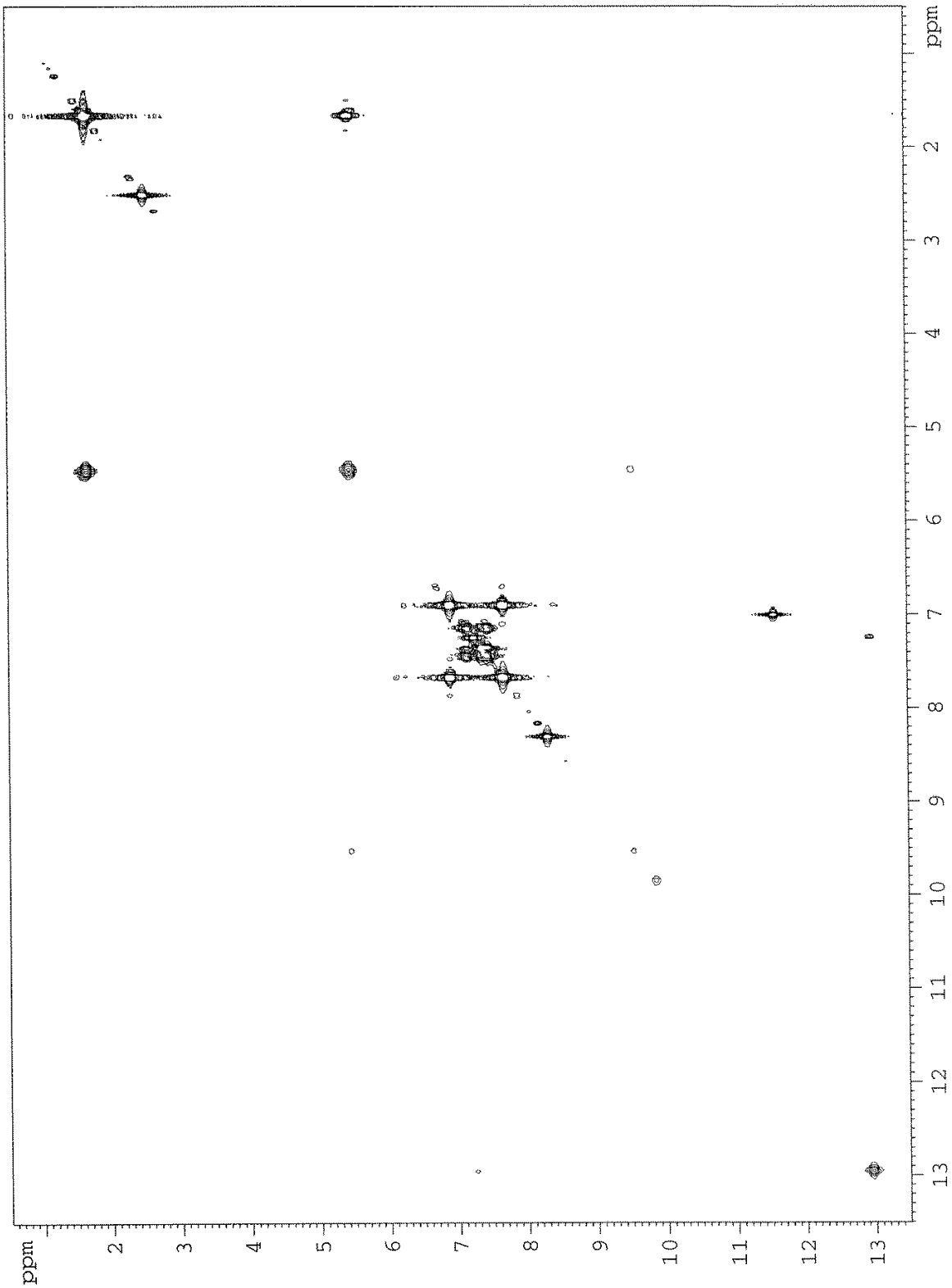

HSQC, 2D Spectrum of Compound 1d

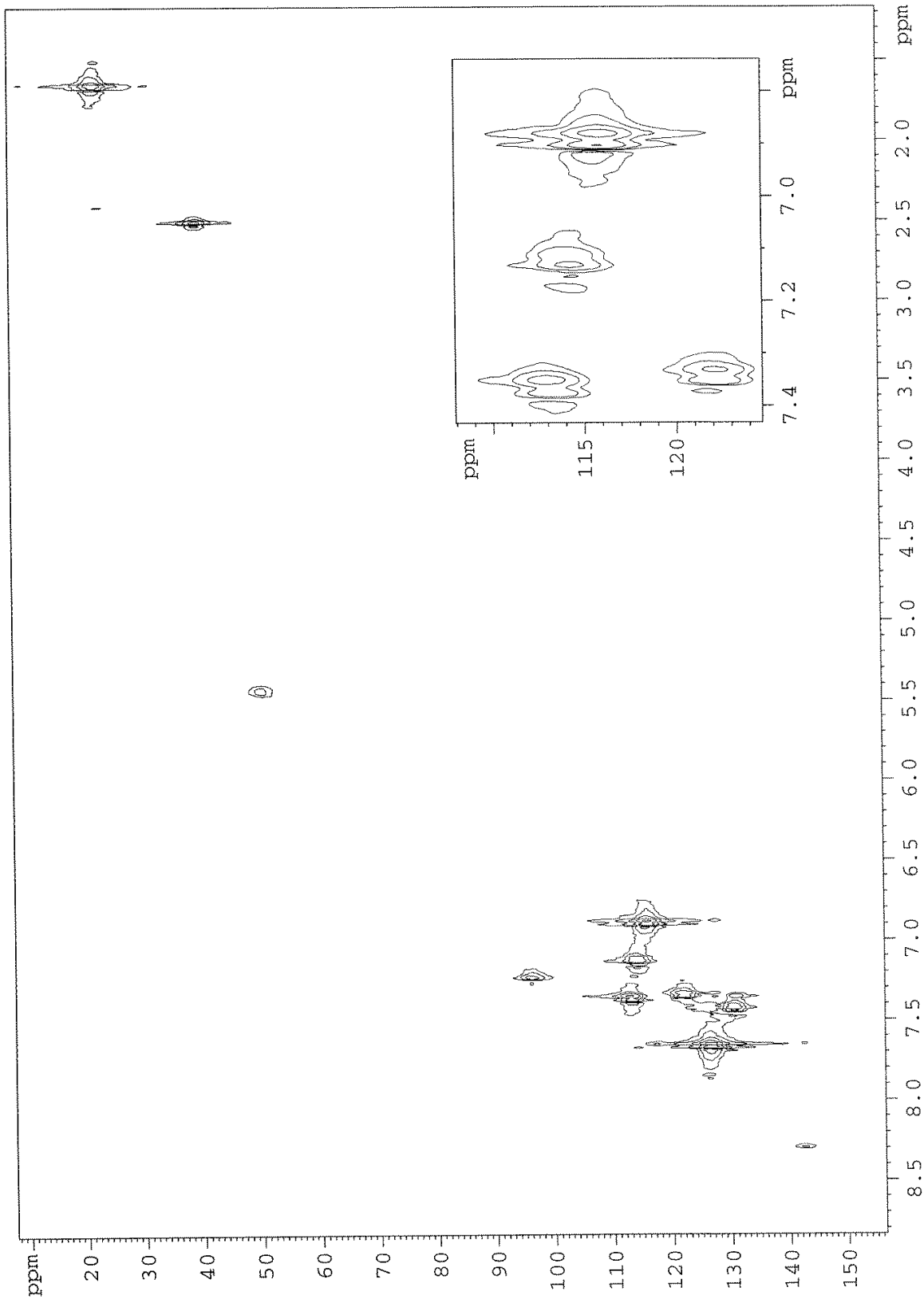

HMBC, 2D Spectrum of Compound 1d

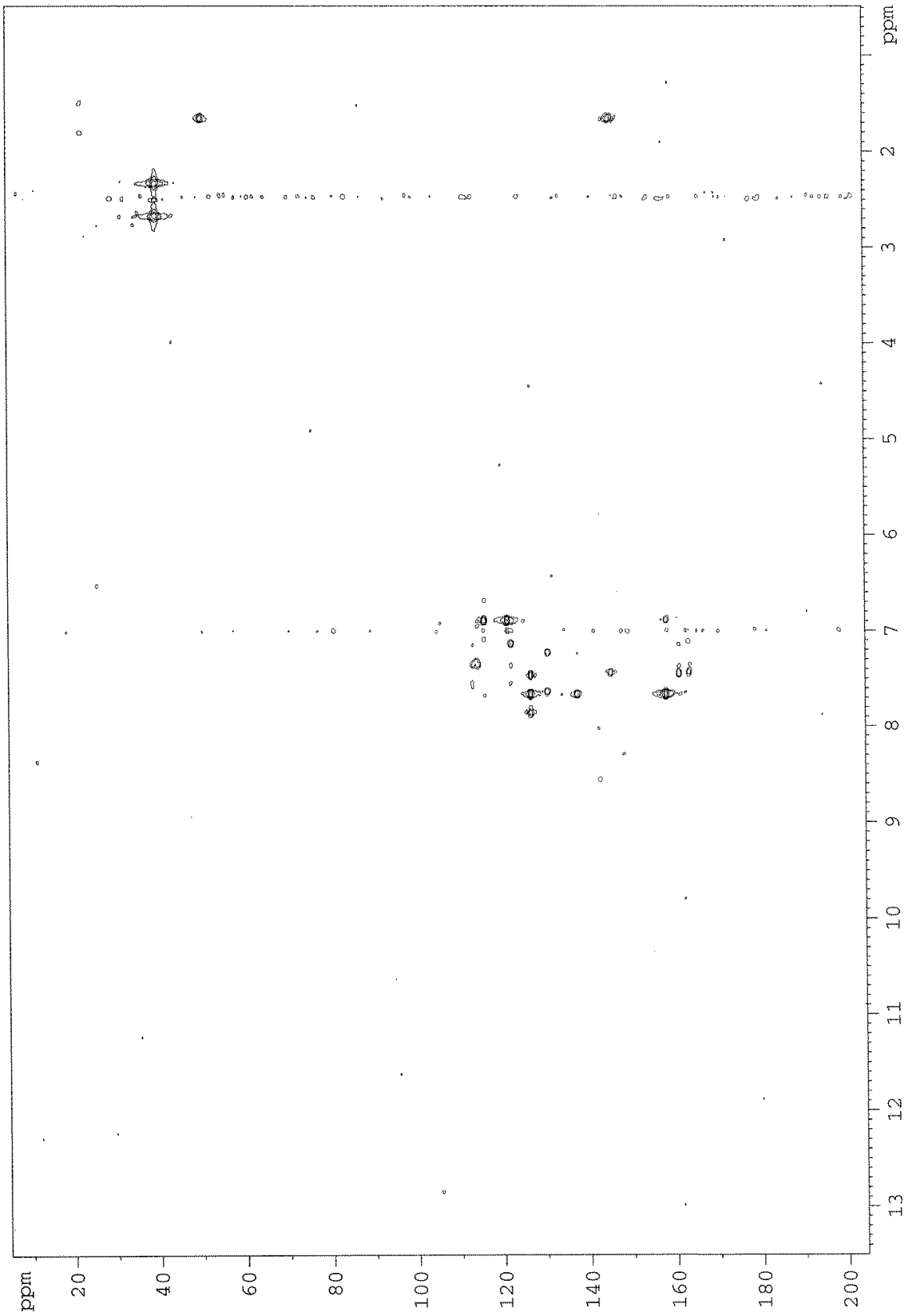

^{19}F – Spectrum of Compound 1d

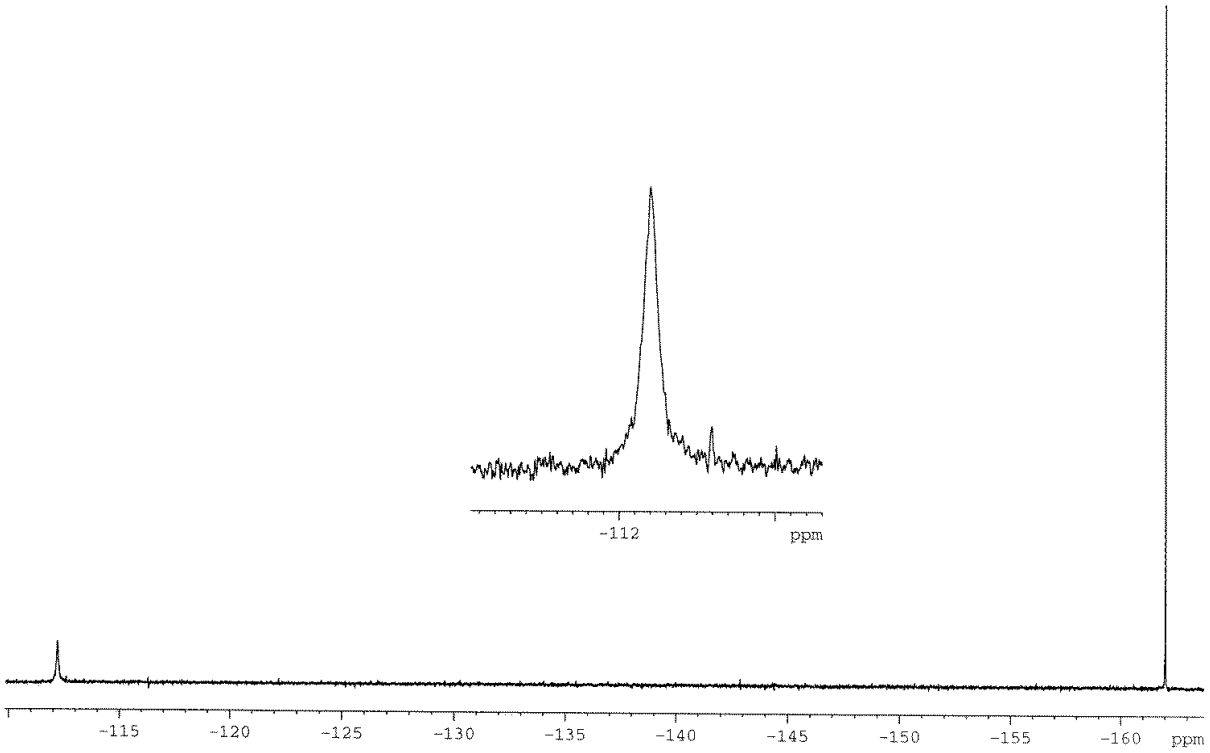

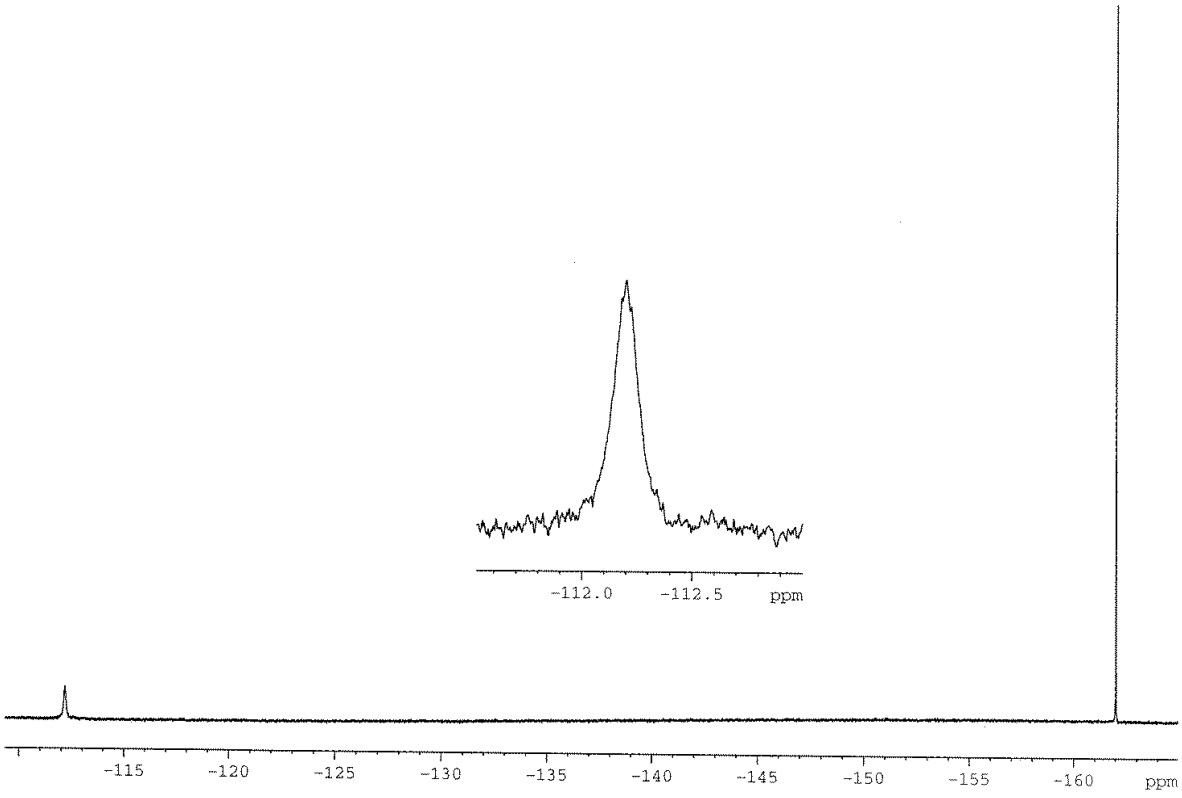

Residual peak of hexafluorobenzene is found at -162.0 ppm. Proton decoupled ^{19}F-NMR experiment is found in the top spectrum, while proton coupled ^{19}F-NMR experiment is found in the bottom spectrum.

A.1.5 – NMR spectra of Compound 1e

^{1}H – Spectrum of Compound 1e

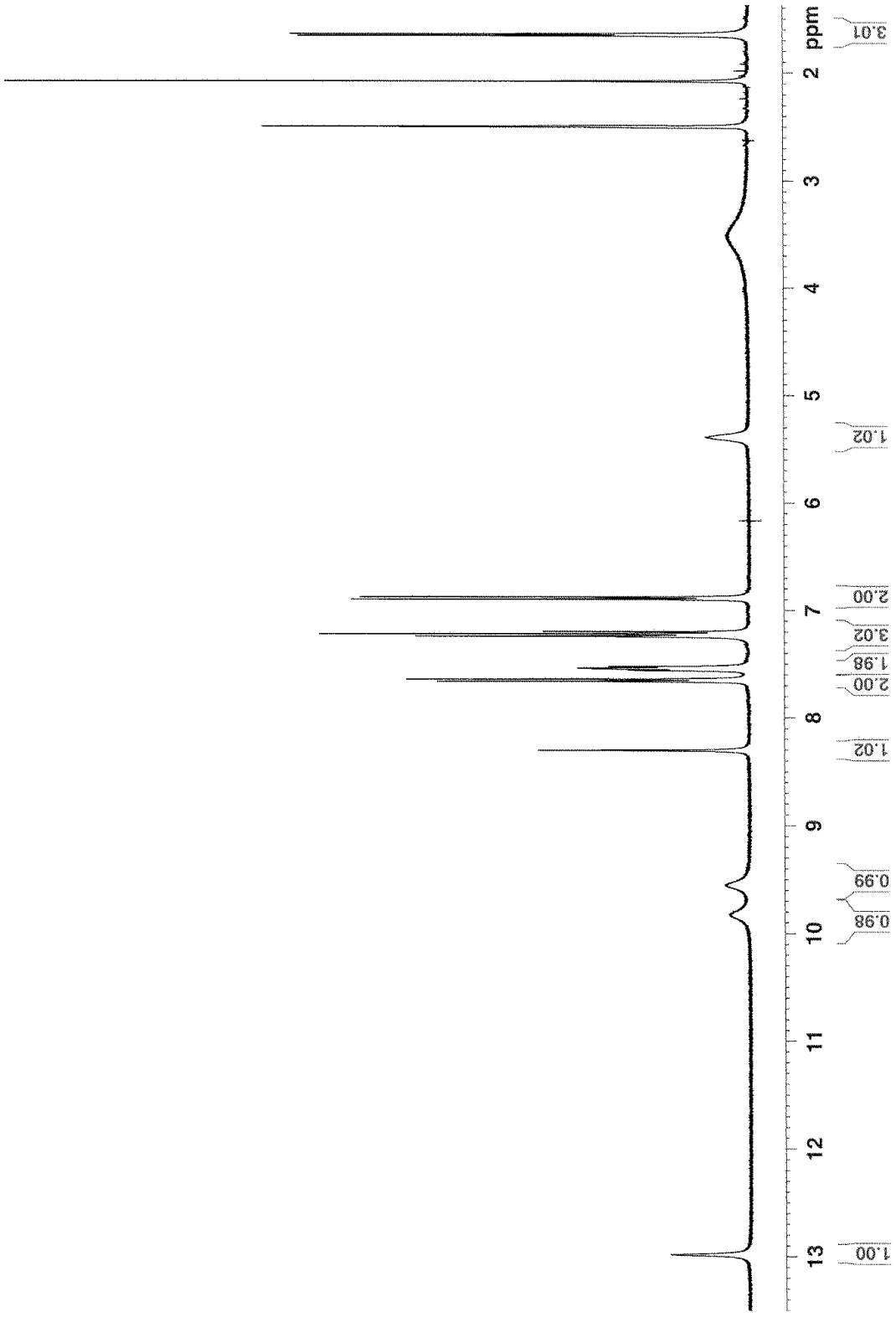

Residual peaks of DMSO, aceton and H_2O are found at 2.50 ppm, 2.09 ppm and 3.33 ppm, respectively.

^{13}C – Spectrum of Compound 1e

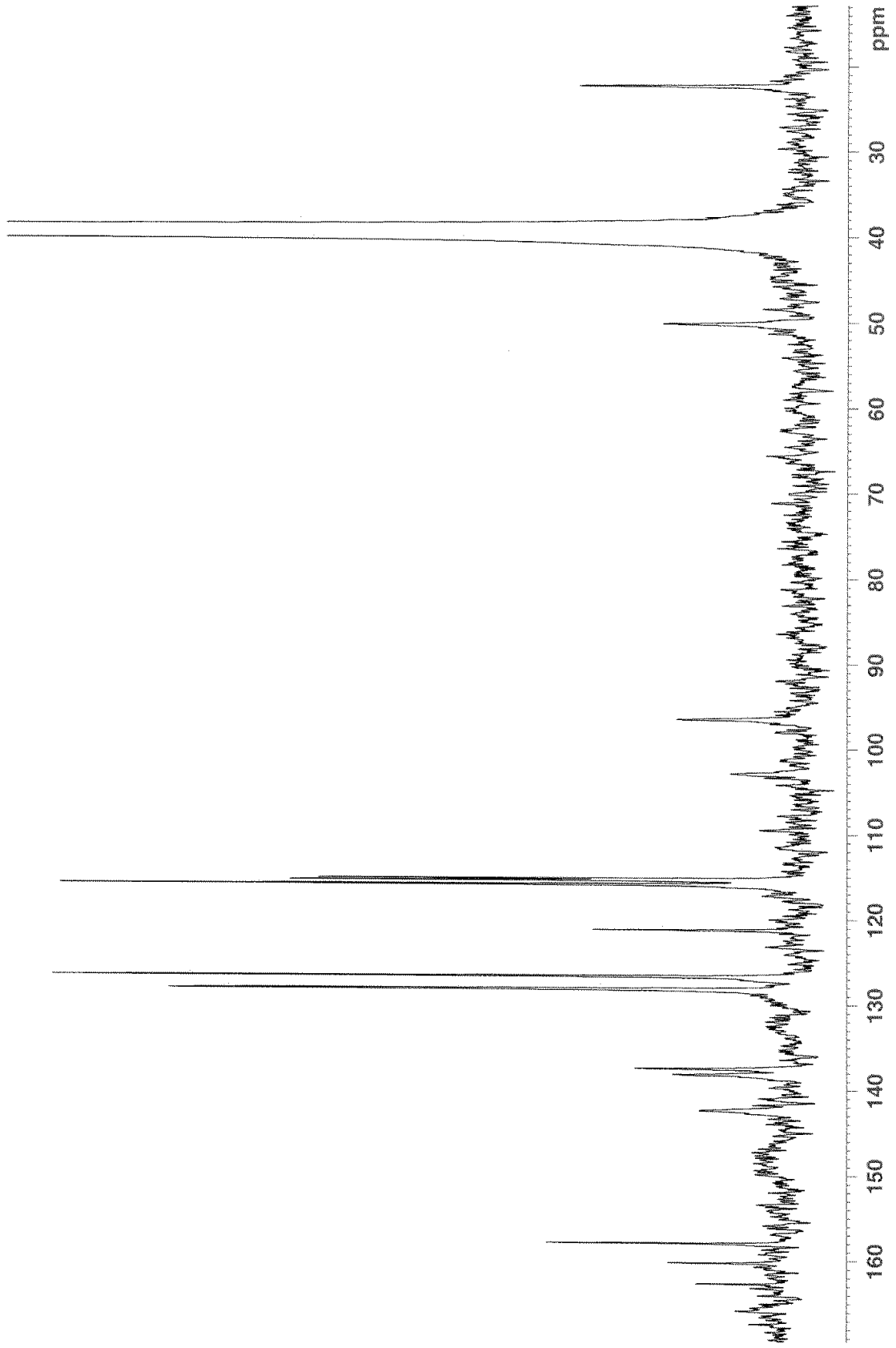

Residual peak of DMSO is found at 39.51 ppm.

COSY, 2D Spectrum of Compound 1e

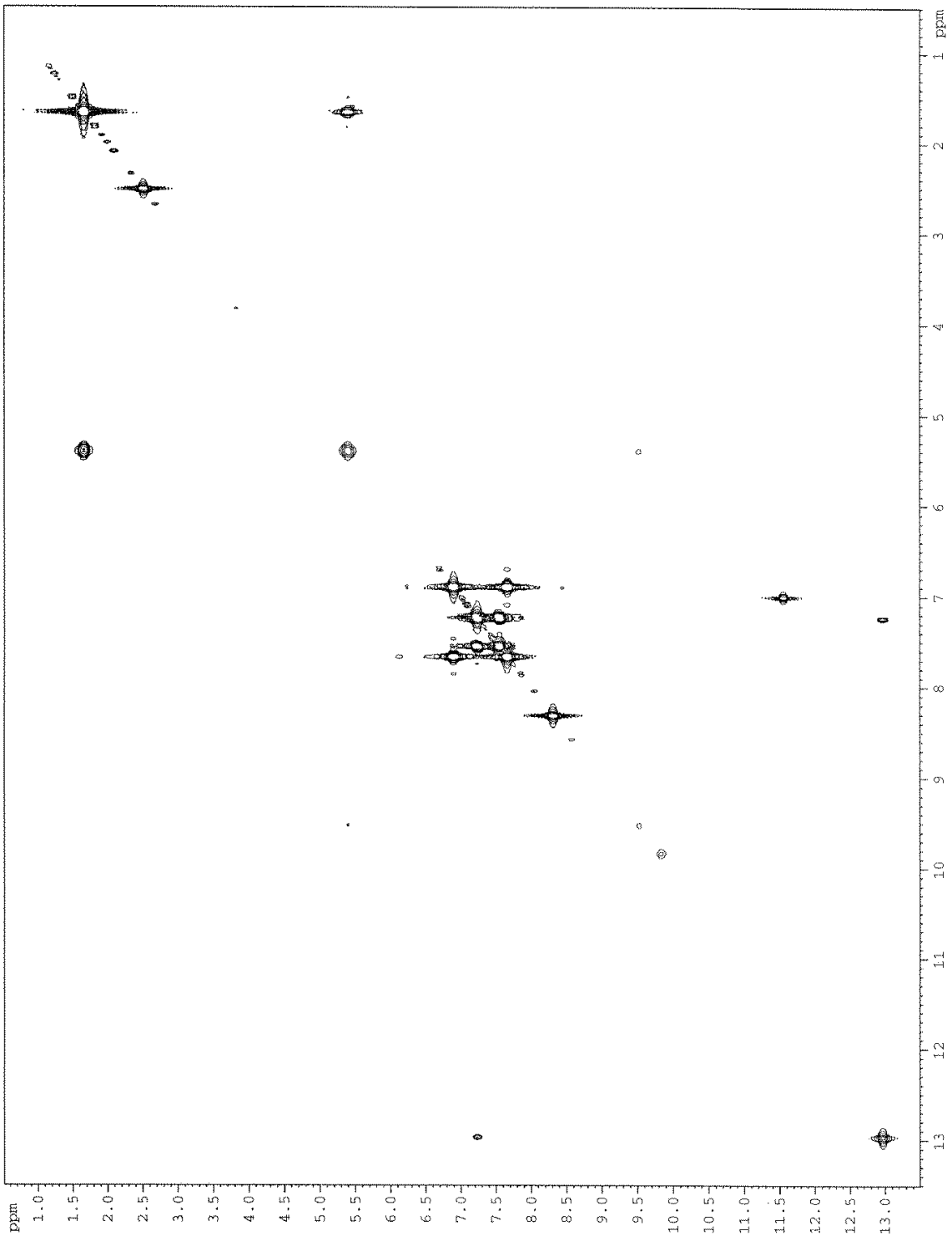

HSQC, 2D Spectrum of Compound 1e

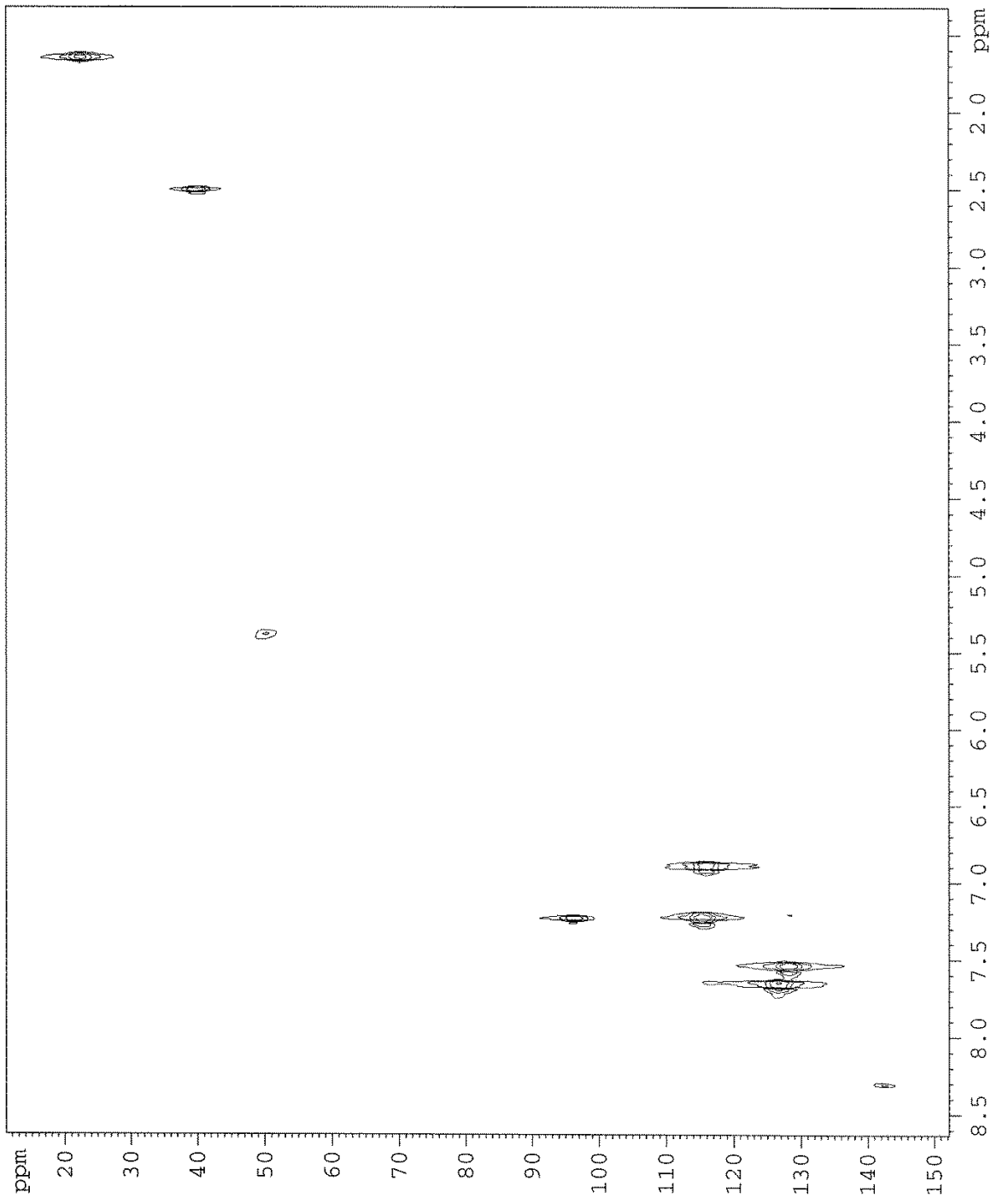

HMBC, 2D Spectrum of Compound 1e

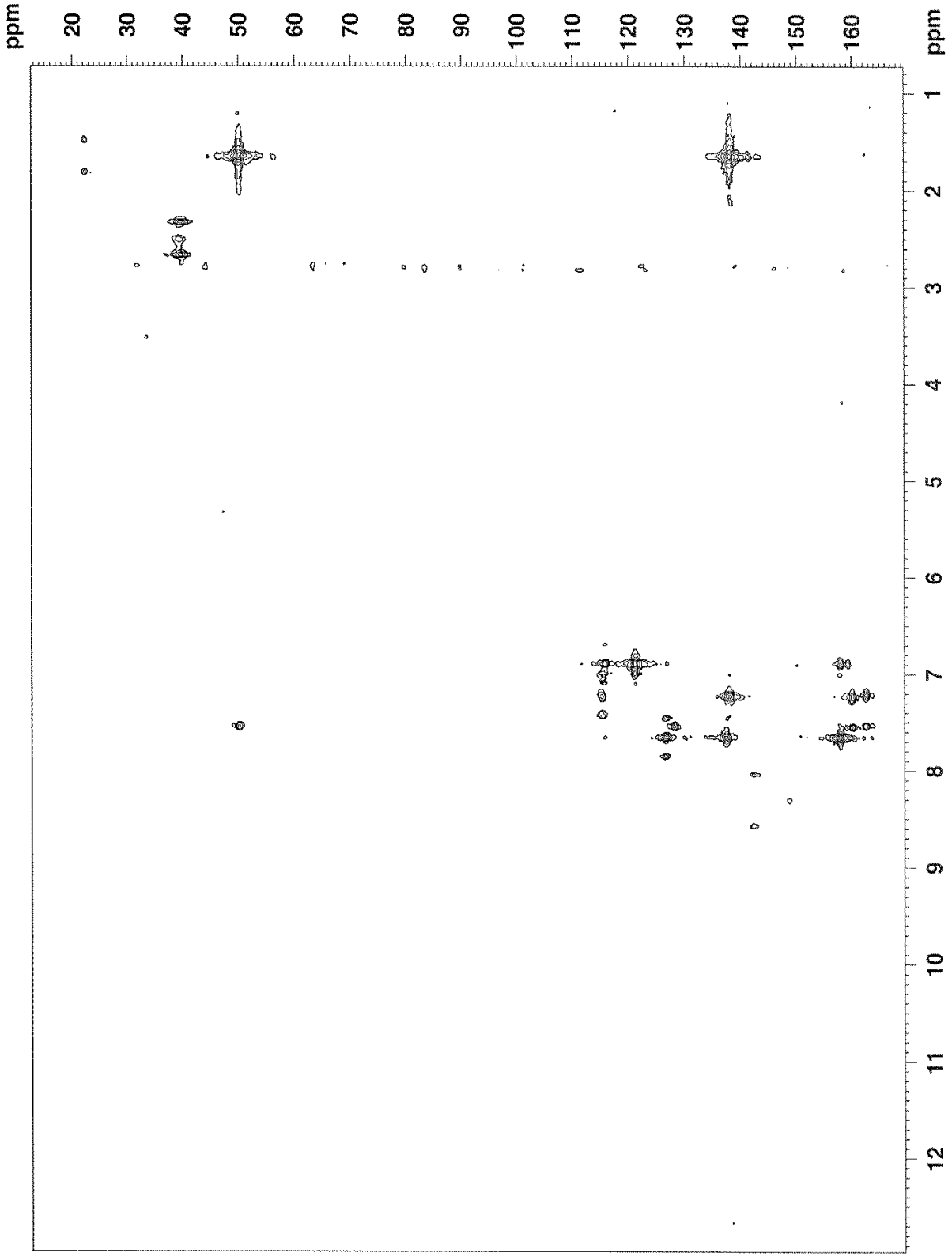

^{19}F – Spectrum of Compound 1e

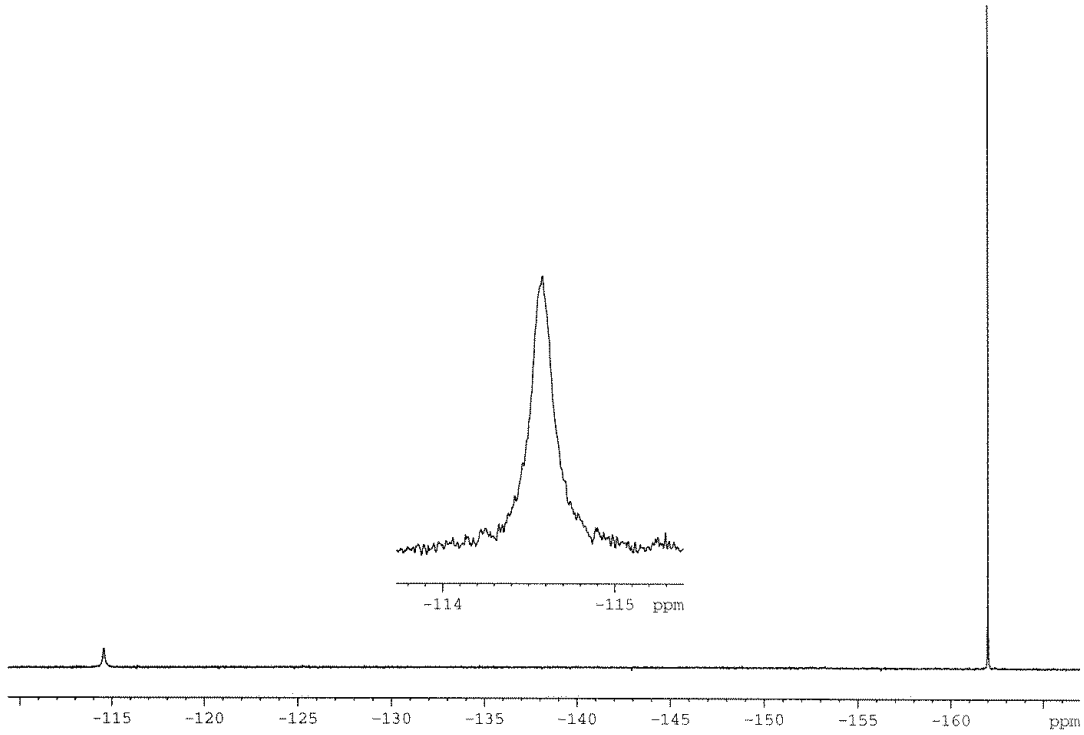

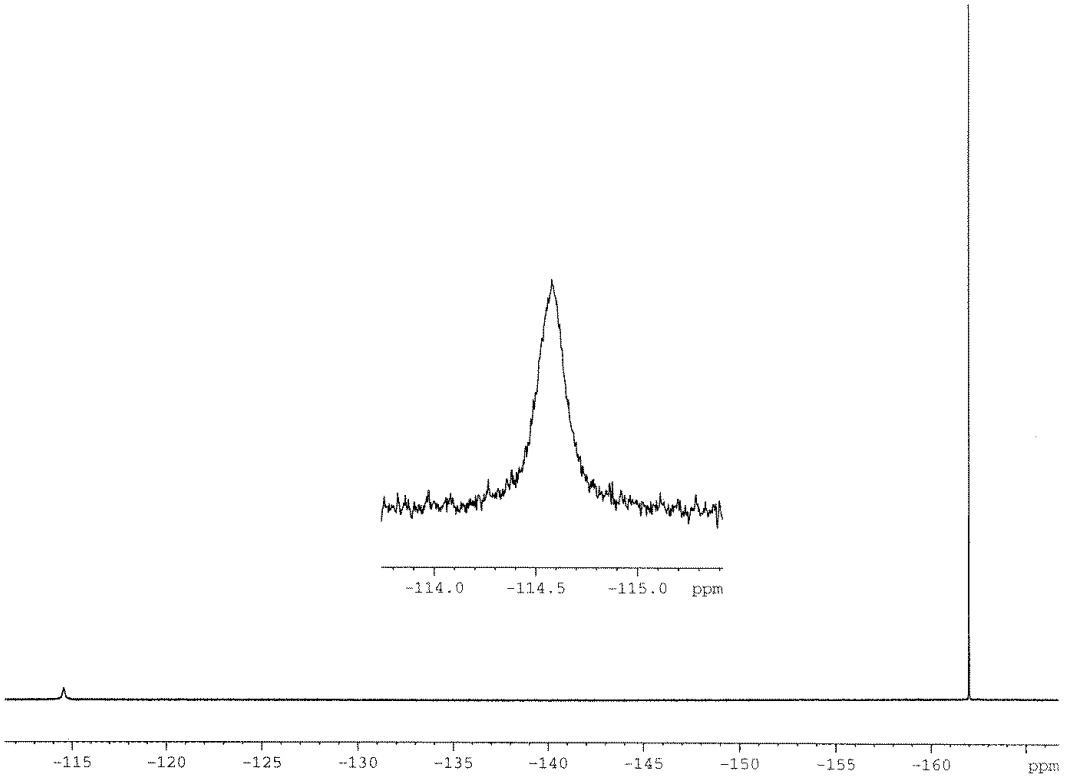

Residual peak of hexafluorobenzene is found at -162.0 ppmProton decoupled 19F-NMR experiment is found in the top spectrum, while proton coupled 19F-NMR experiment is found in the bottom spectrum.

A.1.6 – NMR spectra of Compound 1f

^{1}H – Spectrum of Compound 1f

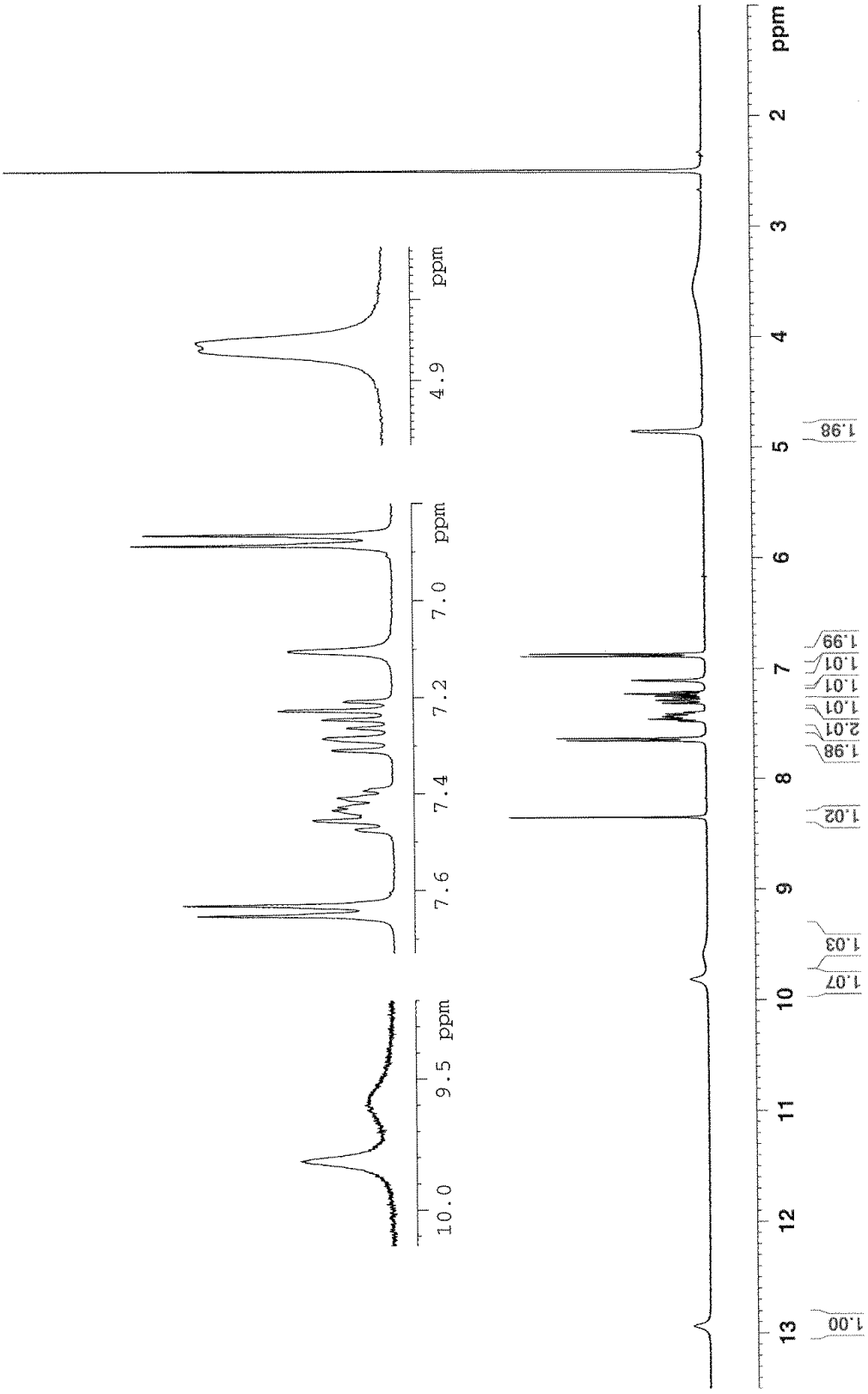

Residual peaks of DMSO and H_2O are found at 2.50 ppm and 3.33 ppm, respectively.

^{13}C – Spectrum of Compound 1f

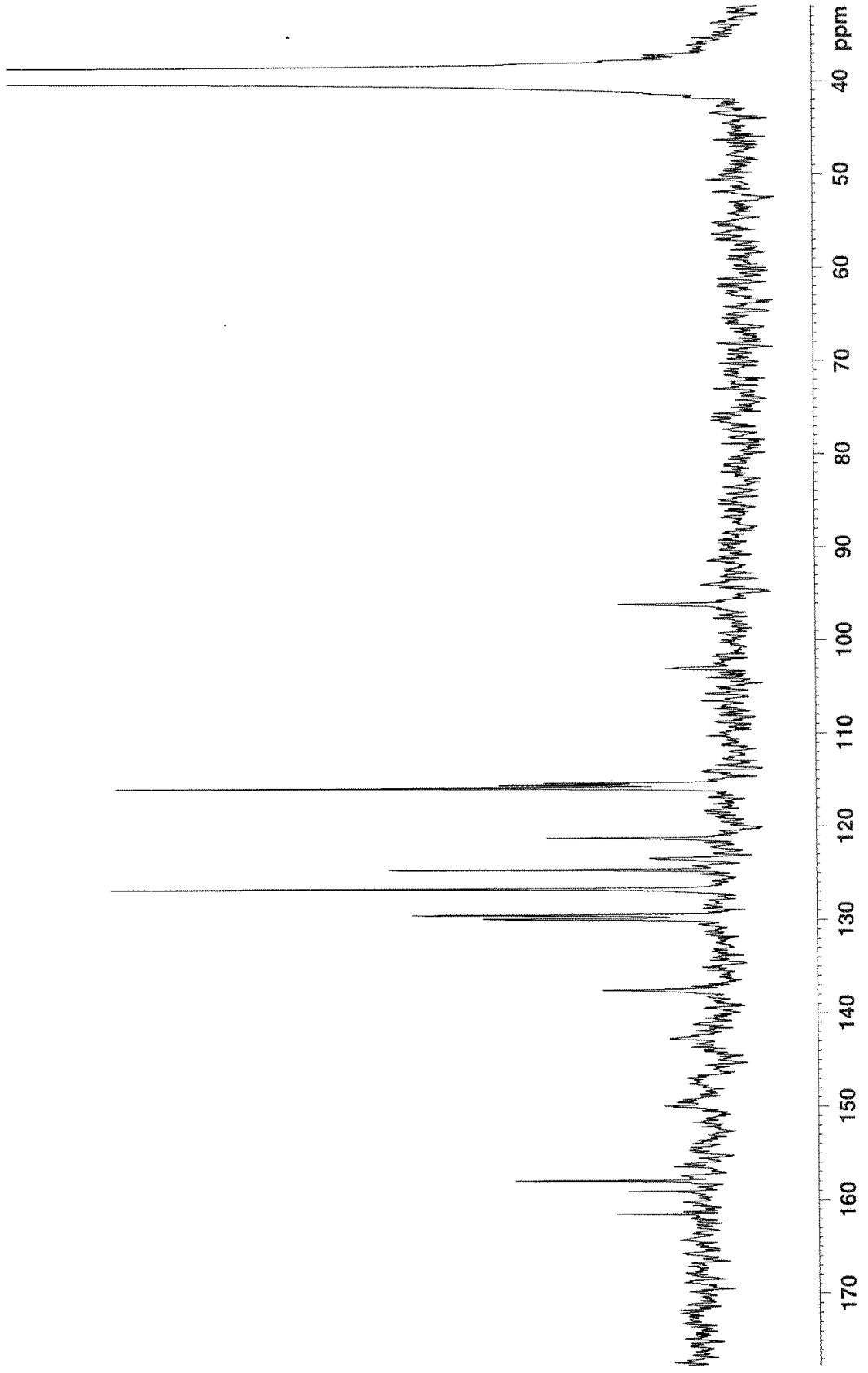

Residual peak of DMSO is found at 39.51 ppm.

COSY, 2D Spectrum of Compound 1f

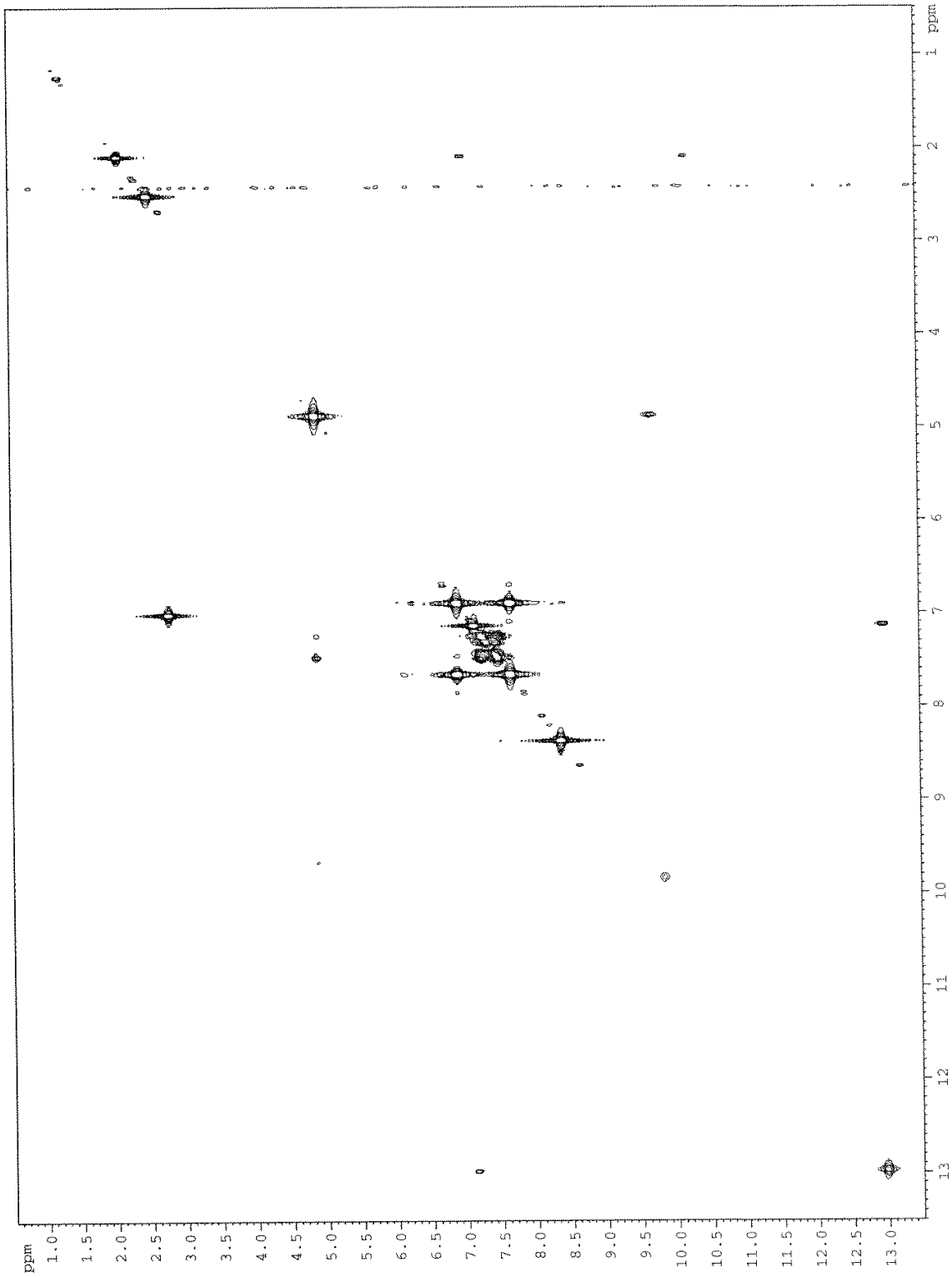

HSQC, 2D Spectrum of Compound 1f

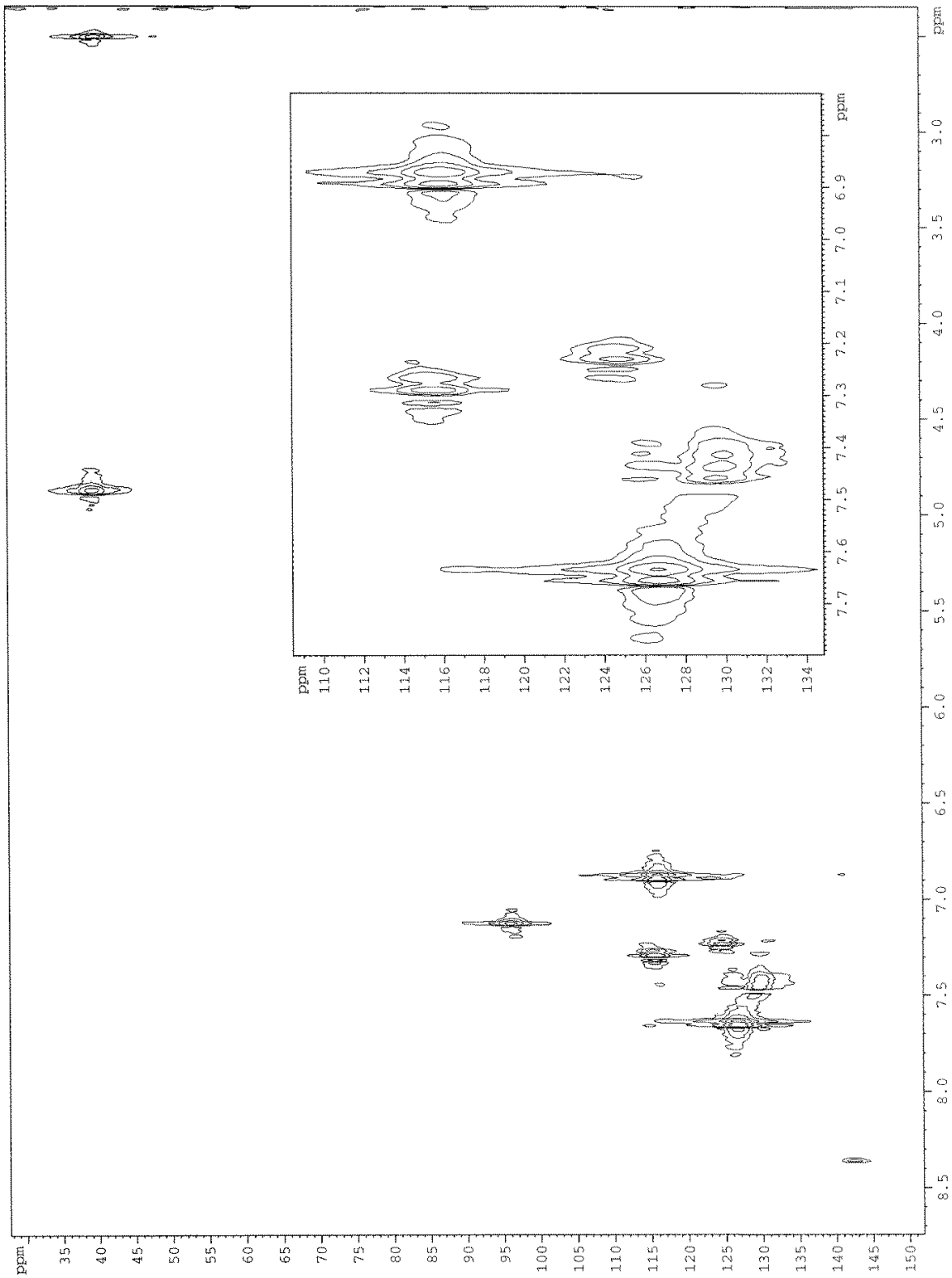

HMBC, 2D Spectrum of Compound 1f

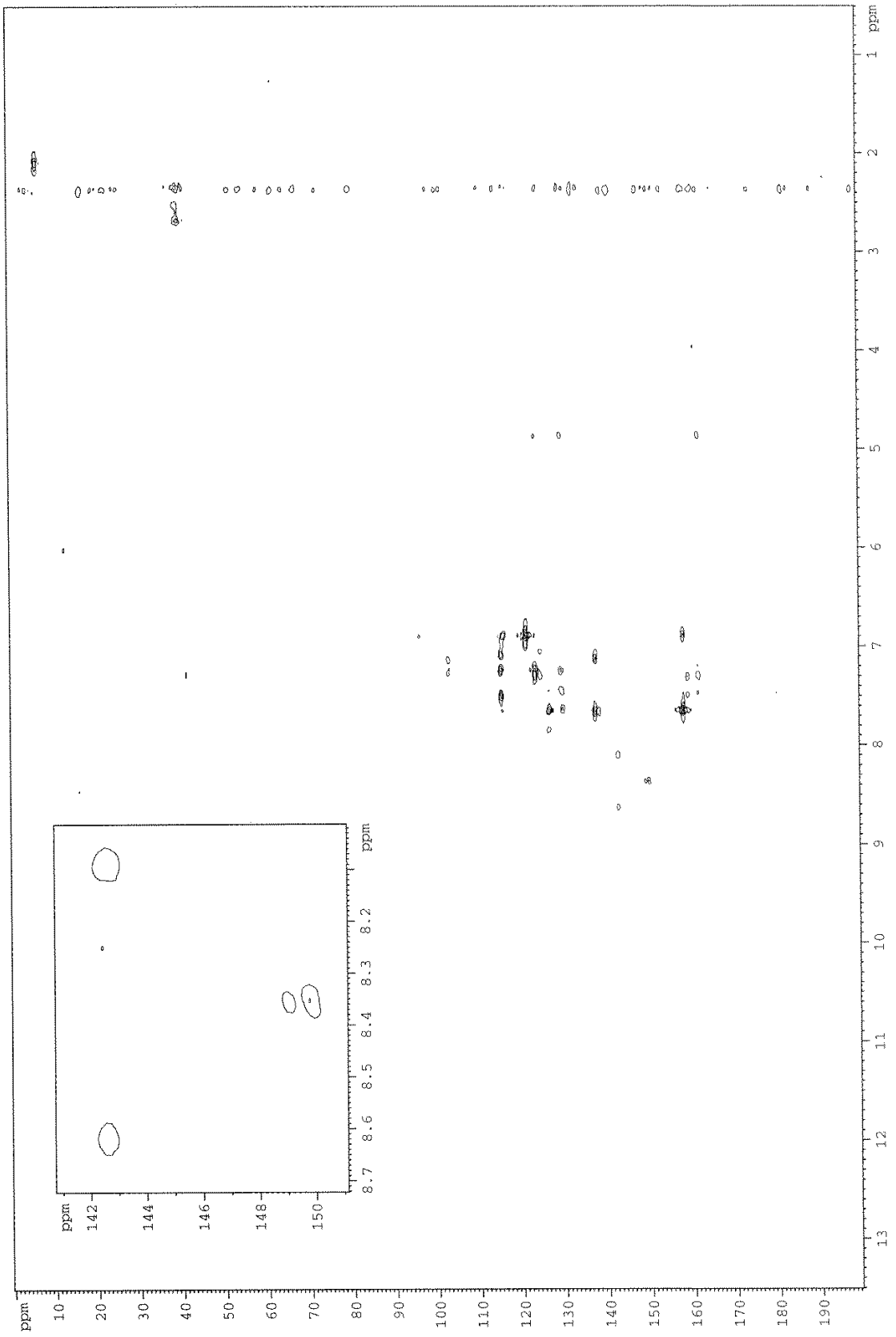

^{19}F – Spectrum of Compound 1f

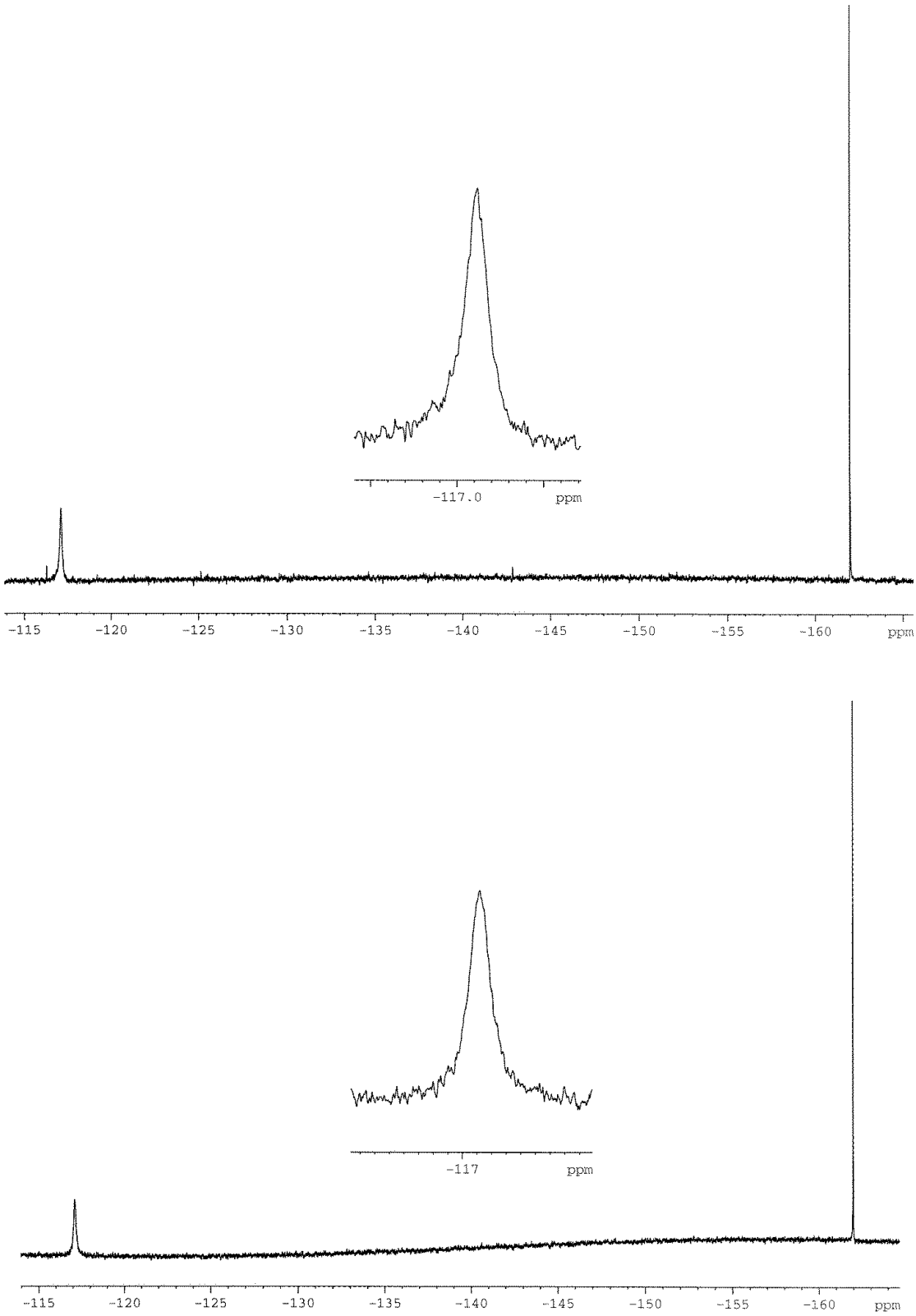

Residual peak of hexafluorobenzene is found at -162.0 ppm. Proton decoupled ^{19}F-NMR experiment is found in the top spectrum, while proton coupled ^{19}F-NMR experiment is found in the bottom spectrum.

A.1.7 – NMR spectra of Compound 1g

^{1}H – Spectrum of Compound 1g

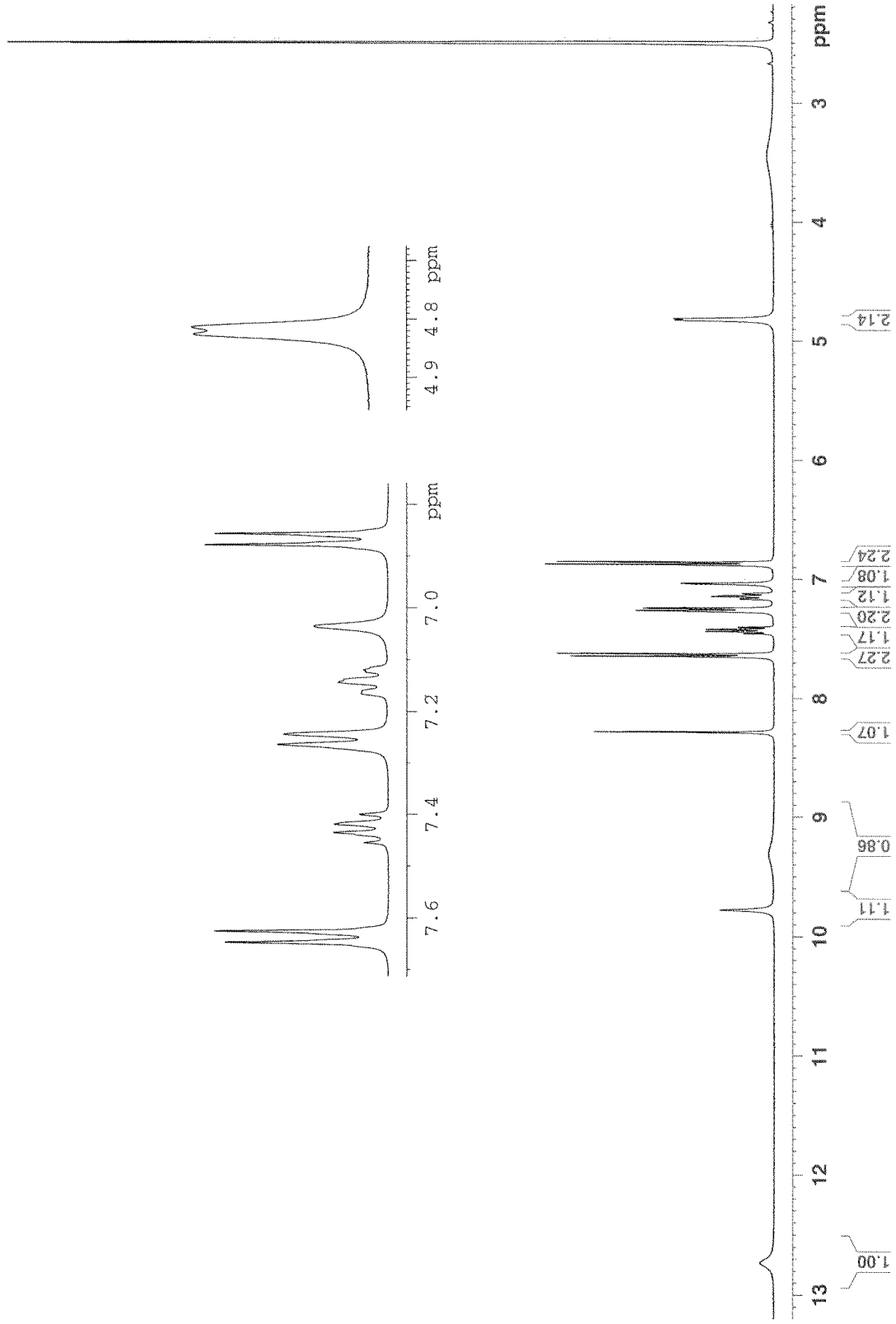

Residual peaks of DMSO and H_2O are found at 2.50 ppm and 3.33 ppm, respectively.

^{13}C – Spectrum of Compound 1g

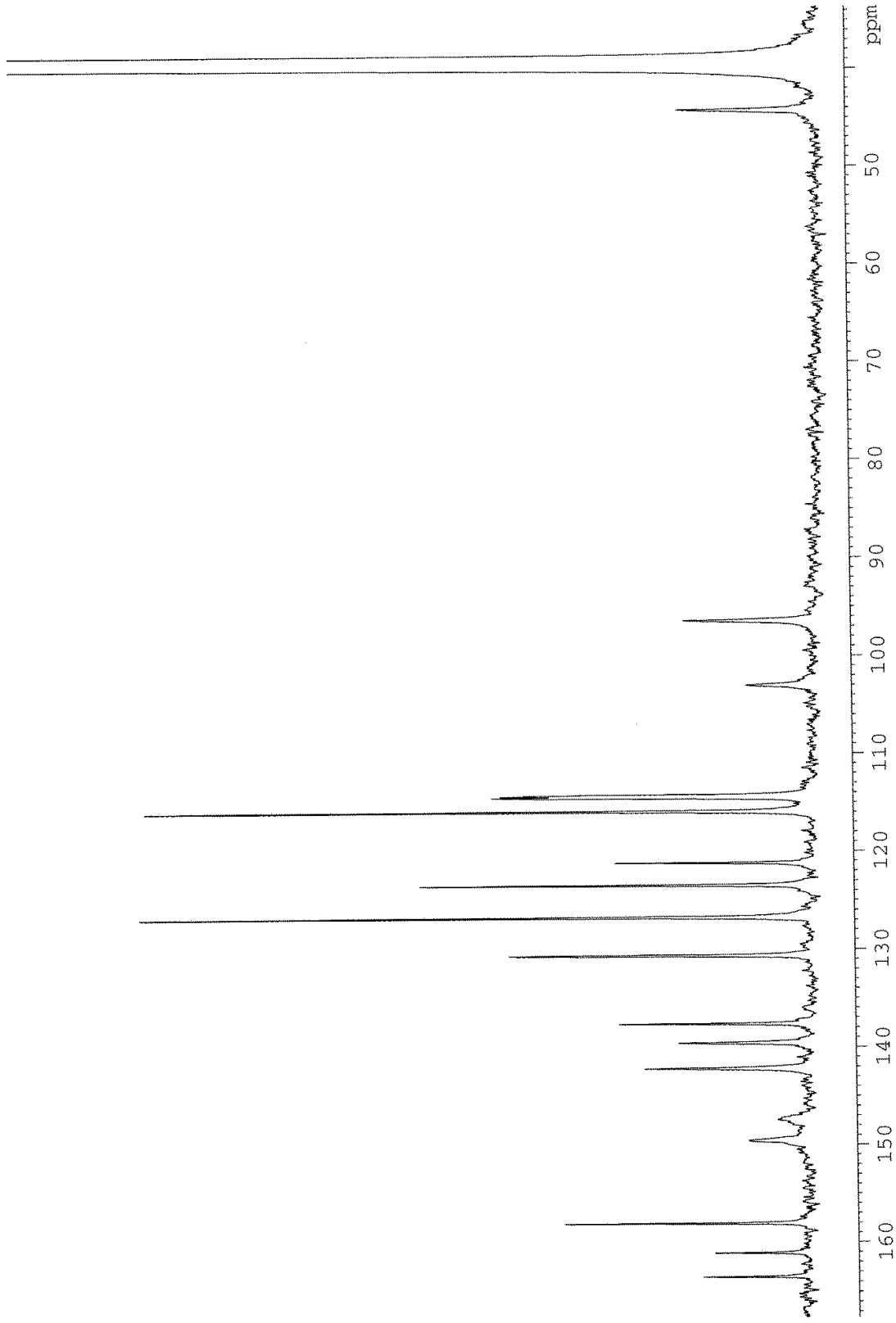

Residual peak of DMSO is found at 39.51 ppm.

COSY, 2D Spectrum of Compound 1g

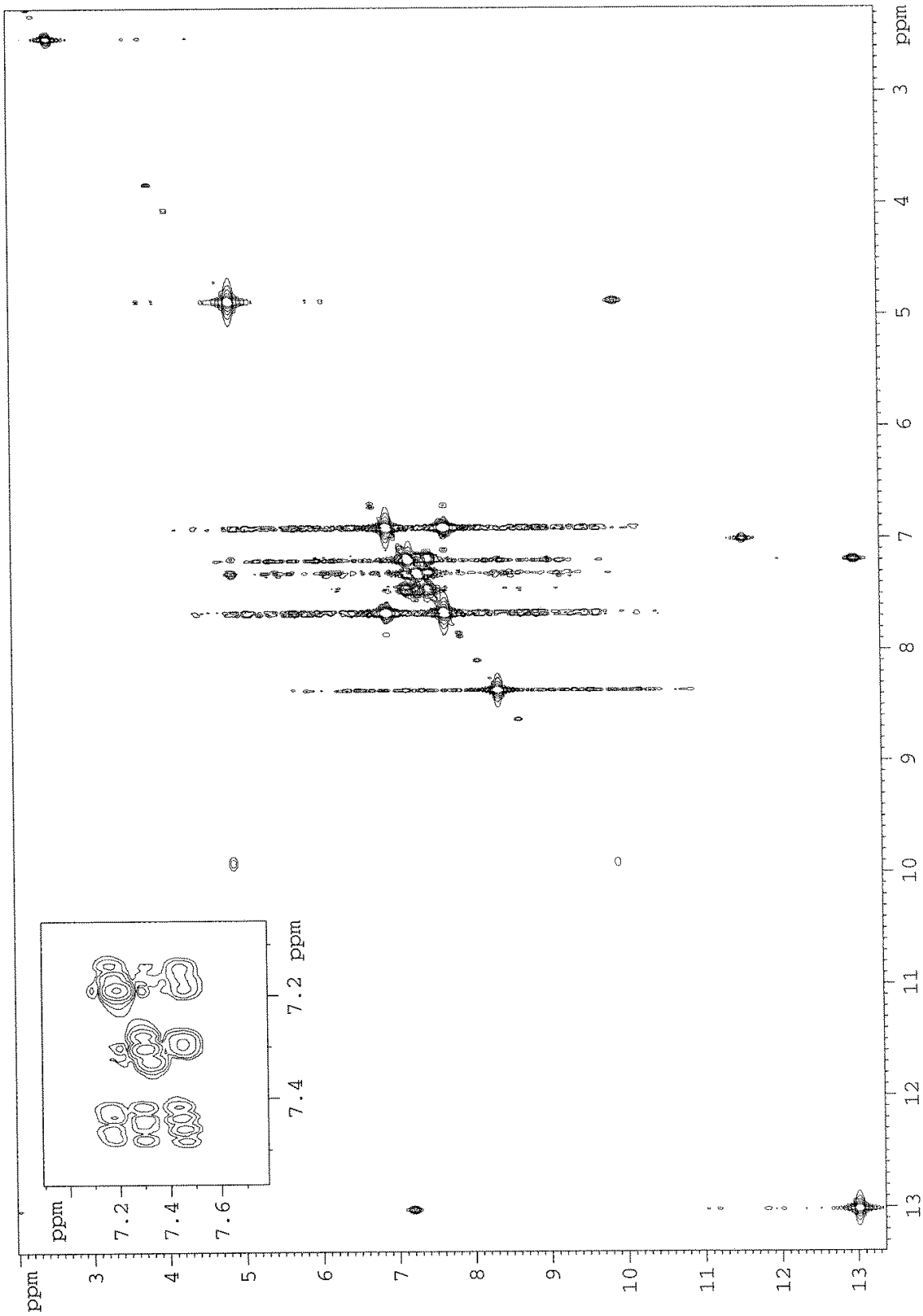

HSQC, 2D Spectrum of Compound 1g

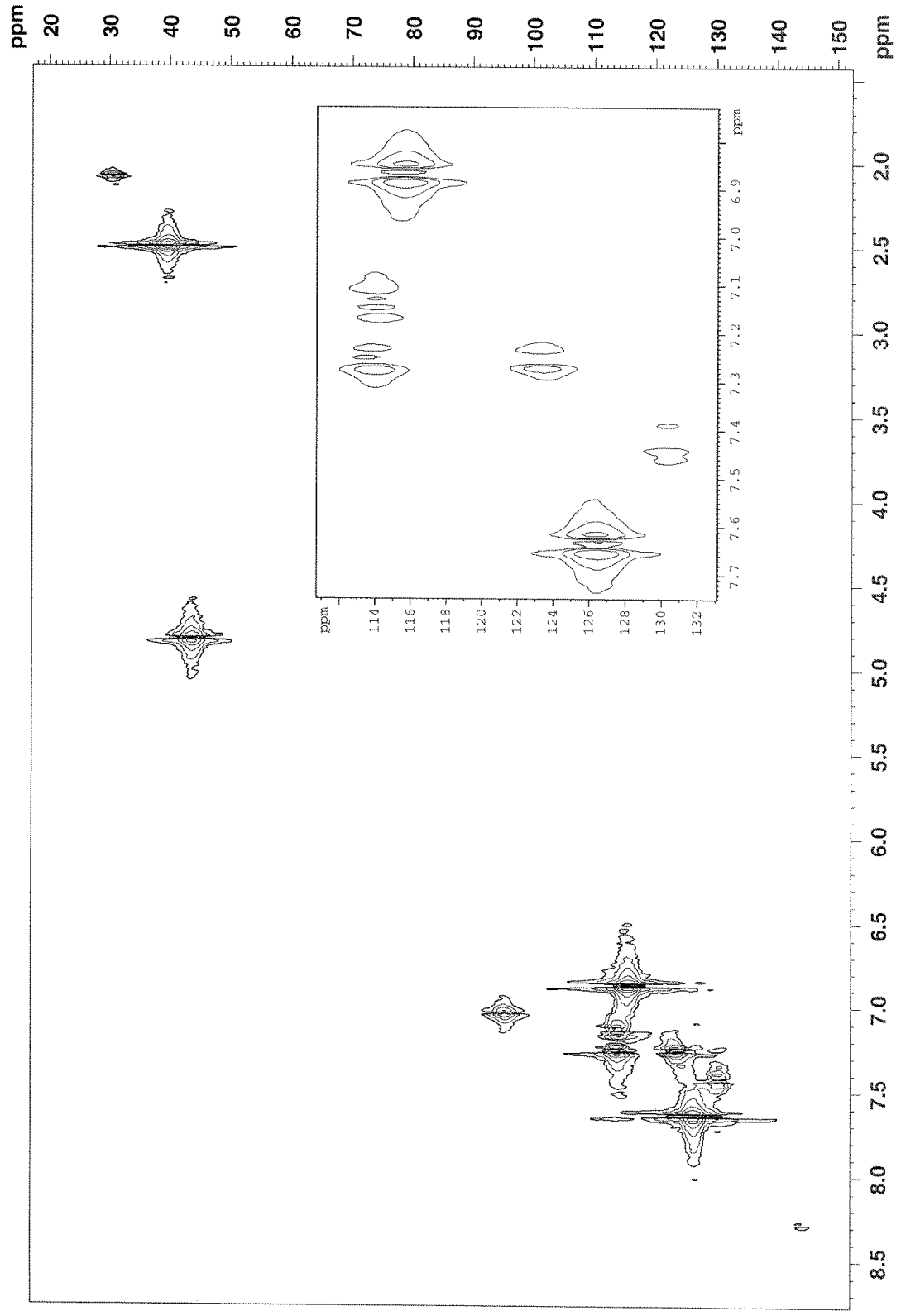

HMBC, 2D Spectrum of Compound 1g

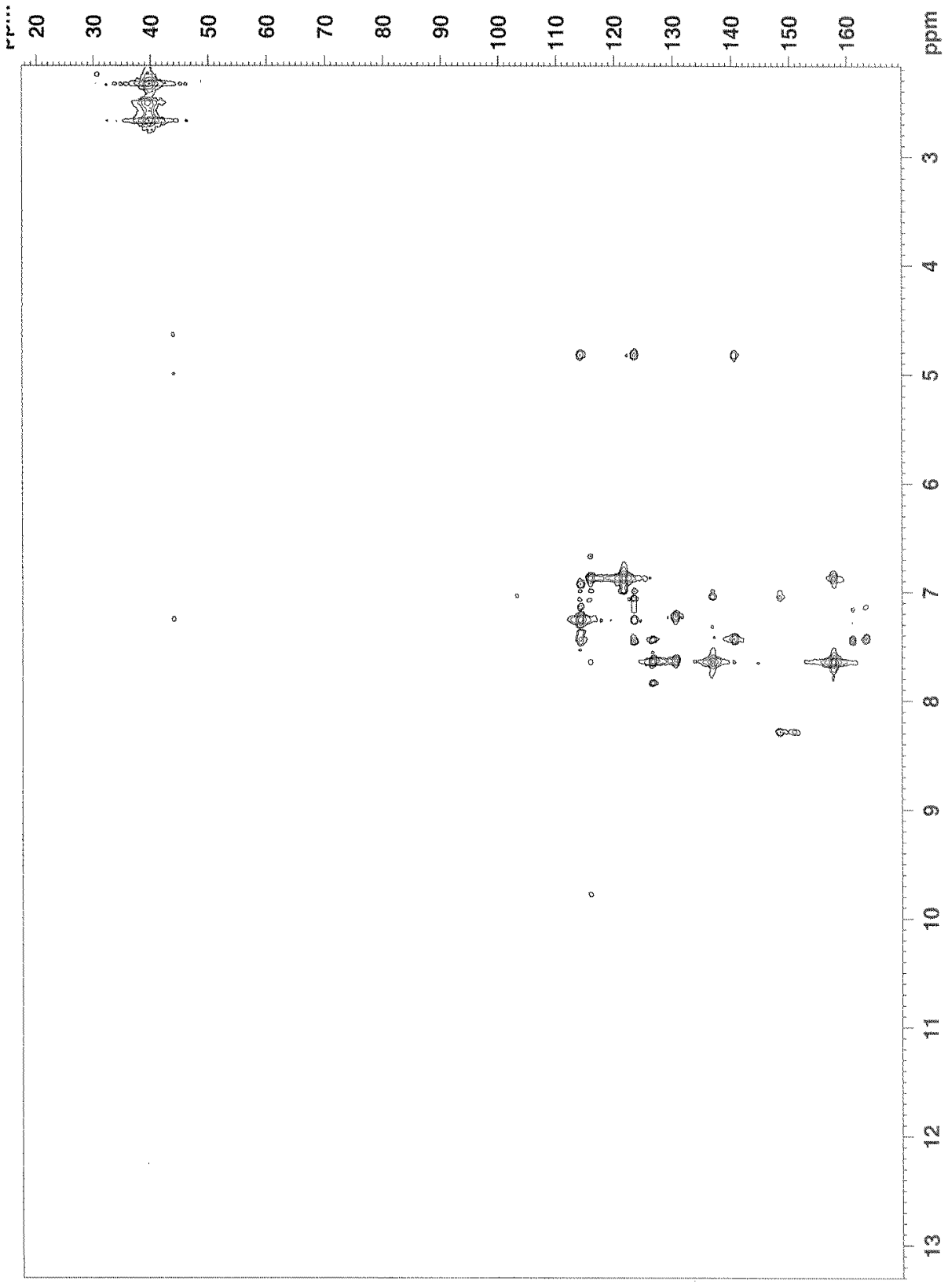

^{19}F – Spectrum of Compound 1g

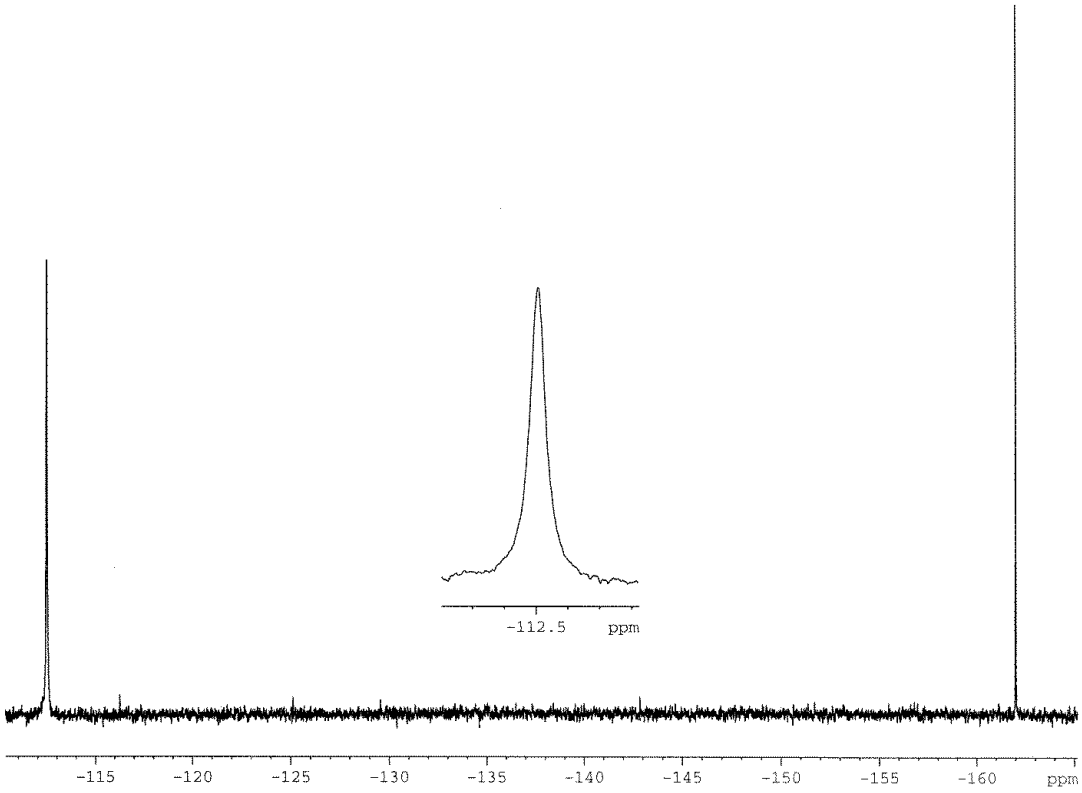

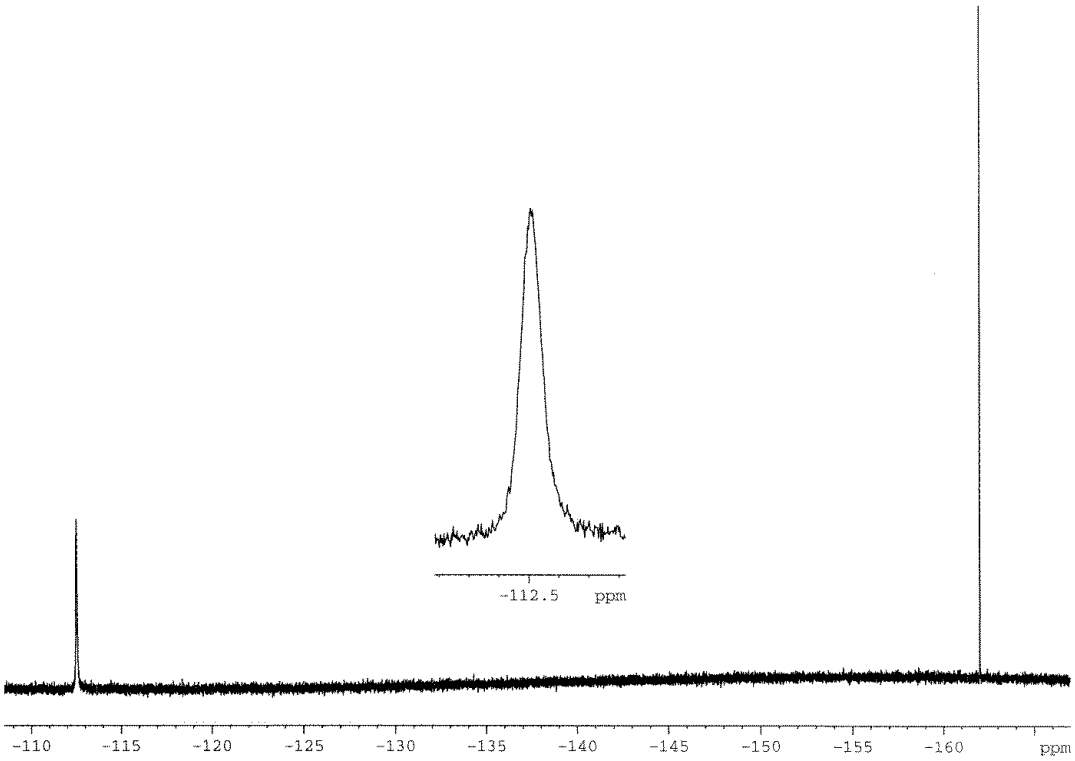

Residual peak of hexafluorobenzene is found at -162.0 ppm. Proton decoupled ^{19}F-NMR experiment is found in the top spectrum, while proton coupled ^{19}F-NMR experiment is found in the bottom spectrum.

A.1.8 – NMR spectra of Compound 1h

^{1}H – Spectrum of Compound 1h

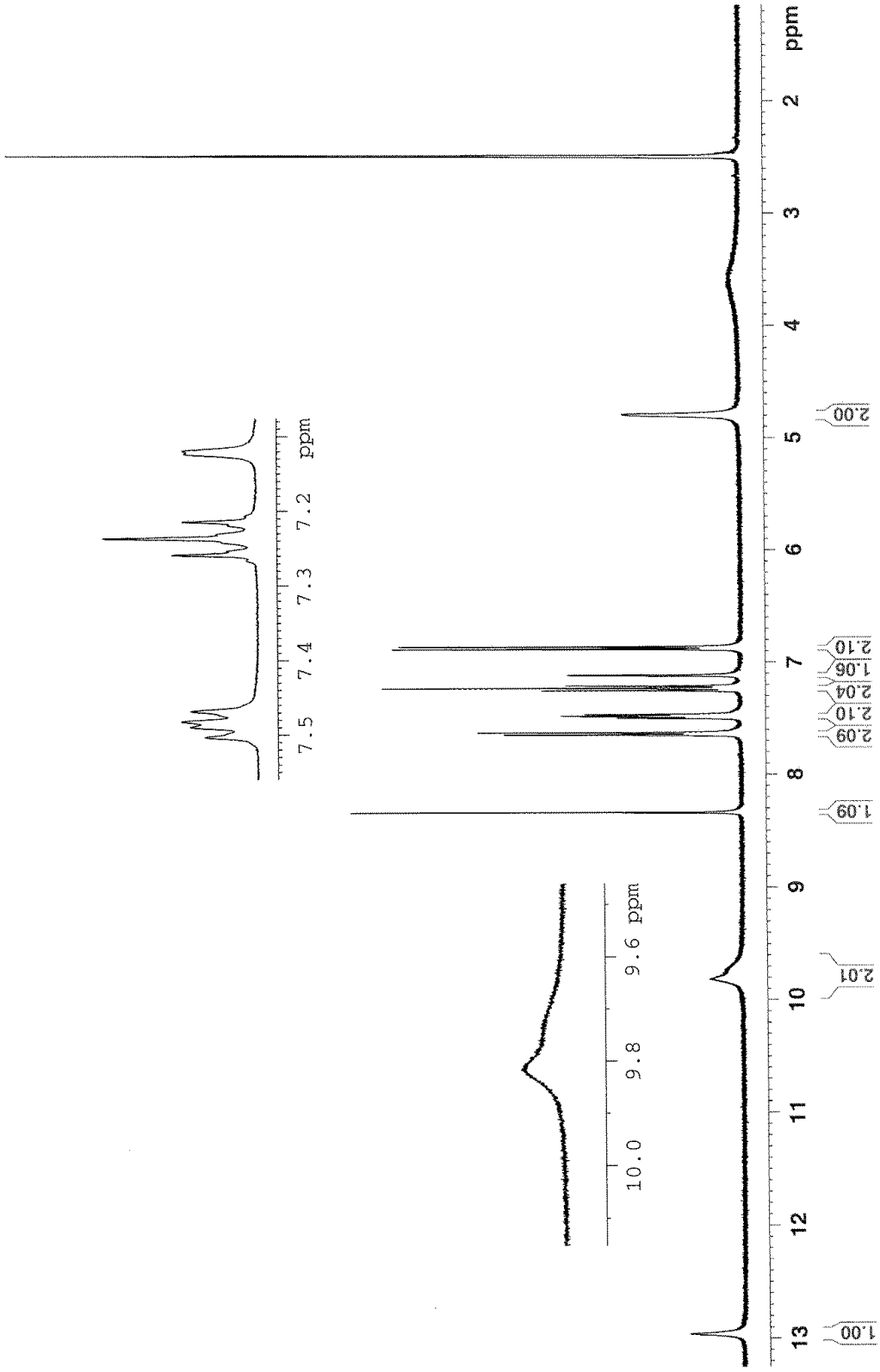

Residual peaks of DMSO and H_2O are found at 2.50 ppm and 3.33 ppm, respectively.

^{13}C – Spectrum of Compound 1h

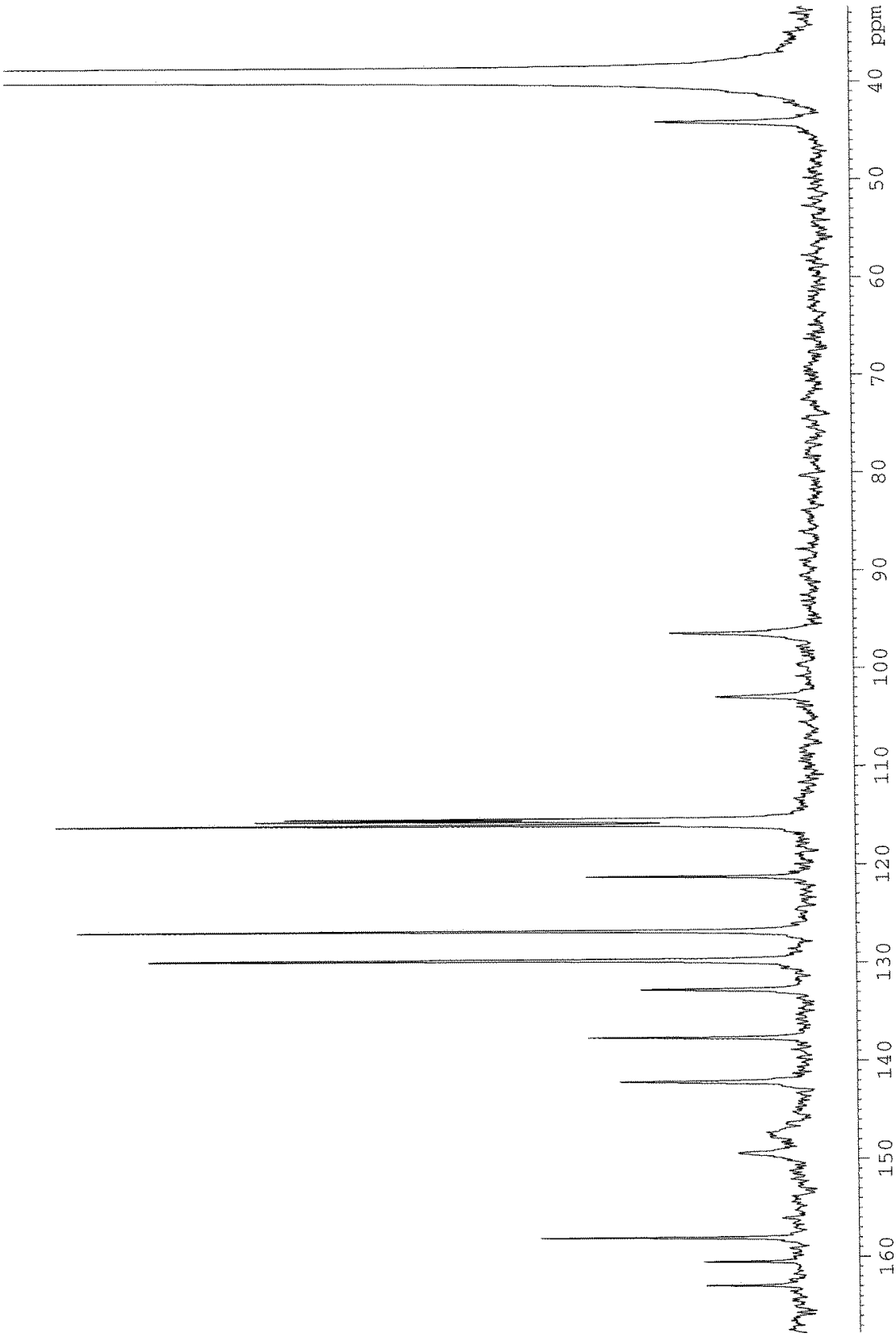

Residual peak of DMSO is found at 39.51 ppm.

COSY, 2D Spectrum of Compound 1h

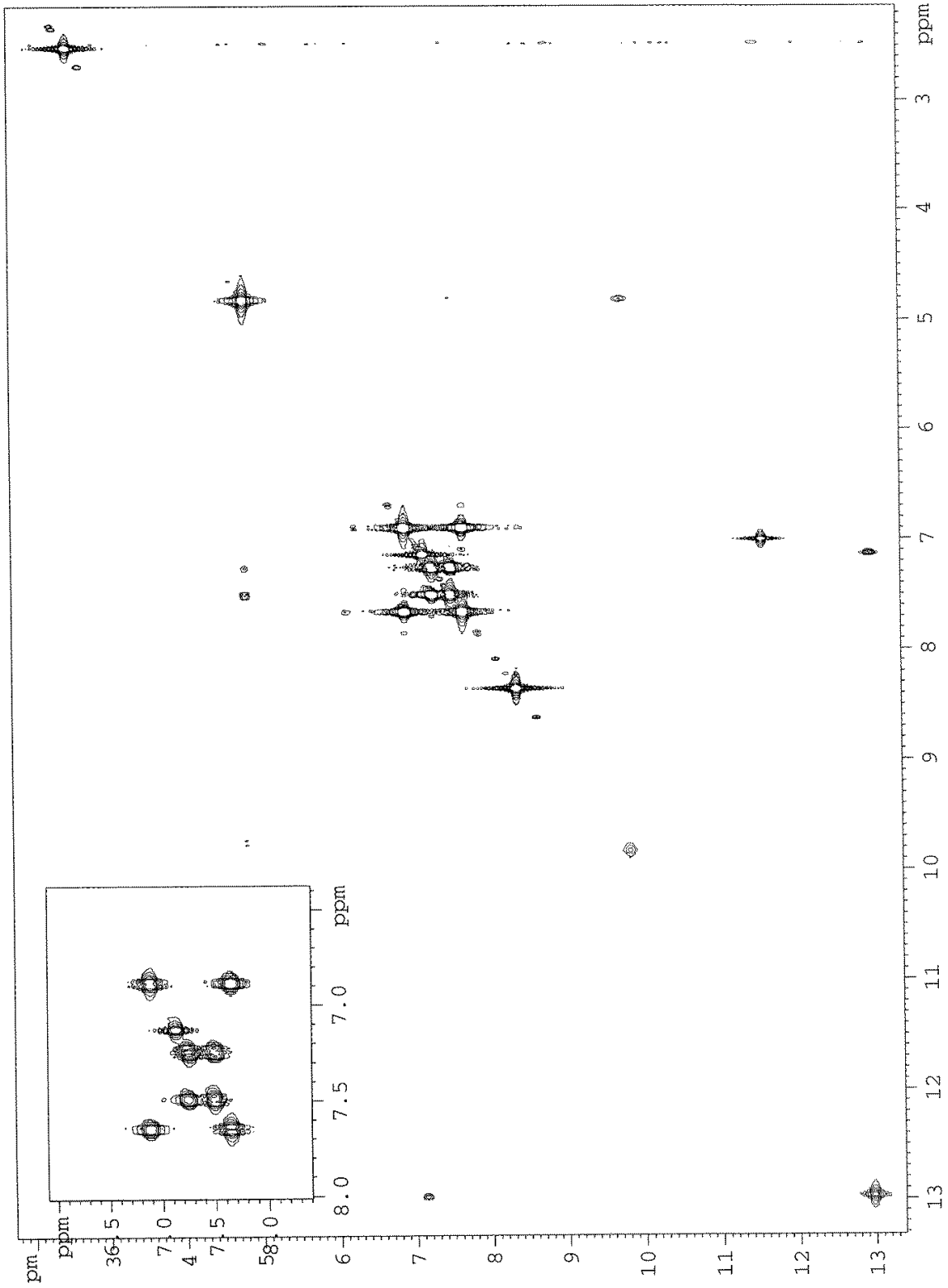

HSQC, 2D Spectrum of Compound 1h

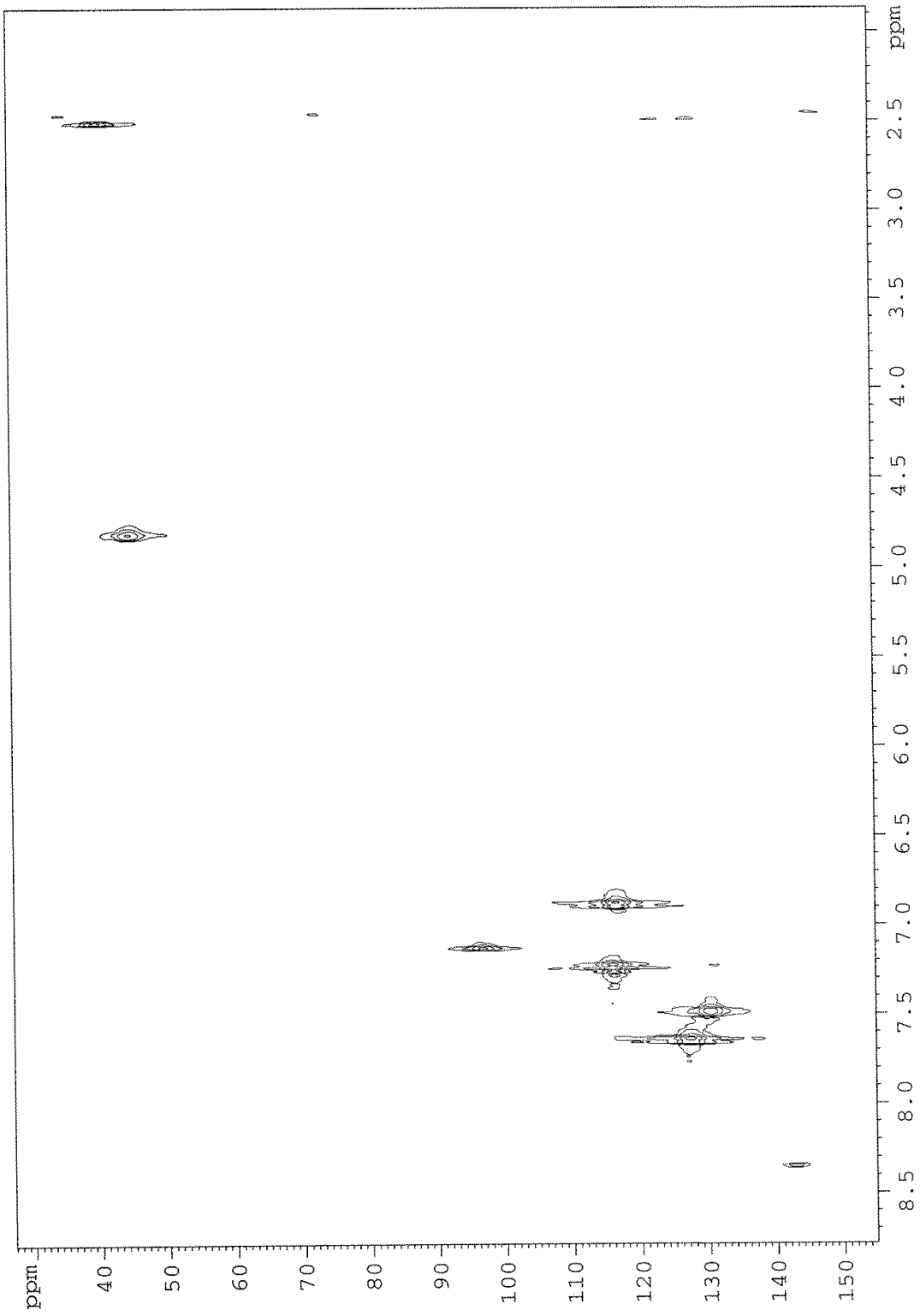

HMBC, 2D Spectrum of Compound 1h

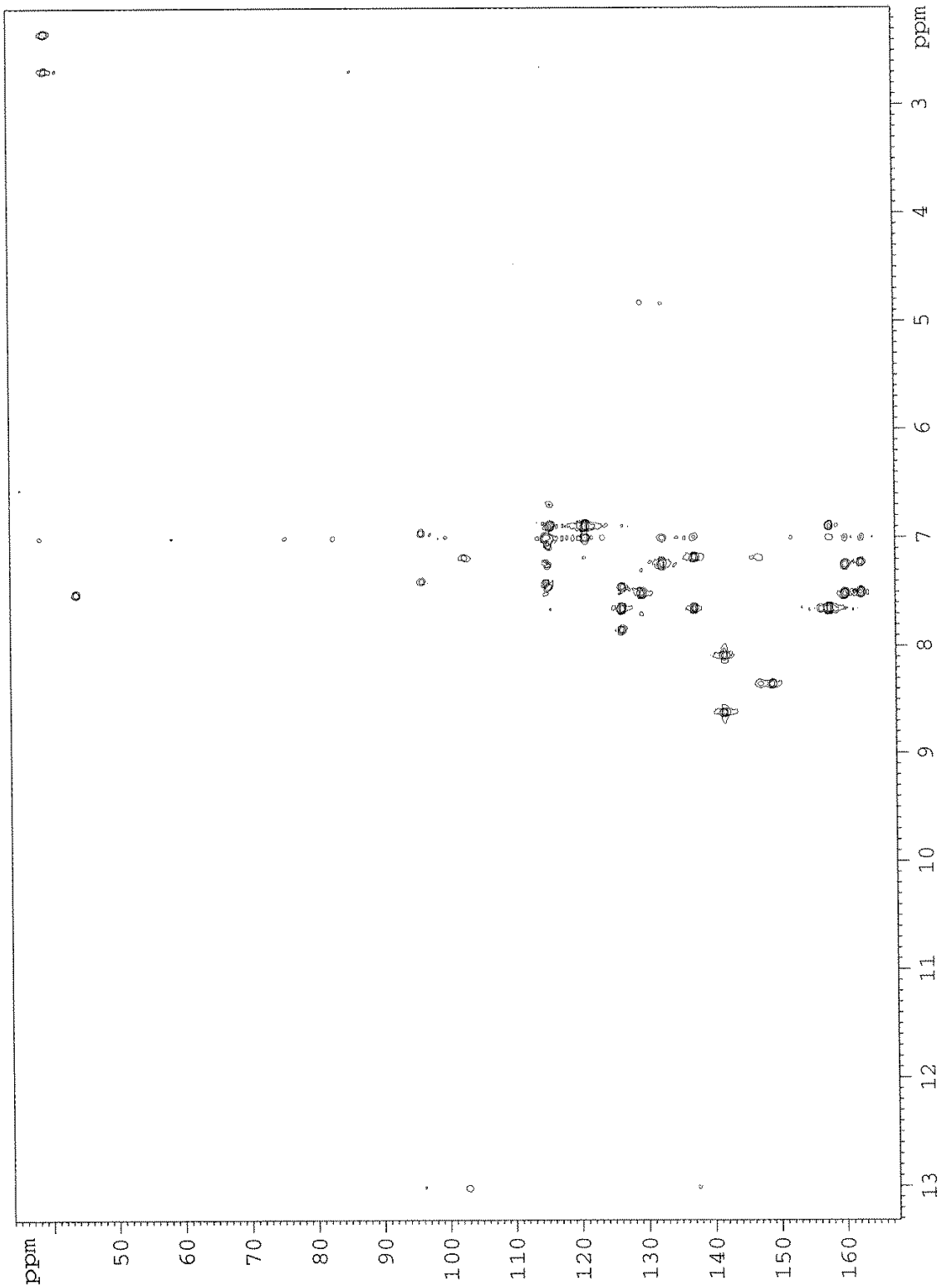

^{19}F – Spectrum of Compound 1h

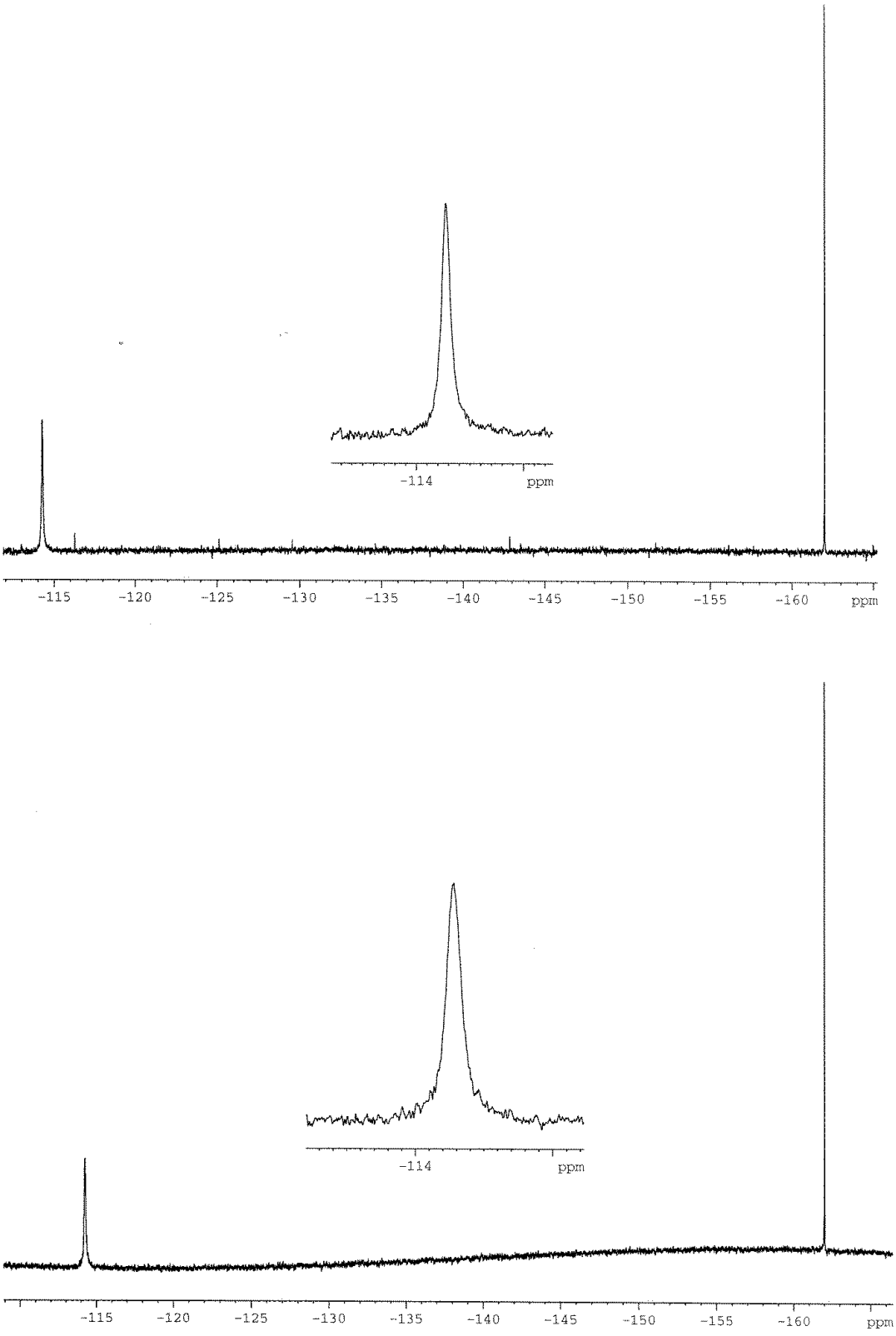

Residual peak of hexafluorobenzene is found at -162.0 ppm. Proton decoupled ^{19}F-NMR experiment is found in the top spectrum, while proton coupled ^{19}F-NMR experiment is found in the bottom spectrum.

A.2 – NMR Spectra of Compounds 2a-h

A.2.1 – NMR spectra of Compound 2a

1H – Spectrum of Compound 2a

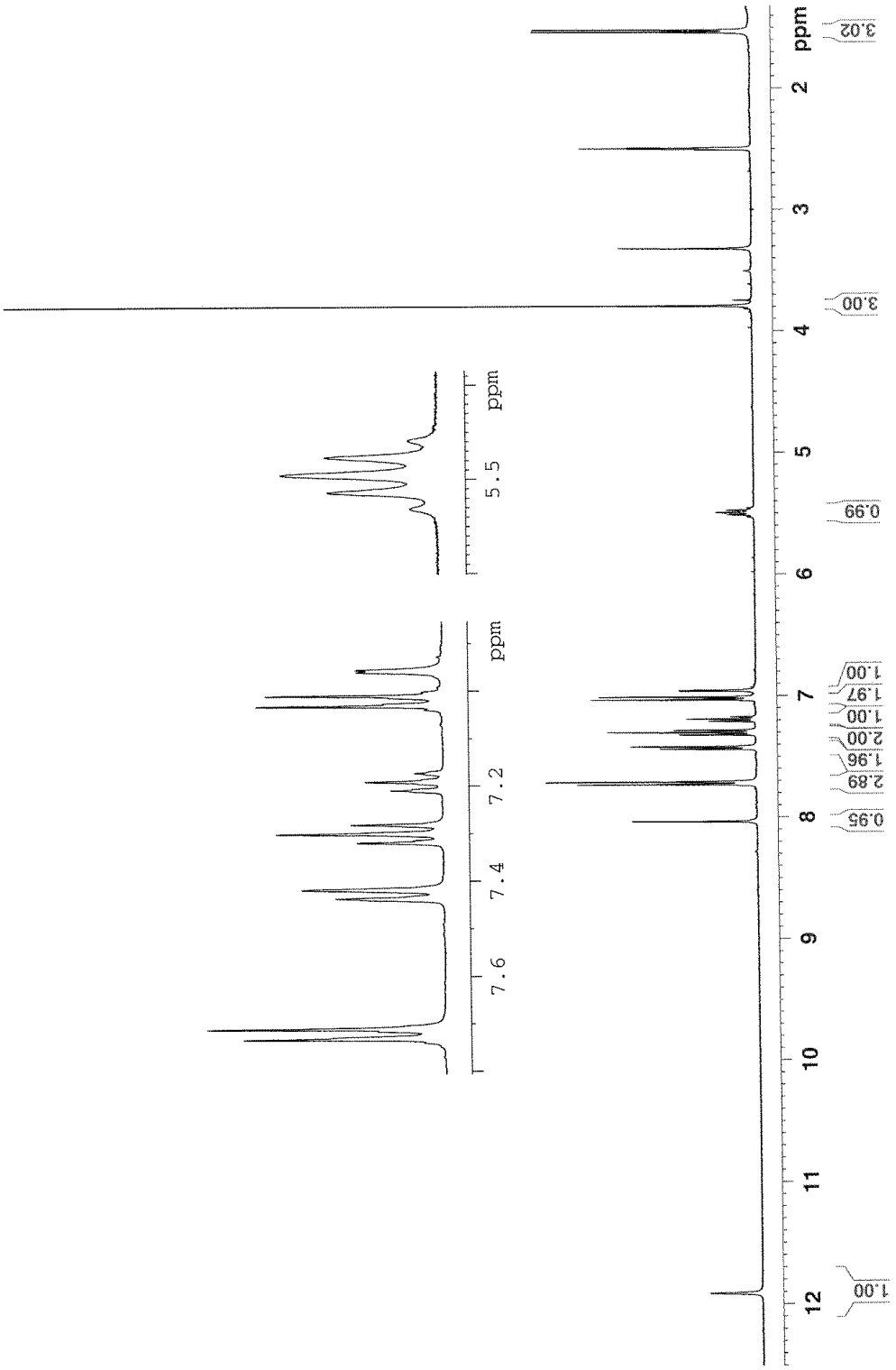

Residual peaks of DMSO and H_2O are found at 2.50 ppm and 3.33 ppm, respectively.

^{13}C – Spectrum of Compound 2a

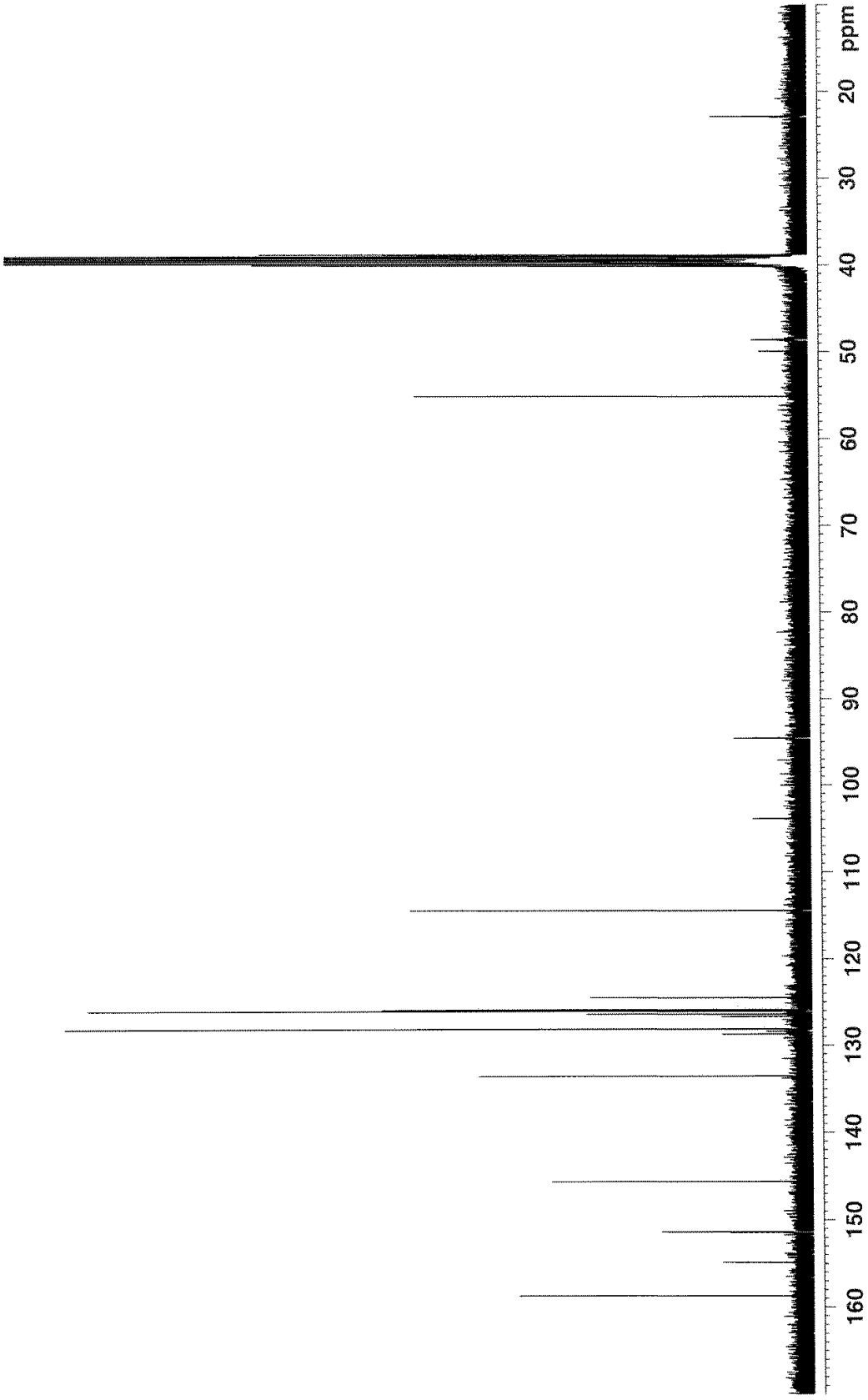

Residual peak of DMSO is found at 39.51 ppm.

COSY, 2D Spectrum of Compound 2a

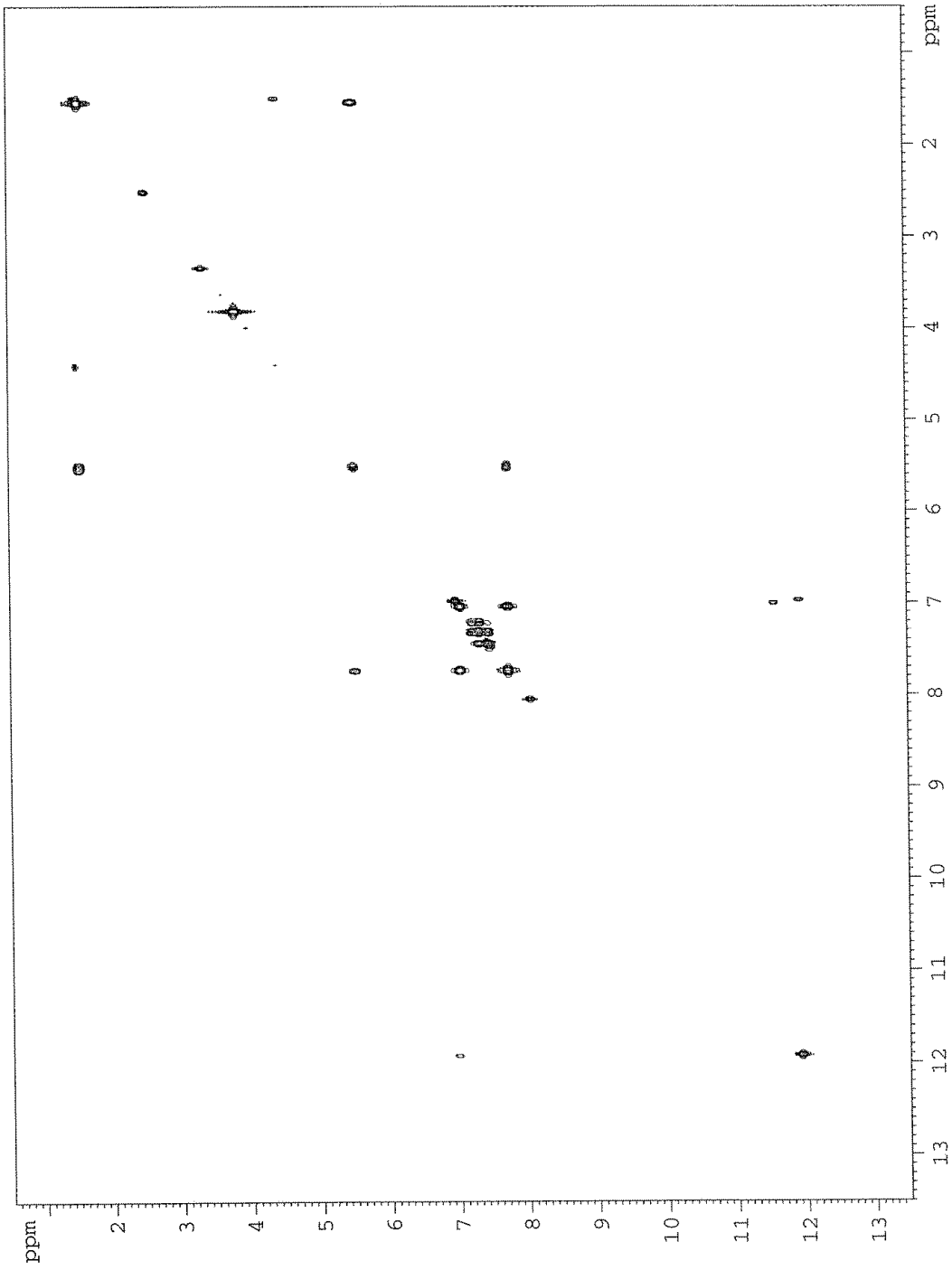

HSQC, 2D Spectrum of Compound 2a

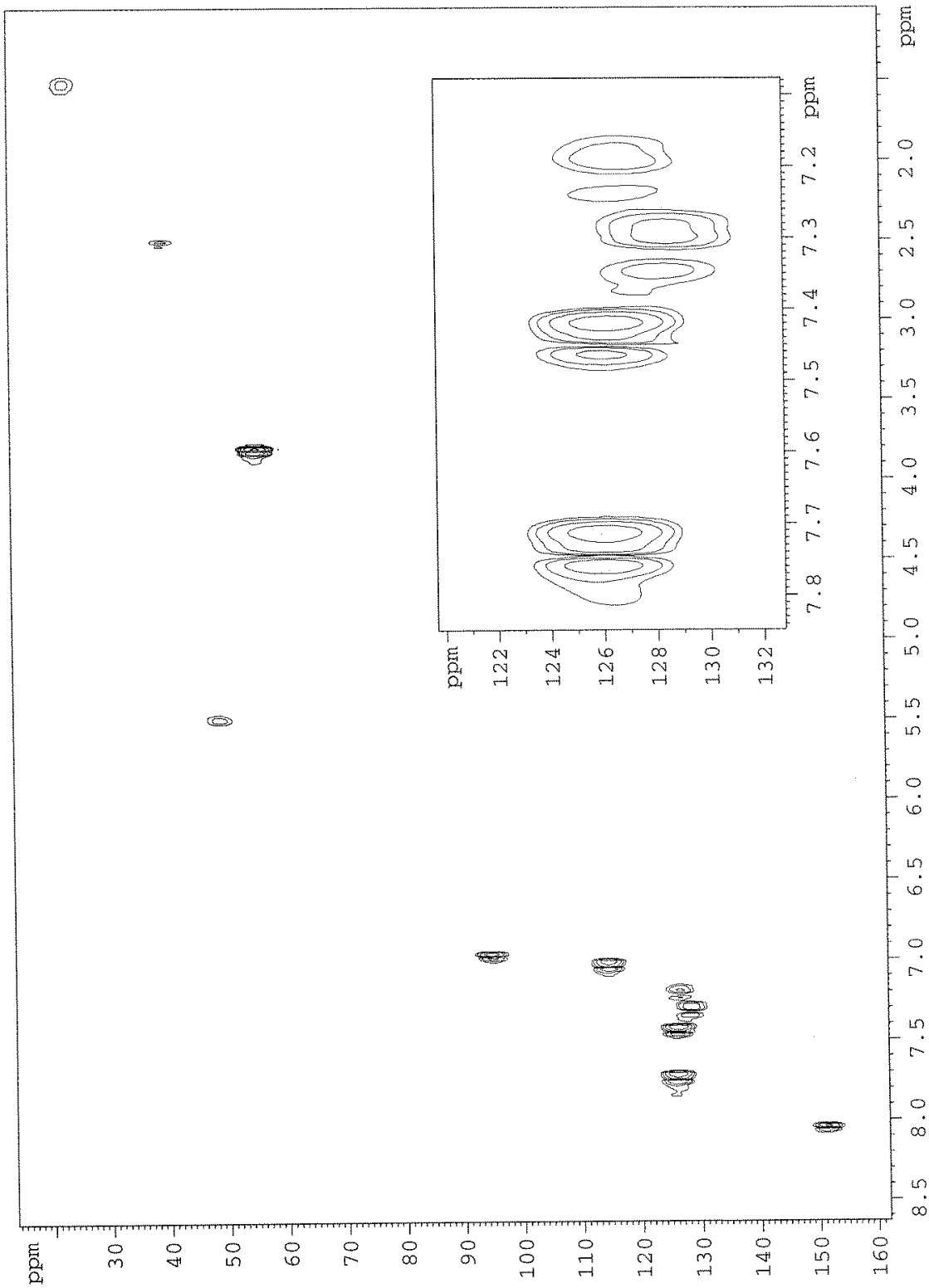

HMBC, 2D Spectrum of Compound 2a

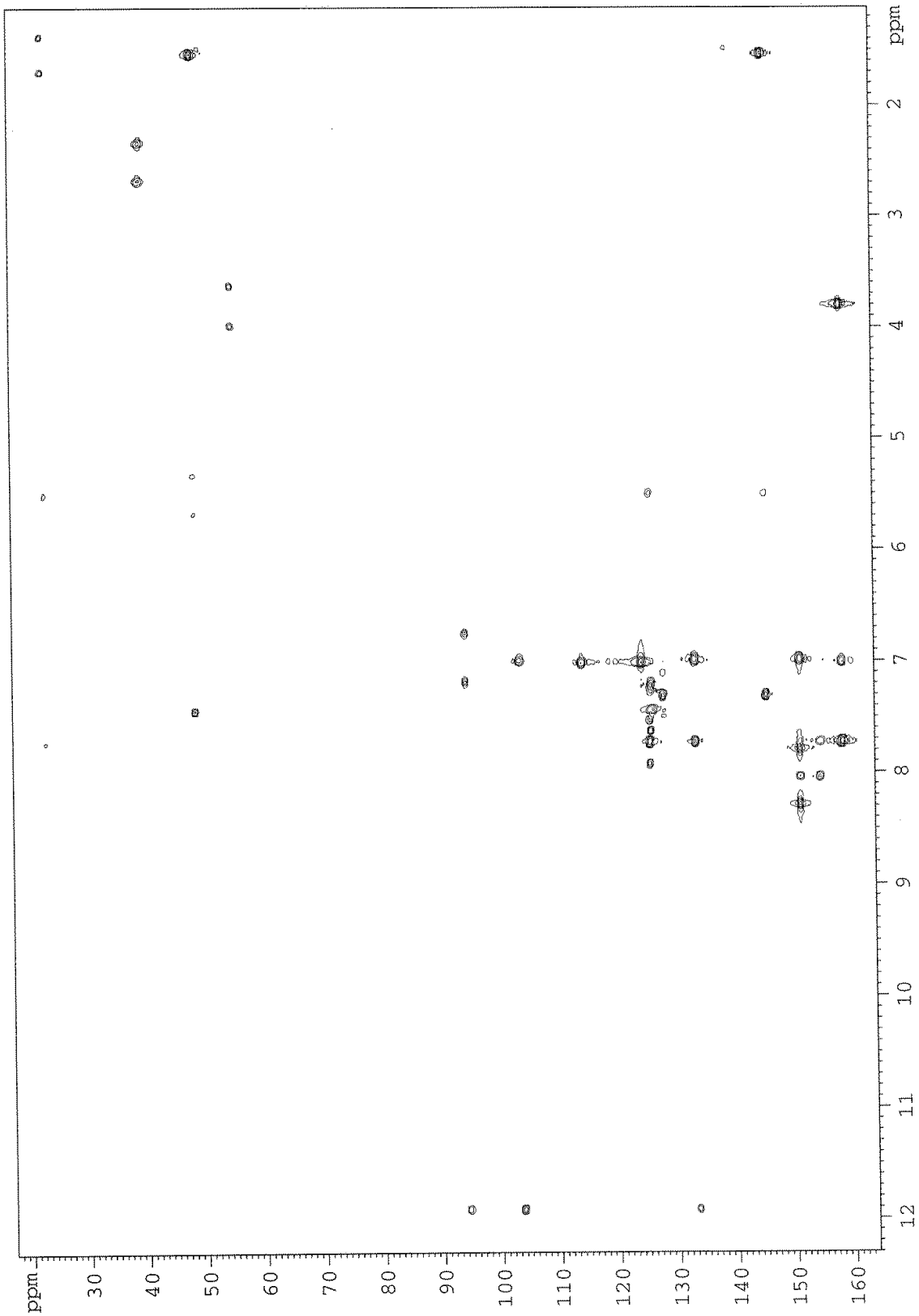

A.2.2 – NMR spectra of Compound 2b

^{1}H – Spectrum of Compound 2b

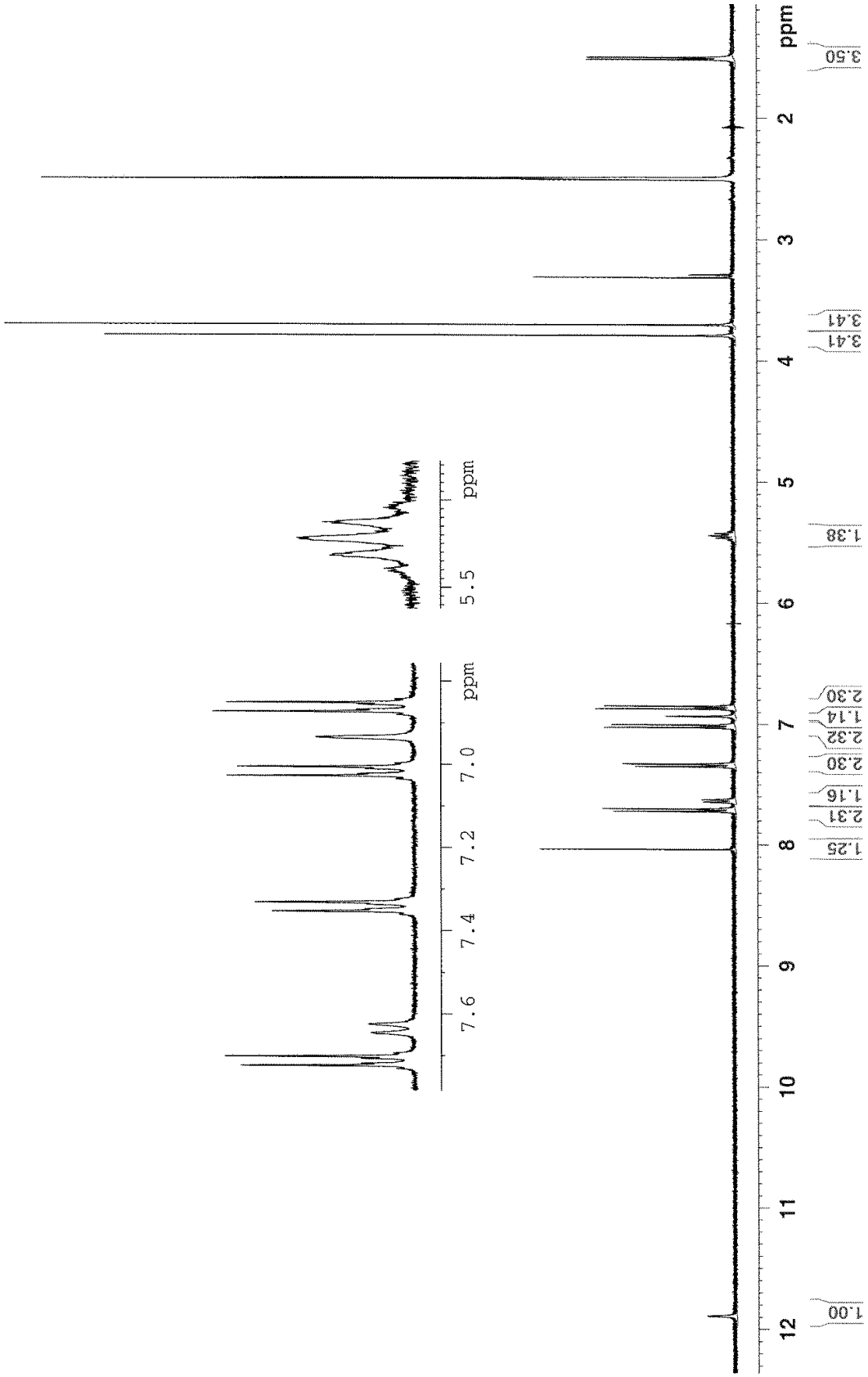

Residual peaks of DMSO and H_2O are found at 2.50 ppm and 3.33 ppm, respectively.

^{13}C – Spectrum of Compound 2b

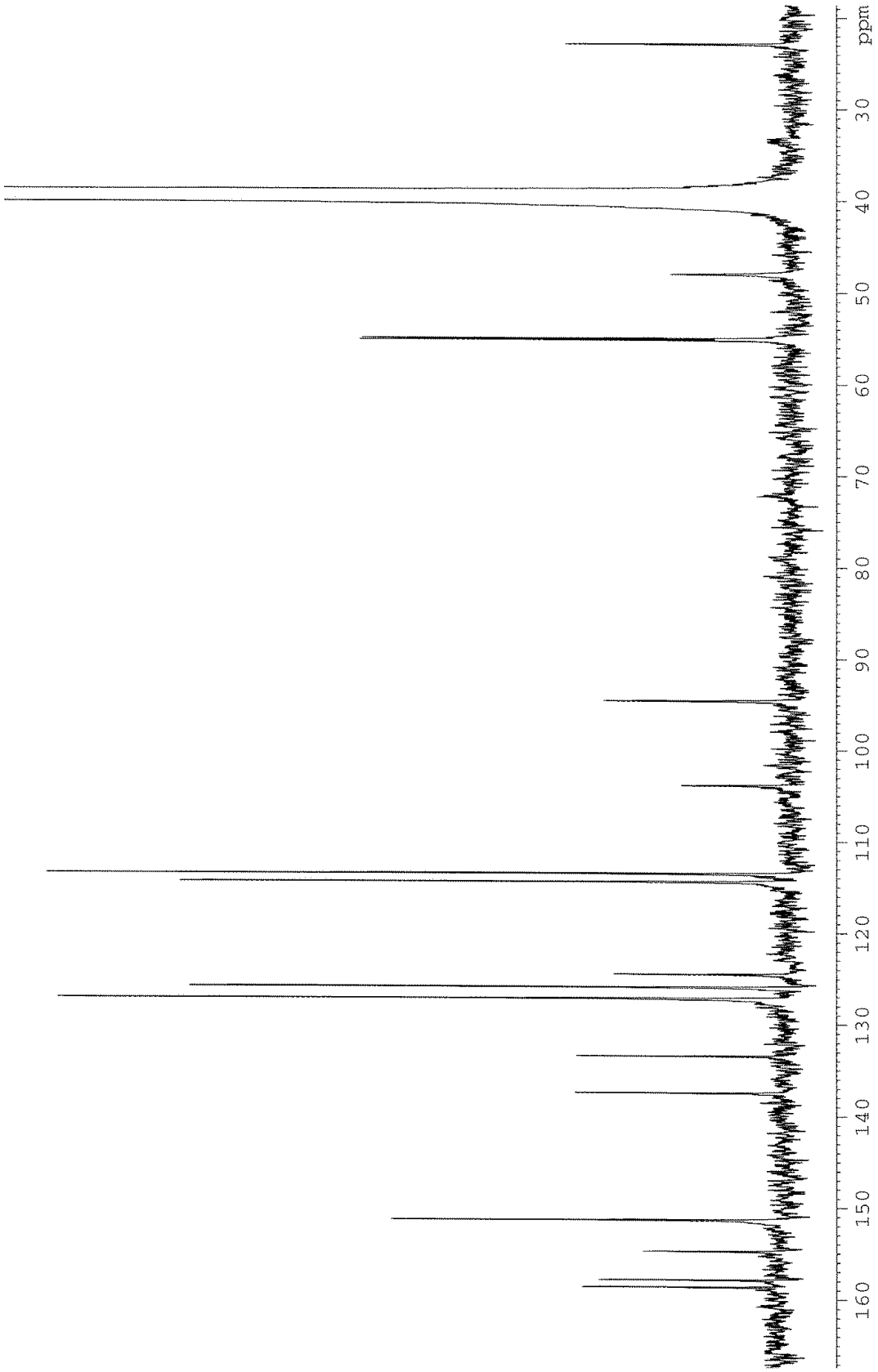

Residual peak of DMSO is found at 39.51 ppm.

COSY, 2D Spectrum of Compound 2b

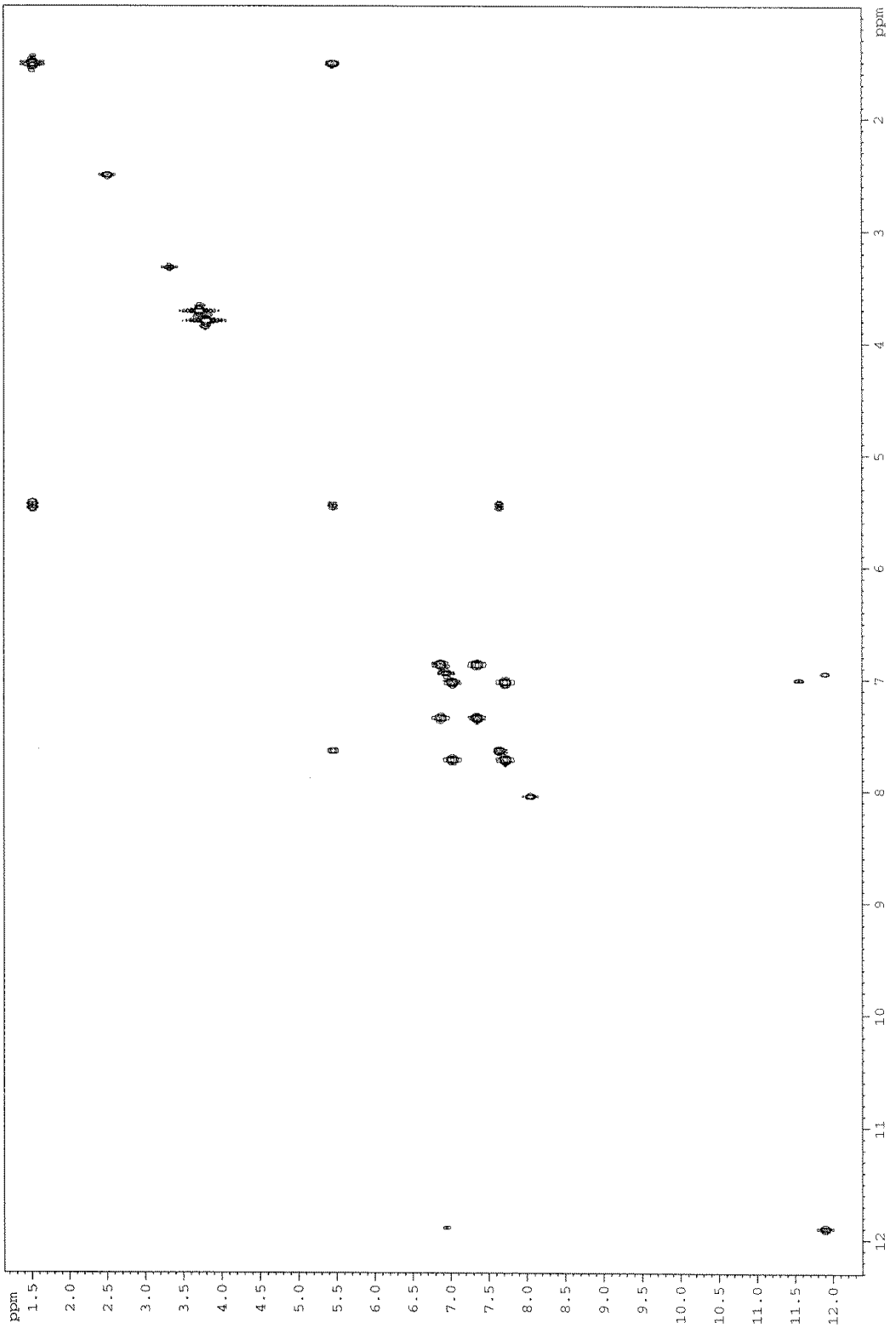

HSQC, 2D Spectrum of Compound 2b

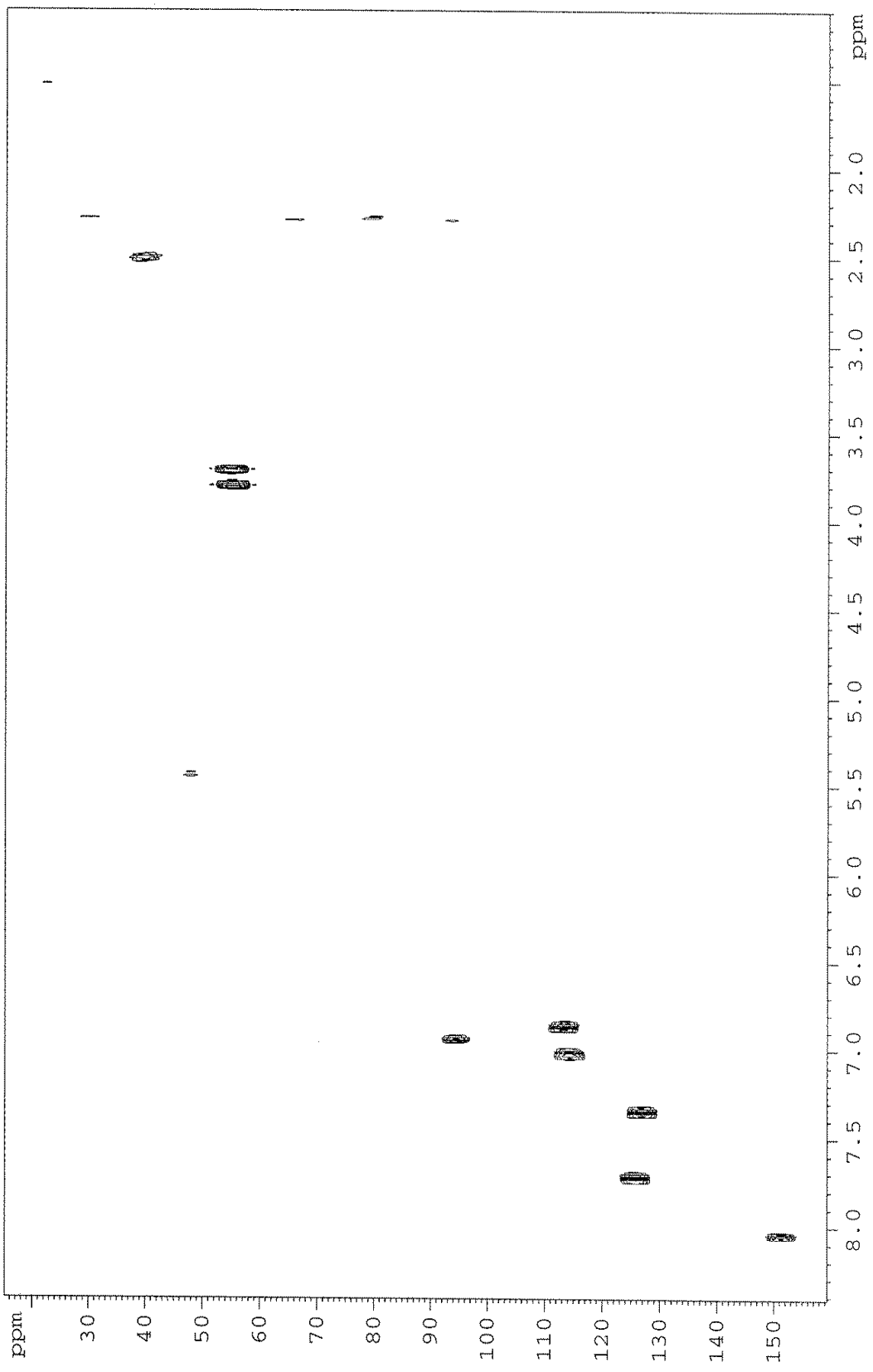

HMBC, 2D Spectrum of Compound 2b

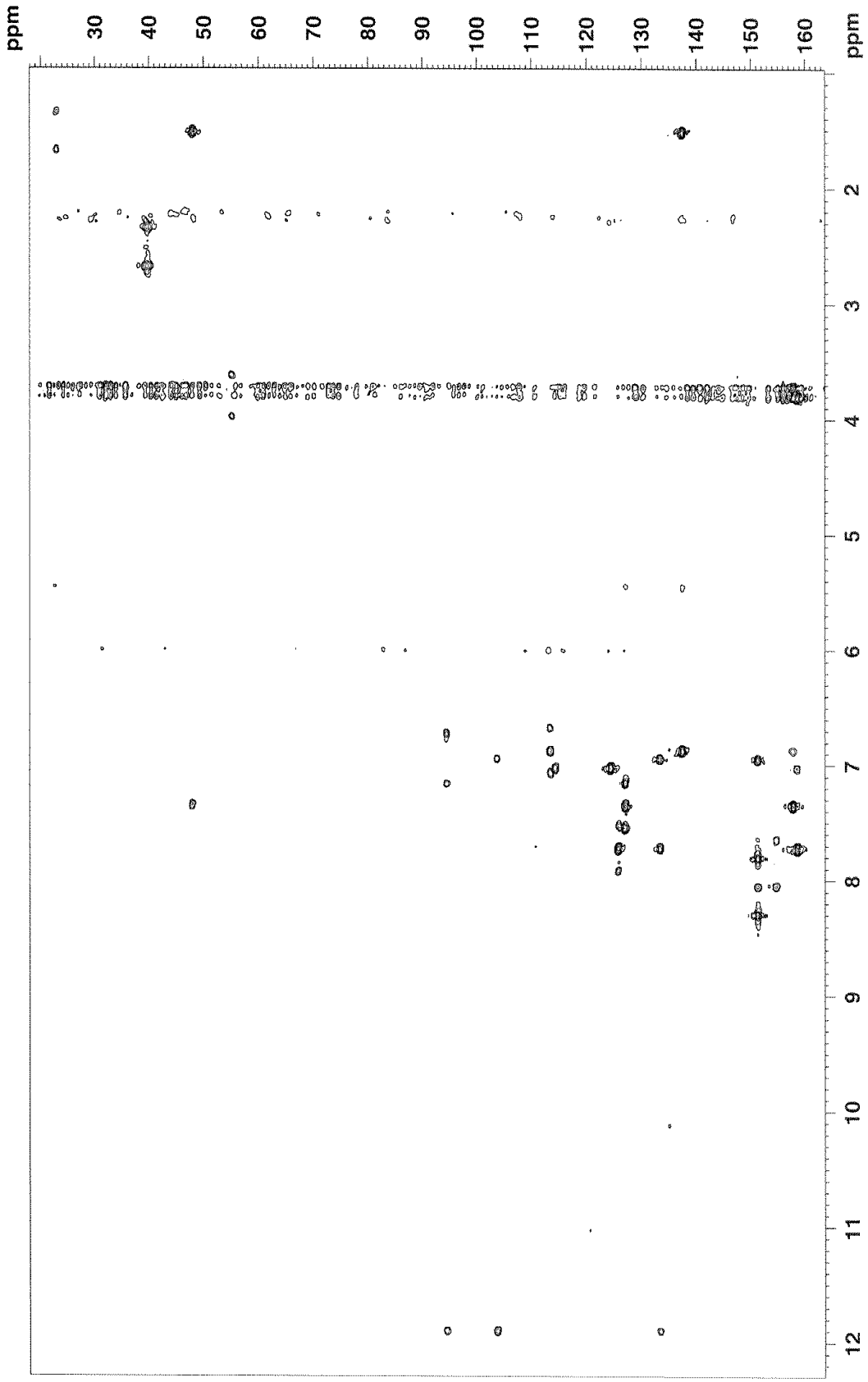

A.2.3 – NMR spectra of Compound 2c

^{1}H – Spectrum of Compound 2c

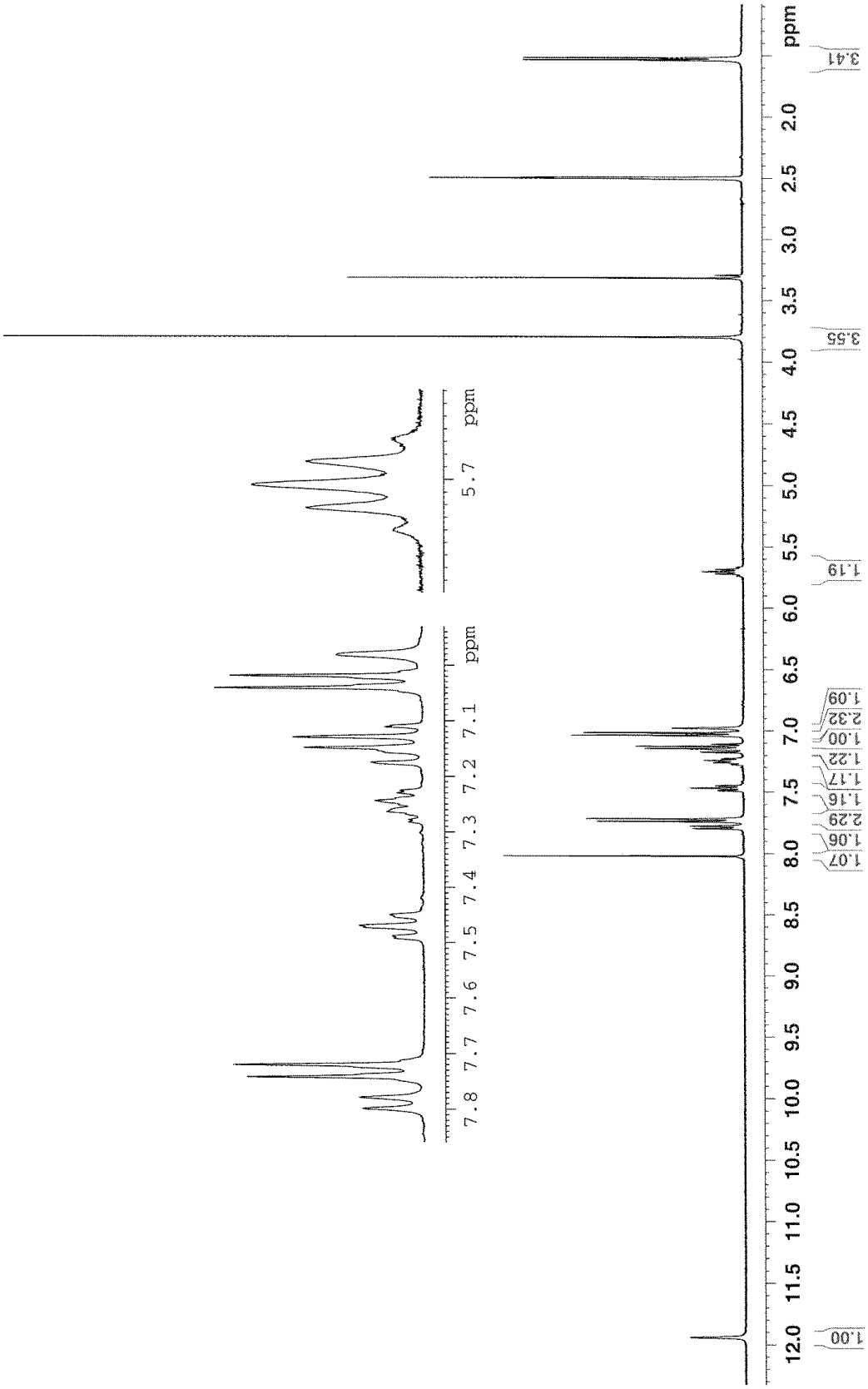

Residual peaks of DMSO and H_2O are found at 2.50 ppm and 3.33 ppm, respectively.

^{13}C – Spectrum of Compound 2c

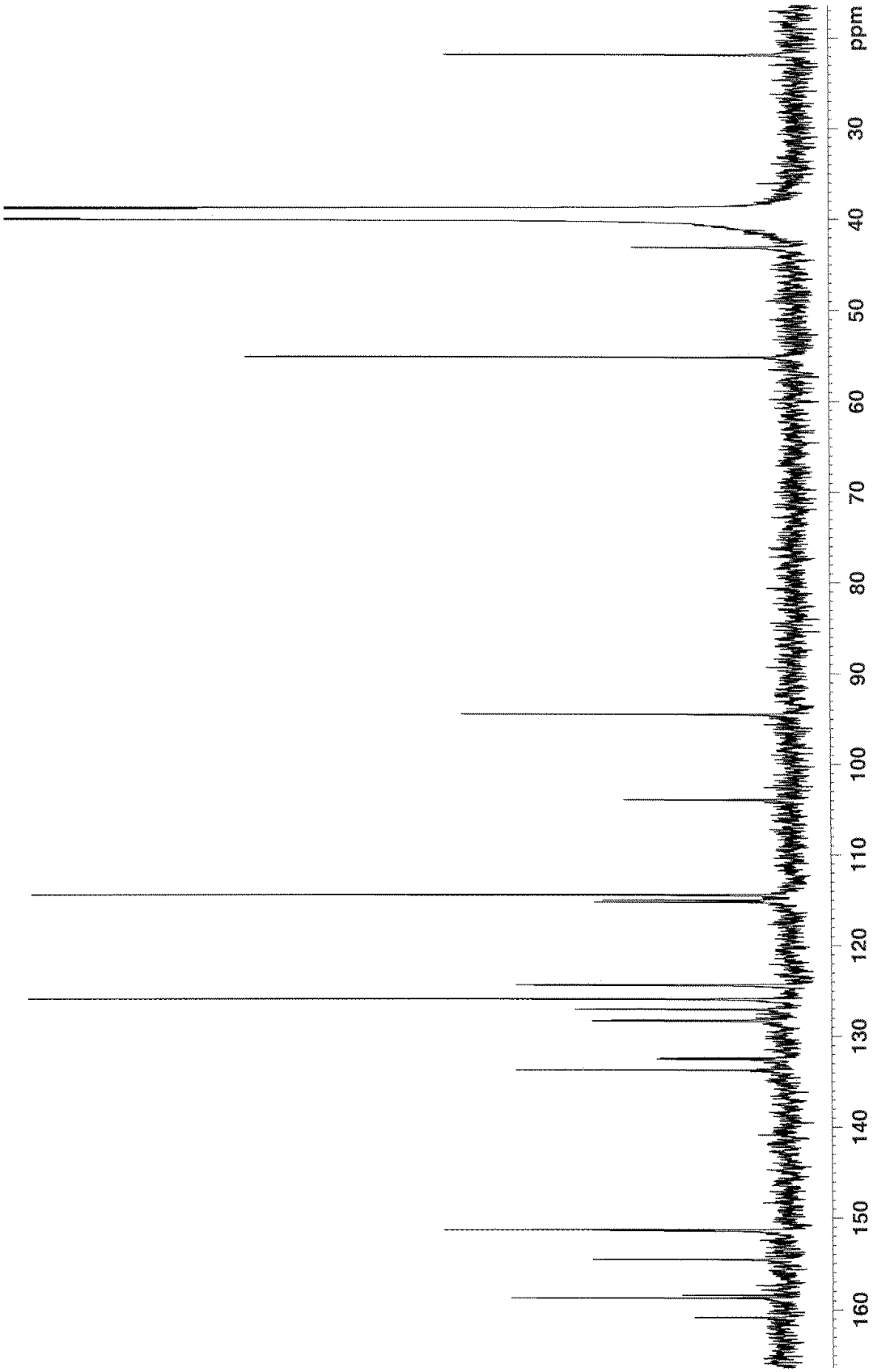

Residual peak of DMSO is found at 39.51 ppm.

COSY, 2D Spectrum of Compound 2c

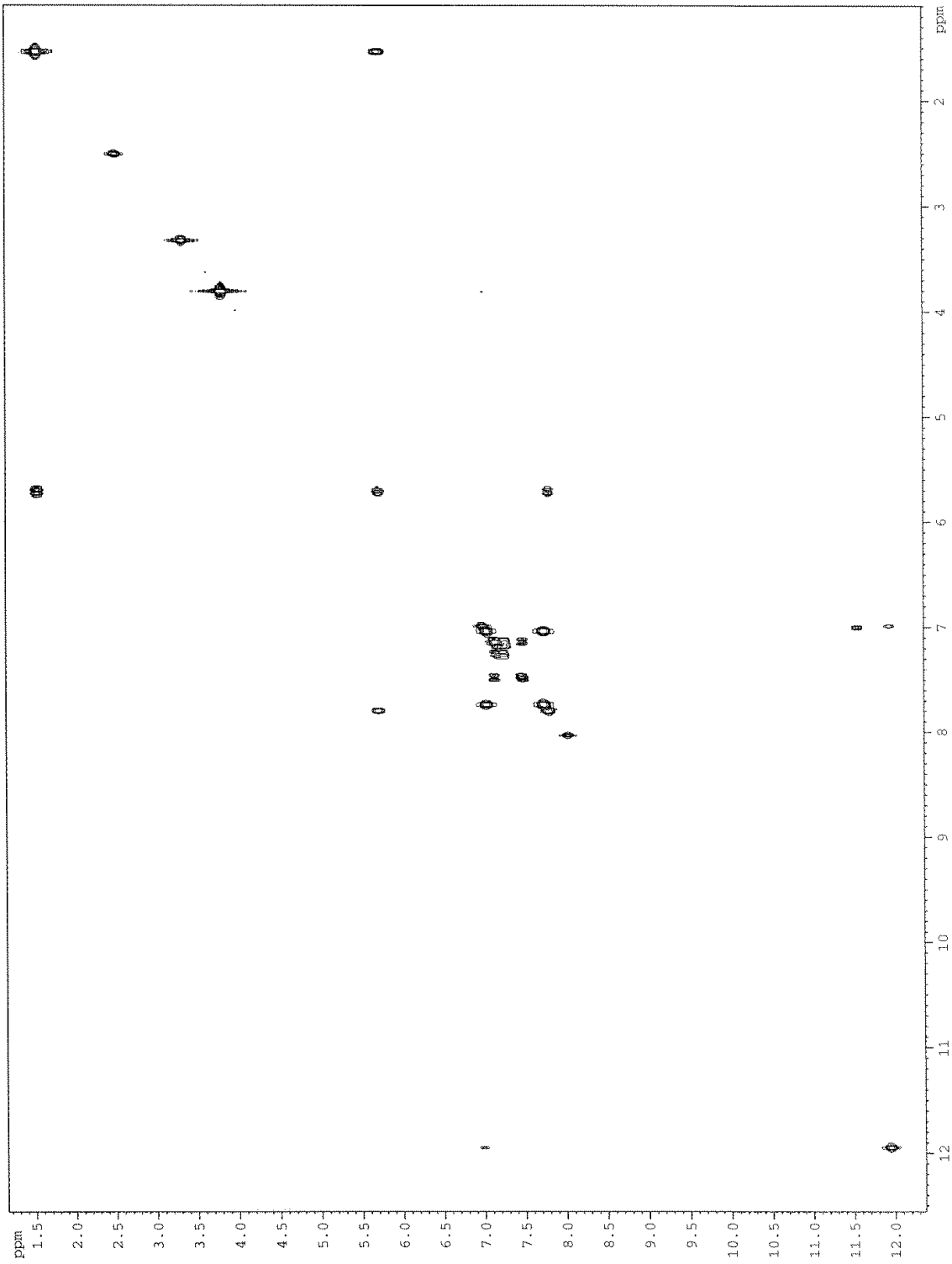

HSQC, 2D Spectrum of Compound 2c

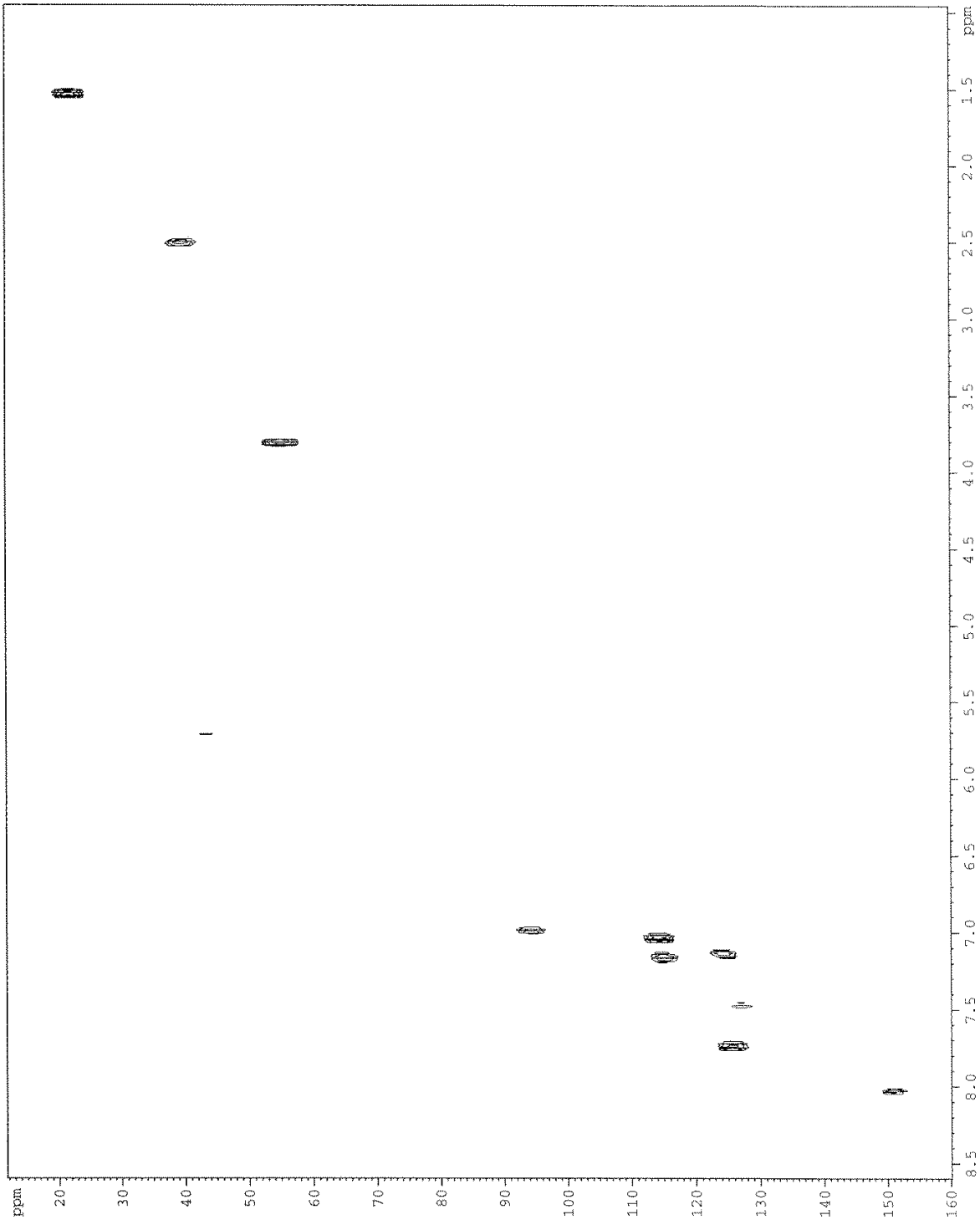

HMBC, 2D Spectrum of Compound 2c

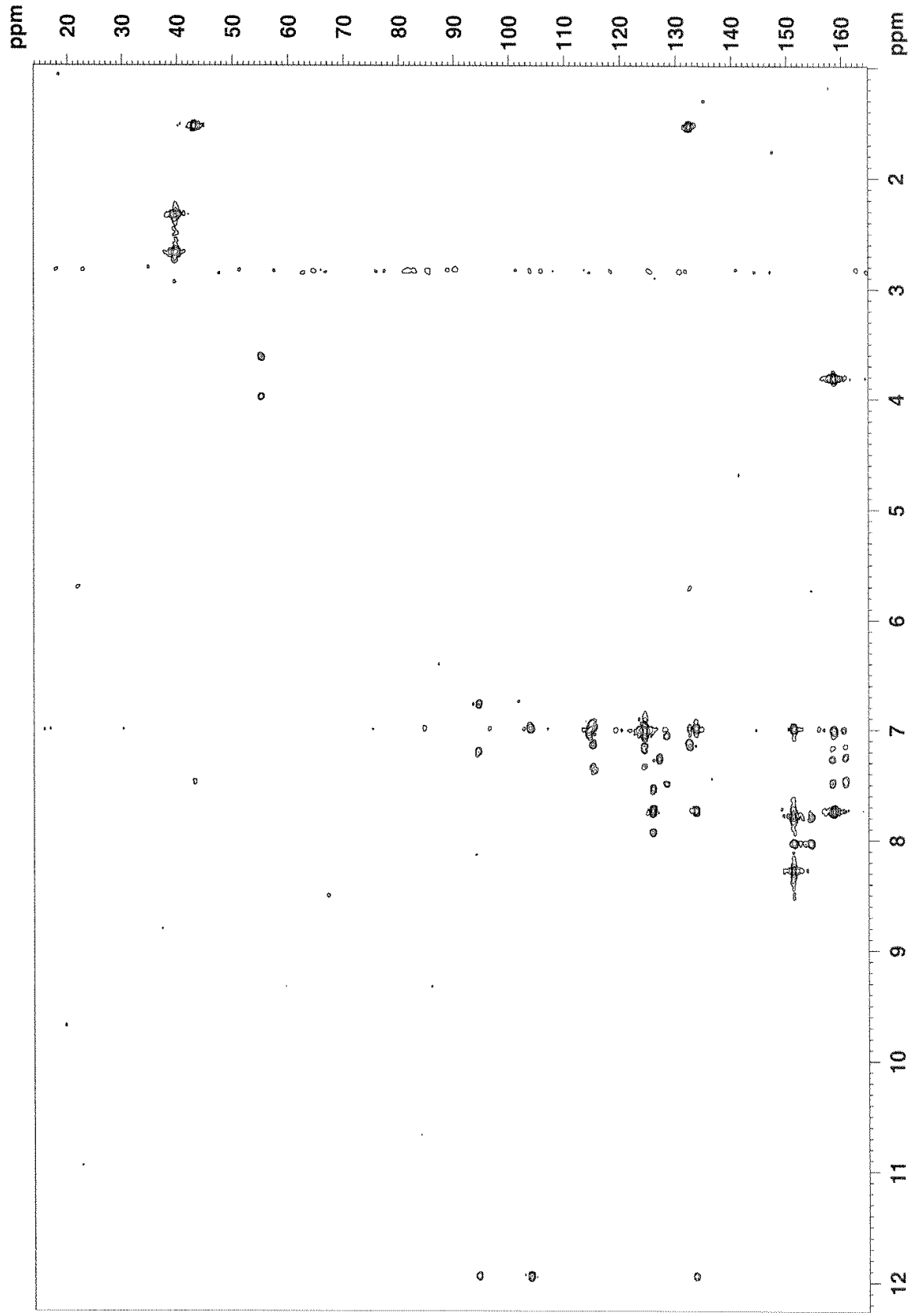

^{19}F – Spectrum of Compound 2c

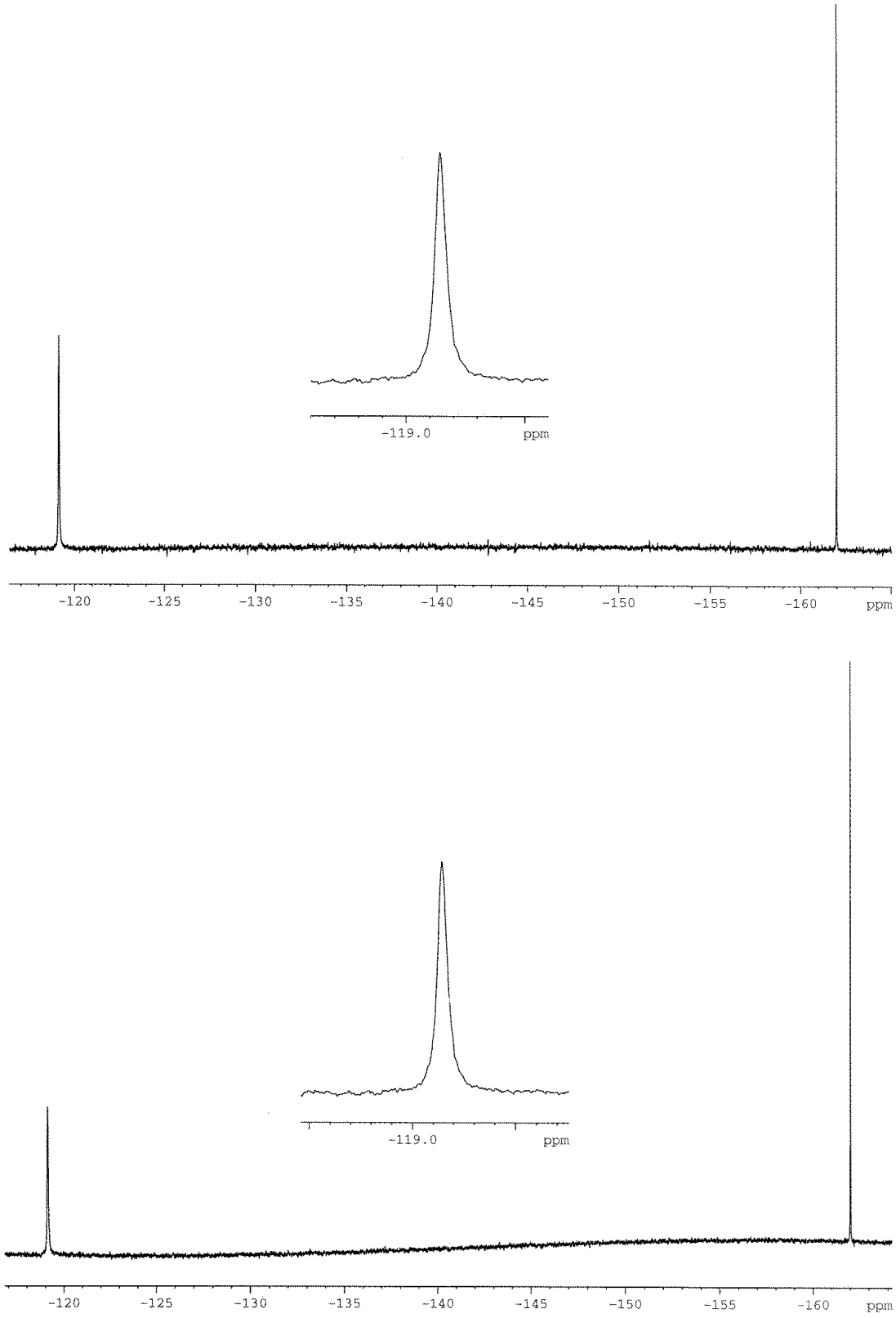

Residual peak of hexafluorobenzene is found at -162.0 ppm. Proton decoupled ^{19}F-NMR experiment is found in the top spectrum, while proton coupled ^{19}F-NMR experiment is found in the bottom spectrum.

A.2.4 – NMR spectra of Compound 2d

^{1}H – Spectrum of Compound 2d

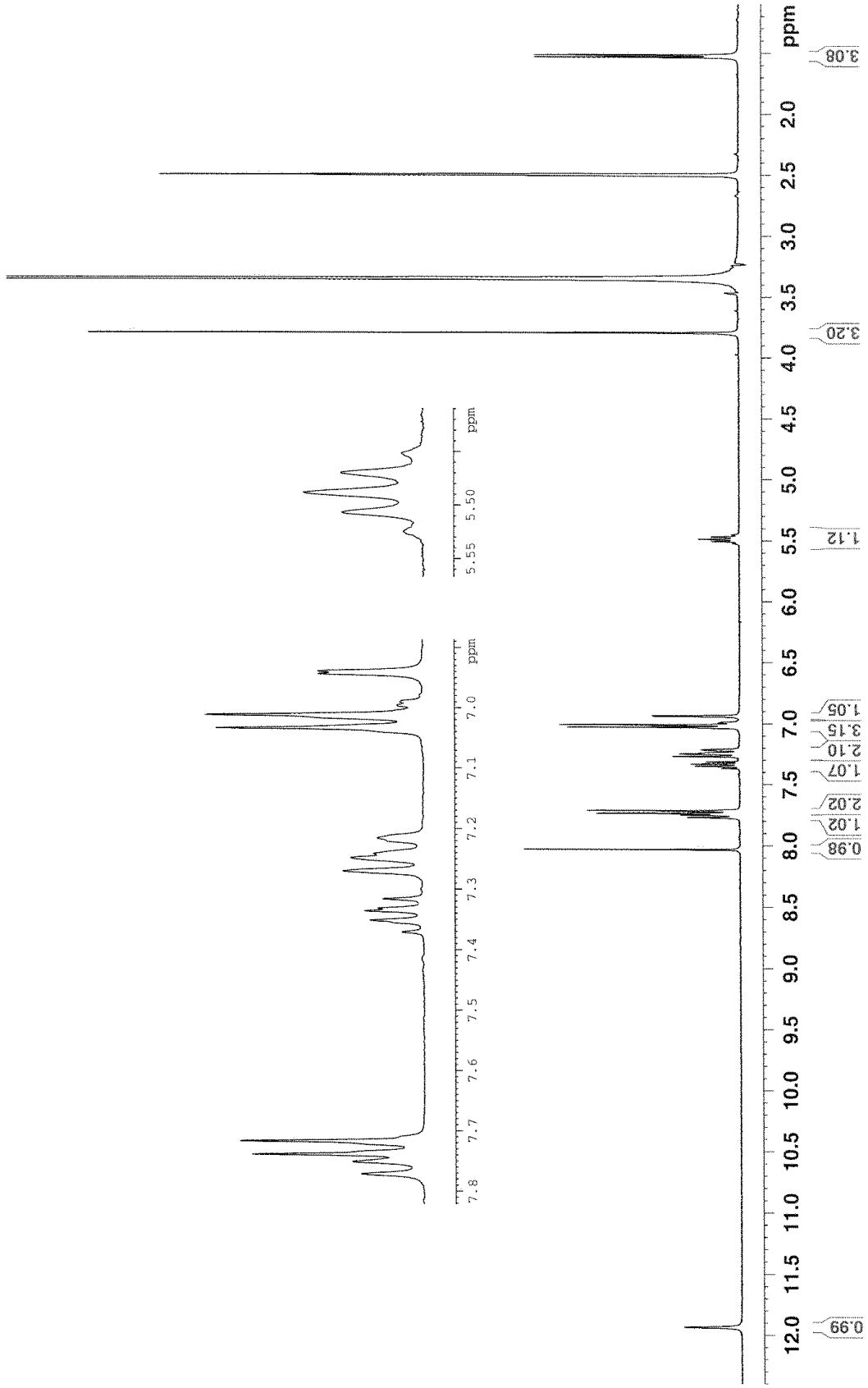

Residual peaks of DMSO and H_2O are found at 2.50 ppm and 3.33 ppm, respectively.

^{13}C – Spectrum of Compound 2d

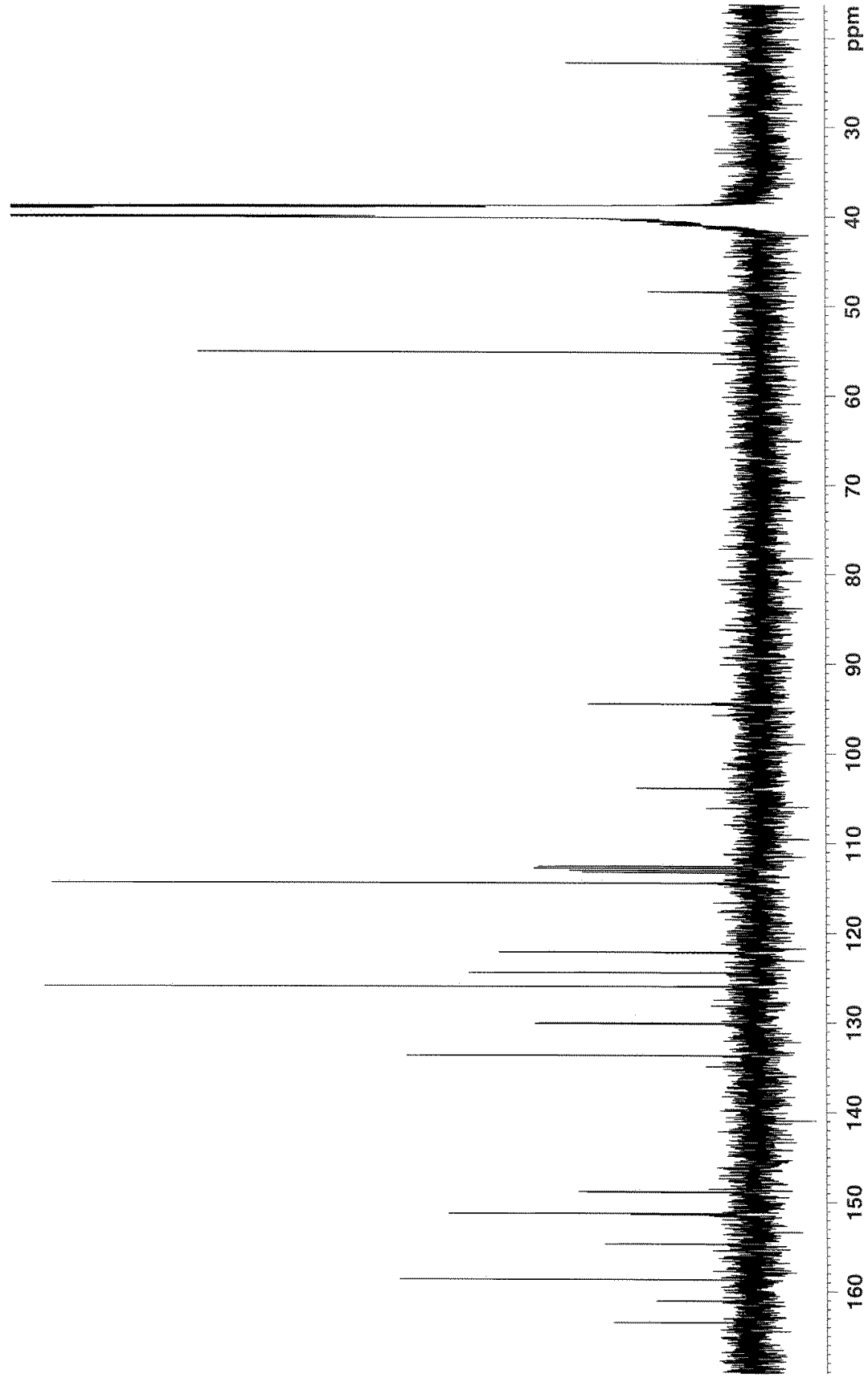

Residual peak of DMSO is found at 39.51 ppm.

COSY, 2D Spectrum of Compound 2d

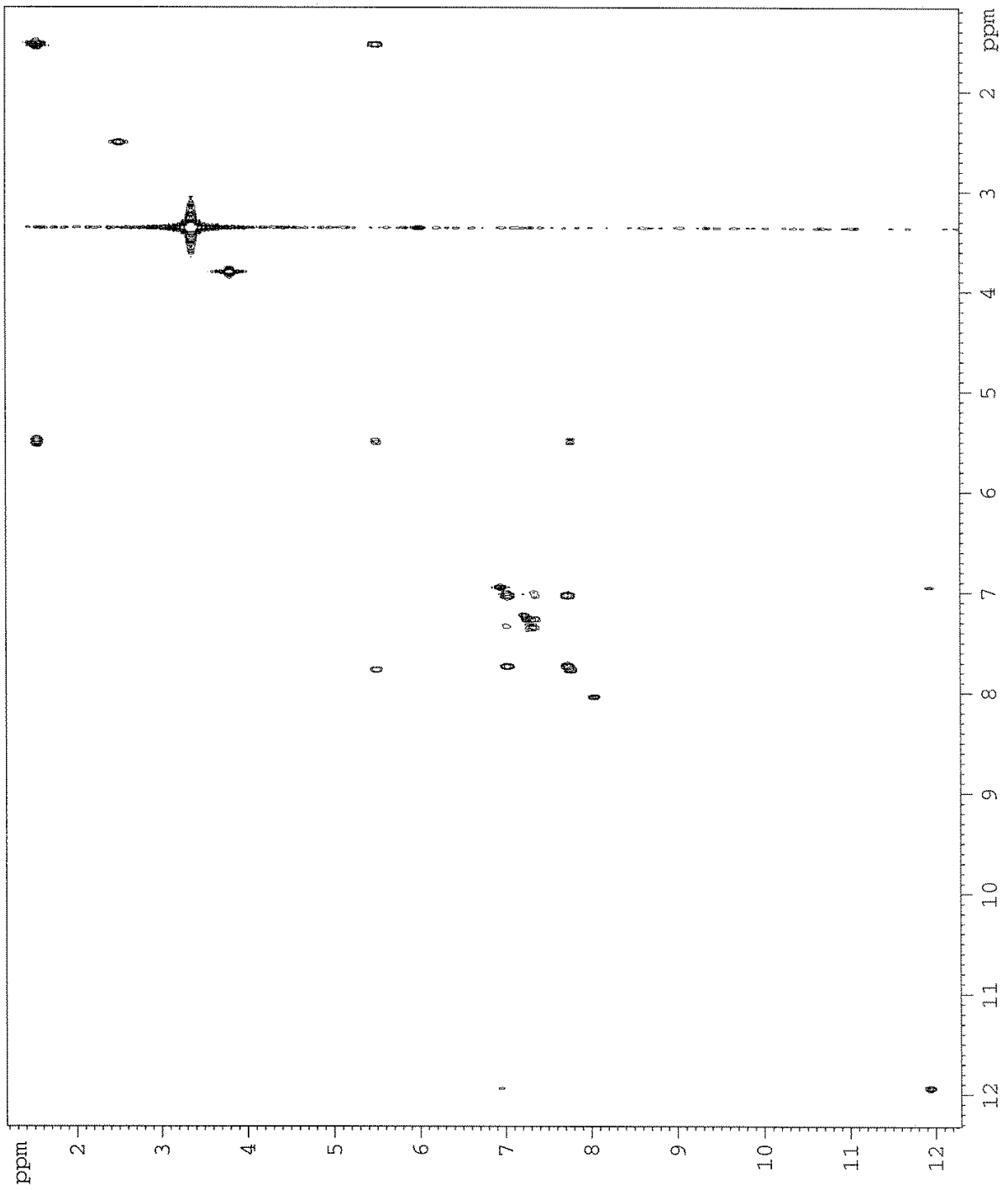

HSQC, 2D Spectrum of Compound 2d

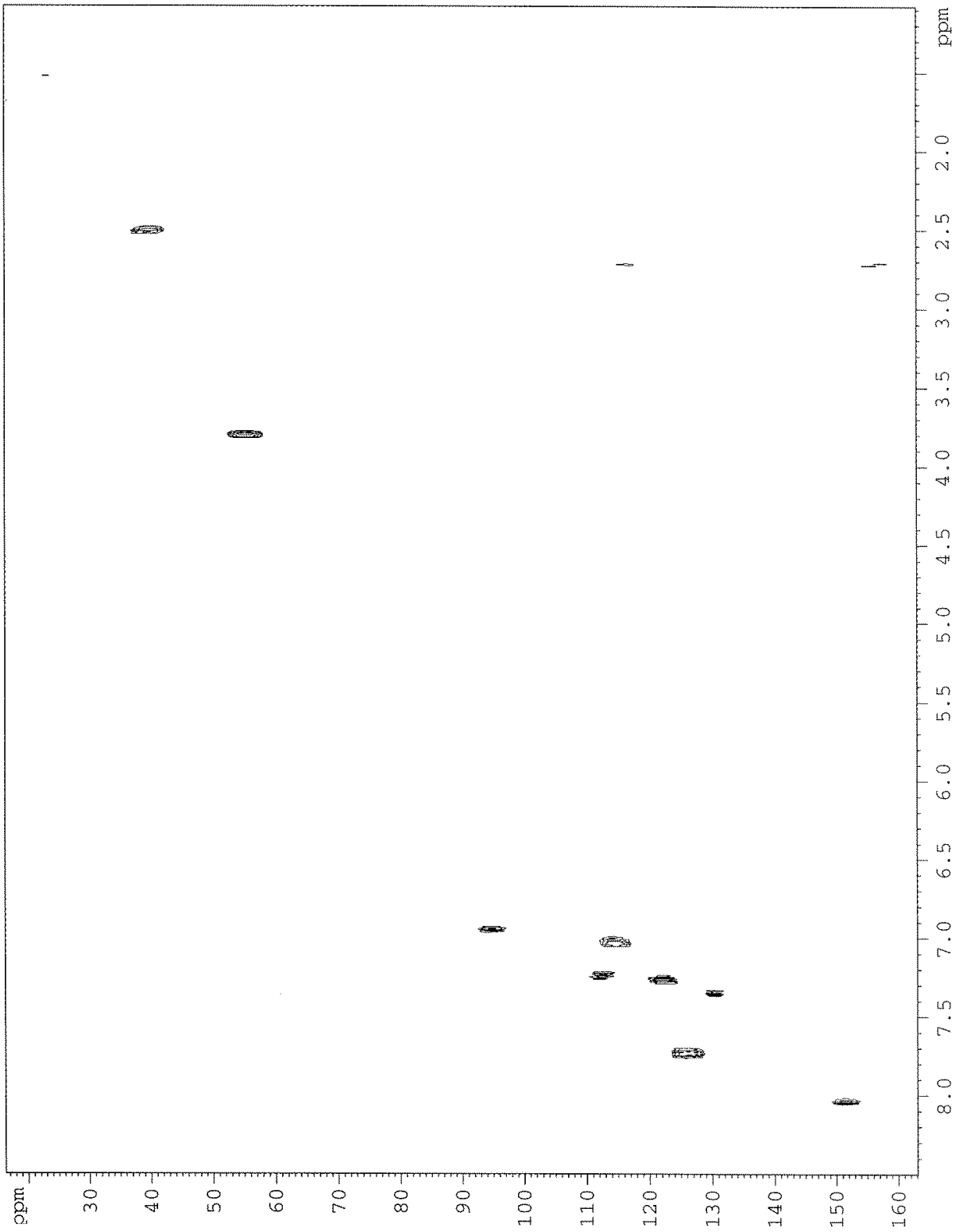

HMBC, 2D Spectrum of Compound 2d

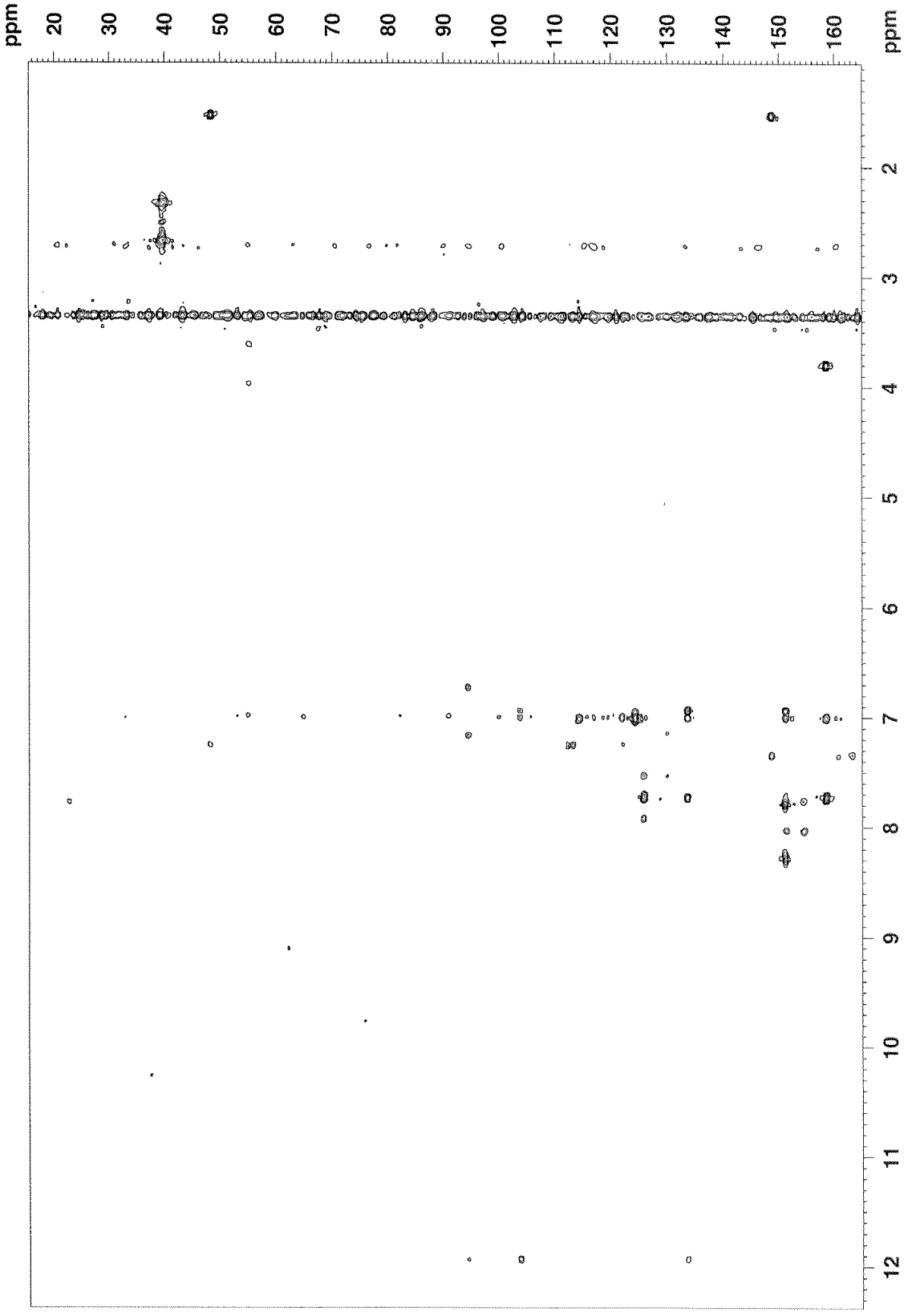

^{19}F – Spectrum of Compound 2d

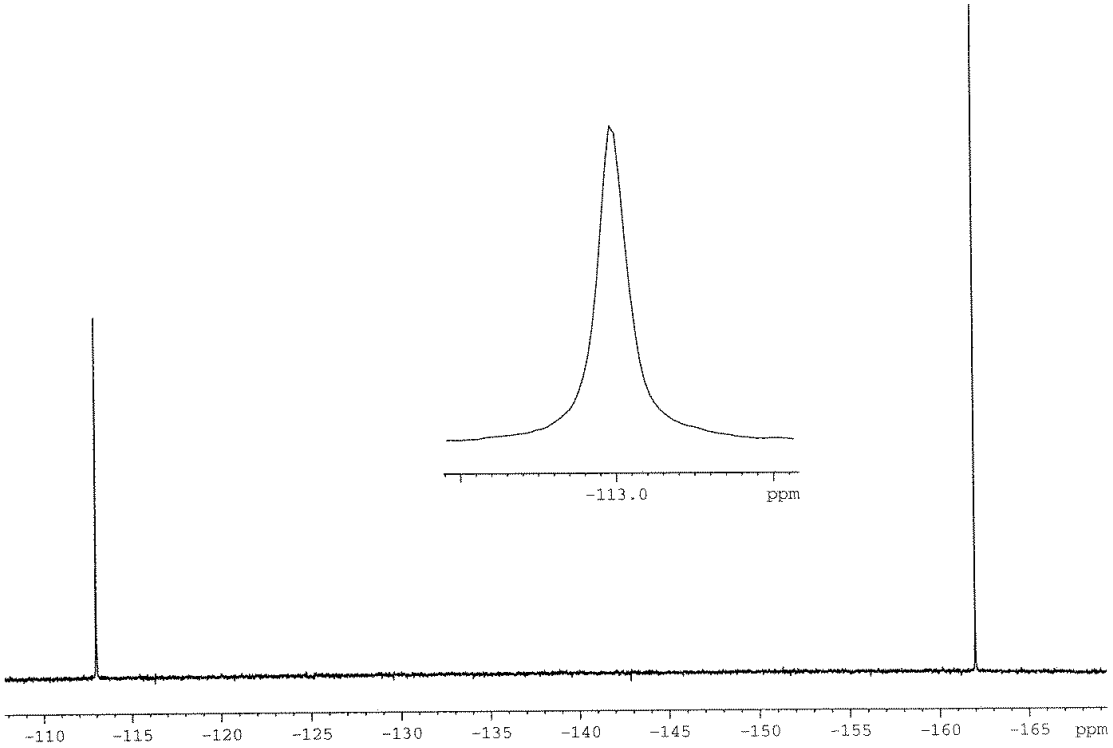

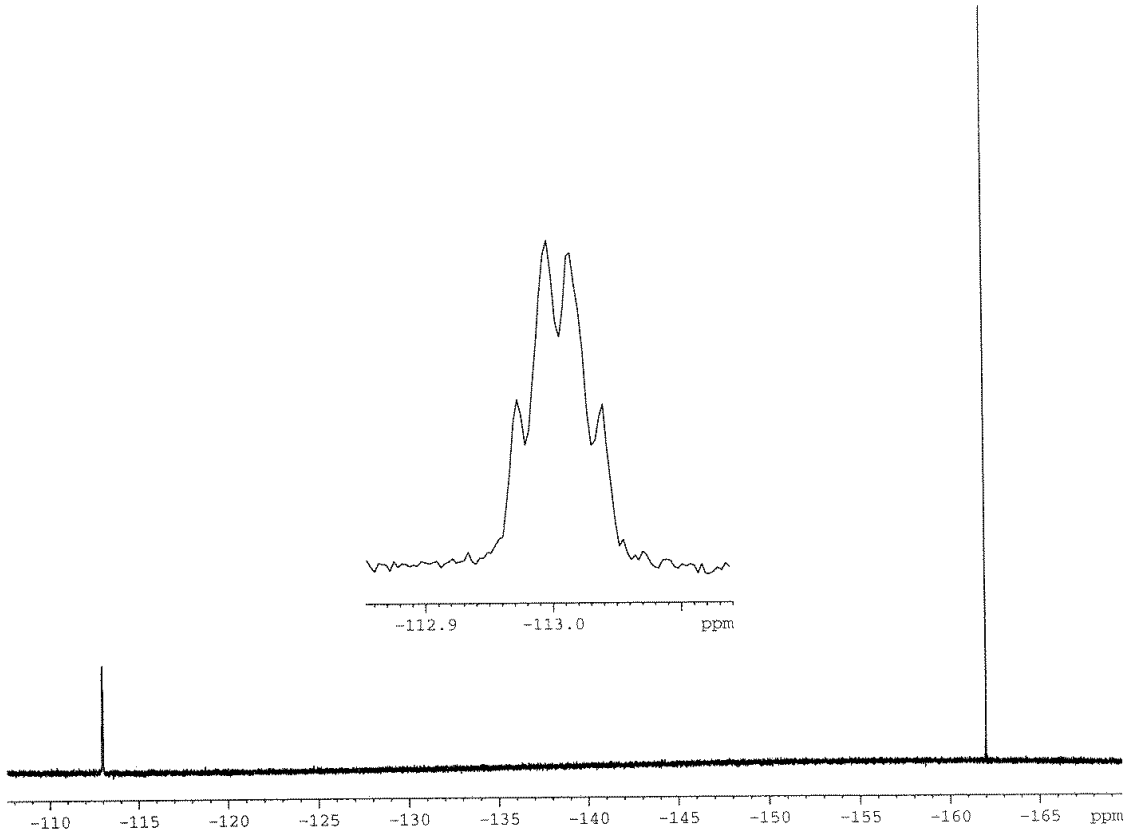

Residual peak of hexafluorobenzene is found at -162.0 ppm. Proton decoupled ^{19}F-NMR experiment is found in the top spectrum, while proton coupled ^{19}F-NMR experiment is found in the bottom spectrum.

A.2.5 – NMR spectra of Compound 2e

^{1}H – Spectrum of Compound 2e

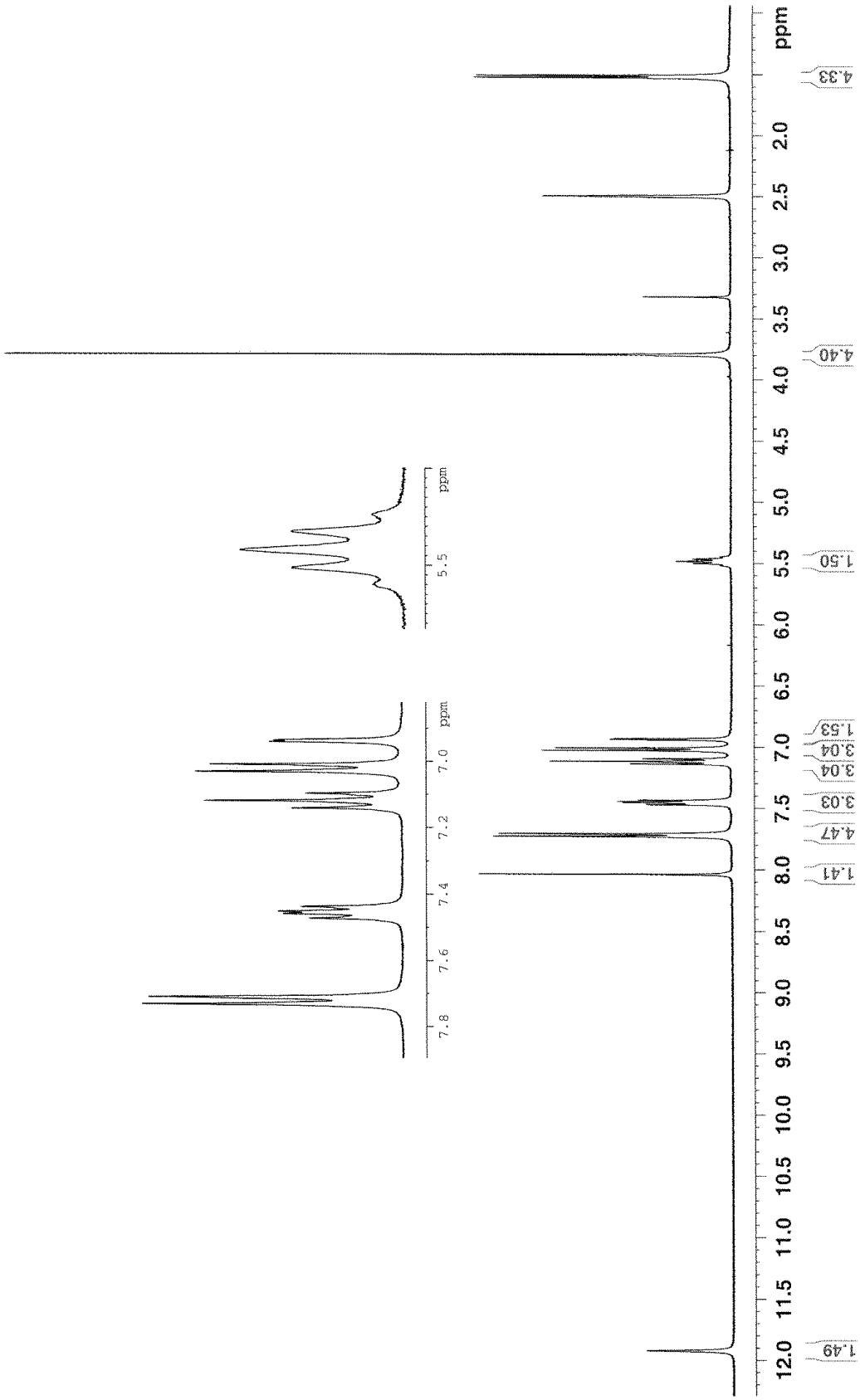

Residual peaks of DMSO and H_2O are found at 2.50 ppm and 3.33 ppm, respectively.

13C – Spectrum of Compound 2e

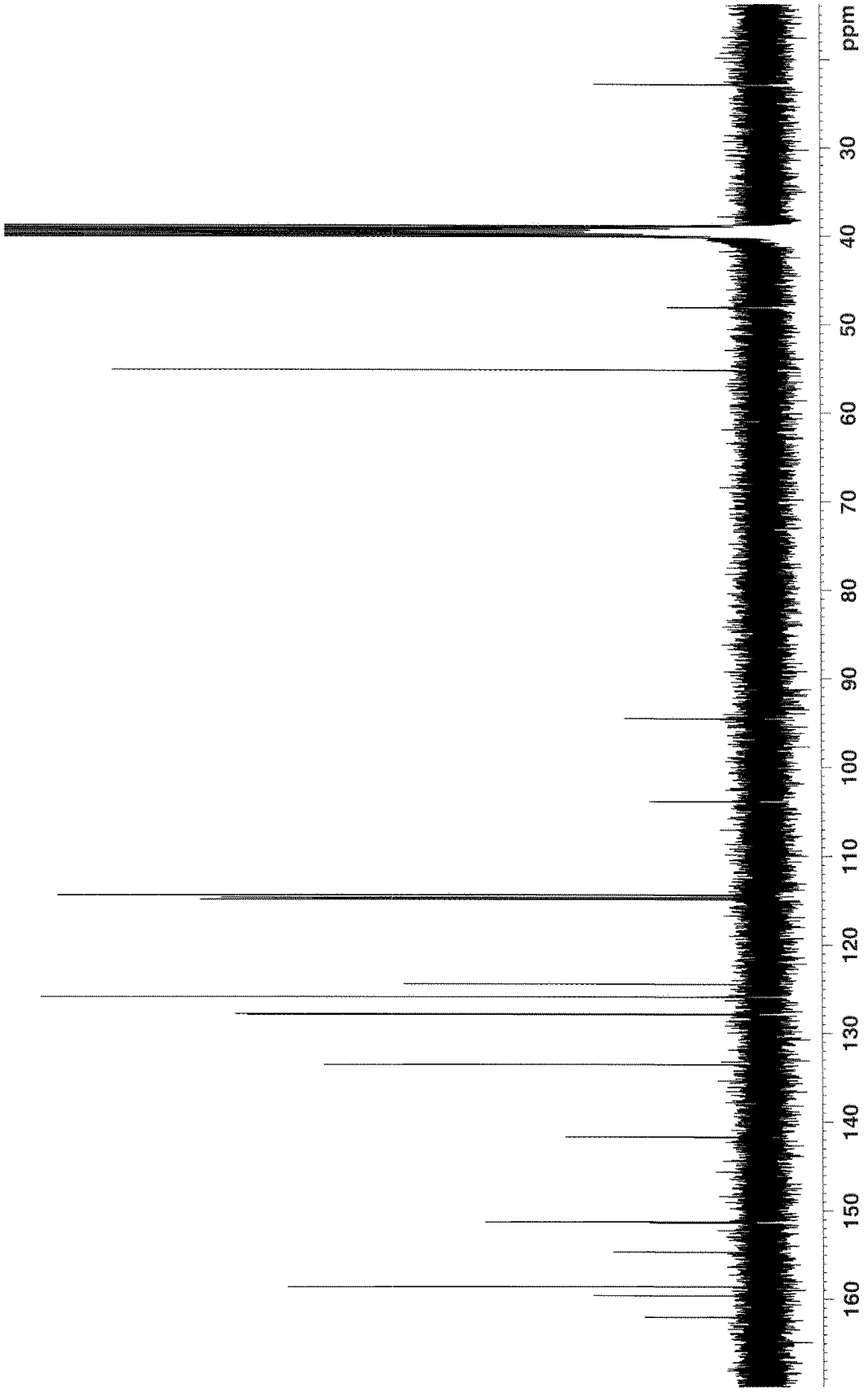

Residual peak of DMSO is found at 39.51 ppm.

COSY, 2D Spectrum of Compound 2e

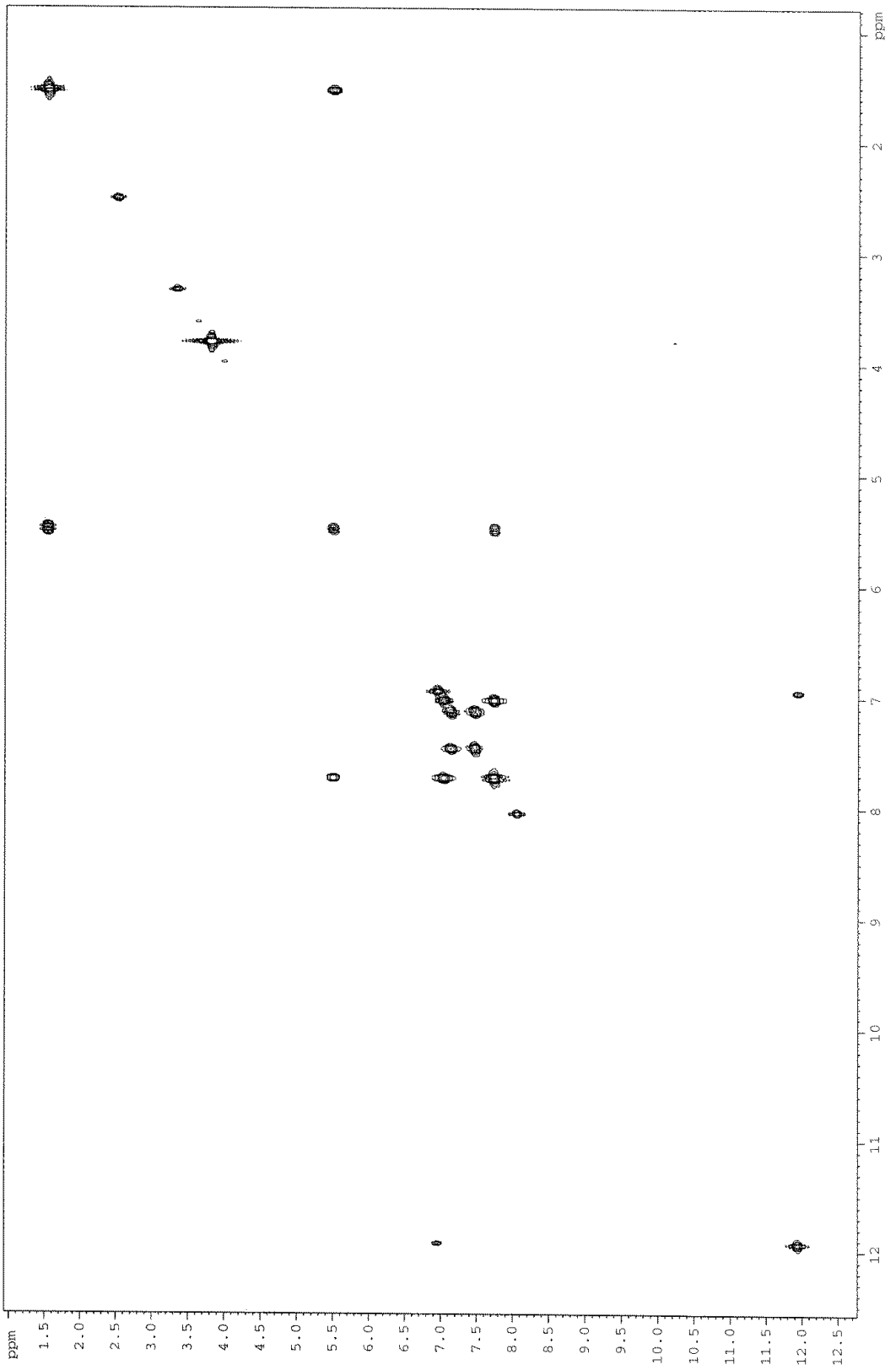

HSQC, 2D Spectrum of Compound 2e

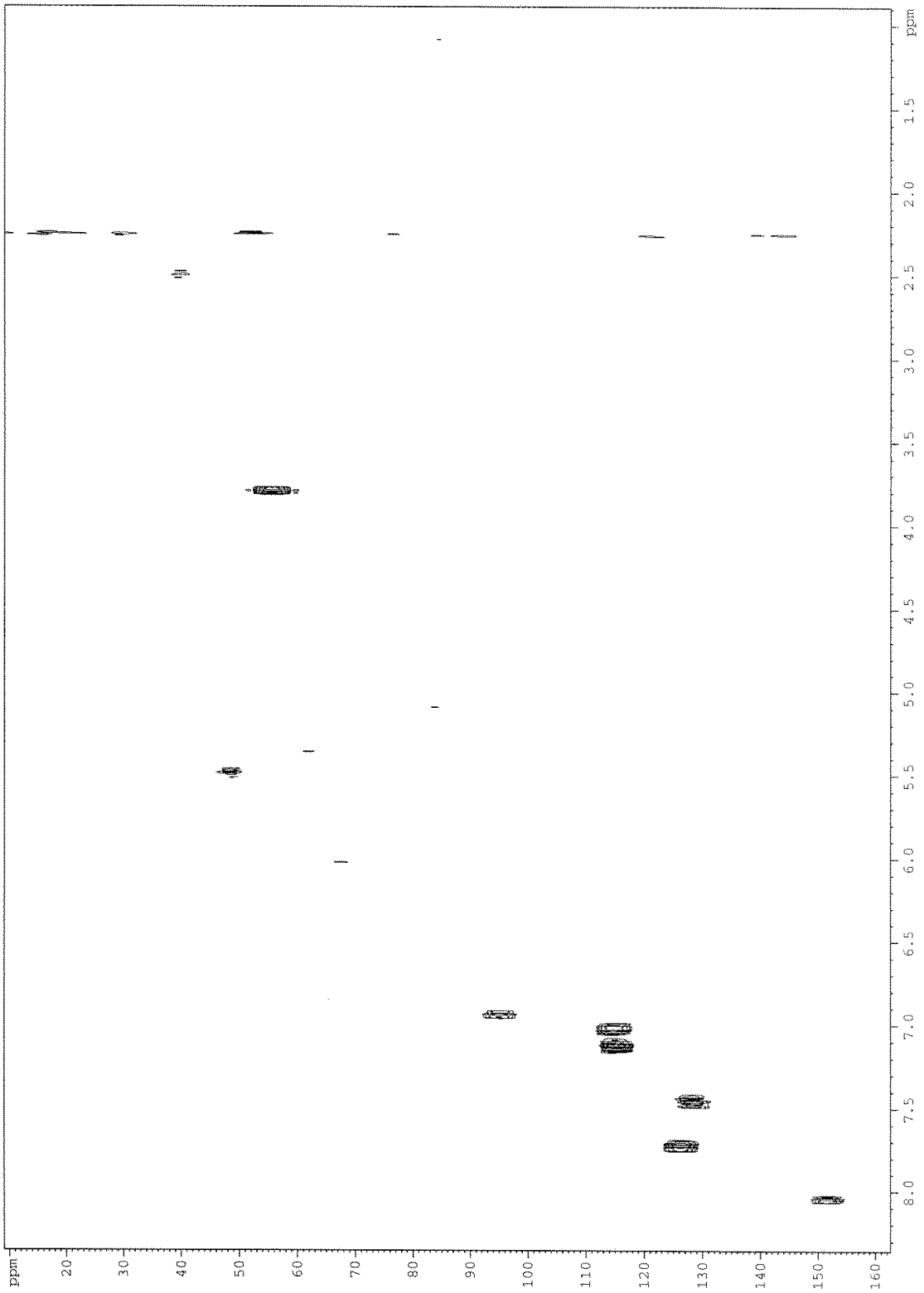

HMBC, 2D Spectrum of Compound 2e

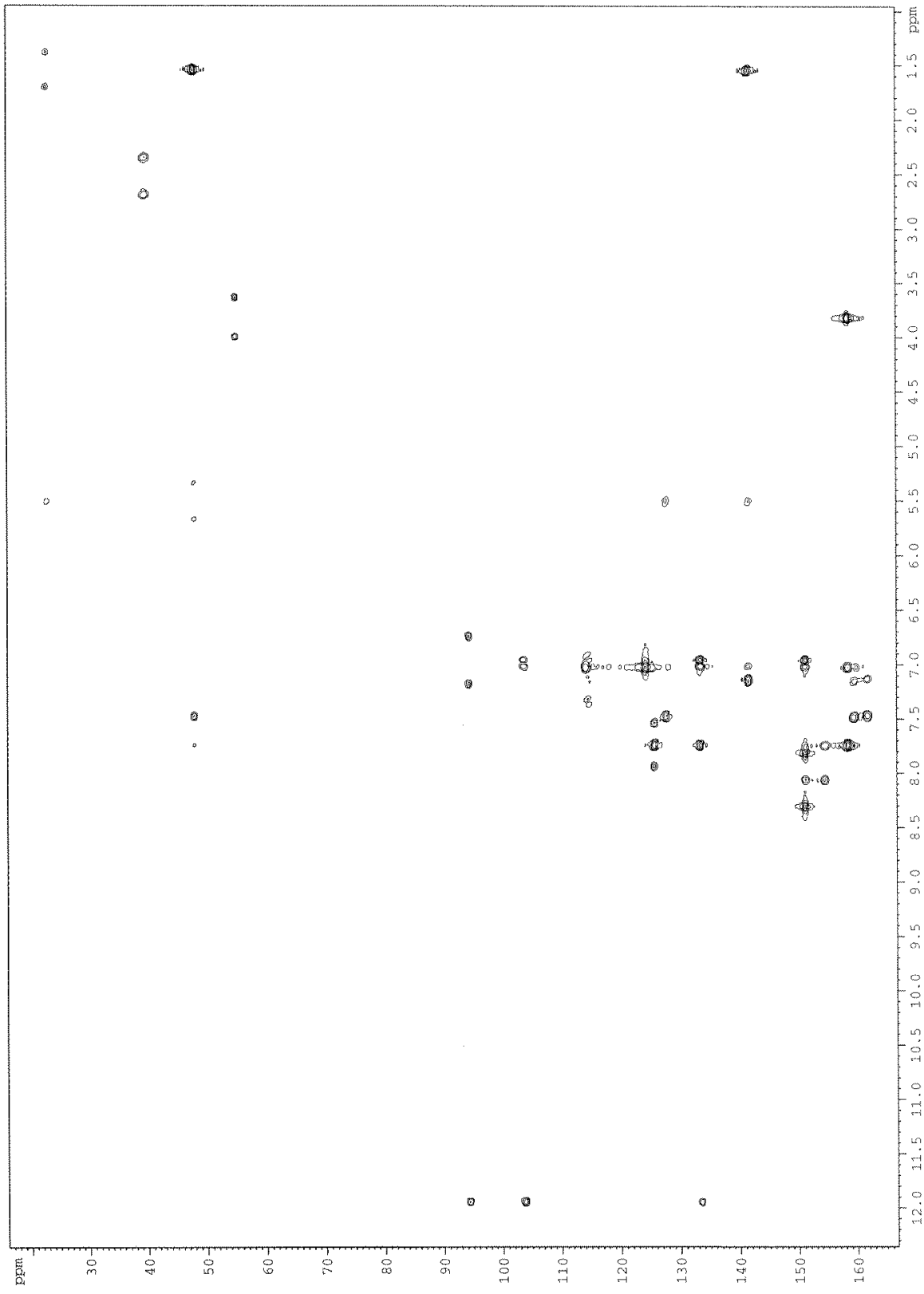

^{19}F – Spectrum of Compound 2e

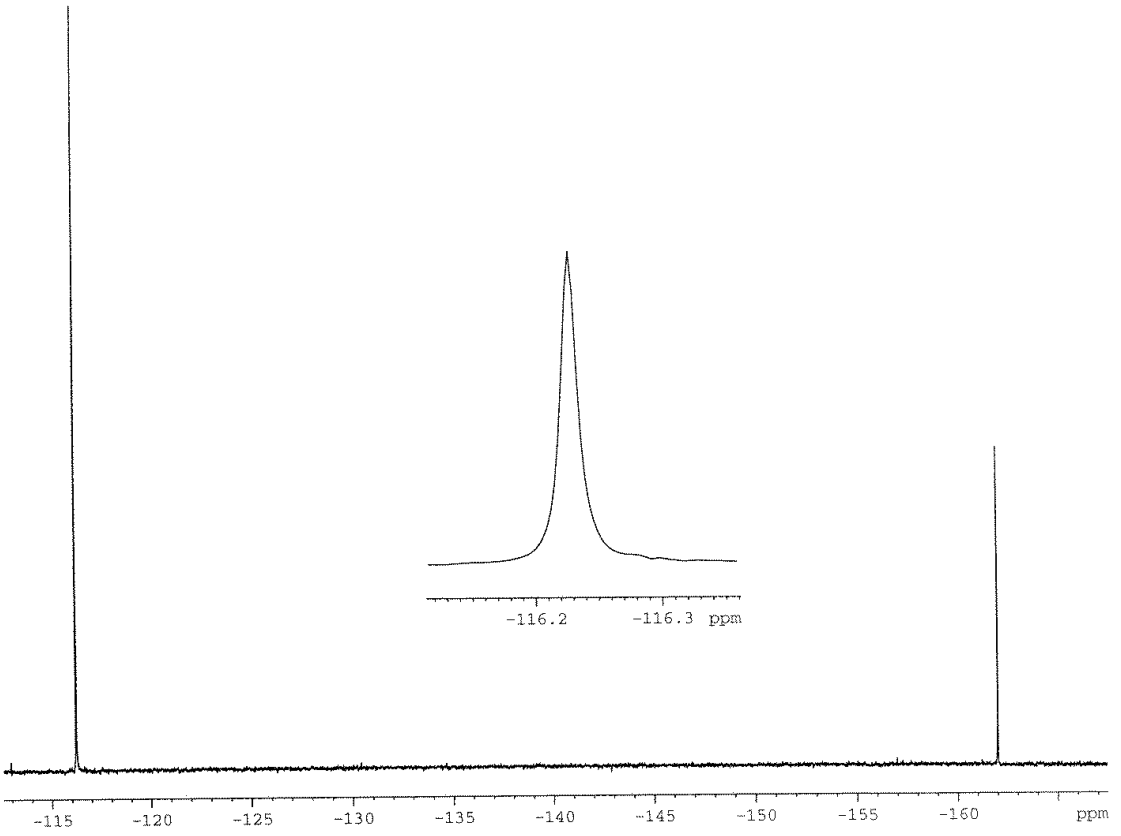

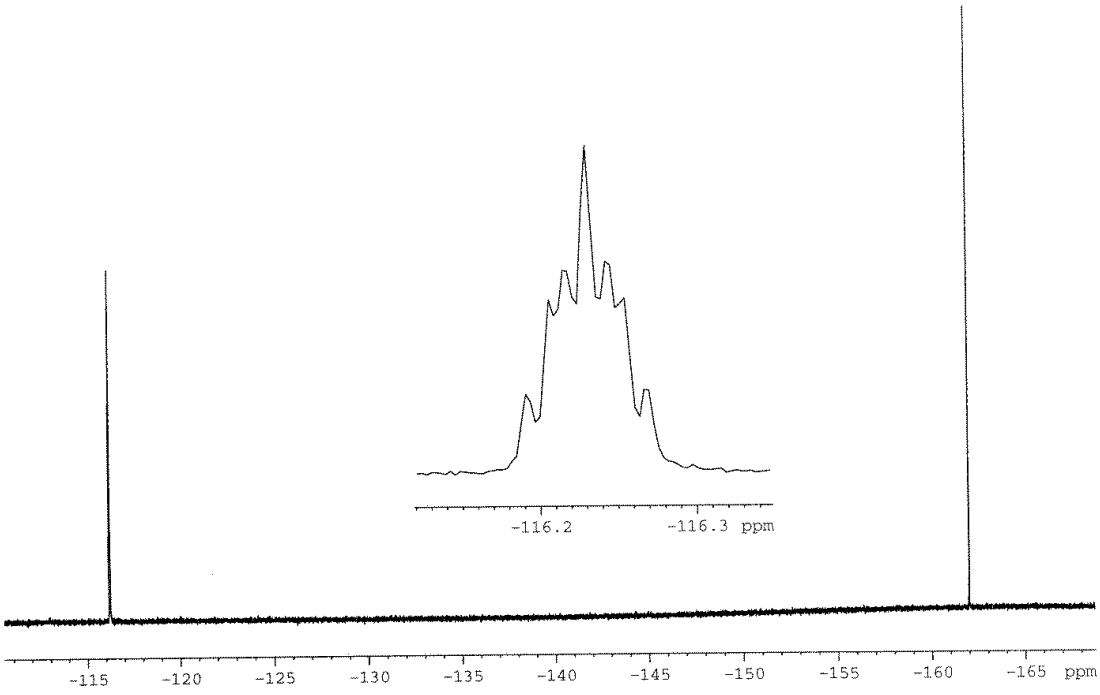

Residual peak of hexafluorobenzene is found at -162.0 ppm. Proton decoupled ^{19}F-NMR experiment is found in the top spectrum, while proton coupled ^{19}F-NMR experiment is found in the bottom spectrum.

A.2.6 – NMR spectra of Compound 2f

^{1}H – Spectrum of Compound 2f

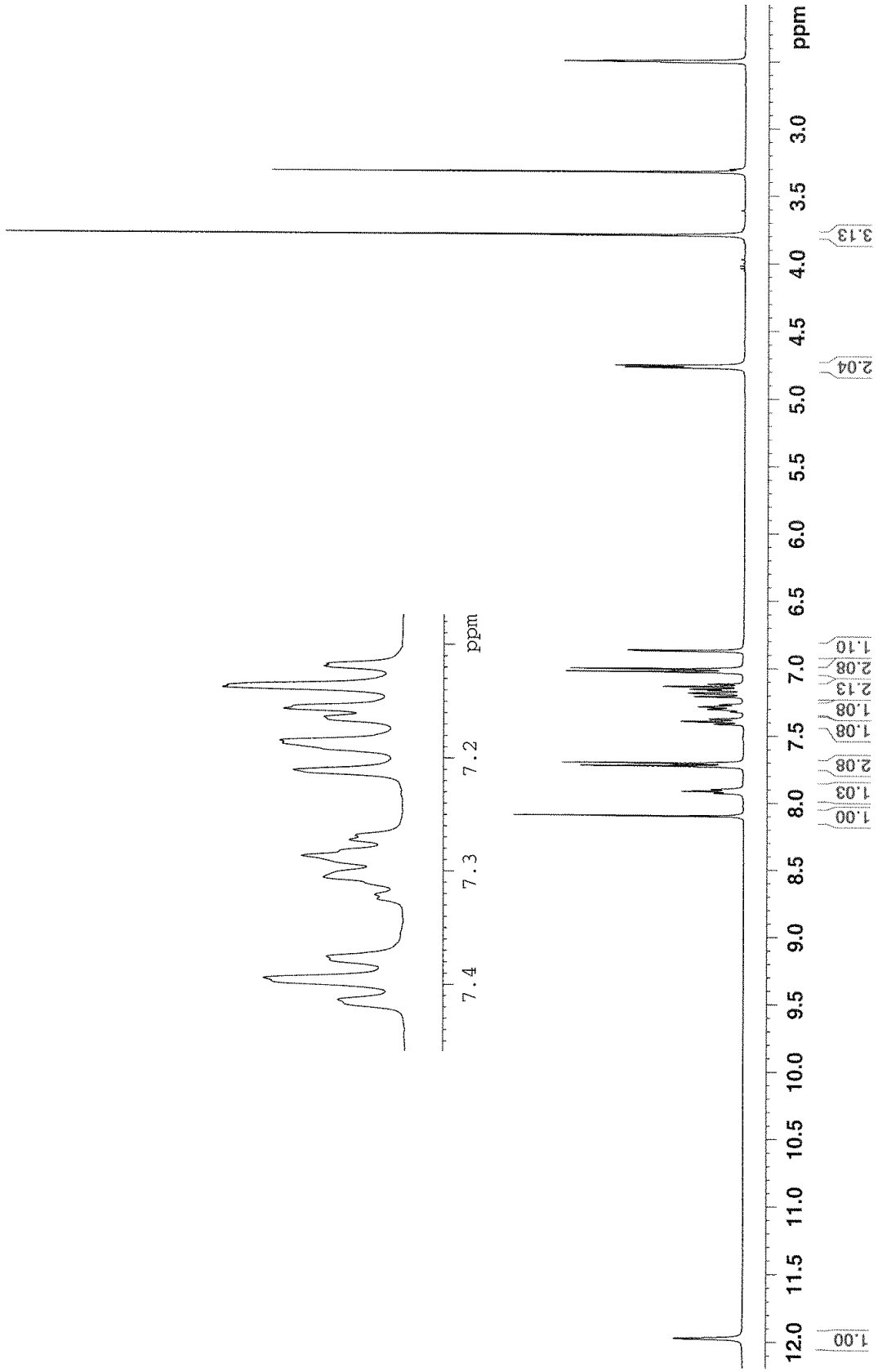

Residual peaks of DMSO and H_2O are found at 2.50 ppm and 3.33 ppm, respectively.

^{13}C – Spectrum of Compound 2f

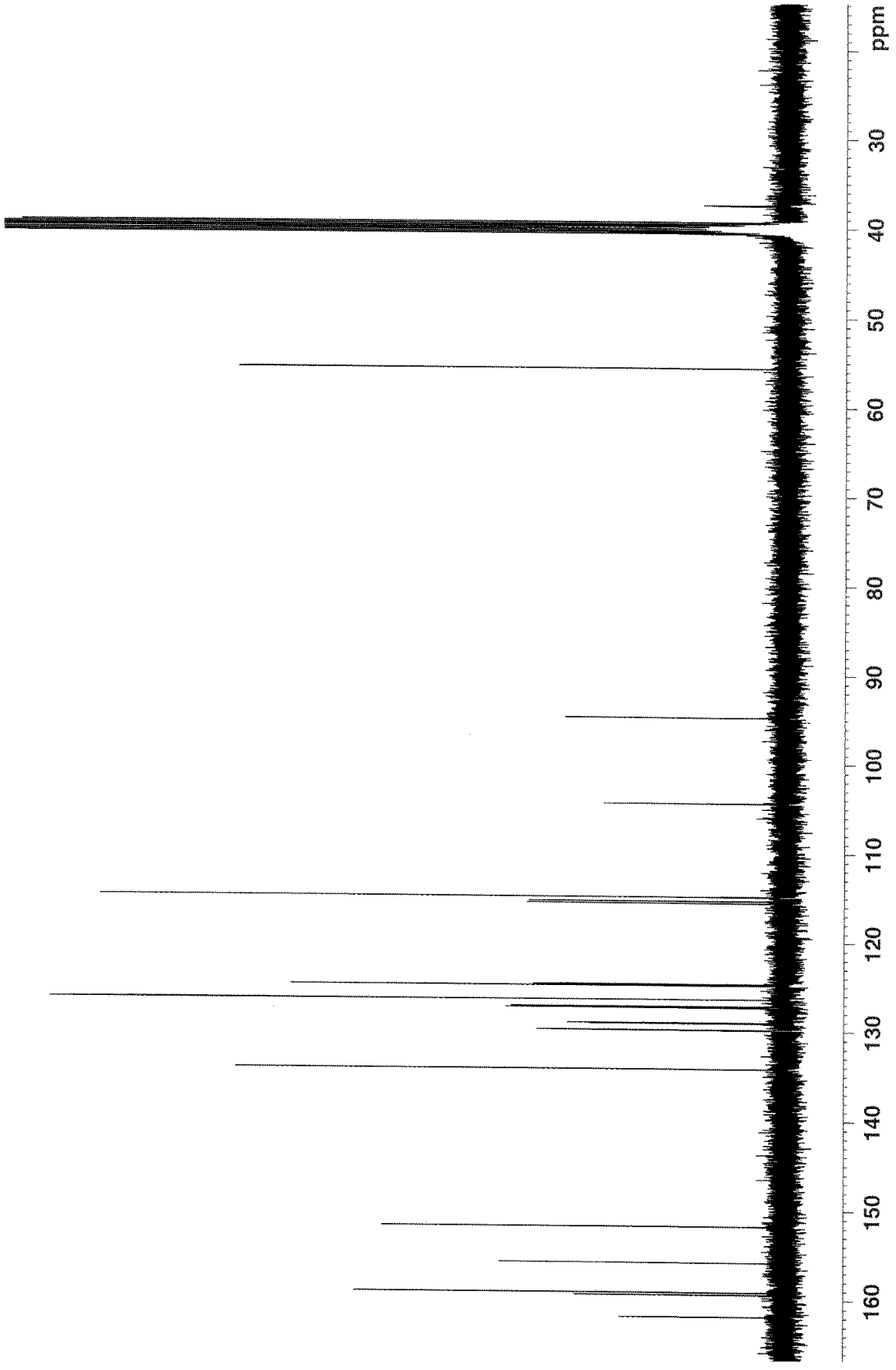

Residual peak of DMSO is found at 39.51 ppm.

COSY, 2D Spectrum of Compound 2f

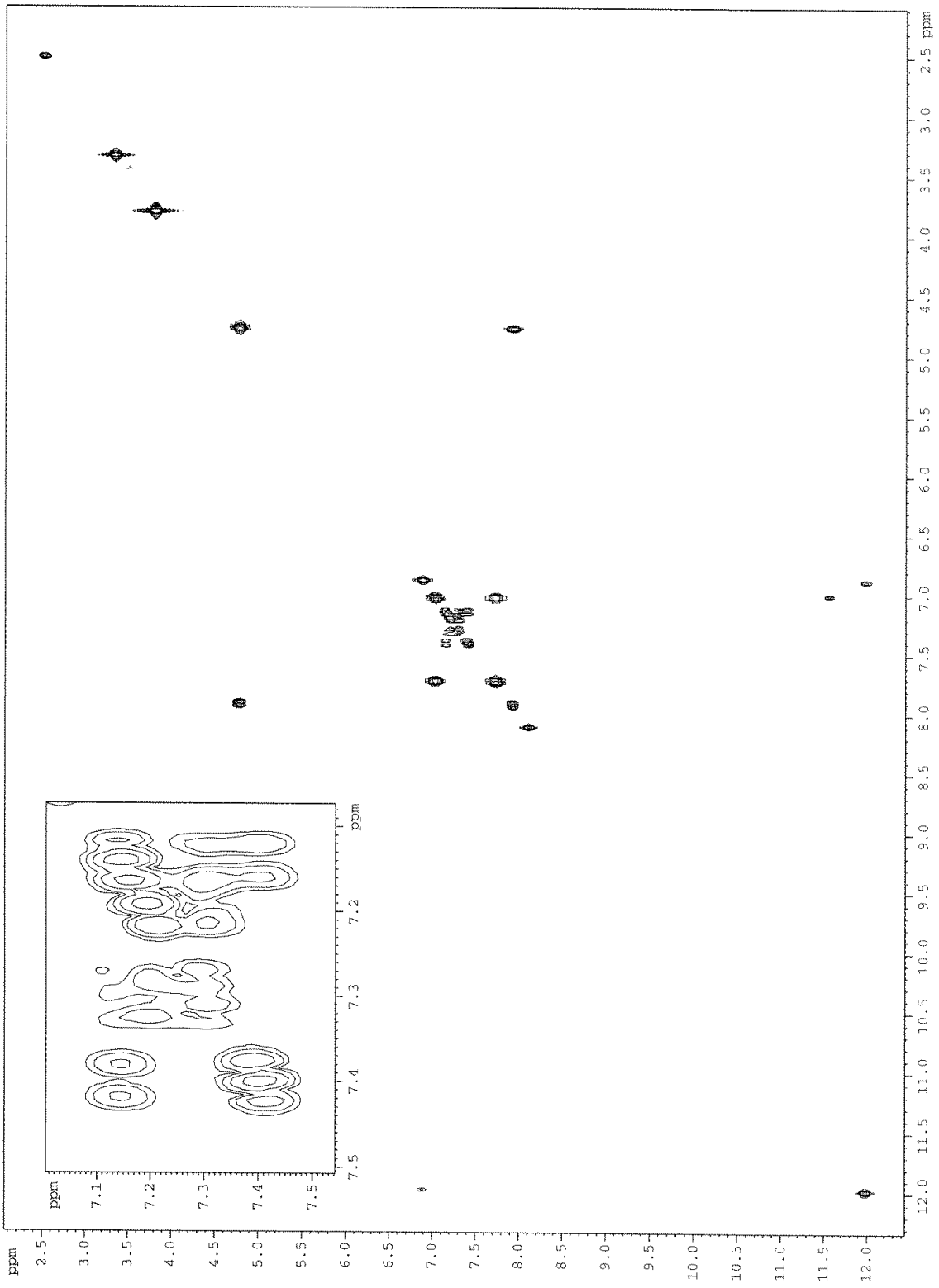

HSQC, 2D Spectrum of Compound 2f

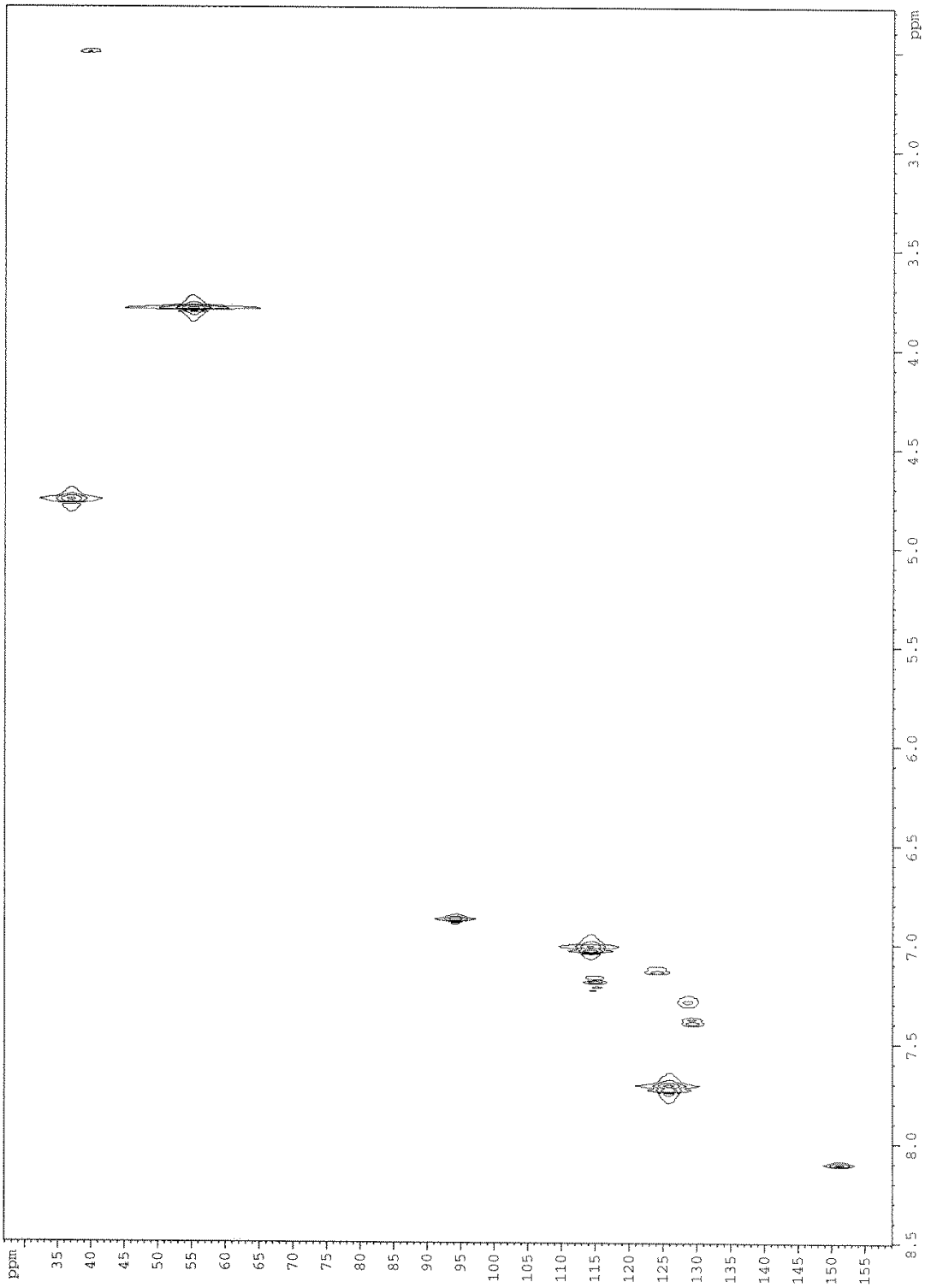

HMBC, 2D Spectrum of Compound 2f

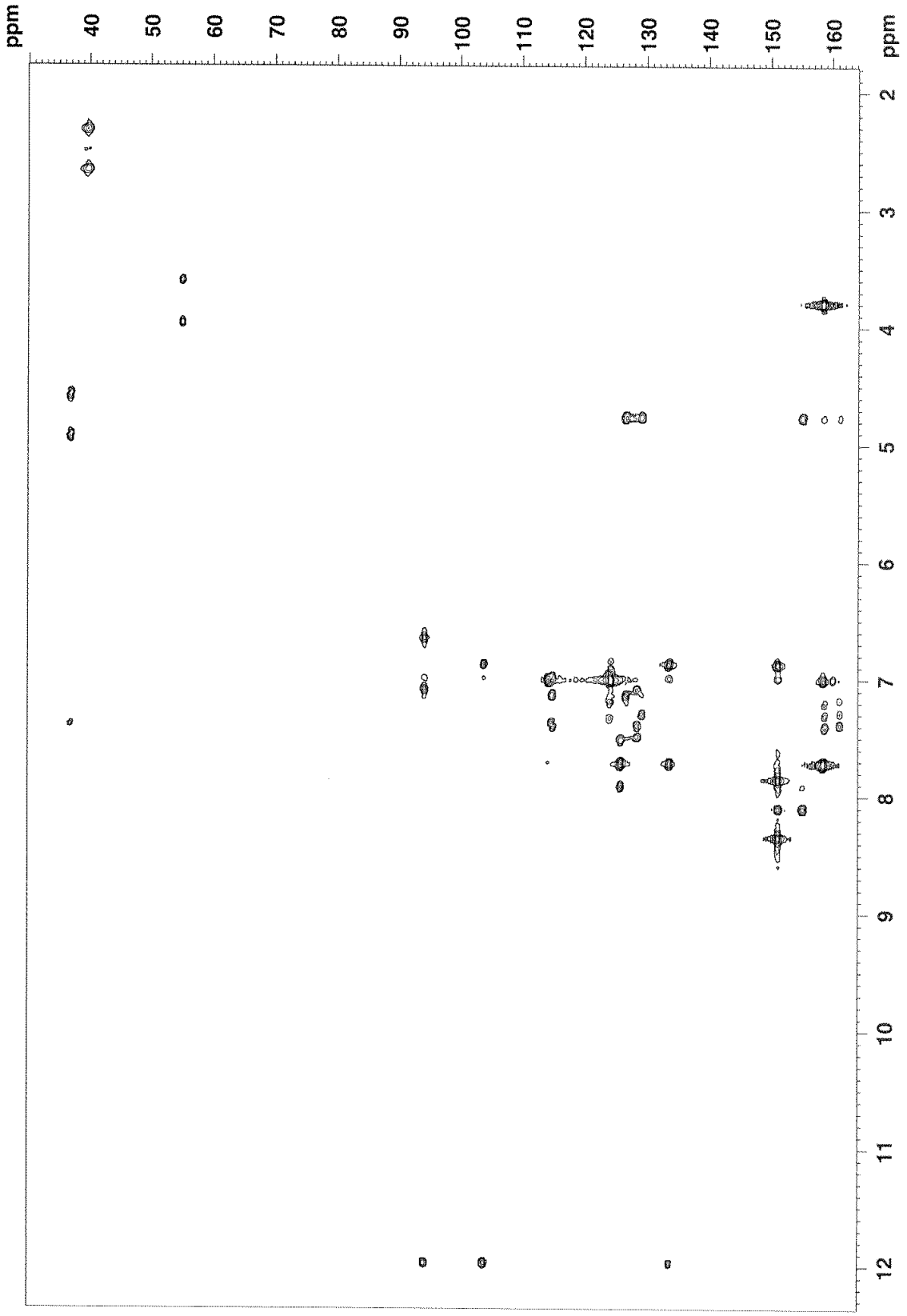

^{19}F – Spectrum of Compound 2f

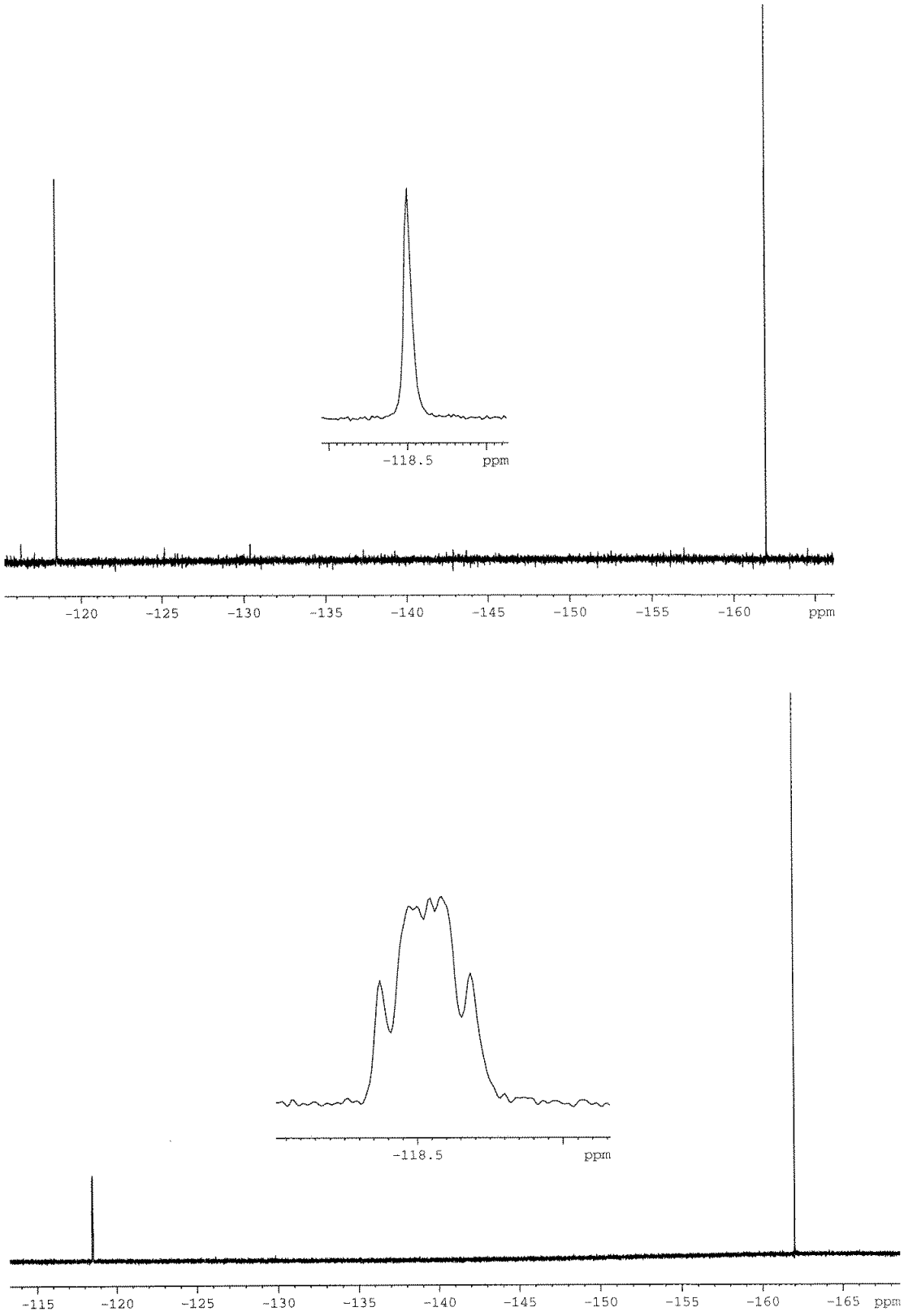

Residual peak of hexafluorobenzene is found at -162.0 ppm. Proton decoupled ^{19}F-NMR experiment is found in the top spectrum, while proton coupled ^{19}F-NMR experiment is found in the bottom spectrum.

A.2.7 – NMR spectra of Compound 2g

^{1}H – Spectrum of Compound 2g

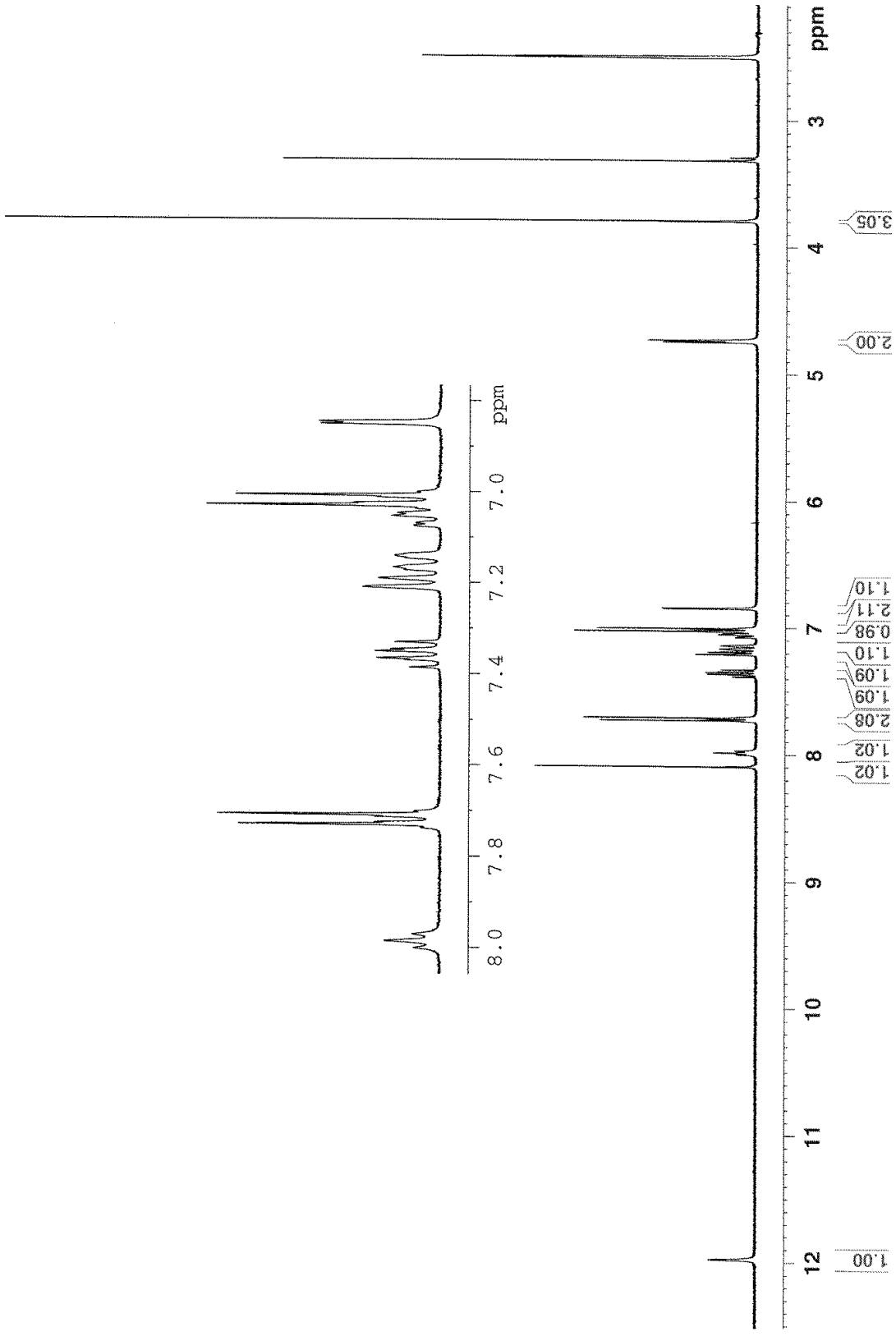

Residual peaks of DMSO and H_2O are found at 2.50 ppm and 3.33 ppm, respectively.

^{13}C – Spectrum of Compound 2g

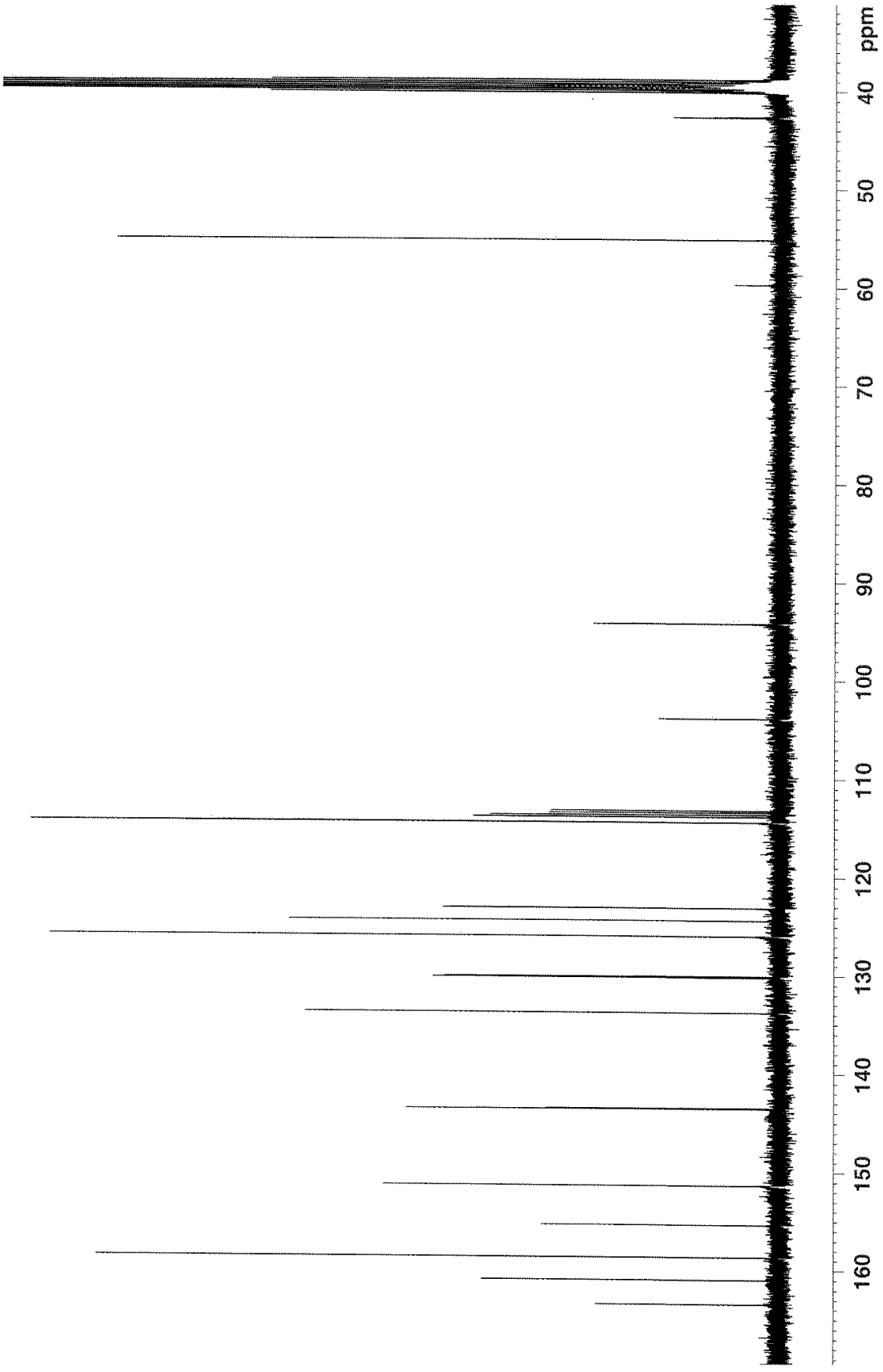

Residual peak of DMSO is found at 39.51 ppm.

COSY, 2D Spectrum of Compound 2g

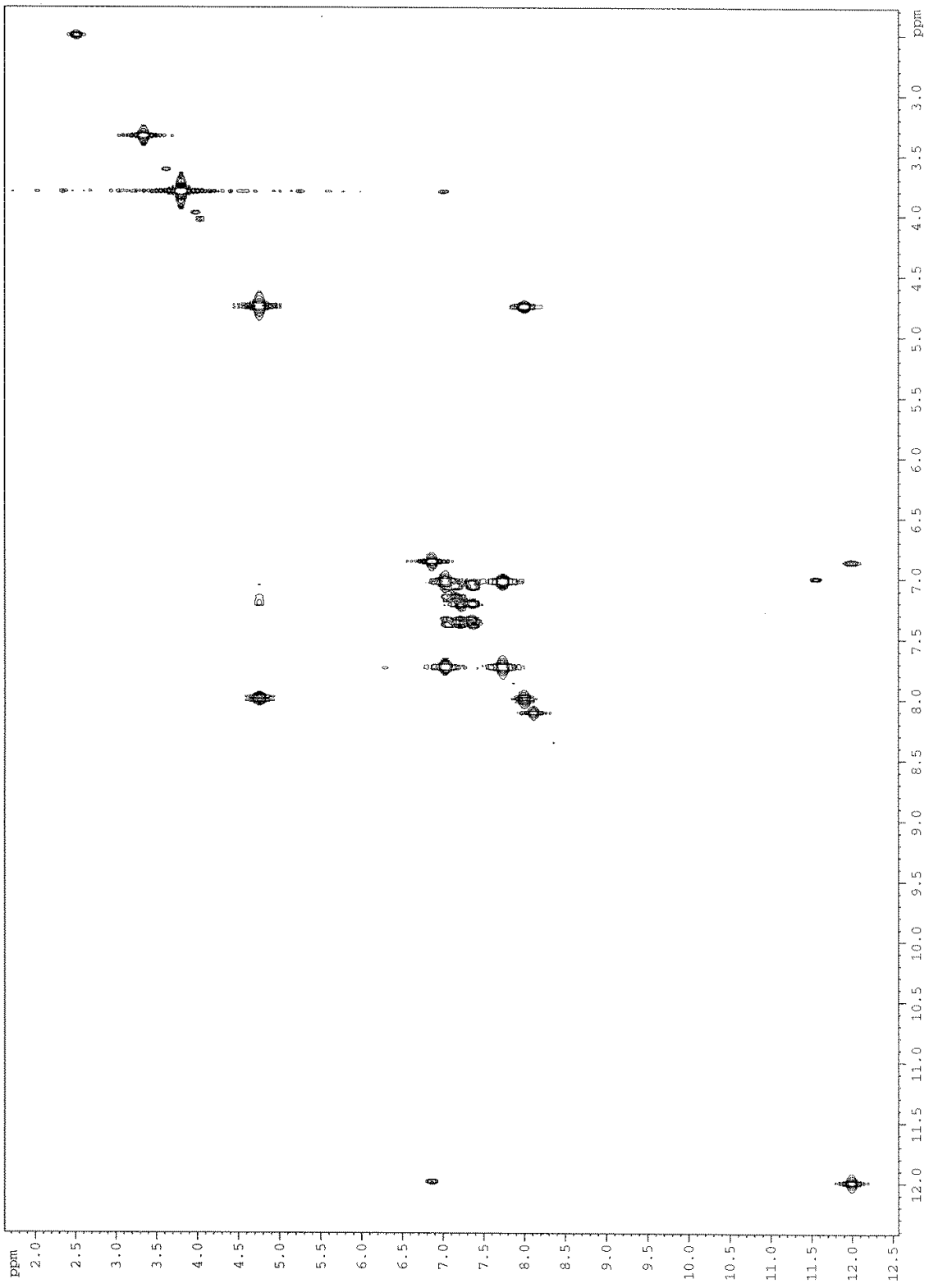

HSQC, 2D Spectrum of Compound 2g

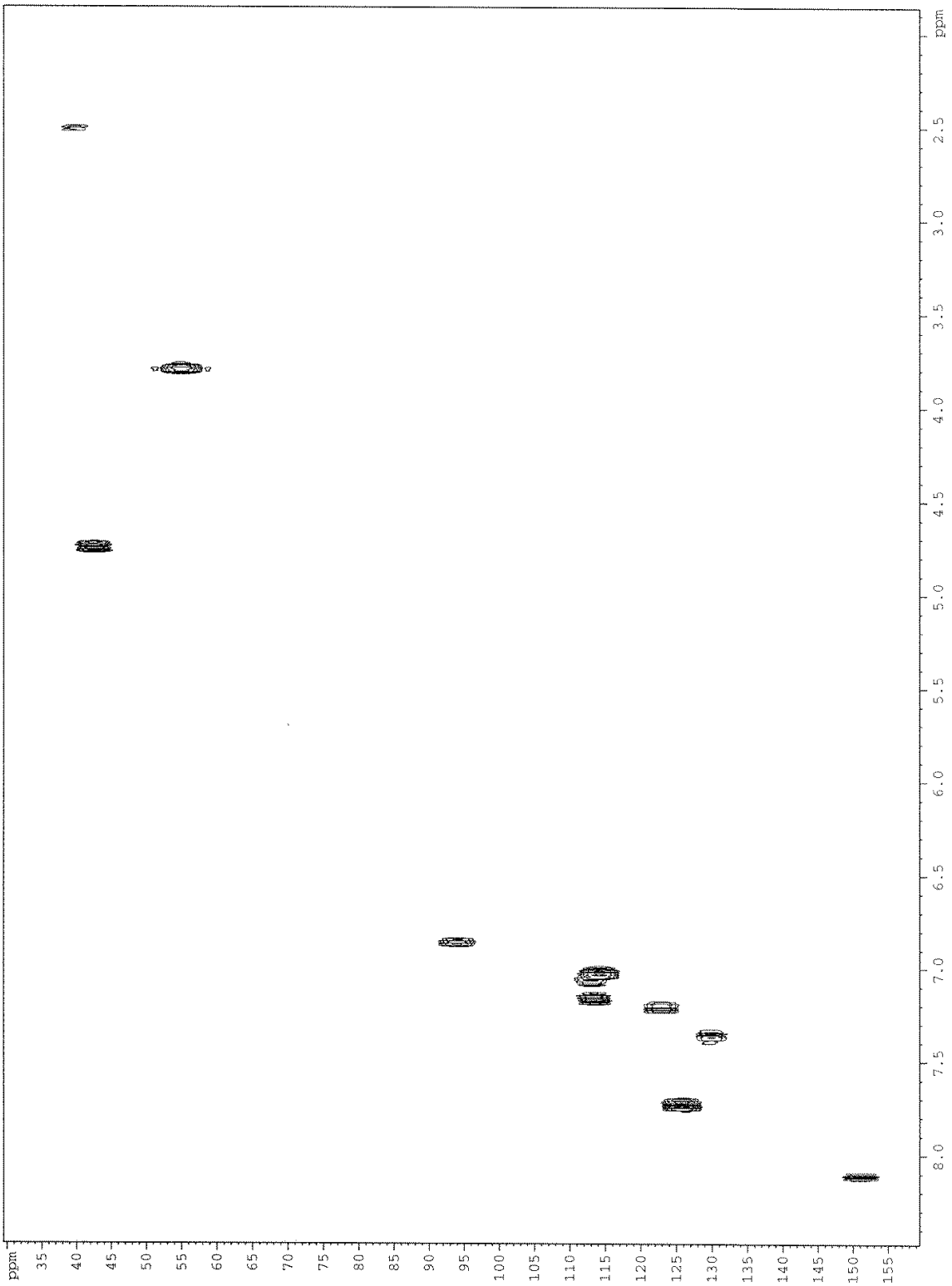

HMBC, 2D Spectrum of Compound 2g

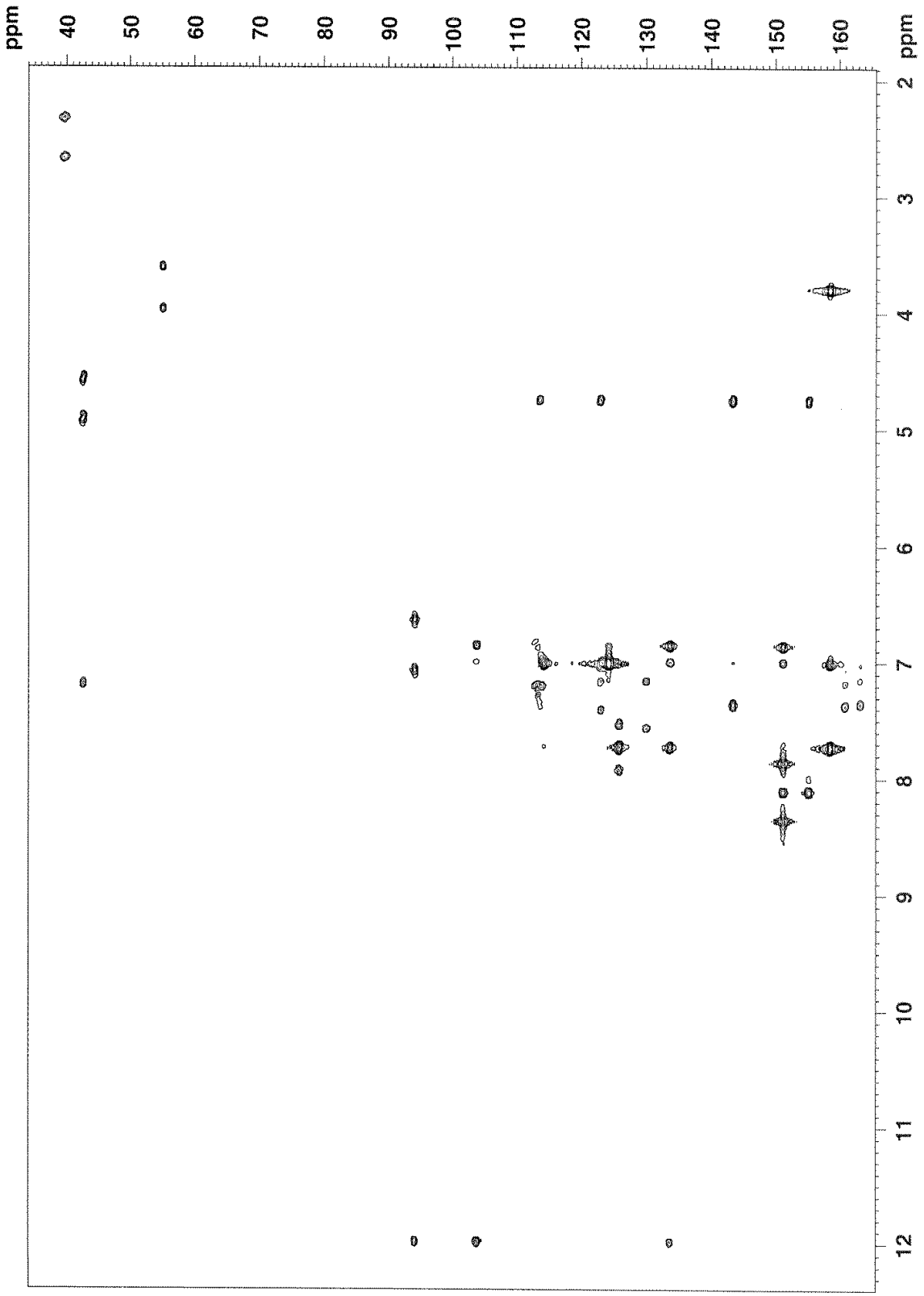

^{19}F – Spectrum of Compound 2g

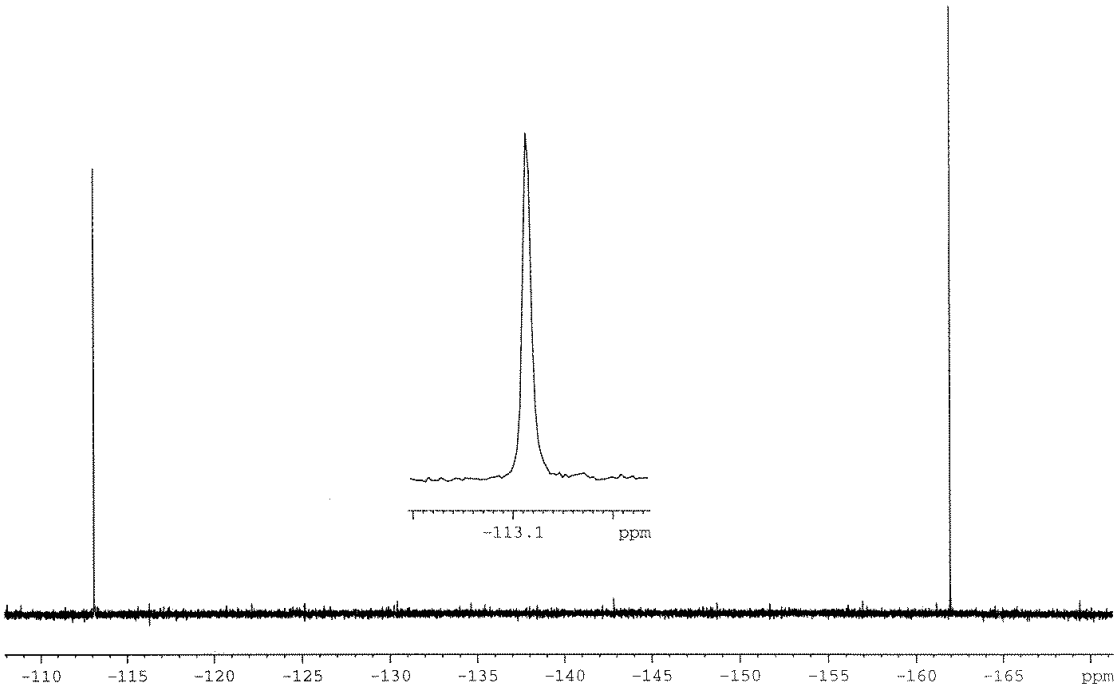

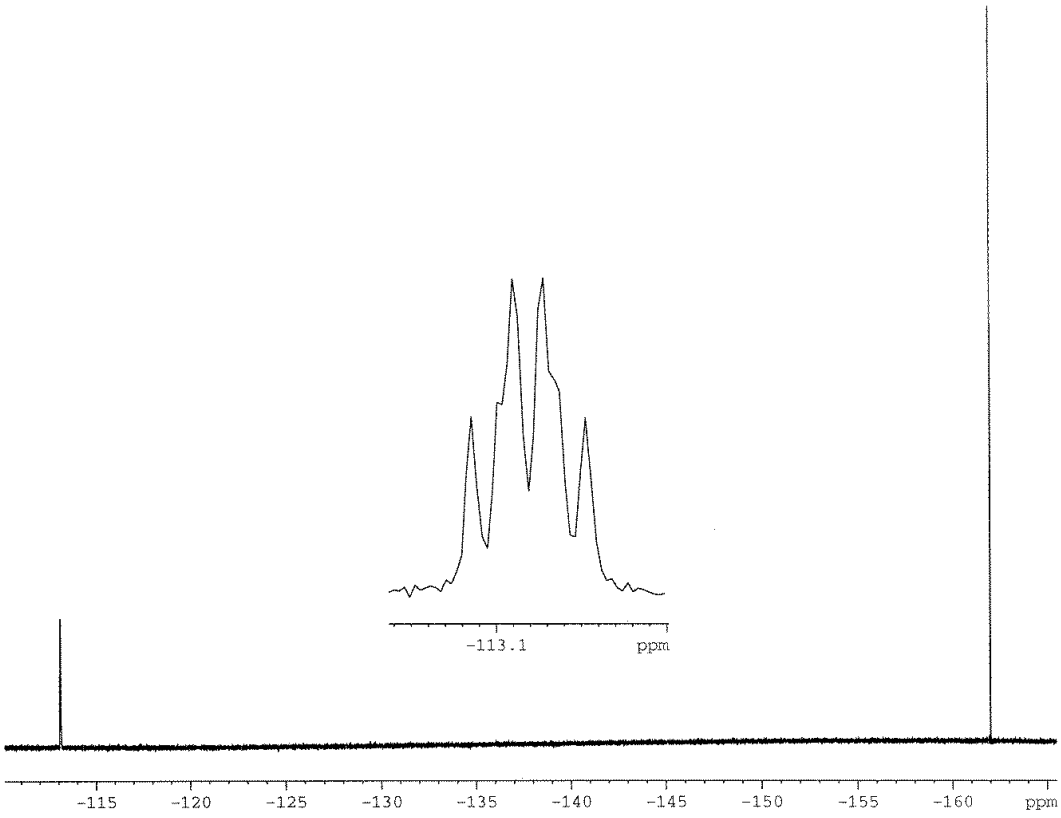

Residual peak of hexafluorobenzene is found at -162.0 ppm. Proton decoupled ^{19}F-NMR experiment is found in the top spectrum, while proton coupled ^{19}F-NMR experiment is found in the bottom spectrum.

A.2.8 – NMR spectra of Compound 2h

^{1}H – Spectrum of Compound 2h

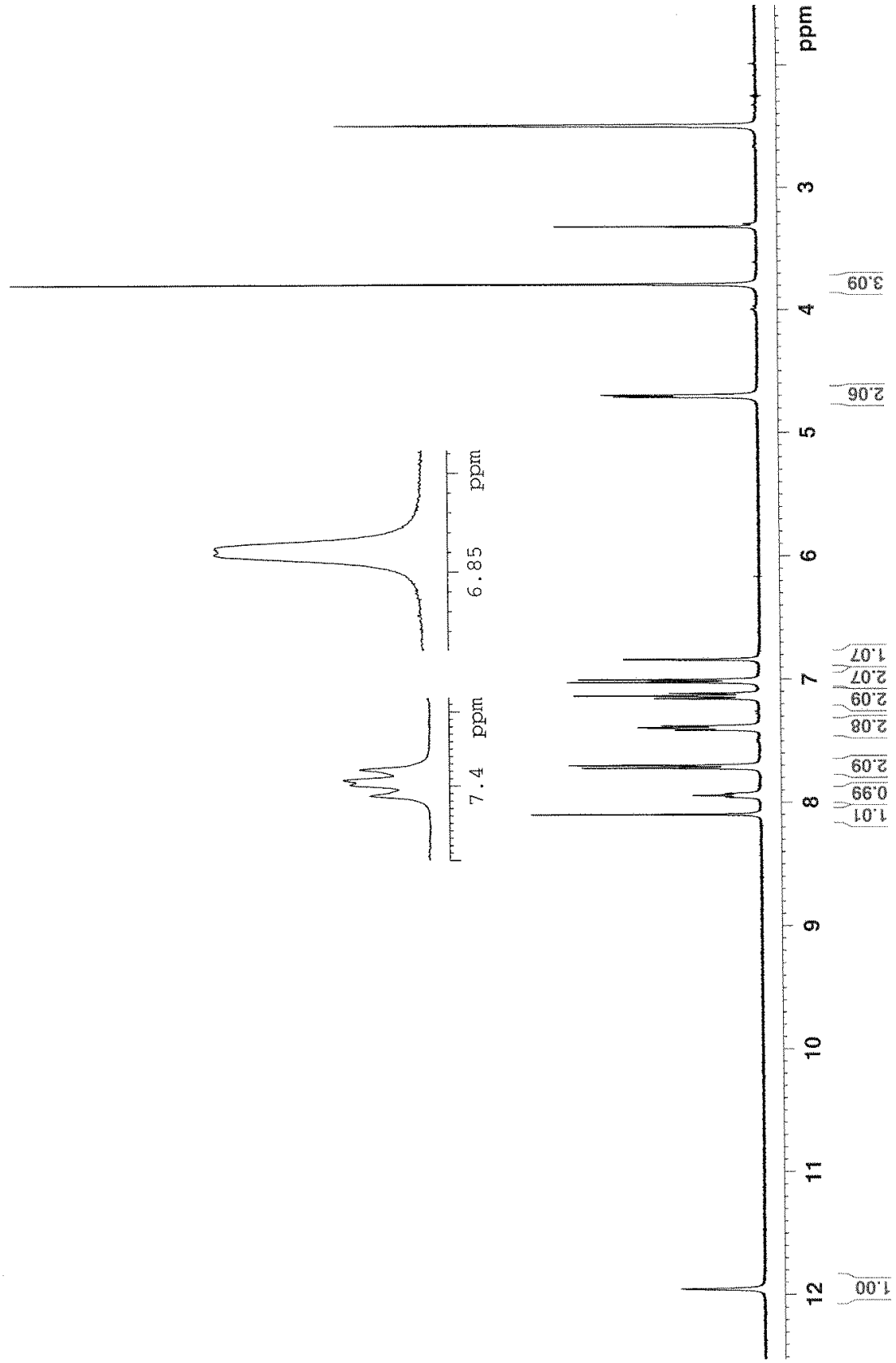

Residual peaks of DMSO and H_2O are found at 2.50 ppm and 3.33 ppm, respectively.

^{13}C – Spectrum of Compound 2h

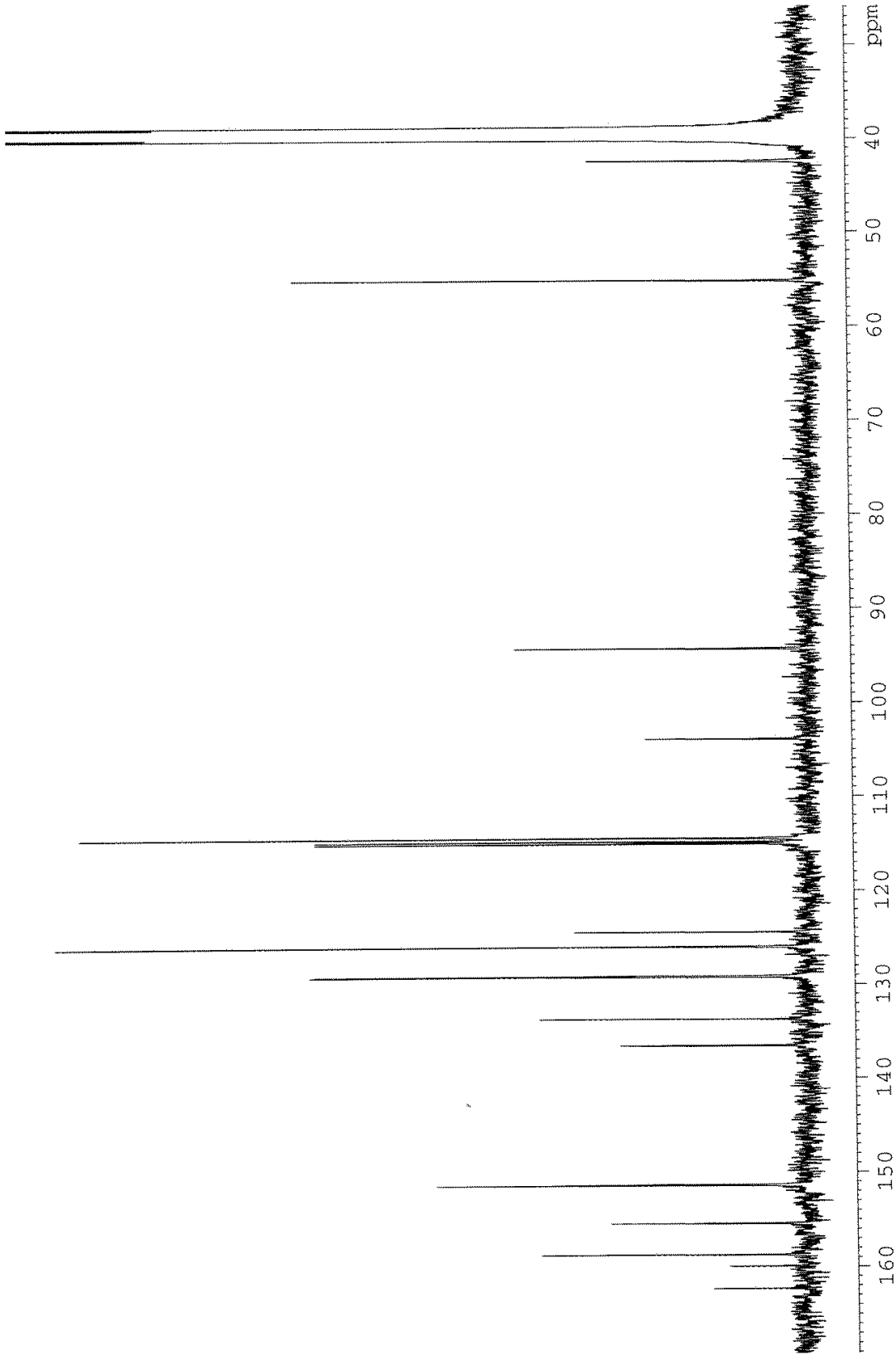

Residual peak of DMSO is found at 39.51 ppm.

COSY, 2D Spectrum of Compound 2h

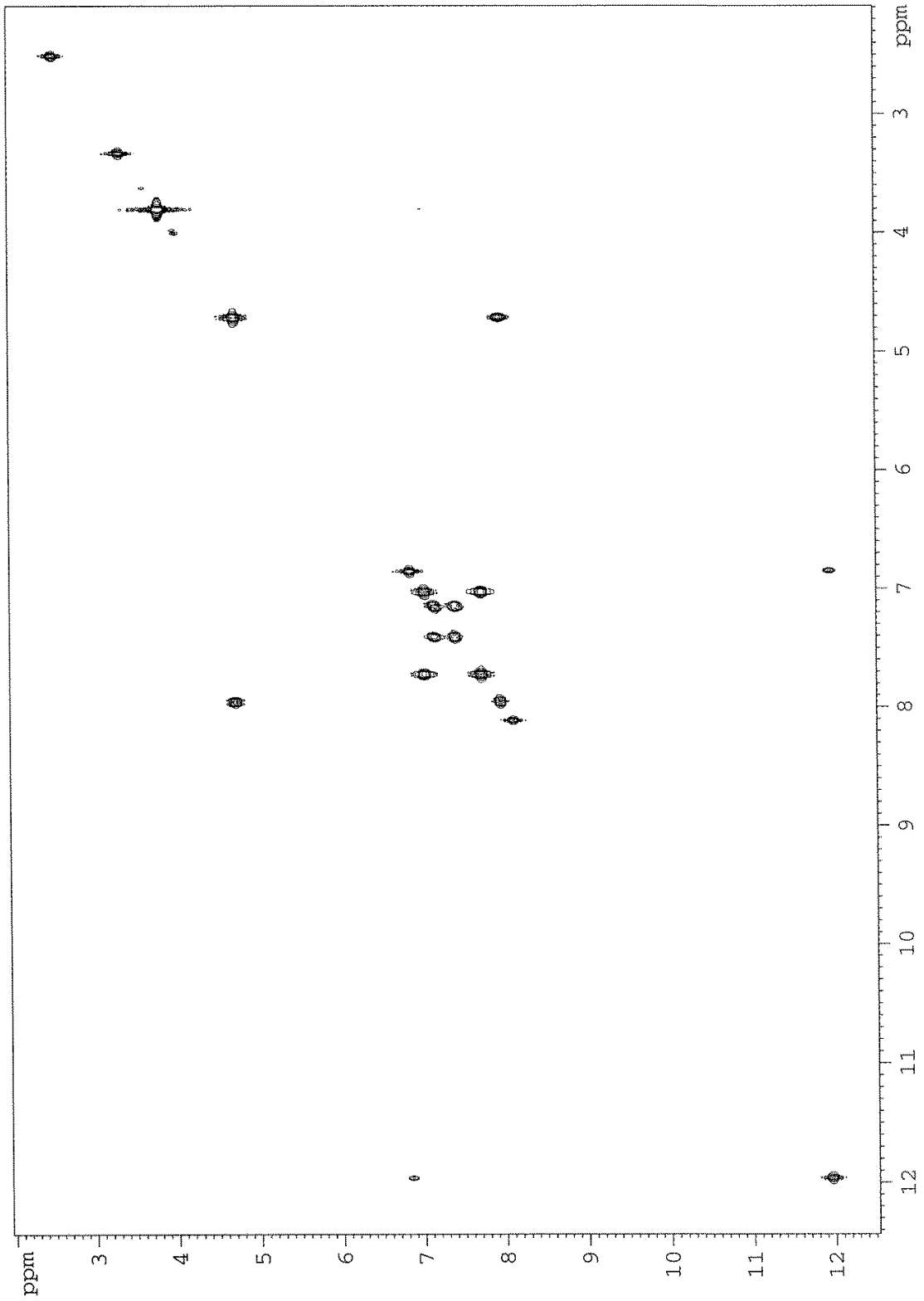

HSQC, 2D Spectrum of Compound 2h

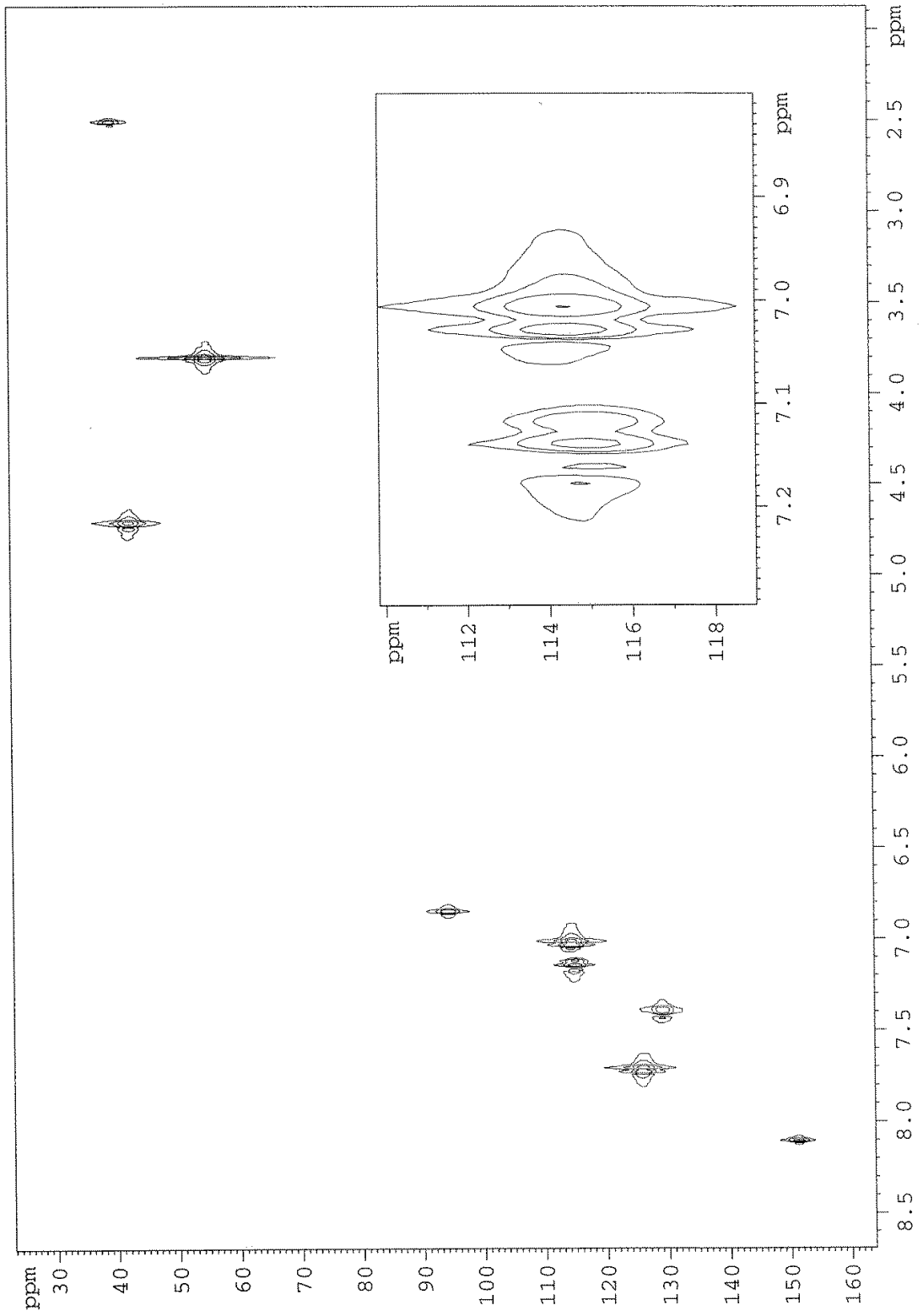

HMBC, 2D Spectrum of Compound 2h

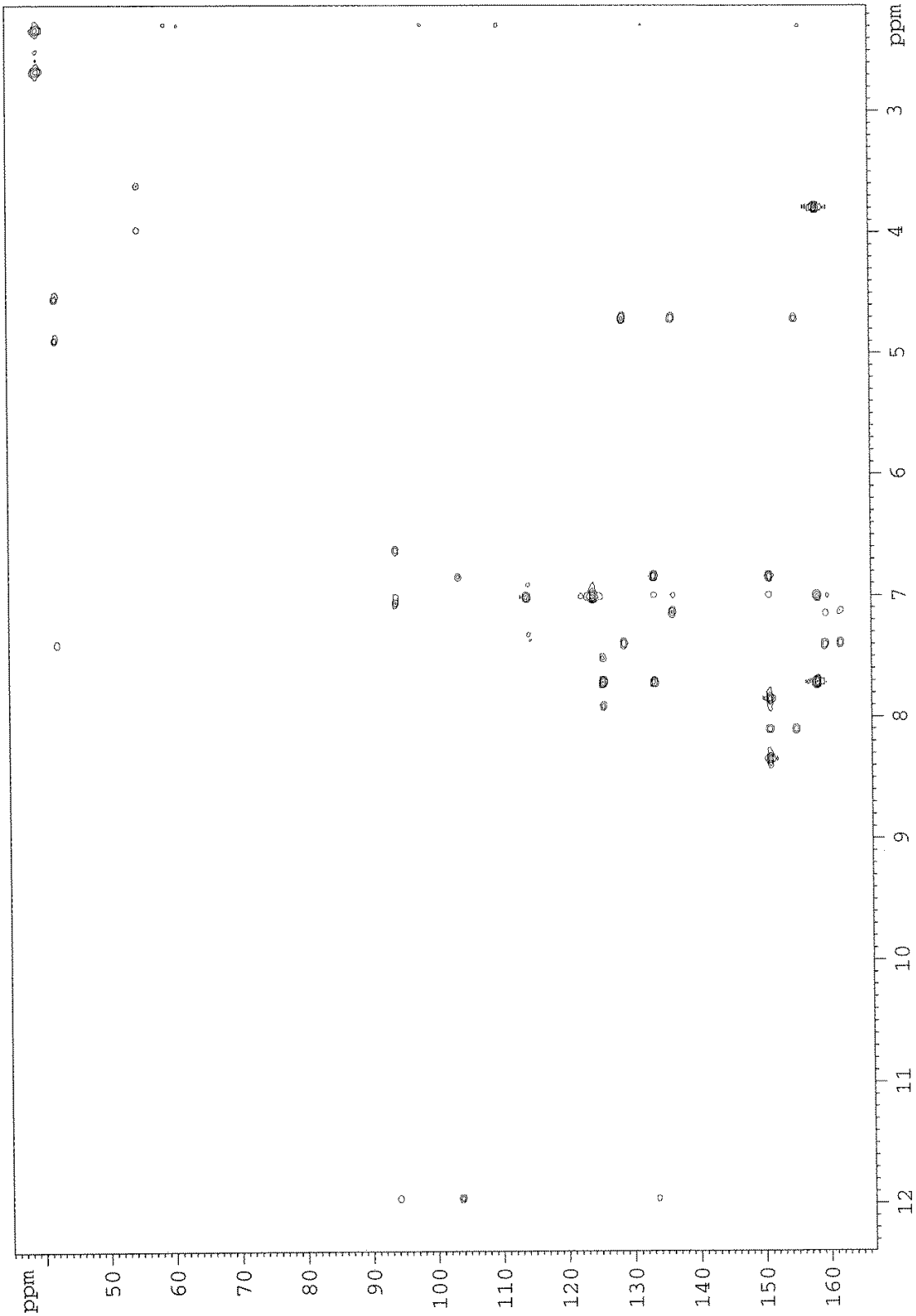

^{19}F – Spectrum of Compound 2h

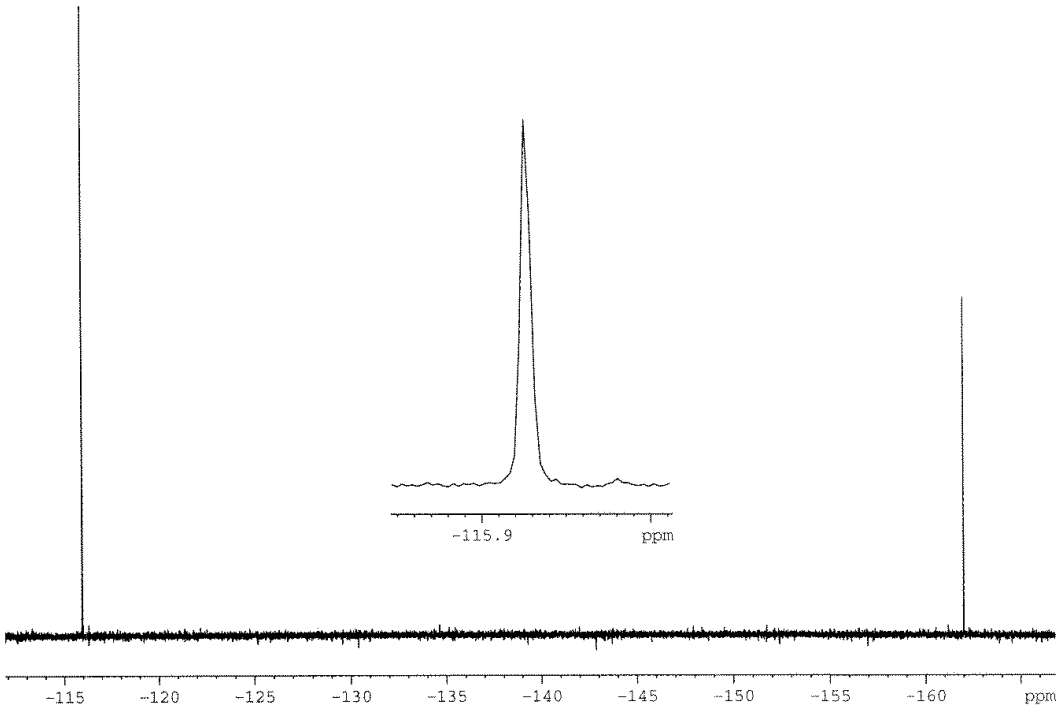

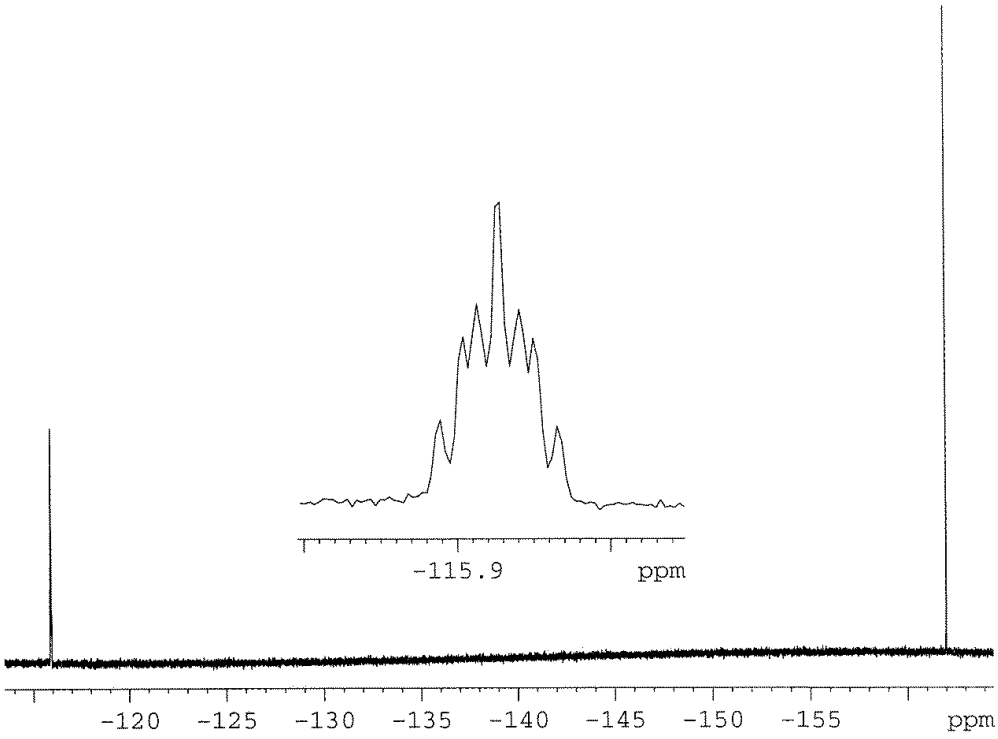

Residual peak of hexafluorobenzene is found at -162.0 ppm. Proton decoupled ^{19}F-NMR experiment is found in the top spectrum, while proton coupled ^{19}F-NMR experiment is found in the bottom spectrum

A.3 – NMR Spectra of Compound 3

^{1}H – Spectrum of Compound 3

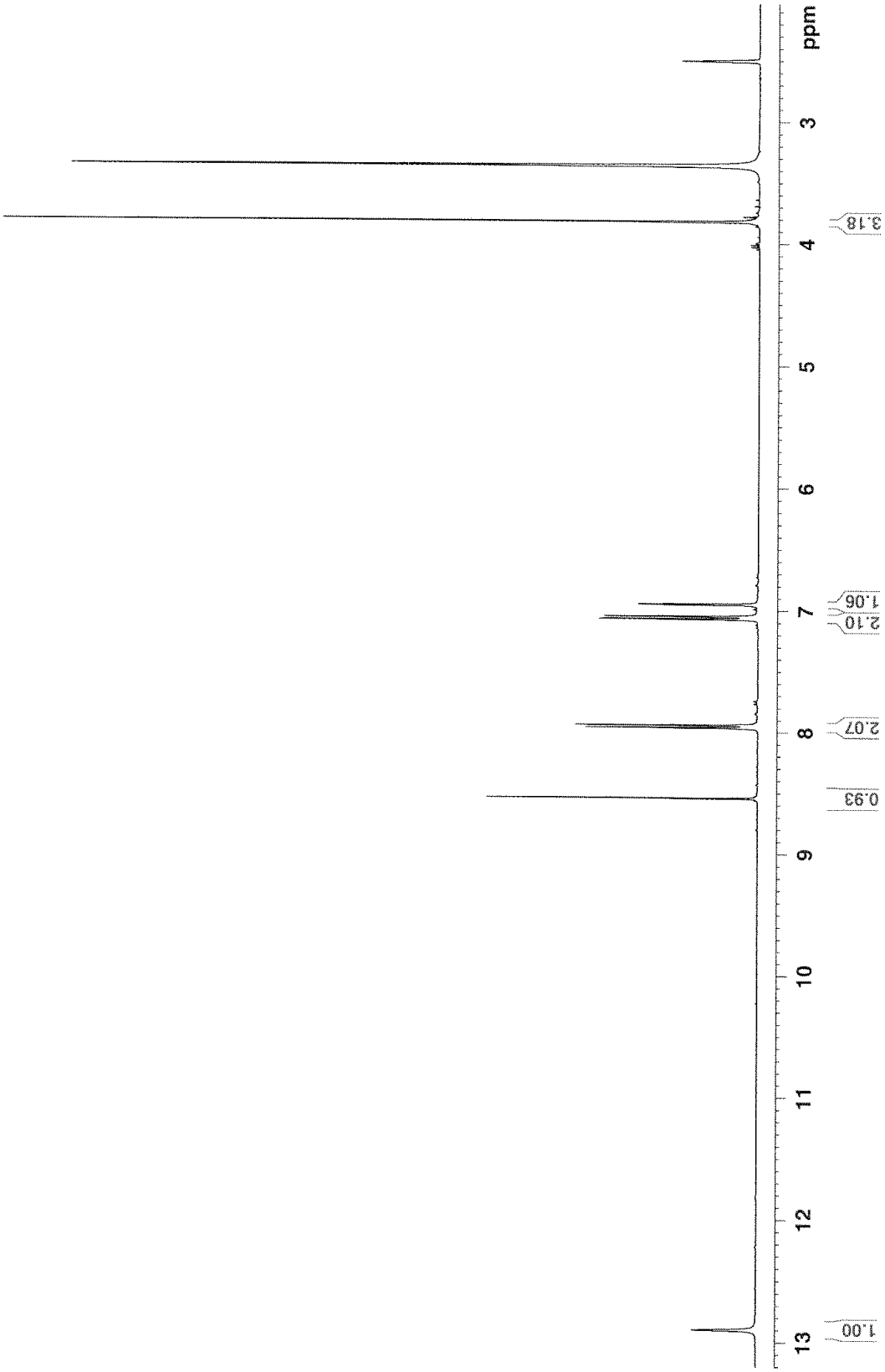

Residual peaks of DMSO and H_2O are found at 2.50 ppm and 3.33 ppm, respectively.

^{13}C – Spectrum of Compound 3

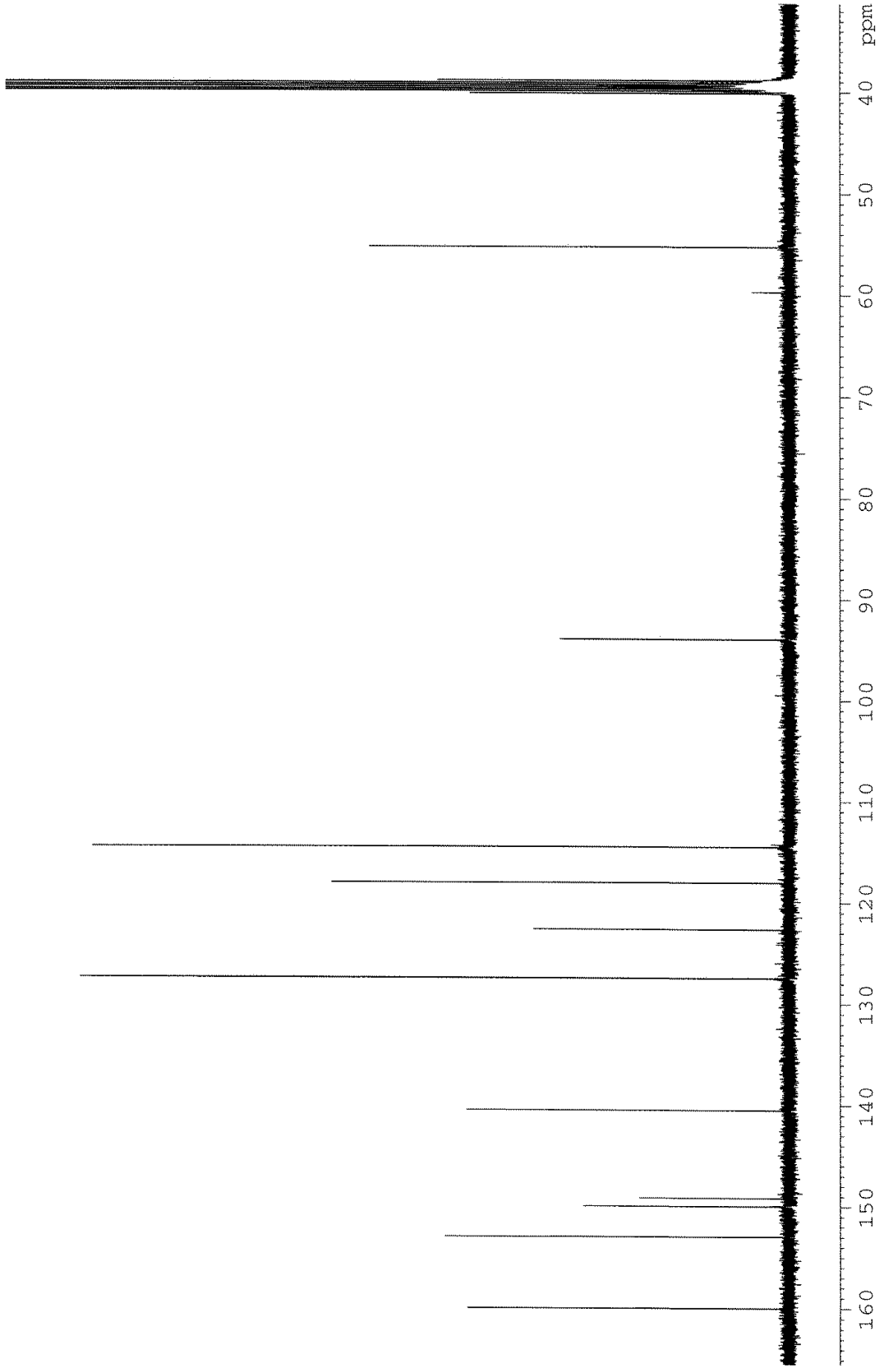

Residual peak of DMSO is found at 39.51 ppm.

COSY, 2D Spectrum of Compound 3

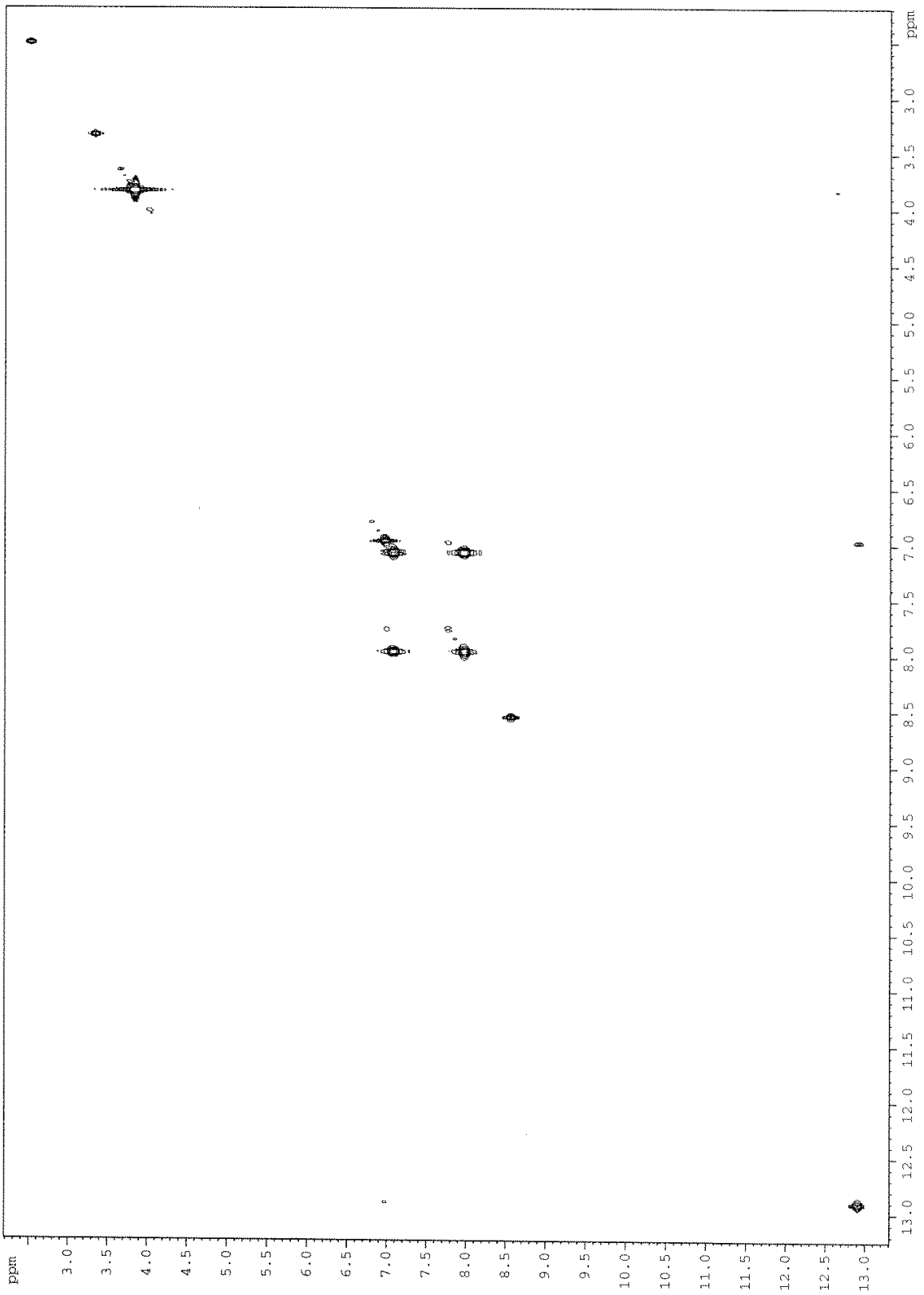

HSQC, 2D Spectrum of Compound 3

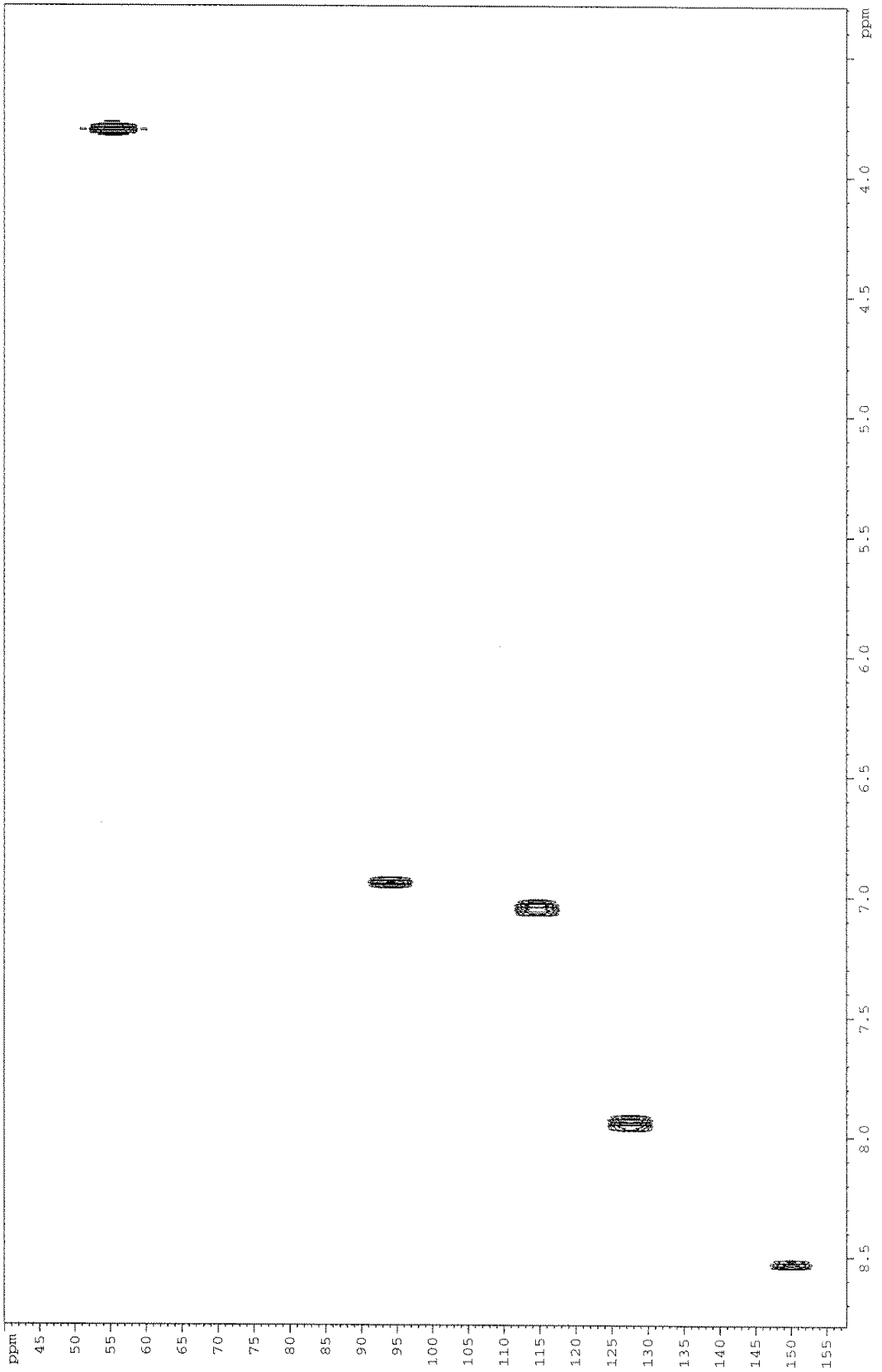

HMBC, 2D Spectrum of Compound 3

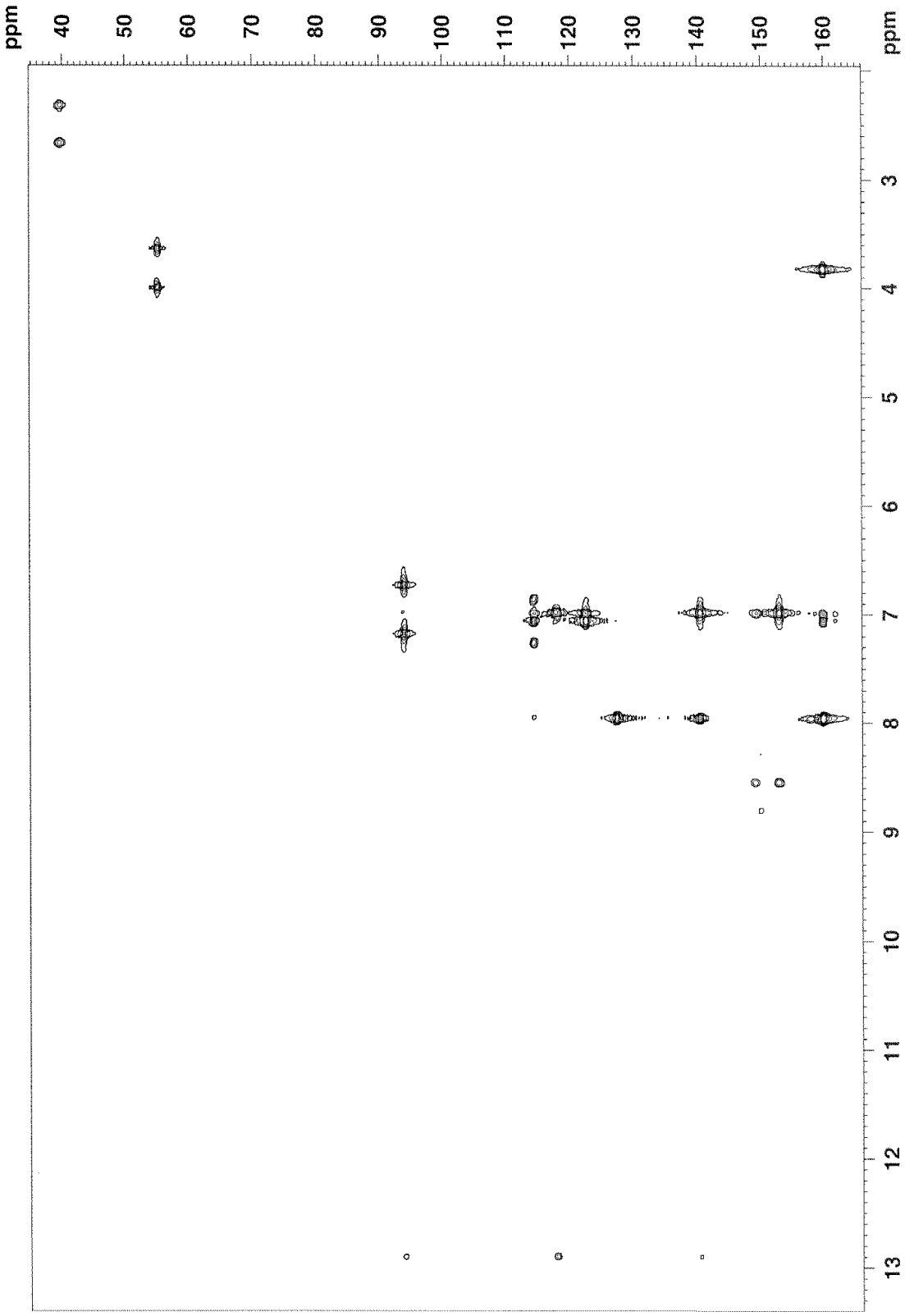

A.4 – NMR Spectra of Compound 4

^{1}H – Spectrum of Compound 4

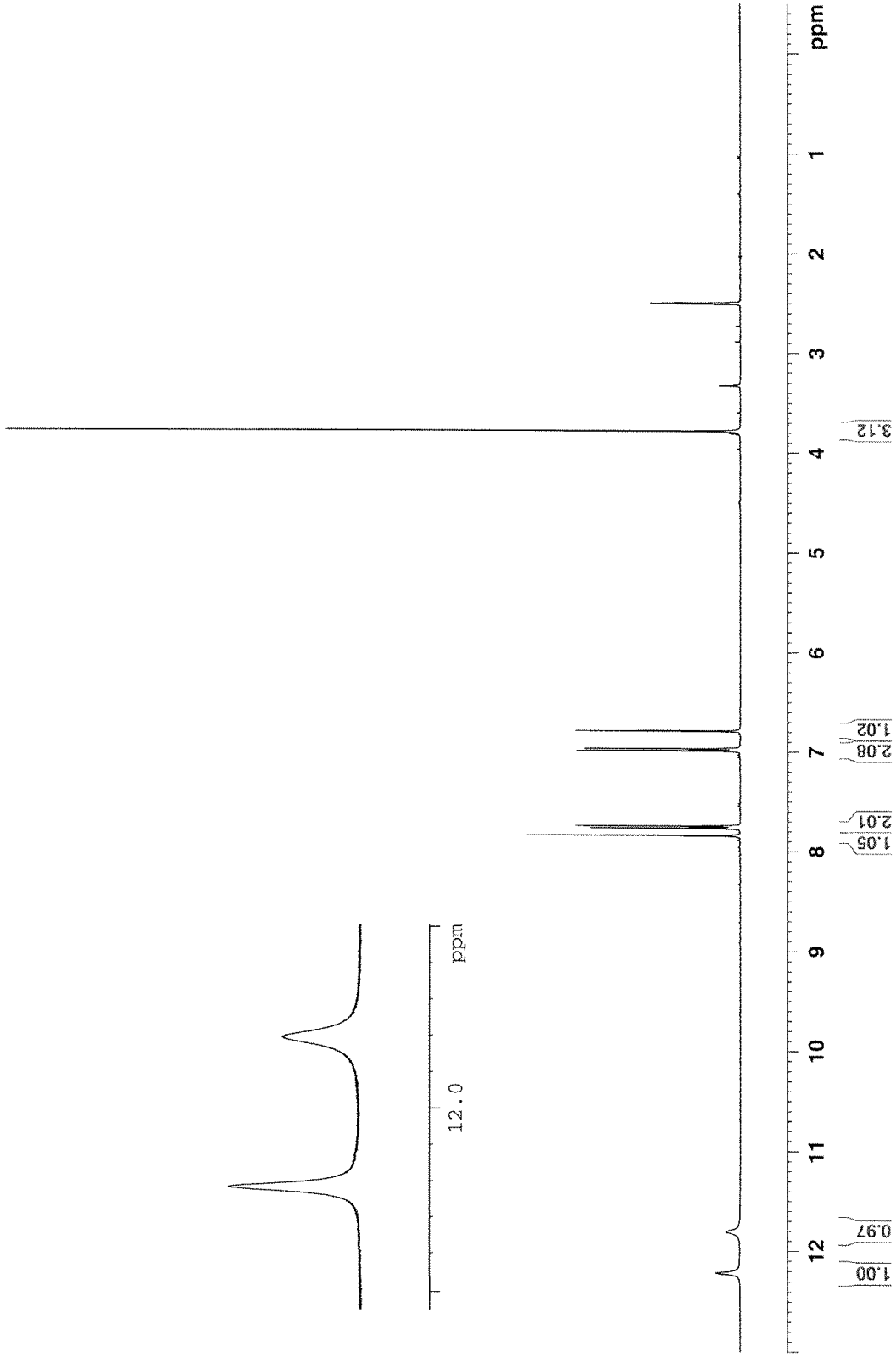

Residual peaks of DMSO and H_2O are found at 2.50 ppm and 3.33 ppm, respectively.

^{13}C – Spectrum of Compound 4

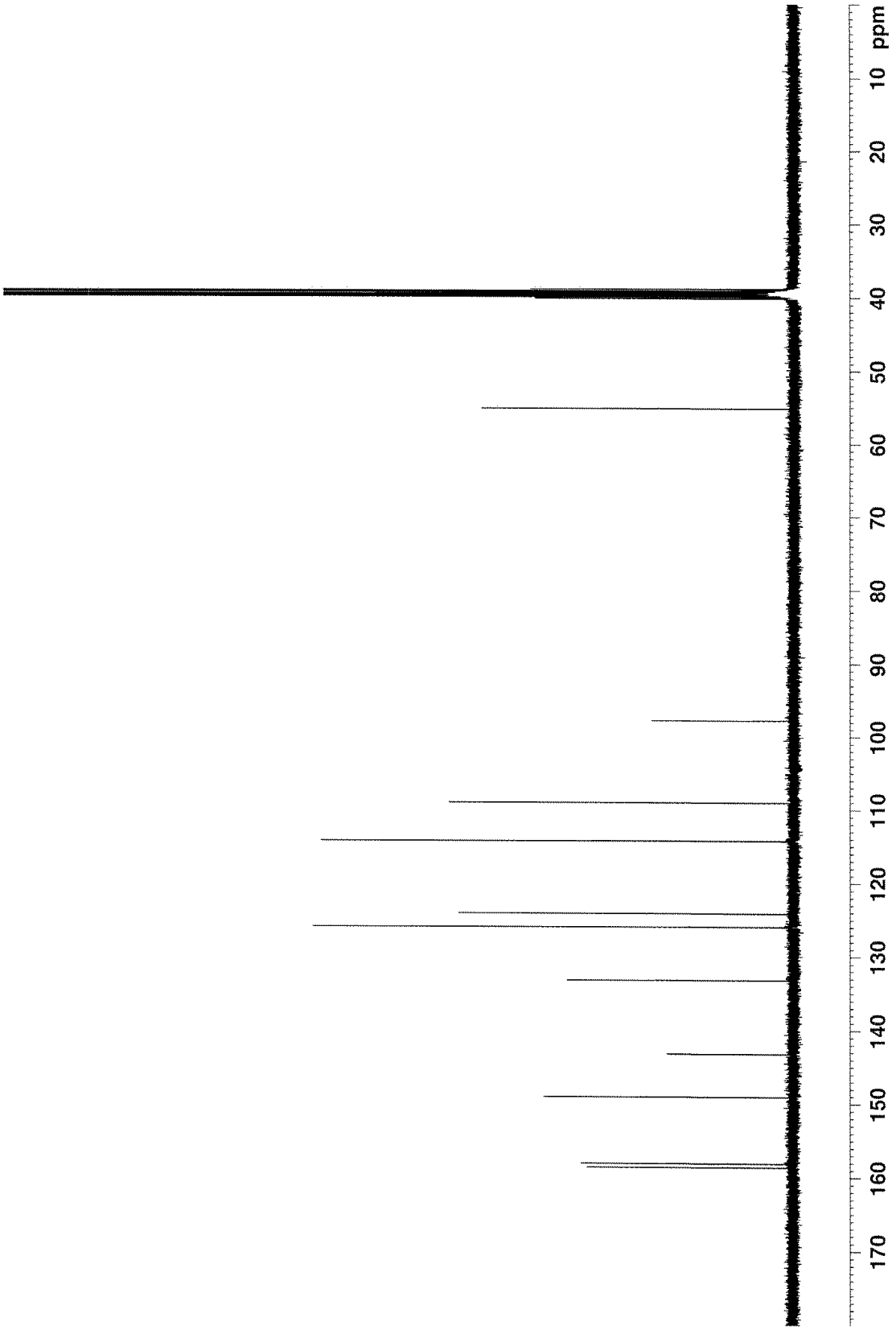

Residual peak of DMSO is found at 39.51 ppm.

A.5 – NMR Spectra of Compound 5

^{1}H – Spectrum of Compound 5

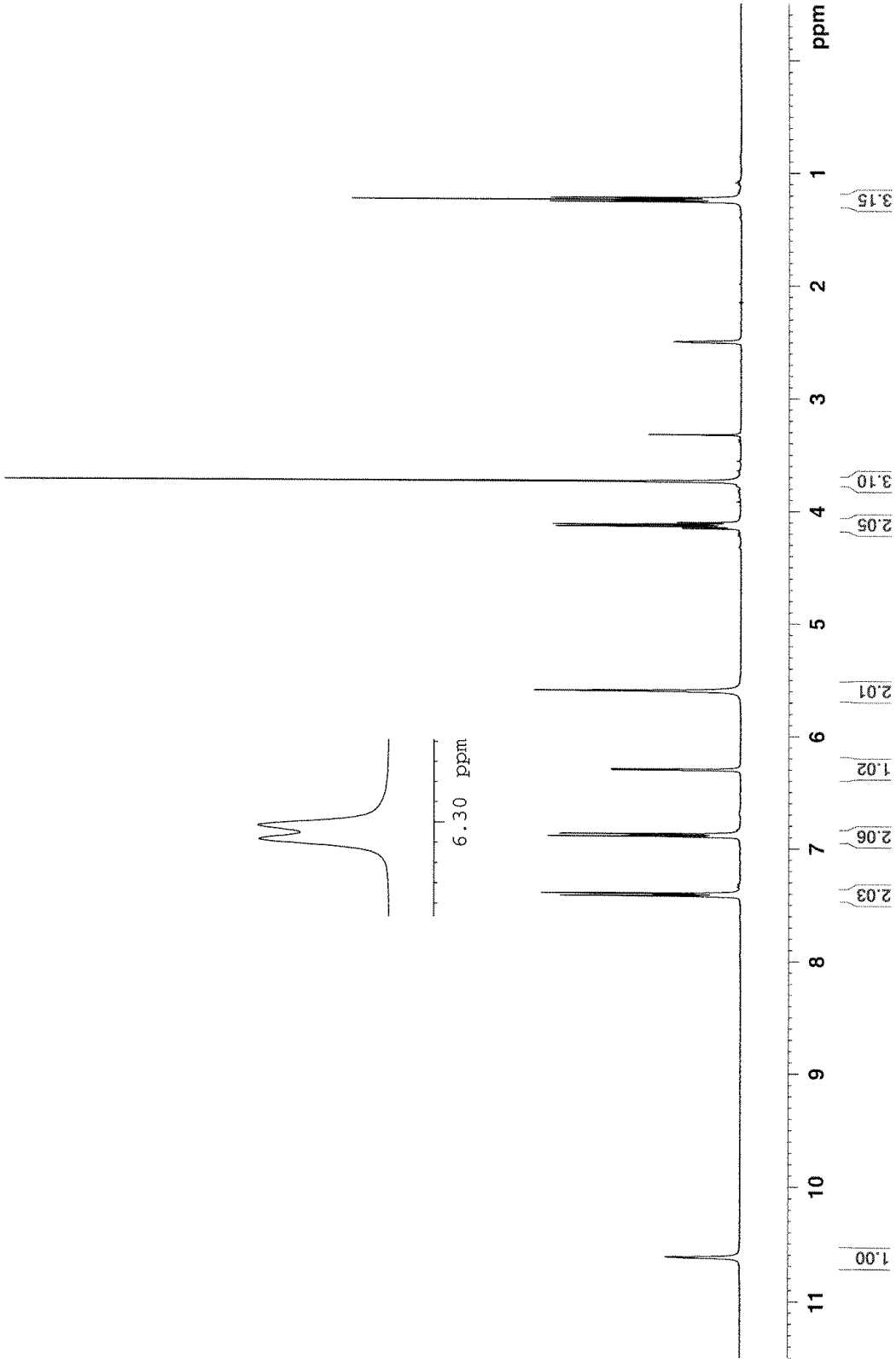

Residual peaks of DMSO and H_2O are found at 2.50 ppm and 3.33 ppm, respectively.

^{13}C – Spectrum of Compound 5

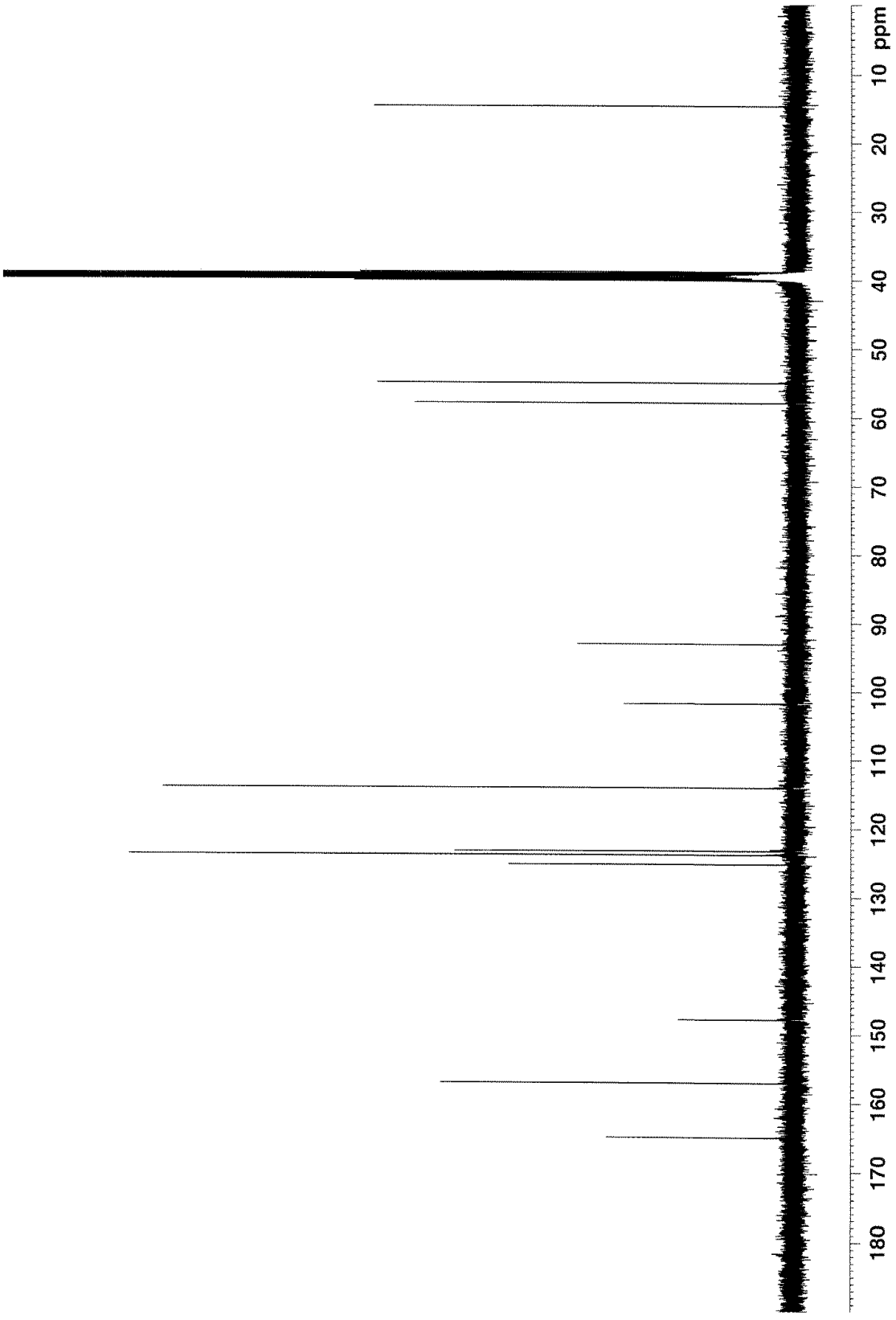

Residual peak of DMSO is found at 39.51 ppm.

A.6 – NMR Spectra of Compound 6

^{1}H – Spectrum of Compound 6

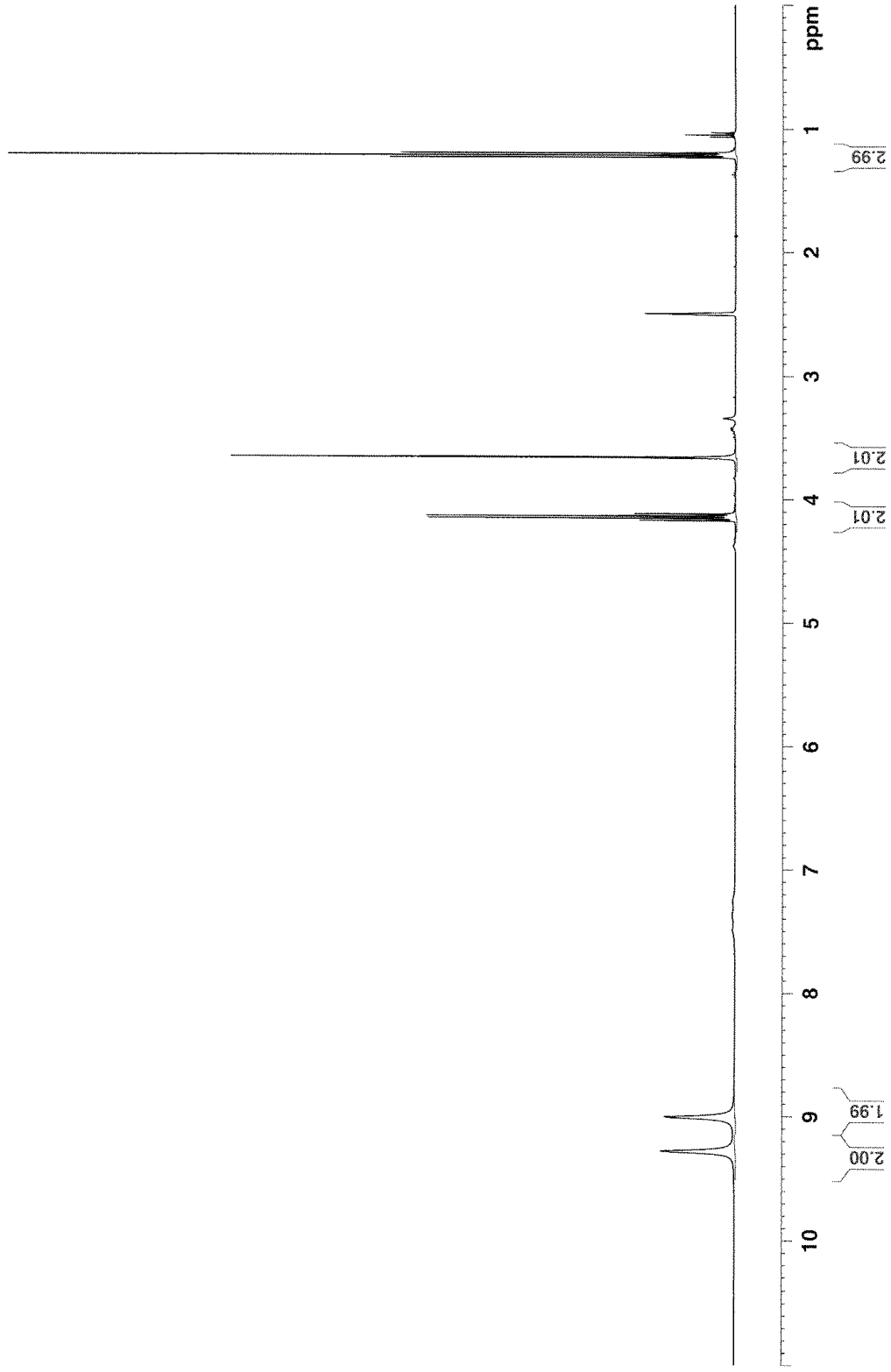

Residual peaks of DMSO and H_2O are found at 2.50 ppm and 3.33 ppm, respectively.

^{13}C – Spectrum of Compound 6

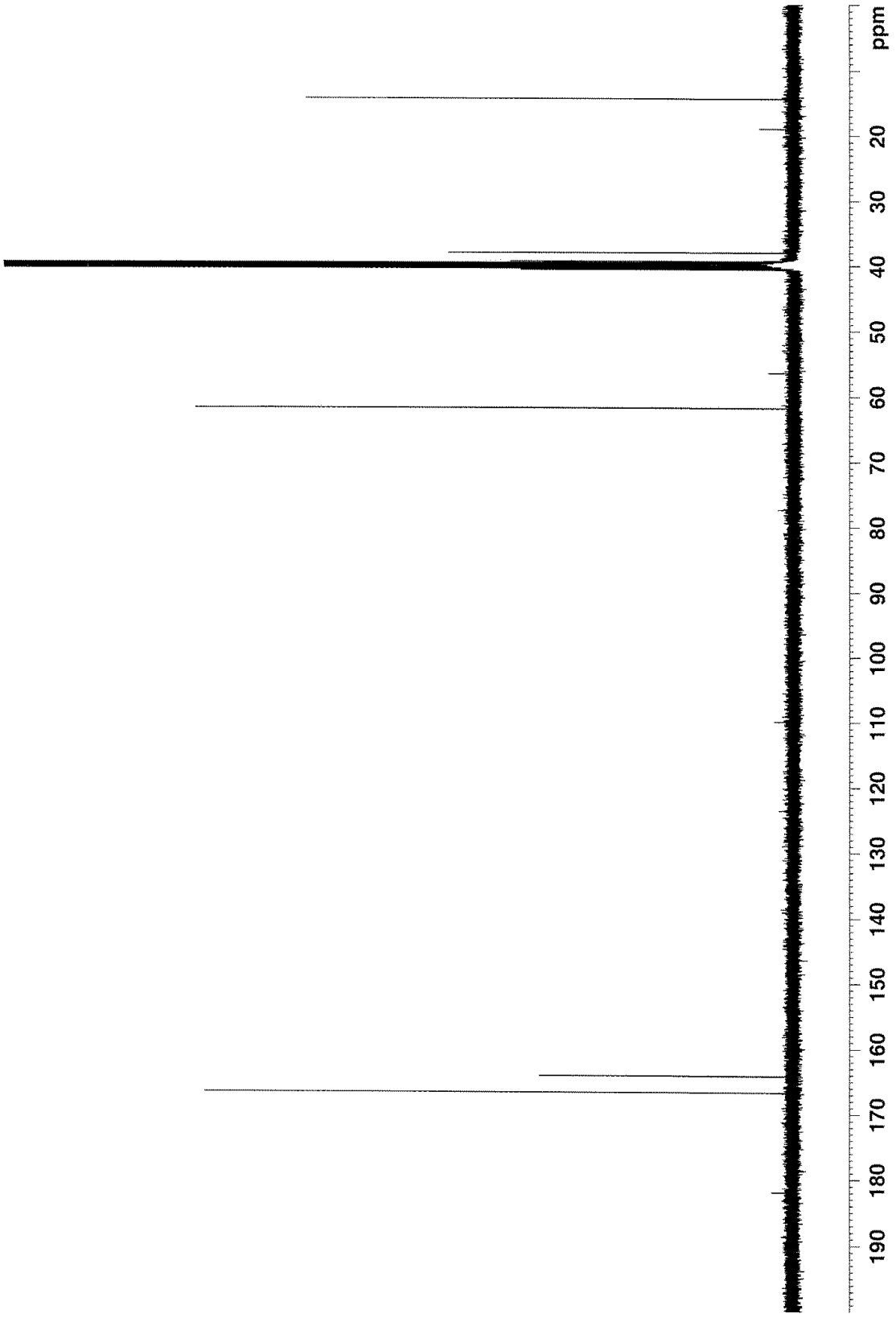

Residual peak of DMSO is found at 39.51 ppm.

A.7 – NMR Spectra of Compound 7

^{1}H – Spectrum of Compound 7

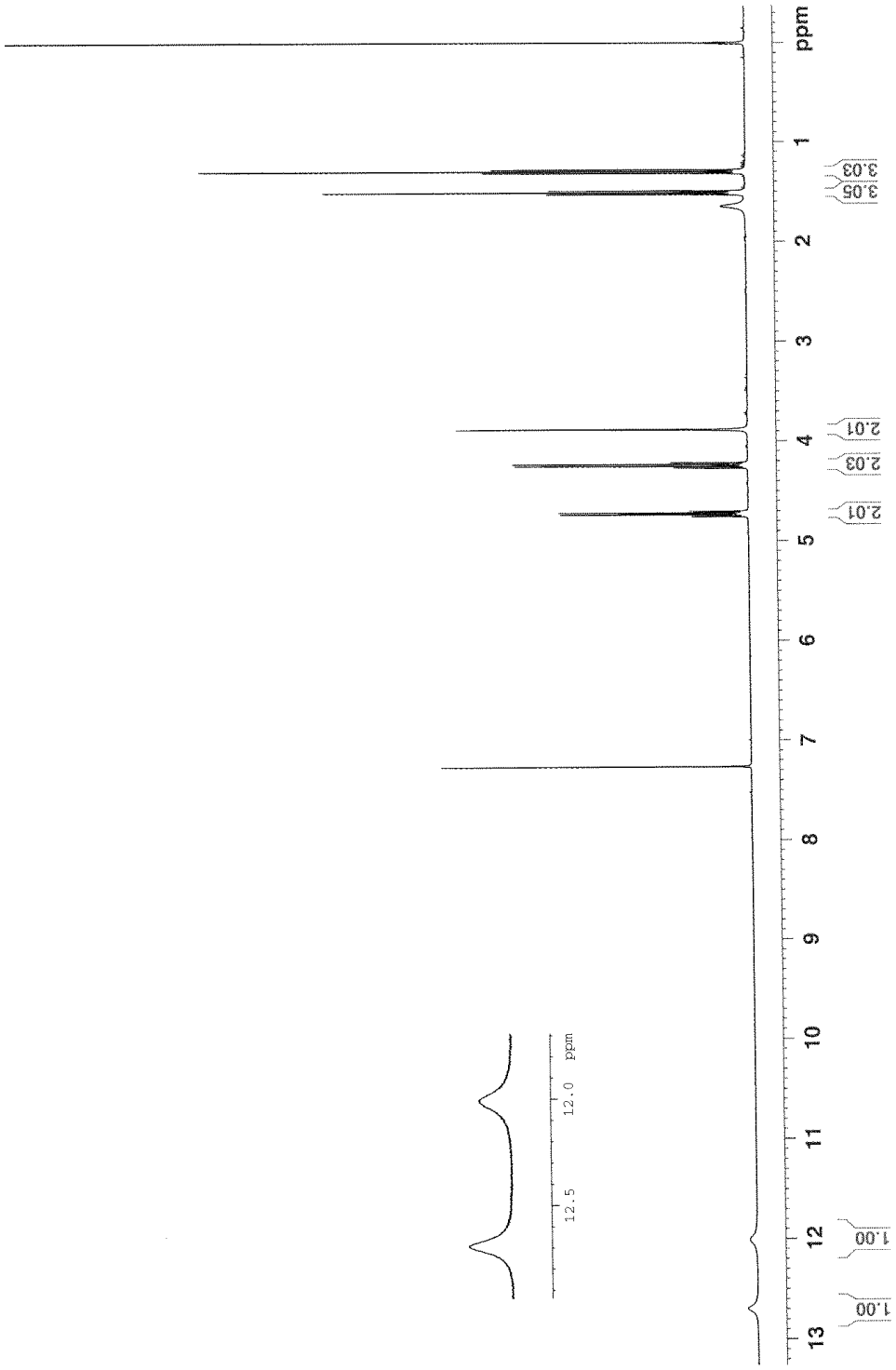

Residual peaks of Chloroform and H_2O are found at 7.24 ppm and 1.56 ppm, respectively.

^{13}C – Spectrum of Compound 7

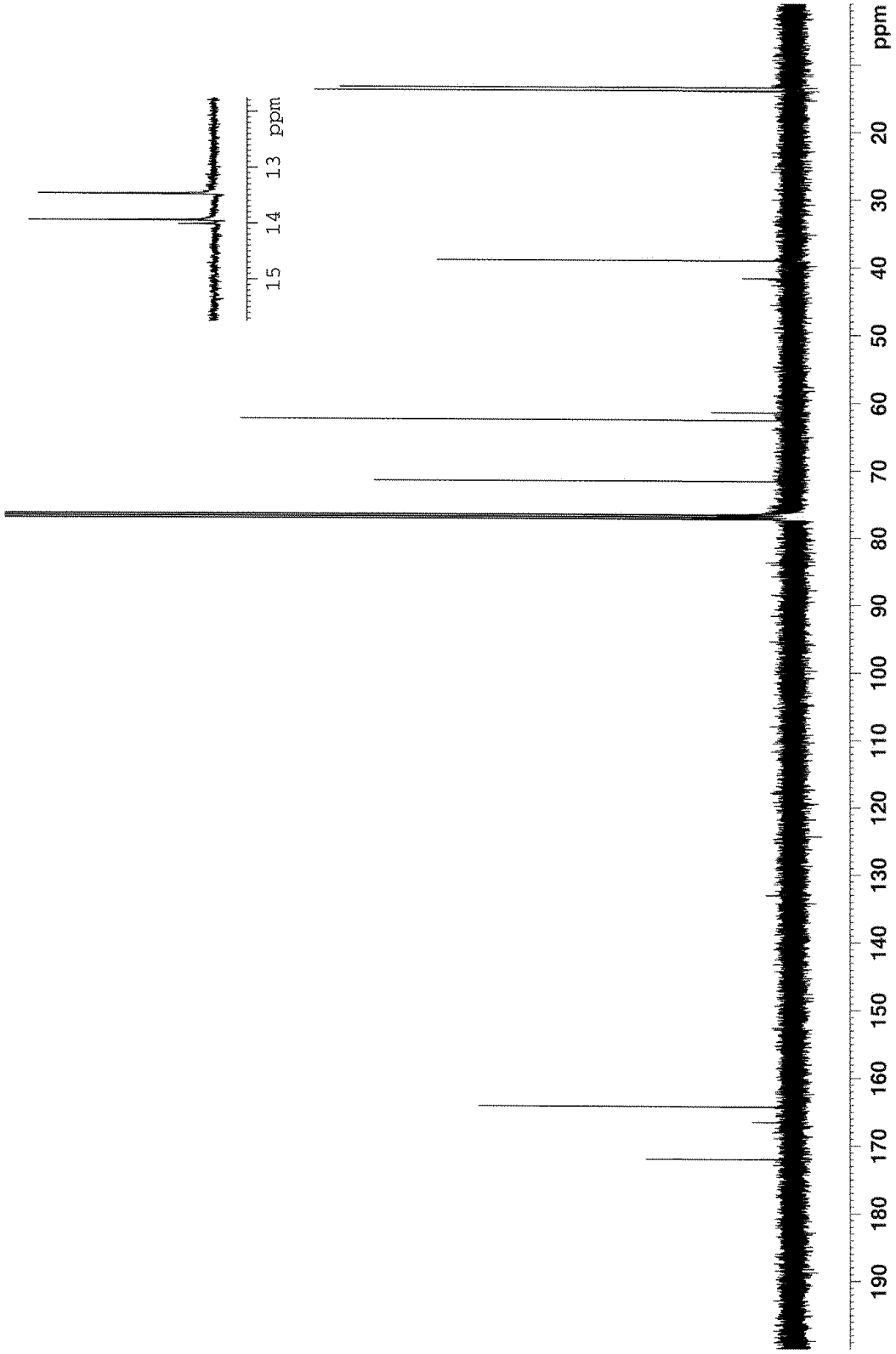

Residual peak of Chloroform is found at 77.23 ppm.

Appendix B – Mass Spectra

B.1 – Mass Spectra of Compounds 1a-h

B.1.1 – Compound 1a

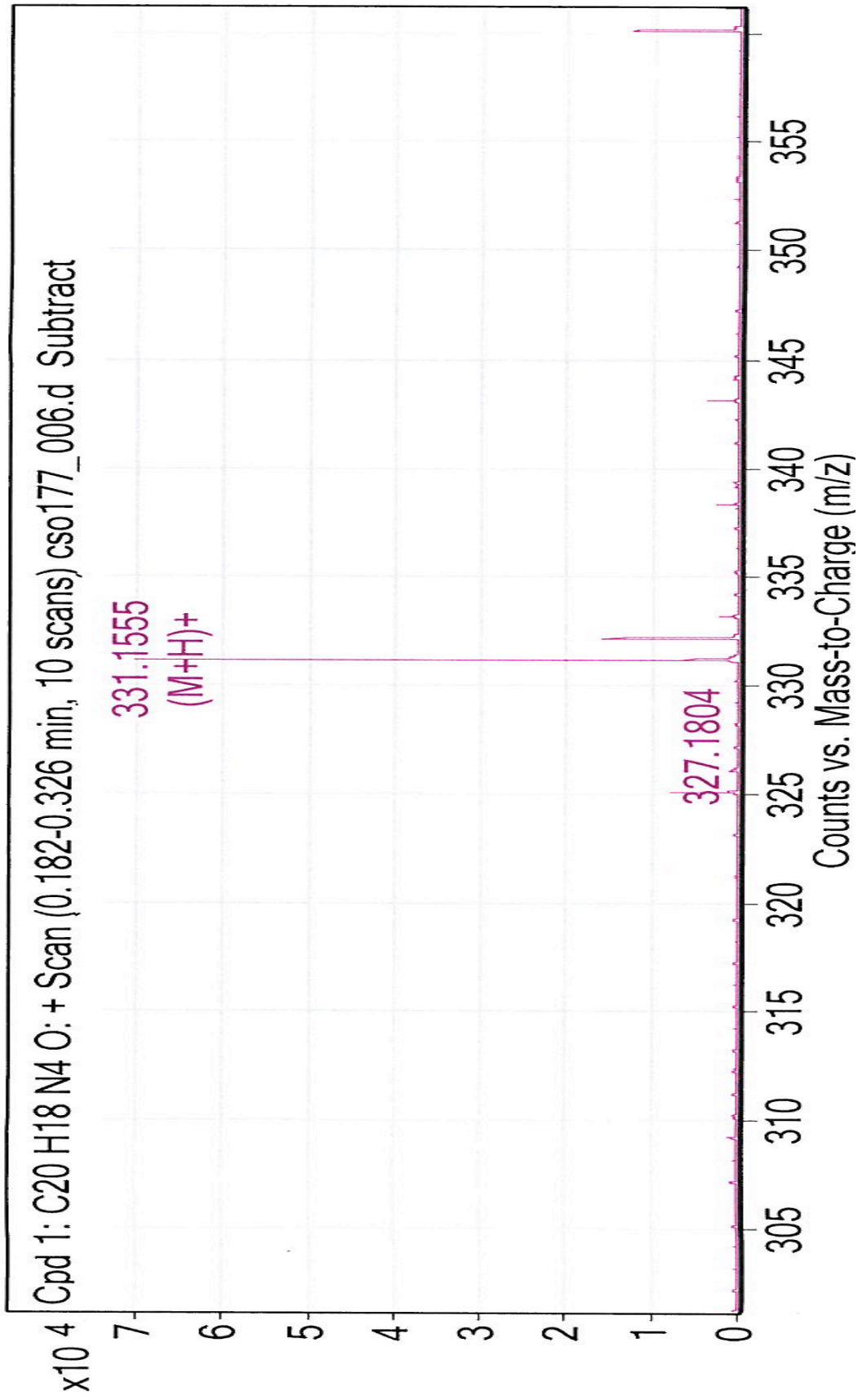

B.1.2 – Compound 1b

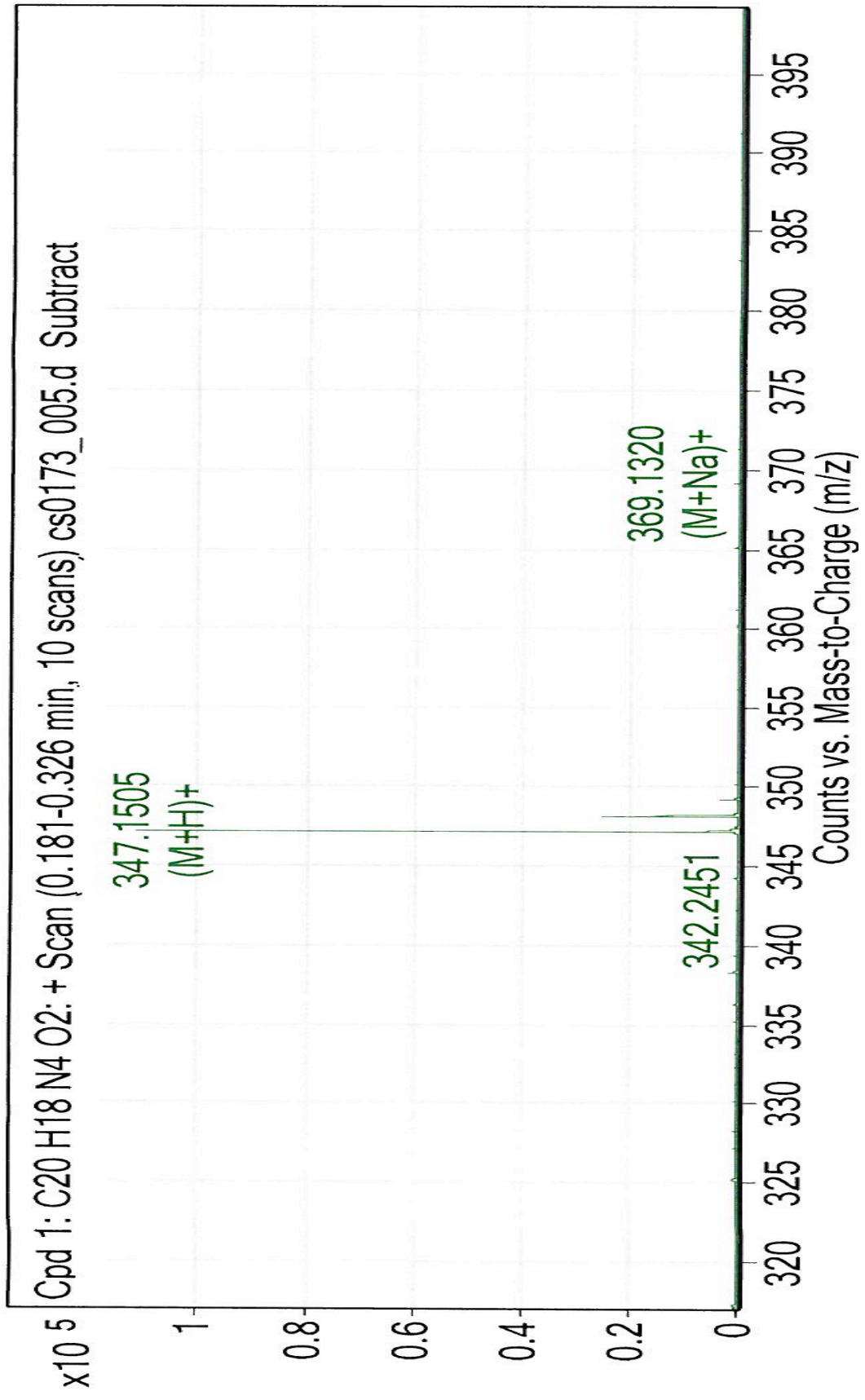

B.1.3 – Compound 1c

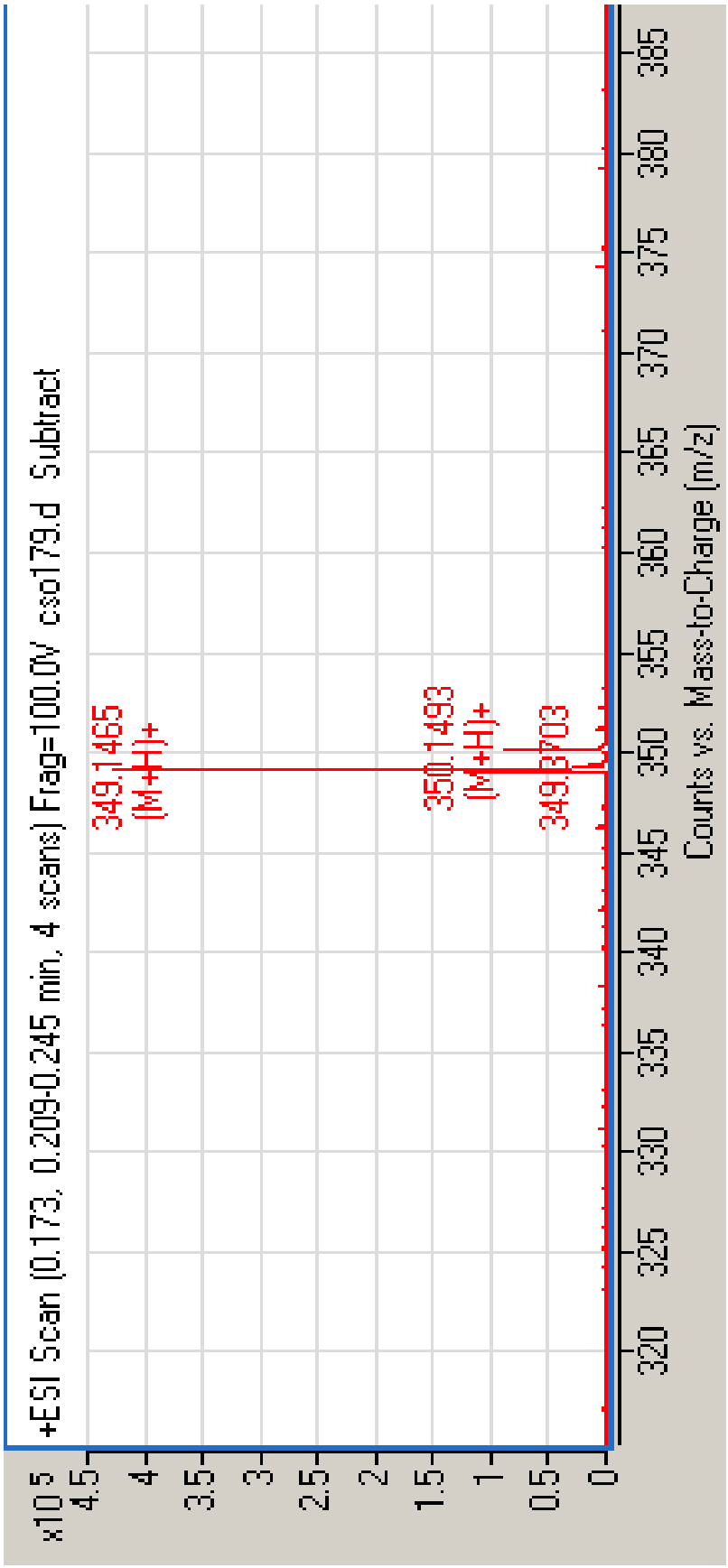

B.1.4 – Compound 1d

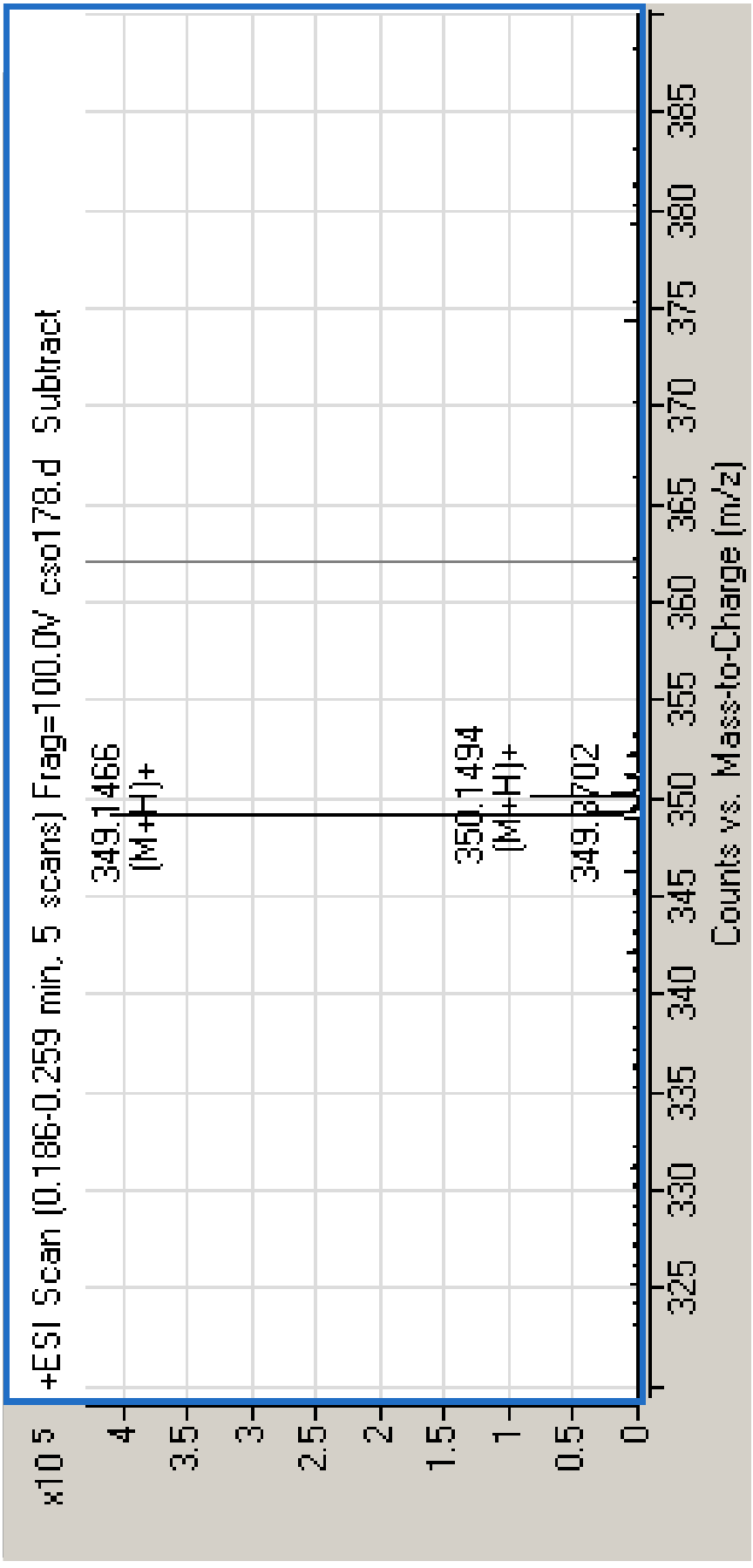

B.1.5 – Compound 1e

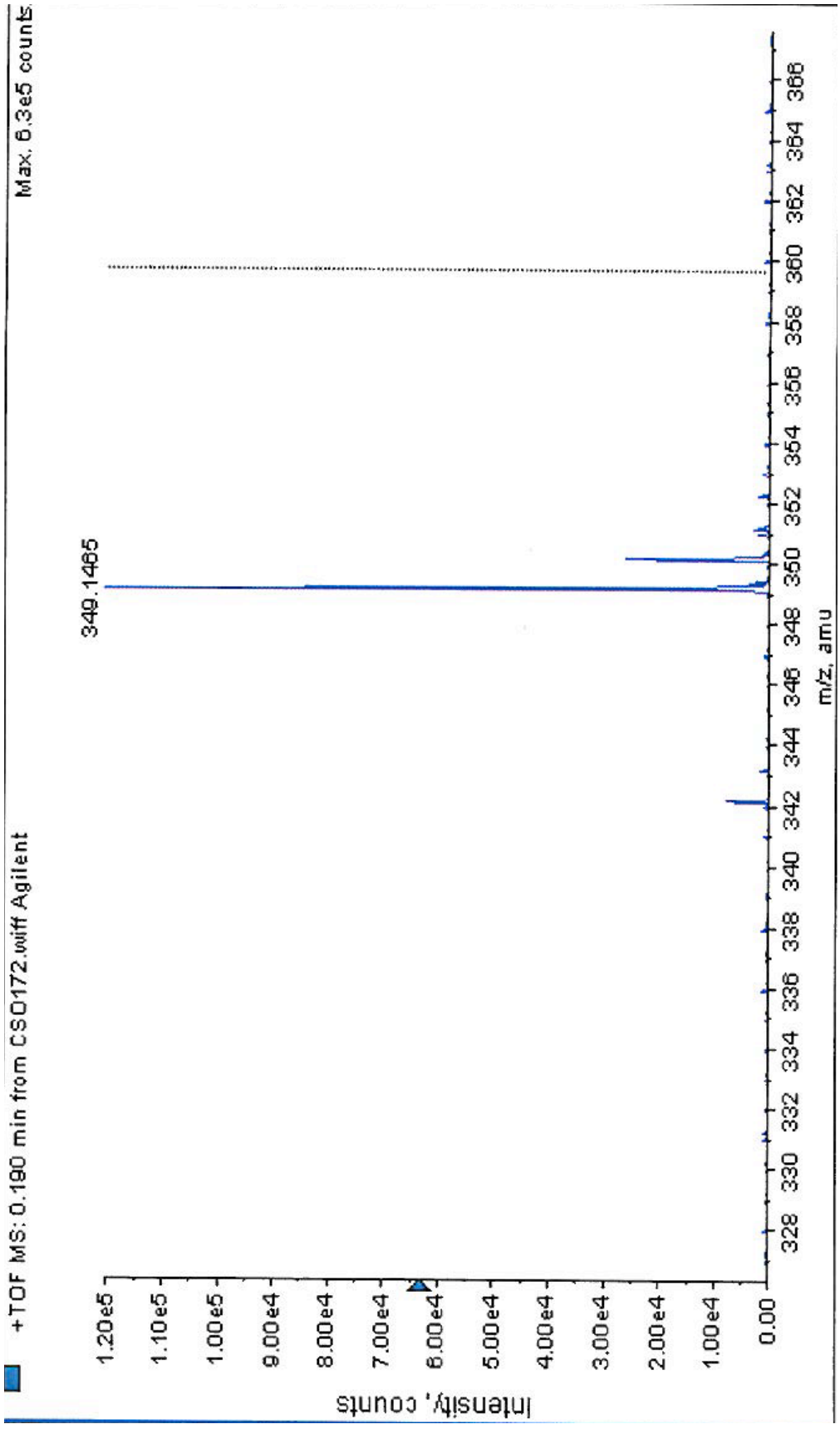

B.1.6 – Compound 1f

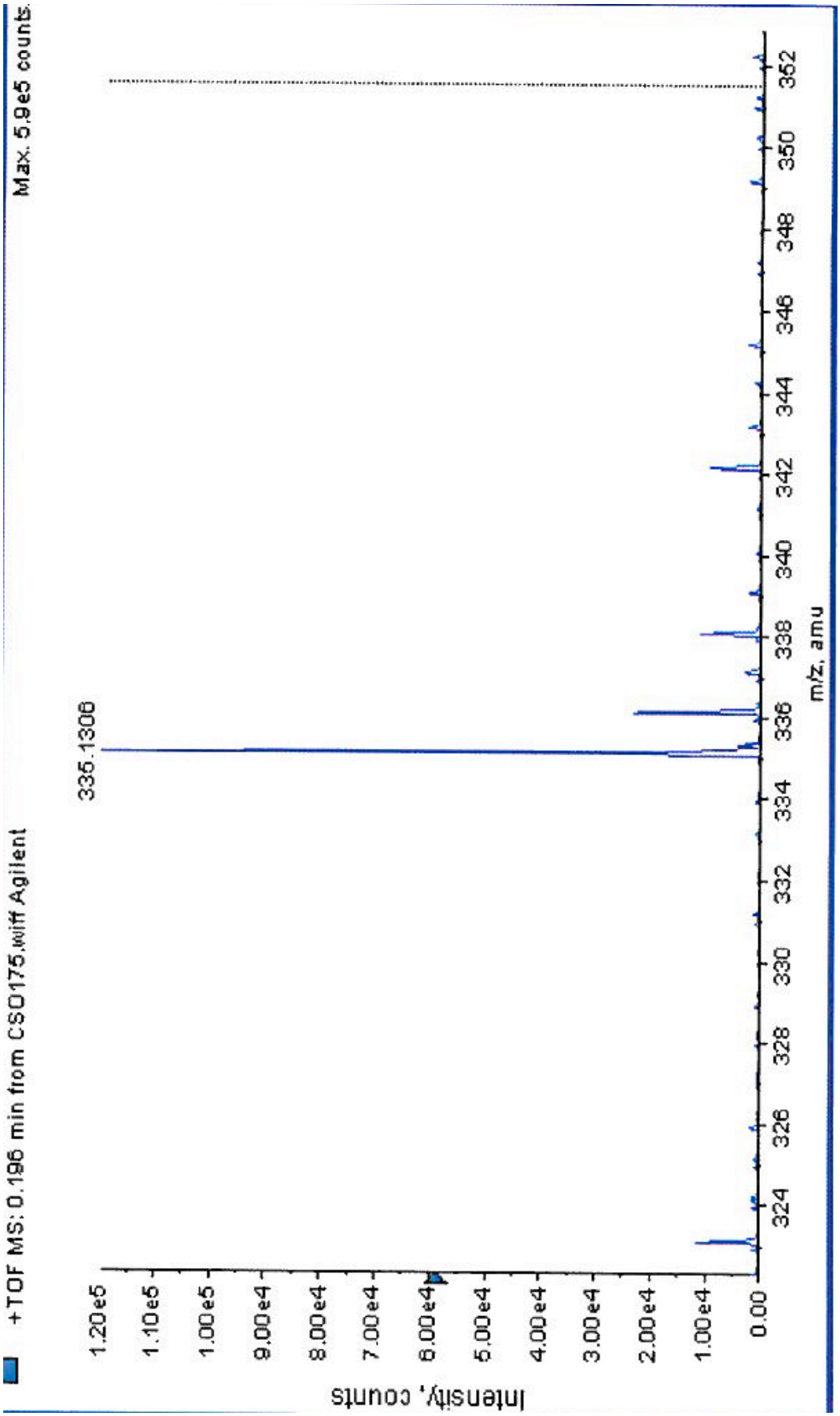

B.1.7 – Compound 1g

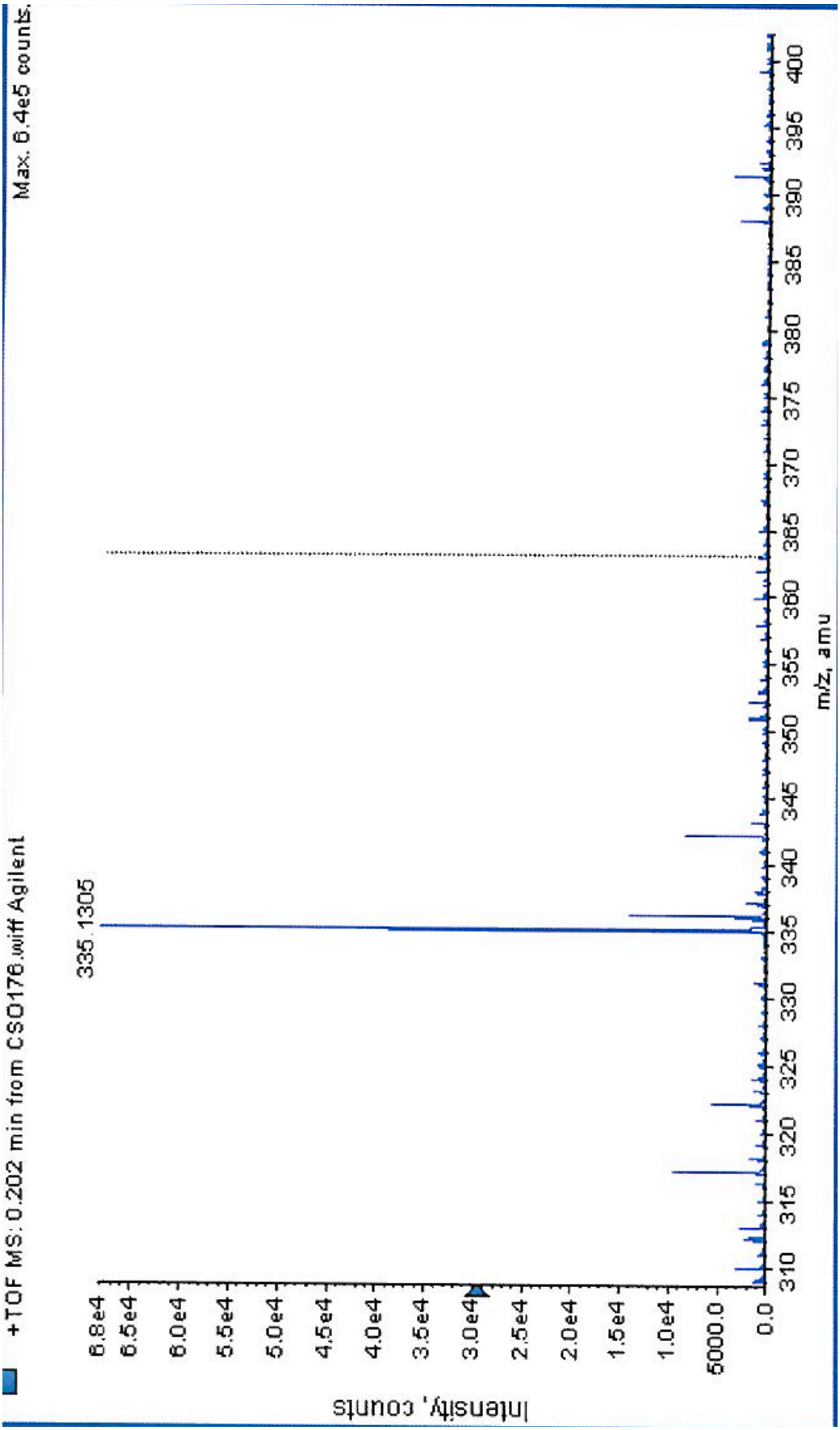

B.1.8 – Compound 1h

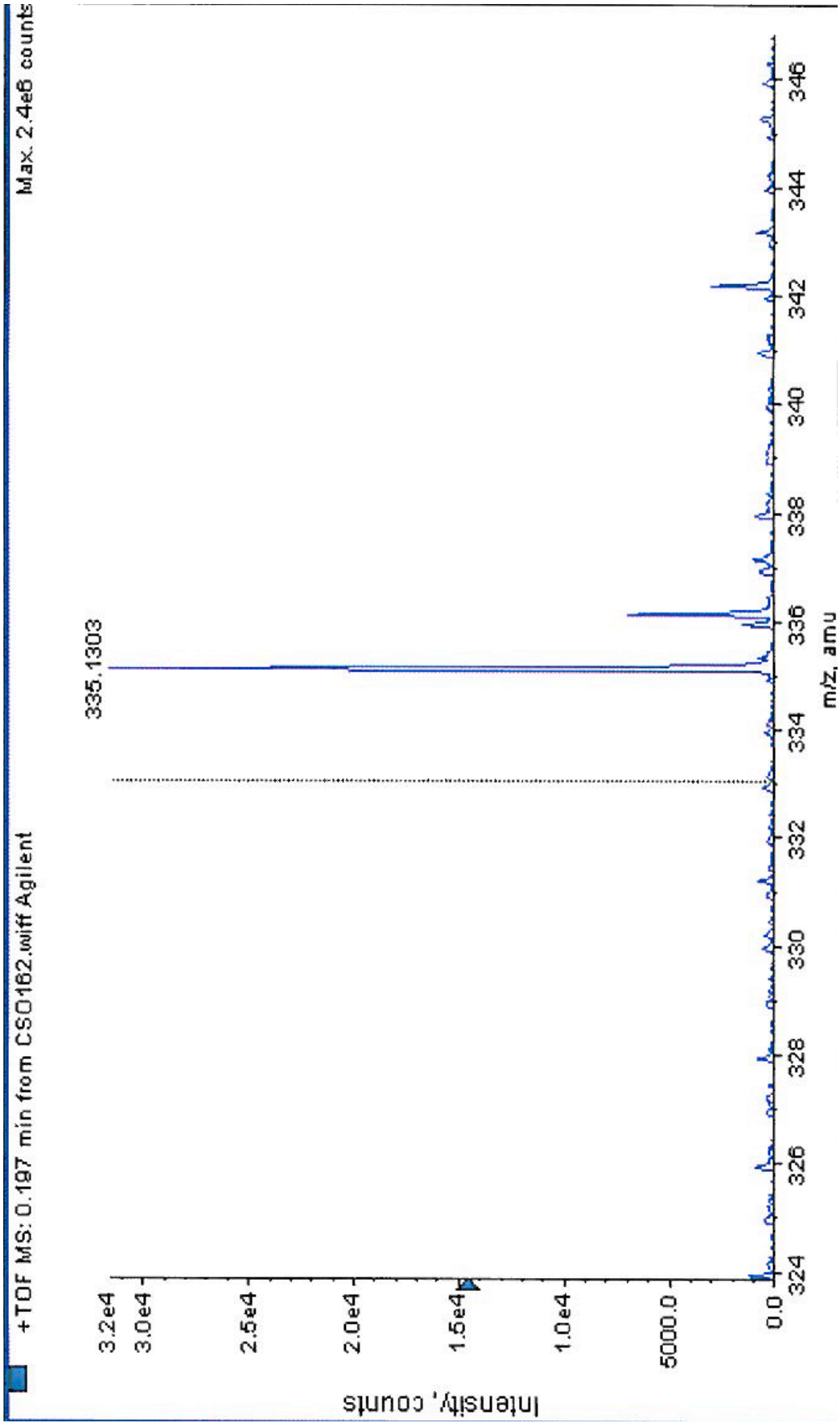

B.2 – Mass Spectra of Compounds 2a-h

B.2.1 – Compound 2a

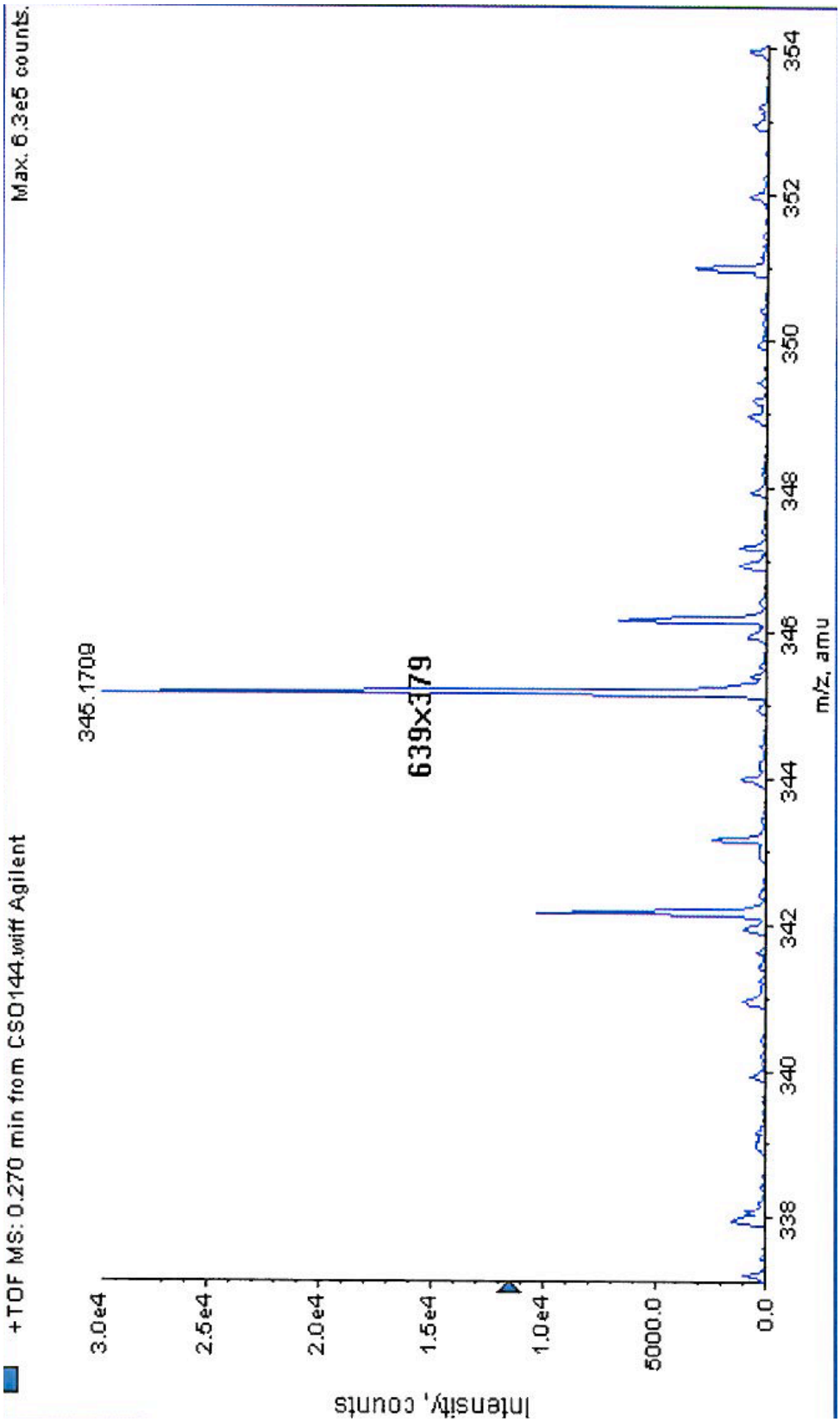

B.2.2 – Compound 2b

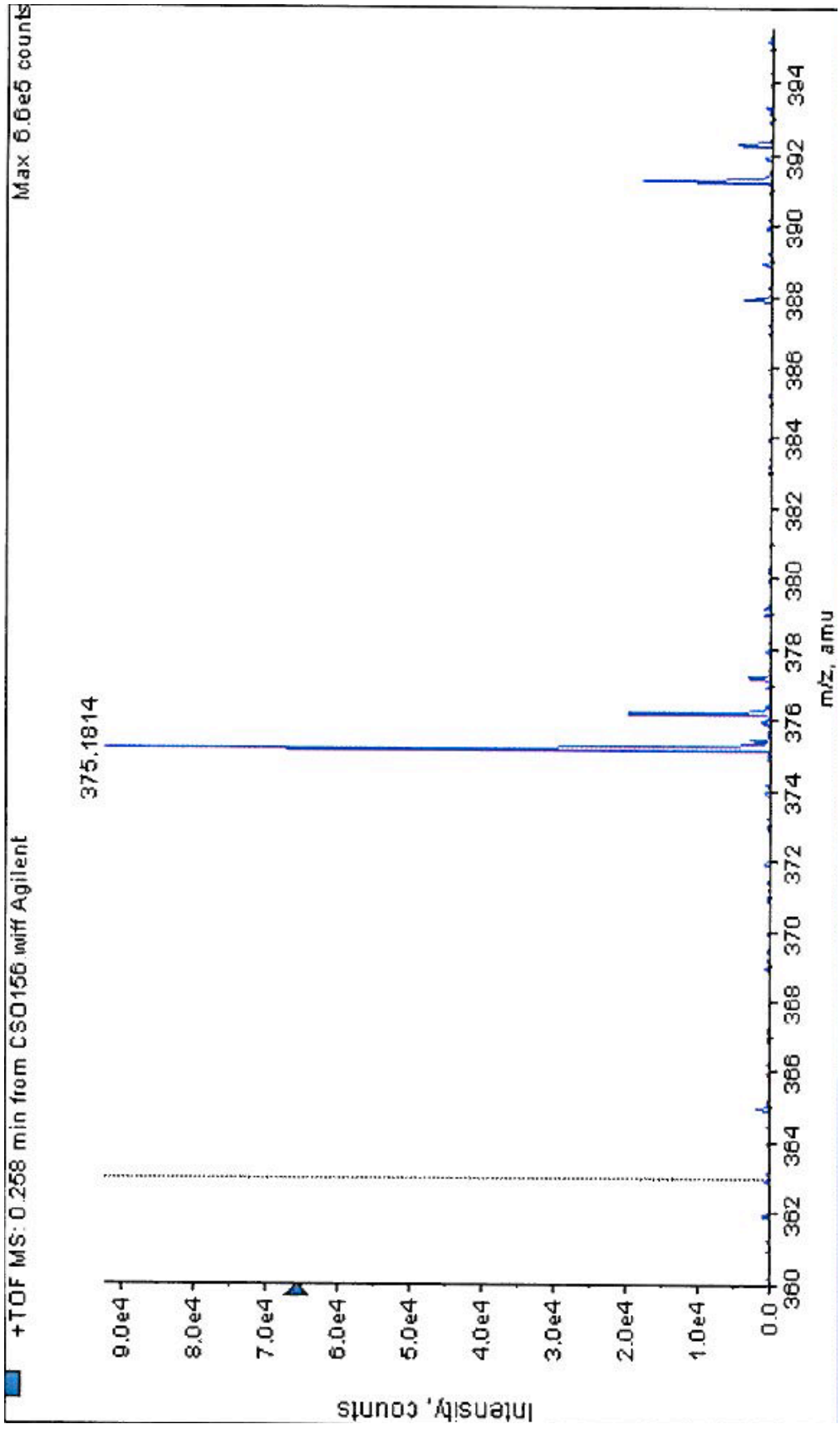

B.2.3 – Compound 2c

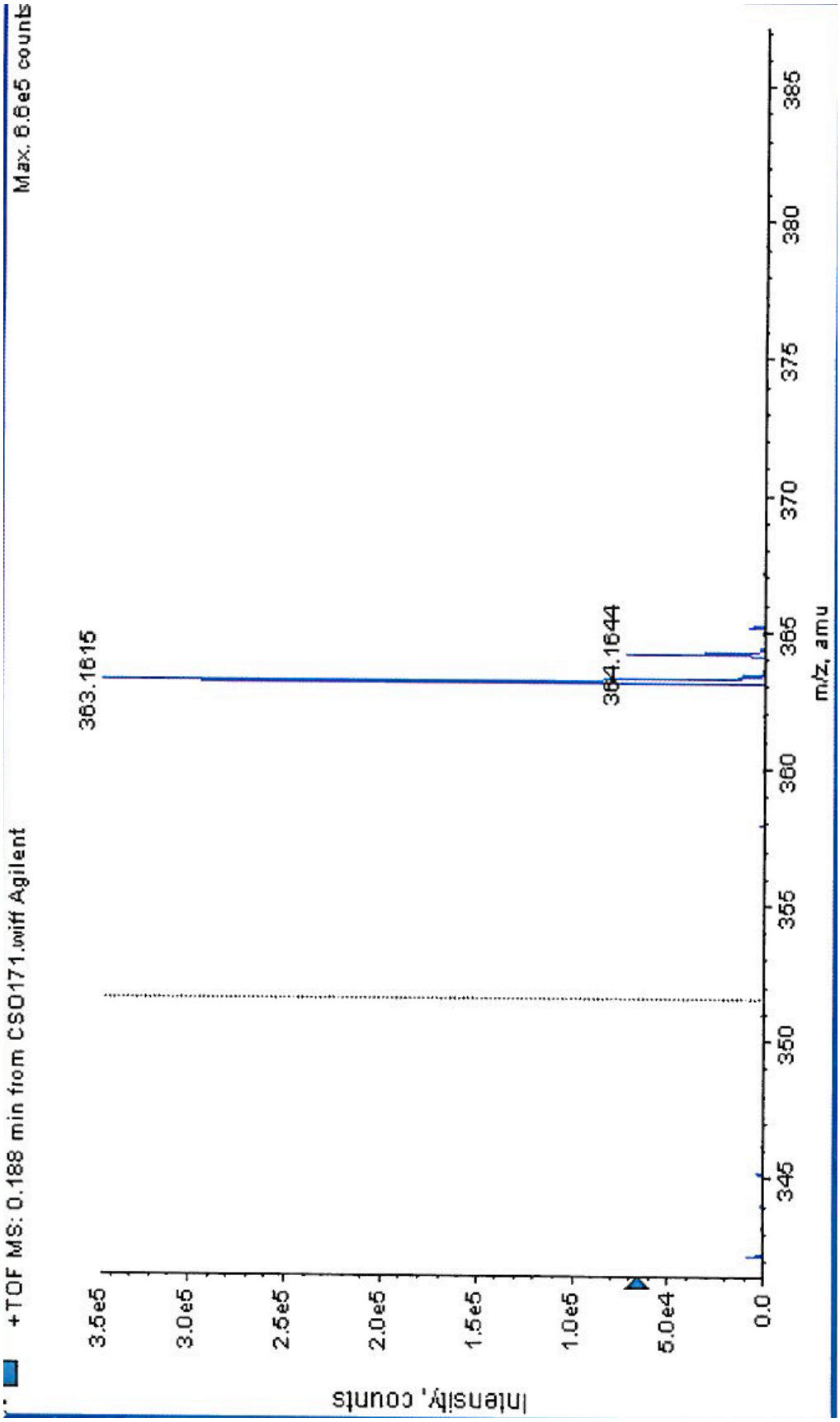

B.2.4 – Compound 2d

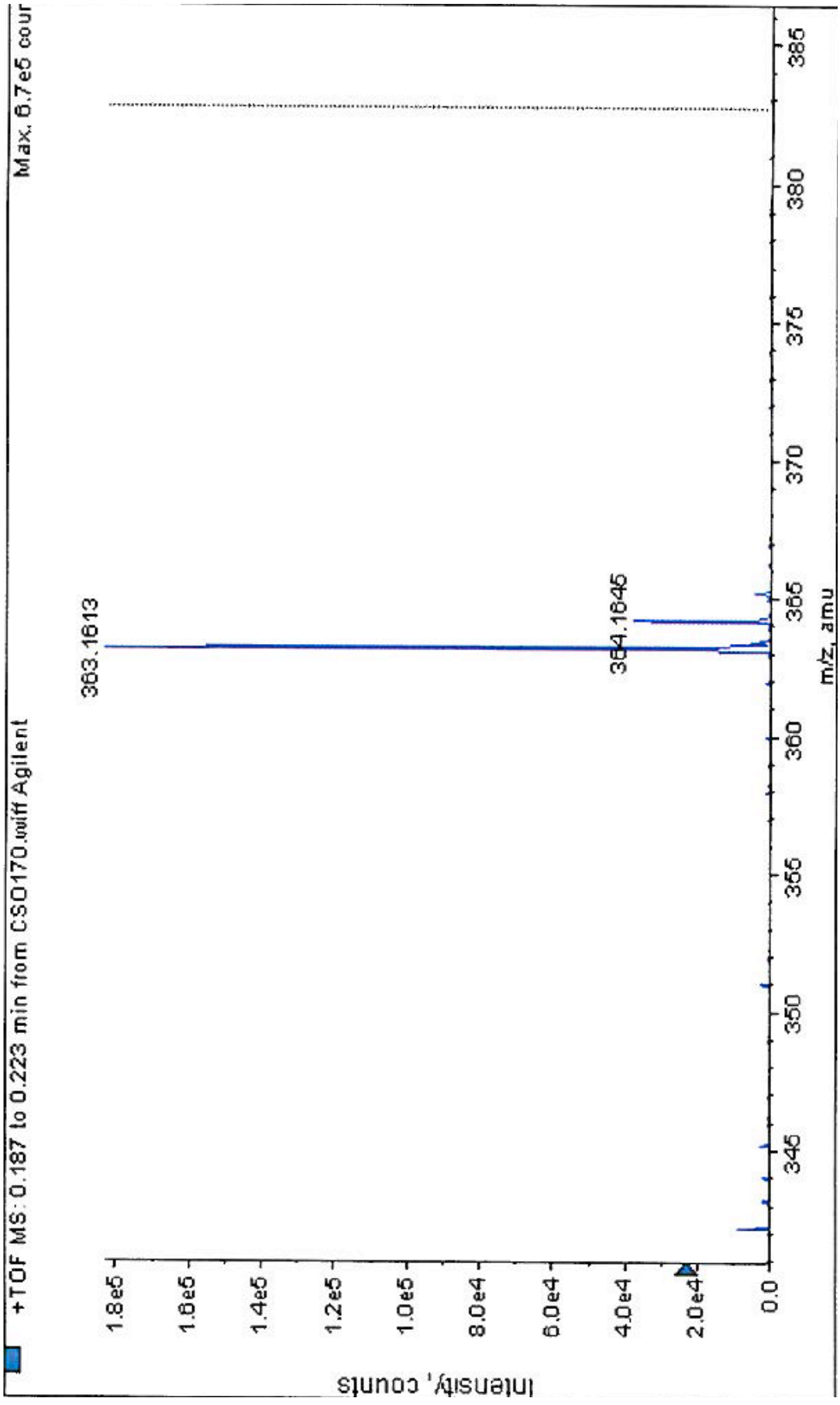

B.2.5 – Compound 2e

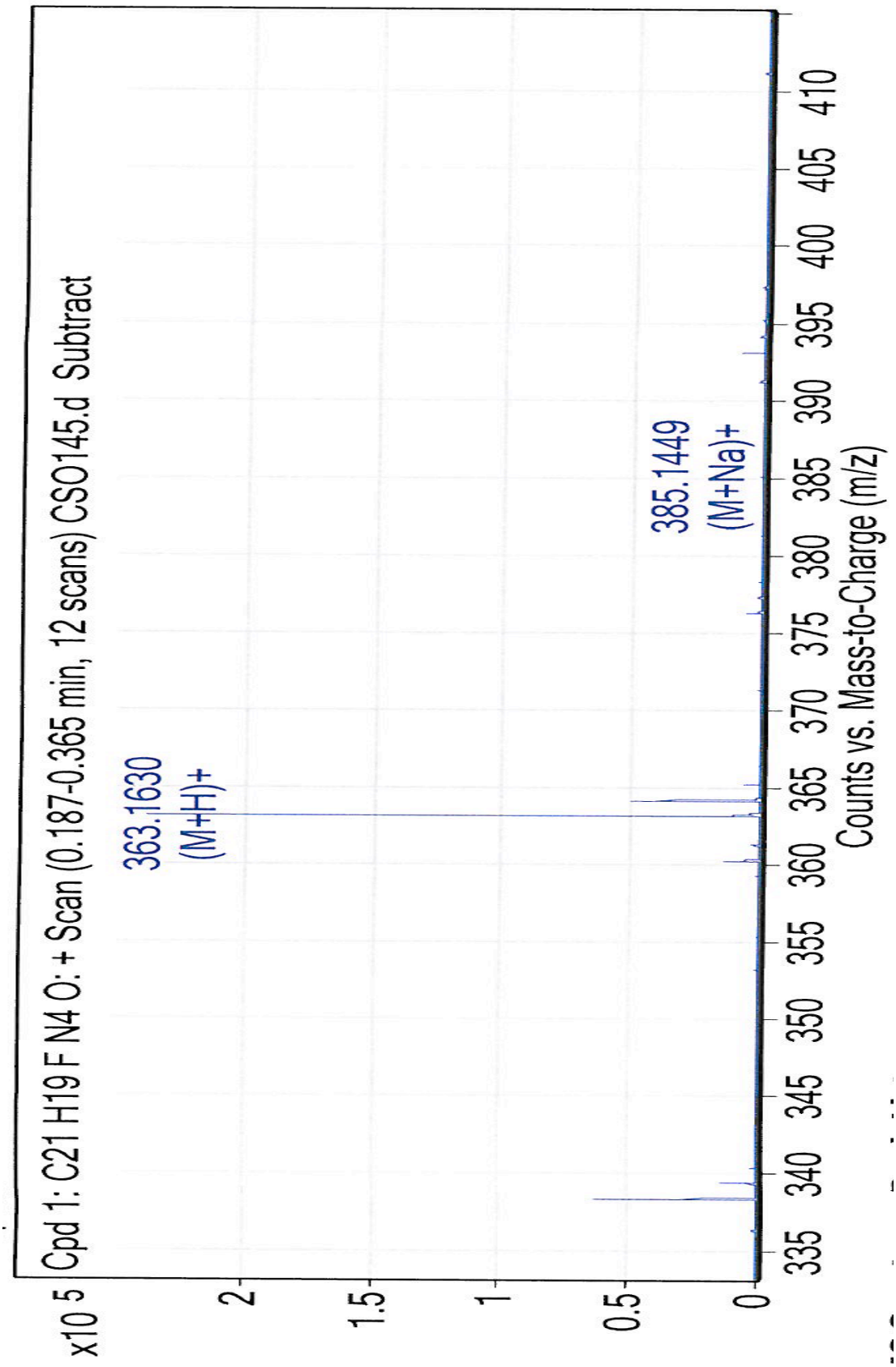

B.2.6 – Compound 2f

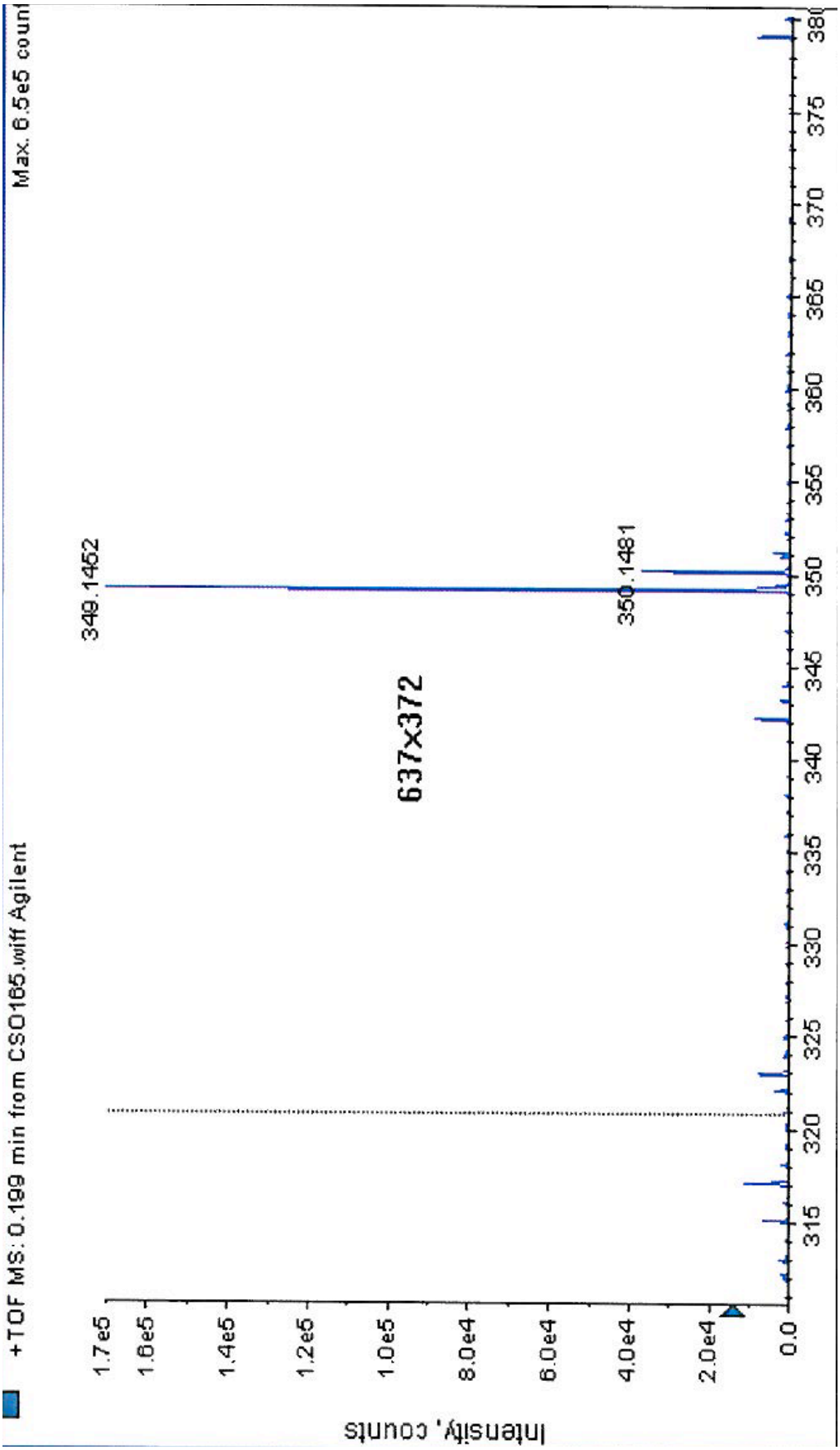

B.2.7 – Compound 2g

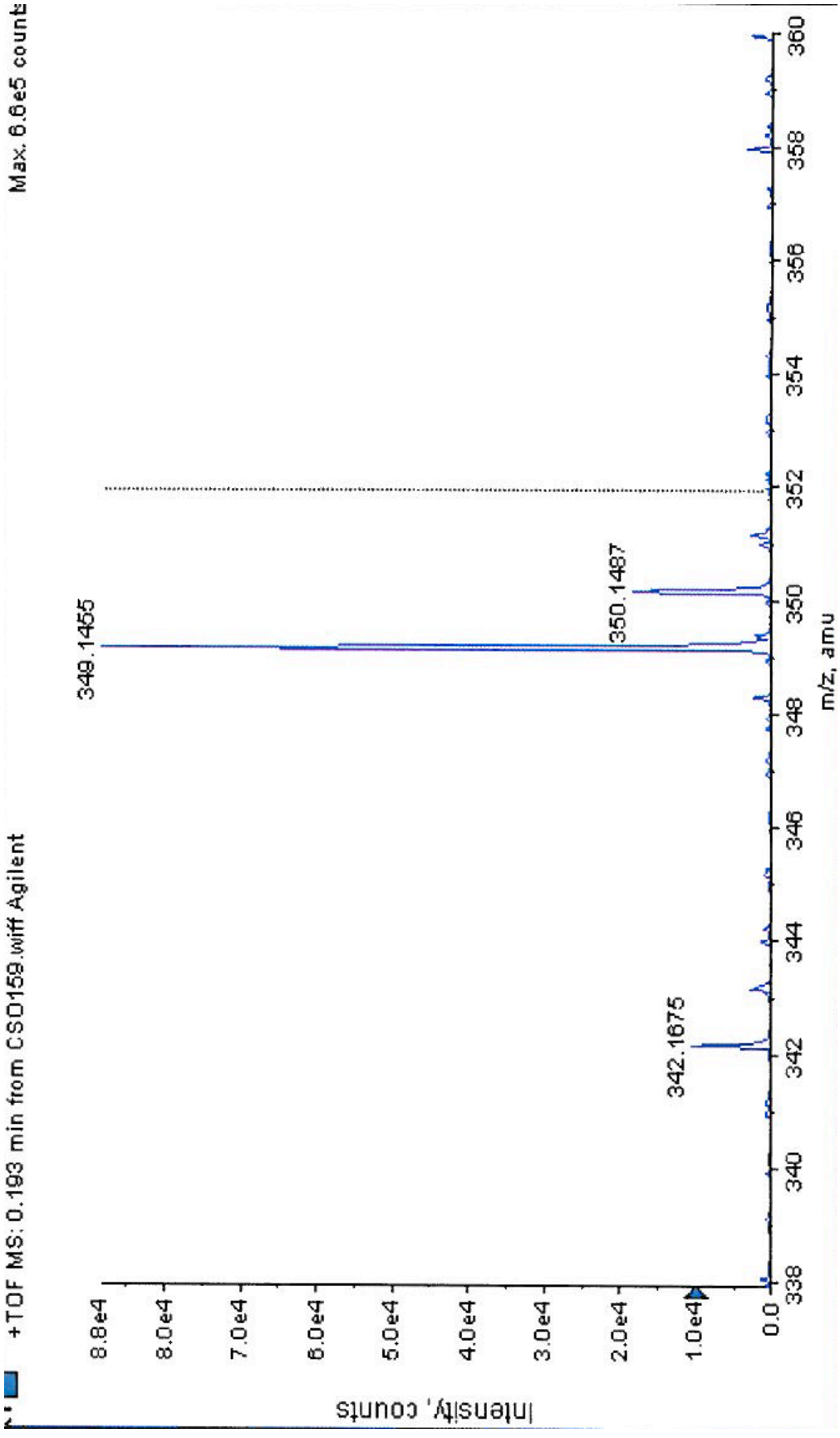

B.2.8 – Compound 2h

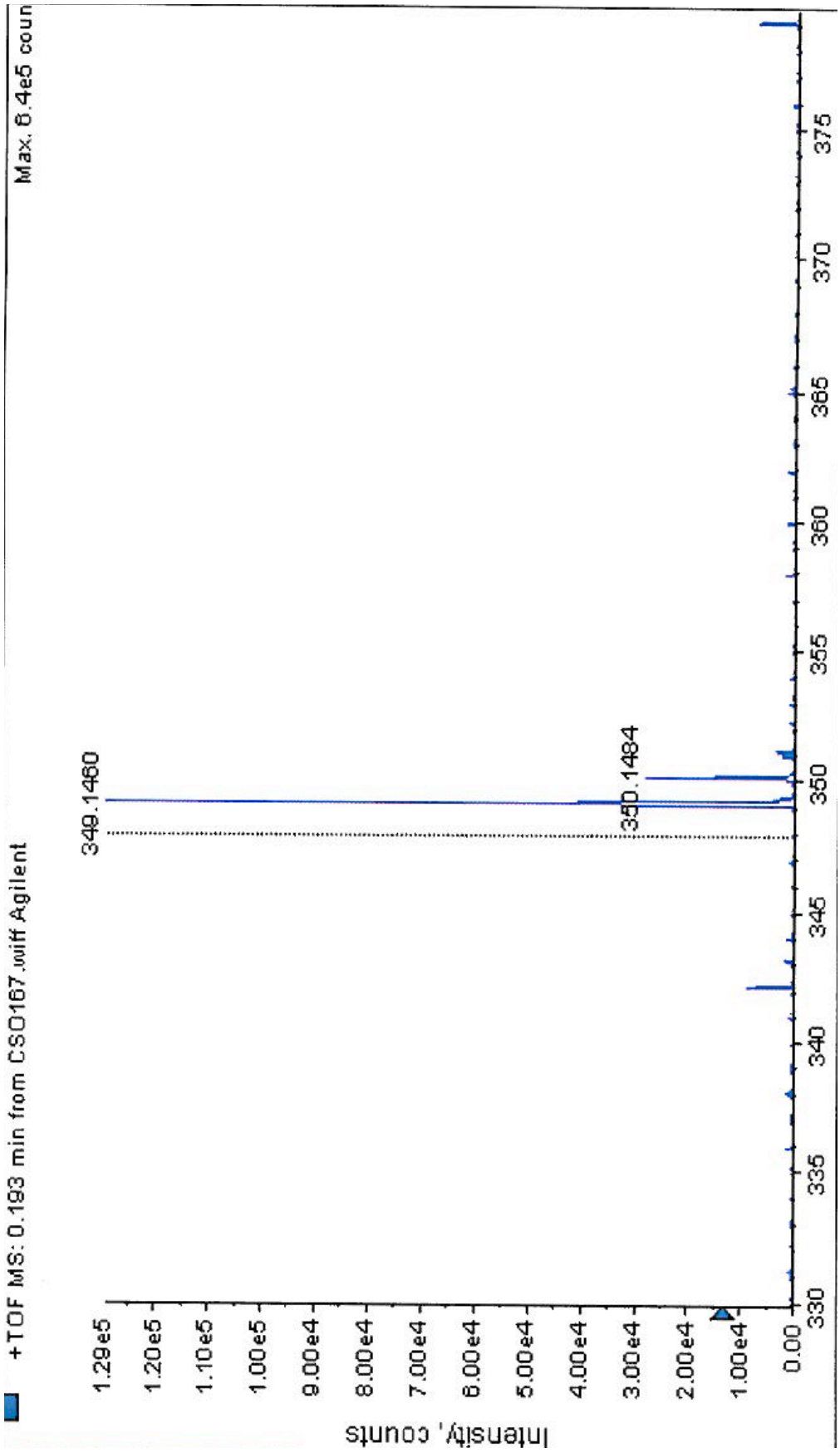

B.3 – Mass Spectra of Compound 3